Available online at www.sciencedirect.com
SCIENCE DIRECT®
ELSEVIER
Progress in Solid State Chemistry 32 (2004) 33–177
Progress in Solid State Chemistry
www.elsevier.nl/locate/pssc

Photoinduced reactivity of titanium dioxide

O. Carp [a,*], C.L. Huisman [b], A. Reller [b]

[a] *Institute of Physical Chemistry 'I.G. Murgulescu', Spl. Independentei 202, Sector 6, Bucharest, Romania*
[b] *Solid State Chemistry, University of Augsburg, Universitätstrasse 1, D-86159 Augsburg, Germany*

Abstract

The utilization of solar irradiation to supply energy or to initiate chemical reactions is already an established idea. If a wide-band gap semiconductor like titanium dioxide (TiO_2) is irradiated with light, excited electron–hole pairs result that can be applied in solar cells to generate electricity or in chemical processes to create or degrade specific compounds. Recently, a new process used on the surface of TiO_2 films, namely, photoinduced super-hydrophilicity, is described. All three appearances of the photoreactivity of TiO_2 are discussed in detail in this review, but the main focus is on the photocatalytic activity towards environmentally hazardous compounds (organic, inorganic, and biological materials), which are found in wastewater or in air. Besides information on the mechanistical aspects and applications of these kinds of reactions, a description of the attempts and possibilities to improve the reactivity is also provided. This paper would like to assist the reader in getting an overview of this exciting, but also complicated, field.
© 2004 Elsevier Ltd. All rights reserved.

Keywords: Titanium dioxide; Photocatalysis; Photoinduced processes; Surface properties; Environmental remediation

Contents

* Corresponding author. Tel./fax: +40-212128871.
E-mail address: carp@apia.ro (O. Carp).

0079-6786/$ - see front matter © 2004 Elsevier Ltd. All rights reserved.
doi:10.1016/j.progsolidstchem.2004.08.001

Nomenclature

A	light absorption coefficient at a given wavelength
A	acceptor
AC	active carbon
Ads	adsorbed species on a surface
AOP	advanced oxidation process
AOTs	advanced oxidation technologies
BOD	biological oxygen demand
BTEX	benzene, toluene, ethyl benzene and xylene
COD	chemical oxygen demand
CB	conduction band
CHQ	chloroquinone,
2-CP, 4-CP	2-, 4-chlorophenol
D	donor
DBPs	disinfection by-products

DCA	dichloroacetic acid
DCB	dichlorobenzene
DCM	dichloromethane
2,4-DCP	2,4-dichlorophenol
e^-	electron formed upon illumination of a semiconductor
EDTA	ethylenediaminetetraacetic acid
E_g	band gap energy
EPA	US Environmental Protection Agency
eV	electron volts
h^+	hole formed upon illumination of a semiconductor
hv	incident photon energy
HAs	humic acids
HHQ	hydroxyhydroquinone
IAQ	indoor air quality
IR	infrared
k_i	reaction rate constant
k(S)	Langmuir adsorption constant of a species S
K_{H_2O}	equilibrium coefficient for dissolved water on a semiconductor
$K_{(OW)}$	1-octanol–water partition coefficient
K(S)	adsorption equilibrium constant of a species S
LH	Langmuir–Hinshelwood
N_d	number of donor atoms
M, M^{n+}	metal, metallic ion with oxidation state n
MIBK	methyl-isobutyl ketone
nm	nanometer
$O_2^{\bullet -}$	superoxide ion radical
$OH^{\bullet}$	hydroxyl radical
Ox	oxidant
PCE	tetrachloroethylene
PCO	photocatalytic oxidation
pH_{zpc}	pH corresponding to the point of zero charge
P_{O_2}	oxygen partial pressure
ppm	parts per million
ppmv	parts per million by volume
PSH	photoinduced superhydrophilicity
Red	reductor
$[S_i]$	initial concentration of substrate
RH	relative humidity
SOD	superoxide dismutase
SBS	sick building syndrome
SS	solid solution
T	temperature (Kelvin)

TCE	trichloroethylene
TOC	total oxygen demand
UV	ultraviolet
VB	valence band
VIS	visible component of light
V_s	surface potential
W	thickness of the space-charge layer
ΔG^0	Gibbs free energy
ε_0	static dielectric constant in vacuum
$\phi_{overall}$	overall quantum yield
ξ	photonic efficiency
σ	Hammet constant

1. Introduction

Photoinduced processes are studied in a manifold ways and various applications have been developed since their first description. Despite the differences in character and utilization, all these processes have the same origin. Semiconductors can be excited by light with higher energy than the band gap and an energy-rich electron–hole pair is formed. This energy can be used electrically (solar cells), chemically (photochemical catalysis), or to change the catalyst surface itself (superhydrophilicity). Several excellent reviews [1,2] have been written in this field, especially on the topic of photocatalysis for pollutant degradation, but recent literature has not been reviewed yet. Here, we give an overview of the recent literature concerning these photoinduced phenomena. We concentrate on titanium dioxide, as it is one of the most important and most widely used compounds in all application areas mentioned above. The first part of this article will be devoted to the introduction of titanium dioxide and its photoinduced processes (Sections 2 and 3), after which we will treat photocatalytic reactions and mechanisms (Sections 4 and 5) in detail. The last part will describe research, performed on the application of titanium dioxide as photoactive material, in which emphasis is placed on the photocatalytic purification/disinfection of water and air. In conclusion, a critical evaluation of the work performed will be given, in which we will emphasize the questions that remained open until now and what kind of research is desired to further develop this field of science.

1.1. Titanium in our world

Titanium, the world's fourth most abundant metal (exceeded only by aluminium, iron, and magnesium) and the ninth most abundant element (constituting about 0.63% of the Earth's crust), was discovered in 1791 in England by Reverend William Gregor, who recognized the presence of a new element in ilmenite. The element was rediscovered several years later by the German chemist Heinrich

Klaporth in rutile ore who named it after Titans, mythological first sons of the goddess Ge (Earth in Greek mythology).

Titanium metal is not found unbound to other elements that are present in various igneous rocks and sediments. It occurs primarily in minerals like rutile, ilmenite, leucoxene, anatase, brookite, perovskite, and sphene, and it is found in titanates and many iron ores. The metal was also found in meteorites and has been detected in Sun and M-type stars. Rocks brought back from moon during the Apollo 17 mission have 12.1% TiO_2. Titanium is also found in coal, ash, plants, and even in the human body.

Mineral sources are rutile, ilmenite, and leucoxene (a weathering product of ilmenite). Ninety-three to 96% of rutile consists of titanium dioxide, ilmenite may contain between 44% and 70% TiO_2 and leucoxene concentrates may contain up to 90% TiO_2. In addition, a high-TiO_2 slag is produced from ilmenite that contains 75–85% TiO_2. About 98% of the world's production is used to make white pigments, and only the remaining 2% is used for making titanium metal, welding rod coatings, fluxes, and other products [3].

Ilmenite also called titanic iron ore is a weakly magnetic iron-black or steel-grey mineral found in metamorphic and plutonic rocks. It is used as a source of titanium metal. Kupffer discovered it in 1827 and named it after the Ural Ilmen Mountain (Russia) where it was first found. It is found in primary massive ore deposits or as secondary alluvial deposits (sands) that contain heavy minerals. Manganese, magnesium, calcium, chromium, silicon, and vanadium are present as impurities. Two-third of the known ilmenite reserves that can economically be worked up are in China, Norway (both having massive deposits), and former Soviet Union (sands and massive deposits); but the countries with the largest outputs are Australia (sands), Canada (massive ore), and the Republic of South Africa (sands).

Rutile is the most stable form of titanium dioxide and the major ore of titanium was discovered in 1803 by Werner in Spain, probably in Cajuelo, Burgos. Its name is derived from the Latin *rutilus*, red, in reference to the deep red color observed in some specimen when the transmitted light is viewed. It is commonly reddish brown but also sometimes yellowish, bluish or violet, being transparent to opaque. Rutile may contain up to 10% iron, and also other impurities such as tantalum, niobium, chromium, vanadium, and tin. It is associated with minerals such as quartz, tourmaline, barite, hematite and silicates. Notable occurrences include Brazil, Swiss Alps, the USA and some African countries.

Brookite was named in honor of the English mineralogist, H.J. Brooke, and was discovered by A. Levy in 1825 at Snowen (Pays de Gales, England). Its crystals are dark brown to greenish black opaque. Crystal forms include the typical tabular to platy crystals with a pseudohexagonal outline. Associate minerals are anatase, rutile, quartz, feldspar, chalcopyrite, hematite, and sphene. Notable occurrences include those in the USA, Austria, Russia, and Switzerland.

Anatase, earlier called octahedrite, was named by R.J. Hauy in 1801 from the Greek word '*anatasis*' meaning 'extension', due to its longer vertical axis compared to that of rutile. It is associated with rock crystal, feldspar, and axinite in crevices

in granite, and mica schist in Dauphiné (France) or to the walls of crevices in the gneisses of the Swiss Alps.

1.2. Photoinduced processes

TiO_2 is characterized by the presence of photoinduced phenomena. These are depicted in Fig. 1.

All these photoinduced processes originate from the semiconductor band gap. When photons have a higher energy, than this band gap, they can be absorbed and an electron is promoted to the CB, leaving a hole in the VB. This excited electron can either be used directly to create electricity in photovoltaic solar cells or drive a chemical reaction, which is called photocatalysis. A special phenomenon was recently discovered: trapping of holes at the TiO_2 surface causes a high wettability and is termed 'photoinduced superhydrophilicity' (PSH). All photoinduced phenomena involve surface bound redox reactions.

TiO_2 mediated photocatalytic reactions are gaining nowadays more and more importance and this is reflected in the increasing number of publications that deal with theoretical aspects and practical applications of these reactions (Fig. 2).

By far, the most active field of TiO_2 photocatalysis is the photodegeneration of organic compounds. TiO_2 has become a photocatalyst in environmental decontamination for a large variety of organics, viruses, bacteria, fungi, algae, and cancer cells, which can be totally degraded and mineralized to CO_2, H_2O, and harmless inorganic anions. This performance is attributed to highly oxidizing holes and hydroxyl radicals ($HO^{\bullet}$) that are known as indiscriminate oxidizing agents [4,5]. The oxidizing potential of this radical is 2.80 V, being exceeded only by fluorine.

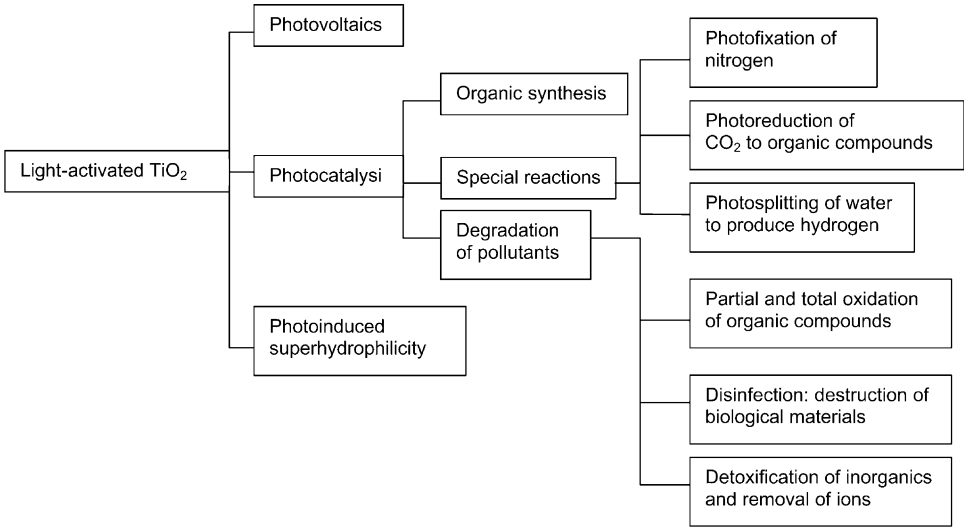

Fig. 1. Photoinduced processes on TiO_2.

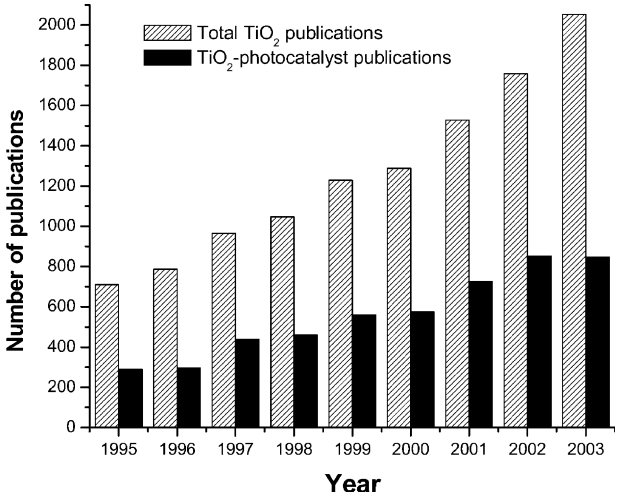

Fig. 2. Number of publications regarding TiO_2/TiO_2-photocatalysis per year (ISI-CD source).

The photoconversion (reduction and oxidation) of inorganic compounds is another group of reactions in which TiO_2 is applied. The photoreduction of metals, usually using hole trapping, is now redirected from a metalized semiconductor photocatalyst synthetic approach [6,7] to a process that removes dissolved metal ions from wastewater [8]. Oxidation is used to isolate metal ions which cannot be reduced and for CN^- decontamination.

The possibility to induce selective, synthetically useful redox transformations in specific organic compounds has also become increasingly more attractive for organic synthesis [9–15].

The ability to control photocatalytic activity is important in many other applications including utilization of TiO_2 in paint pigments [16–22] and cosmetics [23]. A low photoactivity is required for these applications, in order to prevent chalking (physical loss of pigments as the surface is degraded) and reduce UVC-induced pyrimide dimer formation (which can damage the DNA in cells).

Some major cornerstones in the development of TiO_2 in photoactivated processes are:

1972 the first photoelectrochemical cell for water splitting ($2H_2O \rightarrow 2H_2 + O_2$) is reported by Fujishima and Honda [24] using a rutile TiO_2 photoanode and Pt counter electrode;

1977 Frank and Bard [25,26] examined the reduction of CN^- in water, which is the first implication of TiO_2 in environmental purification;

1977 Schrauzer and Guth [27] reported the photocatalytic reduction of molecular nitrogen to ammonia over iron-doped TiO_2.

1978 the first organic photosynthetic reaction is presented, an alternative photo-induced Kolbe reaction [7] ($CH_3COOH \rightarrow CH_4 + CO_2$) that opens the field of organic photosynthesis;

1983 implementation by Ollis [28,29] of semiconductor-sensitized reactions for organic pollutant oxidative mineralization;
1985 application of TiO_2 as microbiocide [30], effective in photokilling of *Lactobacillus acidophilus*, *Saccharomyces cerevisiae* and *Escherichia coli*;
1986 Fujishima et al. [31] reported the first use of TiO_2 in photokilling of tumor cells (HeLa cells);
1991 O'Regan and Grätzel [32] reported about an efficient solar cell using nanosized TiO_2 particles;
1998 highly hydrophilic TiO_2 surfaces with excellent anti-fogging and self-cleaning properties are obtained by Wang et al. [33].

2. Titanium dioxide

2.1. General remarks

Titanium dioxide (TiO_2) belongs to the family of transition metal oxides [34]. In the beginning of the 20th century, industrial production started with titanium dioxide replacing toxic lead oxides as pigments for white paint. At present, the annual production of TiO_2 exceeds 4 million tons [35–37]. It is used as a white pigment in paints (51% of total production), plastic (19%), and paper (17%), which represent the major end-use sectors of TiO_2. The consumption of TiO_2 as a pigment increased in the last few years in a number of minor end-use sectors such as textiles, food (it is approved in food-contact applications and as food coloring (E-171) under a EU legislation on the safety of the food additives [38]), leather, pharmaceuticals (tablet coatings, toothpastes, and as a UV absorber in sunscreen cream with high sun protection factors [39–41] and other cosmetic products), and various titanate pigments (mixed oxides such as $ZnTiO_3$ [42], $ZrTiO_4$ [43,44], etc). Titanium dioxide may be manufactured by either the sulfate or the chlorine process [45]. In the sulfate process, ilmenite is transformed into iron- and titanium sulfates by reaction with sulfuric acid. Titanium hydroxide is precipitated by hydrolysis, filtered, and calcinated at 900 °C. Straight hydrolysis yields only anatase on calcination. To obtain rutile, seed crystals, generated by alkaline hydrolysis of titanyl sulfate or titanium tetrachloride, are added during the hydrolysis step. This sulfate process yields a substantial amount of waste iron sulfides and a poor quality TiO_2, although nowadays, the quality has improved significantly. Therefore, the chlorine process has now become the dominant method. This process uses rutile, which is either excavated or produced in a crude quality from ilmenite using the Becher process. The Becher process reduces the iron oxide in the ilmenite to metallic iron and then reoxidizes it to iron oxide separating out the titanium dioxide as synthetic rutile of about 91–93% purity. The process involves a high temperature furnace to heat the ilmenite with coal and sulfur. The slurry of reduced ilmenite (which consists of a mixture of iron and titanium dioxide in water) is oxidized with air and can be separated in settling ponds. The iron oxide (that represented at least 40% of the ilmenite) is returned to the mine site as waste and for land filling process. The

rutile is reacted with chlorine to produce titanium tetrachloride, which is purified and reoxidized, yielding very pure TiO_2. The chlorine gas is recycled. Although either process may be used to produce the pigment, the decision to use one process instead of the other is based on a number of factors, including raw material availability, freight, and waste disposal costs. The chloride process is less environmentally invasive, although in the last few years, great efforts have been made to operate a sulfate route plant in accordance with strict environmental requirements [46]. On the other hand, the sulfate route presents the advantage that both TiO_2 modifications as well as titanium chemicals can be made from one process.

TiO_2 has received a great deal of attention due to its chemical stability, non-toxicity, low cost, and other advantageous properties. As a result of its high refractive index, it is used as anti-reflection coating in silicon solar cells and in many thin-film optical devices [47]. TiO_2 is successfully used as gas sensor (due to the dependence of the electric conductivity on the ambient gas composition [48–50]) and is utilized in the determination of oxygen [48,51] and CO [52–54] concentrations at high temperatures (>600 °C), and simultaneously determining CO/O_2 [55] and CO/CH_4 [56] concentrations. Due to its hemocompatibility with the human body, TiO_2 is used as a biomaterial (as bone substituent and reinforcing mechanical supports) [57–64].

TiO_2 is also used in catalytic reactions [65] acting as a promoter, a carrier for metals and metal oxides, an additive, or as a catalyst. Reactions carried out with TiO_2 catalysts include selective reduction of NO_x to N_2 [66–76], effective decomposition of VOCs (including dioxines [77–80] and chlorinated [80–82] compounds), hydrogen production by gas shift production [83], Fischer–Tropsch synthesis [84–89], CO oxidation by O_2 [90–94], H_2S oxidation to S [95], reduction of SO_2 to S by CO [96], and NO_2 storage [97]. Photocatalytic reactions will be treated into more detail in the following sections.

Rutile is investigated as a dielectric gate material for MOSFET devices as a result of its high dielectric constant ($\varepsilon > 100$) [98,99] and doped anatase films (using Co) might be used as a ferromagnetic material in spintronics [100,101]. In batteries, the anatase form is used as an anode material in which lithium ions can intercalate reversibly [102]. For solar cell applications, the anatase structure is preferred over the rutile structure, as anatase exhibits a higher electron mobility, lower dielectric constant, lower density, and lower deposition temperature. Nanostructured TiO_2 especially is extensively studied in the field of solar cells as will be discussed in Section 3.2. Other photochemical and photophysical applications include photolysis of water, light-assisted degradation of pollutants, specific catalytic reactions (Section 3.3), and light-induced superhydrophilicity (Section 3.4). This list of applications is far from complete and new ideas concerning the possible use of TiO_2 have been appearing regularly.

2.2. Crystal structure and properties

Besides the four polymorphs of TiO_2 found in nature (i.e., anatase (tetragonal), brookite (orthorhombic), rutile (tetragonal), and TiO_2 (B) (monoclinic)), two

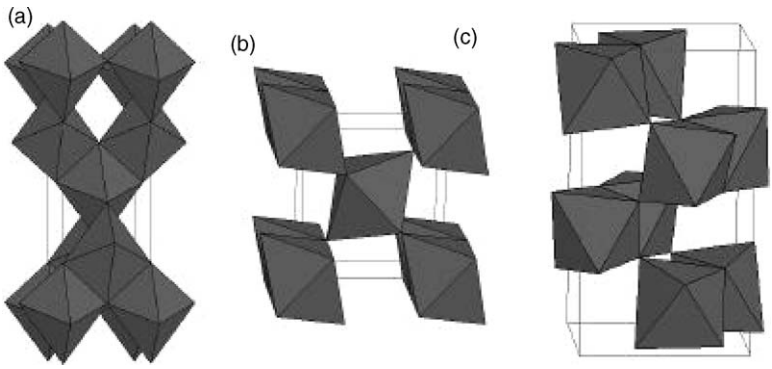

Fig. 3. Crystal structures of anatase (a), rutile (b), and brookite (c).

additional high-pressure forms have been synthesized starting from rutile: TiO_2(II) [103], which has the PbO_2 structure, and TiO_2(H) [104] with the hollandite structure.

The structures of rutile, anatase and brookite can be discussed in terms of (TiO_2^{6-}) octahedrals. The three crystal structures differ by the distortion of each octahedral and by the assembly patterns of the octahedral chains. Anatase can be regarded to be builtup from octahedrals that are connected by their vertices, in rutile, the edges are connected, and in brookite, both vertices and edges are connected (Fig. 3).

Thermodynamic calculations based on calorimetric data predict that rutile is the stablest phase at all temperatures and pressures up to 60 kbar, where TiO_2(II) becomes the thermodynamic favourable phase [105,106]. The small differences in the Gibbs free energy (4–20 kJ/mole) between the three phases suggest that the metastable polymorphs are almost as stable as rutile at normal pressures and temperatures. Particle size experiments affirm that the relative phase stability may reverse when particle sizes decrease to sufficiently low values due to surface-energy effects (surface free energy and surface stress, which depend on particle size) [107]. If the particle sizes of the three crystalline phases are equal, anatase is most thermodynamically stable at sizes less than 11 nm, brookite is most stable between 11 and 35 nm, and rutile is most stable at sizes greater than 35 nm [108]. This agrees with the observation that anatase is the common product of the industrial sulfate process [109]. Similar reverse phase stability is also described for graphite and diamond [110,111] and polymorphoxides such as ZrO_2 [112] and Al_2O_3 [113].

The enthalpy of the anatase → rutile phase transformation is low. A survey of the literature reveals widespread disagreement, with values ranging from -1.3 to -6.0 ± 0.8 kJ/mol [114–117]. Kinetically, anatase is stable, i.e., its transformation into rutile at room temperature is so slow that the transformation practically does not occur. At macroscopic scale, the transformation reaches a measurable speed for bulk TiO_2 at $T > 600\ ^\circ C$ [118–120]. During the transformation, anatase pseudoclosed-packed planes of oxygen [112] are retained as rutile closed-packed planes

[100], and a co-operative rearrangement of titanium and oxygen ions occurs within this configuration. The proposed mechanism implies at least spatial disturbance of the oxygen ion framework and a minimum breaking of Ti–O bonds [121] as a result of surface nucleation and growth [122,123]. The nucleation process is very much affected by the interfacial contact in nanocrystalline solids [124], and once initiated, it quickly spreads out and grain growth occurs [122,125].

The monotropic [126] anatase → rutile conversion has been studied for both mechanistic and application-driven reasons [127–129], because the TiO_2 phase (i.e., anatase or rutile) is one of the most critical parameters determining the use as a photocatalyst, catalyst, or as ceramic membrane material [15,130–132]. This transformation, achieved by increased temperature or pressure, is influenced by several factors, of which we mention:

(a) *concentration of lattice and surface defects*, which mainly depend on the synthetic method [133] and the presence of dopants [134,135]. An increase of *surface defects* enhances the rutile transformation rate, as these defects act as nucleation sites. On the other hand, since the transformation involves an overall contraction or shrinking of the oxygen structure (as indicated by a volume shrinkage of approximately 8%) and a co-operative movement of the ions, the removal of oxygen ions (i.e., the formation of oxygen vacancies) accelerates the transformation. The stoichiometry of TiO_2 and thus the *oxygen vacancy* concentration [135–138], may be controlled by the nature, amount, and lattice-adopted positions of impurities. Interstitial ions decrease the concentration of oxygen vacancies and inhibit the transformation, whereas substitutional cations, depending on their oxidation state, can inhibit or accelerate transformation. Ions with valency less than four and having small radius in substitutional positions (e.g., Cr^{3+}, Cu^{2+}, Co^{2+}, Li^{+}, Fe^{3+}, Mn^{2+}), even in mmol% concentration, are found to increase the oxygen vacancy concentration, which presumably reduces the strain energy which must be overcome before structural rearrangement can occur [121,139,140]. Ions of valency greater than four (e.g., P^{6+}, S^{6+}) would correspondingly reduce the oxygen vacancy concentration and the rate of transformation. Similarly, the substitution of an oxygen ion with two F^{-} or Cl^{-} ions would reduce the number of anion vacancies and inhibit the transformation [135,141,142]. Recently, it has been reported that brookite, which may accompany anatase formation in some preparation techniques [143,144], is responsible for an enhancement of the anatase → rutile transformation [107]. The high interfacial energy between brookite and anatase is thought to provide potential nucleation sites for this transformation [145].

(b) *particle size.* From a physical point of view, the conversion temperature and the rate of transformation depend on how fast the primary particles in the anatase phase sinter together to reach the critical size [146–148]. From circumstantial evidence, it is expected that the critical nucleus size of rutile crystallites is at least three times larger than that of anatase [149]. This means that if sintering of anatase particles is retarded by a suitable technique (e.g., synthesis methods [150], dispersion on a support [151,152], or addition of certain compounds like

Ln_2O_3 [153,154], ZrO_2 [155–158] or SiO_2 [13,15,159], which prevent anatase particles from adhering together), the probability of reaching the critical nucleus size is lowered, delaying the transformation, and stabilizing anatase up to 1000 °C [158]. On the other hand, smaller grain sizes are usually associated with higher specific surfaces. In these conditions, the total boundary energy of the TiO_2 powder increases, the driving force for rutile grain growth increases, and the conversion of anatase to rutile is promoted [160]. Once the critical particle size is achieved using nanosized anatase as starting material, the transformation reaches a measurable speed at lower temperatures ($T > 400$ °C) [121,135,161].

(c) by applying *pressure*, both surface free energy and surface stress may be tuned with sufficient accuracy. An increase of pressure from 1 to 23 kbar lowered the transformation temperature with 500 °C opening the way for pressure-assisted low temperature synthesis [162].

Some of the most important bulk properties of TiO_2 are presented in Table 1

2.3. Synthesis and morphologies

TiO_2 can be prepared in the form of powder, crystals, or thin films. Both powders and films can be built up from crystallites ranging from a few nanometers to several micrometers. It should be noted that nanosized crystallites tend to agglomerate. If separate nanosized particles are desired, often a deagglomeration step is necessary. Many novel methods lead to nanoparticles without an additional deagglomeration step.

2.3.1. Solution routes

For some applications, especially the synthesis of thin films, liquid-phase processing is one of the most convenient and utilized methods of synthesis. This method has the advantage of control over the stoichiometry, producing homogeneous materials, allowing formation of complex shapes, and preparation of composite materials. However, there are several disadvantages among which can (but need not) be: expensive precursors, long processing times, and the presence of carbon as an impurity. The most commonly used solution routes in the synthesis of TiO_2 are presented below.

2.3.1.1 Precipitation(co-)methods. These involve precipitation of hydroxides by the addition of a basic solution (NaOH, NH_4OH, urea) to a raw material followed by calcination to crystallize the oxide. It usually produces anatase even though sulfate or chloride is used [166,167]. In particular conditions, rutile may be obtained at room temperature [168]. The disadvantage is the tedious control of particle size and size distribution, as fast (uncontrolled) precipitation often causes formation of larger particles instead of nanoparticles. As raw materials, $TiCl_3$ [167,168] or $TiCl_4$ [166,169] are mainly used.

2.3.1.2 Solvothermal methods. These methods employ chemical reactions in aqueous [170] (hydrothermal method) or organic media (solvothermal method) such as

Table 1
Some bulk properties of the three main polymorphs of TiO_2 (anatase, rutile, and brookite) [163–165]

Crystal structure	System	Space group	Lattice constants (nm)			
			a	*b*	*c*	*c*/*a*
Rutile	Tetragonal	D_{4h}^{14}-$P4_2/mmm$	0.4584	–	0.2953	0.644
Anatase	Tetragonal	D_{4h}^{19}-$I4_1/amd$	0.3733	–	0.937	2.51
Brookite	Rhombohedral	D_{2h}^{15}-Pbca	0.5436	0.9166	–	0.944
Density (kg/m^3)						
Rutile	4240					
Anatase	3830					
Brookite	4170					
Dielectric properties	Frequency (Hz)	Temperature (K)	Dielectric constant			
Rutile, perpendicular to optical *c*-axis	10^8	290–295	86			
Rutile, parallel to optical *c*-axis	–	290–295	170			
Rutile, perpendicular to optical *c*-axis	10^4	298	160			
Rutile, along *c*-axis	10^7	303	100			
Anatase, average	10^4	298	55			
Band gap (eV)						
Rutile	3.05					
Anatase	3.26					
Refractive index	n_g	n_p				
Rutile	2.9467	2.6506				
Anatase	2.5688	2.6584				
Brookite	2.809	2.677				

methanol [170], 1,4 butanol [171], toluene [172] under self-produced pressures at low temperatures (usually under 250 °C). Generally, but not always, a subsequent thermal treatment is required to crystallize the final material. The solvothermal treatment could be useful to control grain size, particle morphology, crystalline phase, and surface chemistry by regulating the solution composition, reaction temperature, pressure, solvent properties, additives, and ageing time. A high level of attention is paid to the hydrothermal treatment of $TiO_2 \cdot nH_2O$ amorphous gels [148,173–175] either in pure distilled water or in the presence of different mineralizers, such as hydroxides, chlorides, and fluorides of alkali metals at different pH values [176,177]. As sources of TiO_2, in hydrothermal synthesis, $TiOSO_4$ [157,175,178,179], $H_2TiO(C_2O_4)_2$ [180], $H_2Ti_4O_9 \cdot 0.25\ H_2O$ [170], $TiCl_4$ in acidic solution [181], and Ti powder [182] are reported as examples.

2.3.1.3 Sol–gel methods. These methods are used for the synthesis of thin films, powders, and membranes. Two types are known: the non-alkoxide and the alkoxide route. Depending on the synthetic approach used, oxides with different

physical and chemical properties may be obtained. The sol–gel method has many advantages over other fabrication techniques such as purity, homogeneity, felicity, and flexibility in introducing dopants in large concentrations, stoichiometry control, ease of processing, control over the composition, and the ability to coat large and complex areas. The non-alkoxide route uses inorganic salts [183–186] (such as nitrates, chlorides, acetates, carbonates, acetylacetonates, etc.), which requires an additional removal of the inorganic anion, while the alkoxide route (the most employed) uses metal alkoxides as starting material [187–189]. This method involves the formation of a TiO_2 sol or gel or precipitation by hydrolysis and condensation (with polymer formation) of titanium alkoxides. In order to exhibit better control over the evolution of the microstructure, it is desirable to separate and temper the steps of hydrolysis and condensation [190]. In order to achieve this goal, several approaches were adopted. One of them is alkoxide modification by complexation with coordination agents such as carboxylates [191–197], or β-diketonates [151,194,198] that hydrolyze slower than alkoxide ligands. Additionally, the preferred coordination mode of these ligands can be exploited to control the evolution of the structure. In general, β-diketone ligands predominately form metal chelates [199] which can cap the surface of the structure [200]. Carboxylate ligands have a strong tendency to bridge metal centers [199,201], being likely to become trapped in the bulk of materials and on the surface of the particle [202]. Acid–base catalysis can also be used to enable separation of hydrolysis and condensation steps [190,203] It has been demonstrated that acid catalysis increases hydrolysis rates and ultimately crystalline powders are formed from fully hydrolyzed precursors. Base catalysis is thought to promote condensation with the result that amorphous powders are obtained containing unhydrolyzed alkoxide ligands. On the other hand, acetic acid may be used in order to initiate hydrolysis via an esterification reaction, and alcoholic sols prepared from titanium alkoxide using amino alcohols have been shown to stabilize the sol, reducing or preventing the condensation and the precipitation of titania [137,204]. These reactions are followed by a thermal treatment (450–600 $^{\circ}$C) to remove the organic part and to crystallize either anatase or rutile TiO_2. Recent variants of the sol–gel method lowered the necessary temperature to less than 100 $^{\circ}$C [205]. The calcination process will inevitably cause a decline in surface area (due to sintering and crystal growth), loss of surface hydroxyl groups, and even induce phase transformation. Washing steps have been also reported to cause surface modifications [206,207]. Cleaning of particles is usually achieved by washing the surface with a solvent, followed by centrifugation. The solvent can affect the chemical composition and crystallization [206]. It was also reported that particle washing could affect the surface charge of the particles by bonding onto the surface [207]. An alternative washing technique is to dialyze particles against double-distilled water [208], which could be an effective method of removing soluble impurities without introducing new species.

As titanium sources, Ti(*O*-E)$_4$ [209] Ti(*i*-OP)$_4$ [162,210–212], and Ti(O-*n*Bu)$_4$ [213–215] are most commonly used. The sol–gel method has been widely studied particularly for multicomponent oxides where intimate mixing is required to form

a homogeneous phase at the molecular level. Thus, metal ions such as Ca^{2+} [137], Sr^{2+} [137], Ba^{2+} [137], Cu^{2+} [216,217], Fe^{3+} [211,218–221], V^{5+} [221,222], Cr^{3+} [221], Mn^{2+} [139,221], Pt^{4+} [223], Co^{2+} [224], Ni^{2+} [221], Pb^{2+} [225], W^{6+} [224], Zn^{2+} [226], Ag^{+} [134,162], Au^{3+} [227], Zr^{2+} [228], La^{3+} [229], and Eu^{3+} [213] were introduced into TiO_2 powders and films by this method and the photocatalytic activity was improved to varying extent. Most nanocrystalline-TiO_2 (nc-TiO_2) particles that are commercially obtainable are synthesized using sol–gel methods.

Very recently, sol–gel and templating synthetic methods were applied to prepare very large surface area titania phases [230–232], which exhibit a mesoporous structure. Ionic and neutral surfactants have been successfully employed as templates to prepare mesoporous TiO_2 [233,234,236–239]. Block copolymers can also be used as templates to direct formation of mesoporous TiO_2 [240–242]. In addition, many non-surfactant organic compounds have been used as pore formers such as diolates [230,243,244] and glycerine [245,246]. Sol–gel methods coupled with hydrothermal routes for mesoporous structures [246,247] lead to large surface area even after heating at temperatures up to 500 °C. This may be explained as follows: generally, mesopores collapse during calcination due to crystallization of the wall. When a hydrothermal treatment induces the crystallization of amorphous powders, the obtained powders can effectively sustain the local strain during calcination and prevent the mesopores from collapsing.

For nanostructured thin films, the sols are often treated in an autoclave to allow controlled growth of the particles until they reach the desired size. Oswald ripening takes place during this process, leading to a homogeneous particle-size distribution. If a film is made using these particles, substances can be added to prevent cracking and agglomeration or increase the binding and viscosity after this ripening process. The resulting paste can be deposited on a substrate using doctor blading or screen printing. The solvent is evaporated and the particles are interconnected by a sintering process, normally at air temperatures around 450 °C. At this temperature, organic additives are also removed from the film. Slow heating and cooling is important to prevent cracking of the film. In most cases, the resulting film has a porosity of 50%. Thin films can also be made from the sol by dip coating.

2.3.1.4 Microemulsion methods. Water in oil microemulsion has been successfully utilized for the synthesis of nanoparticles. Microemulsions may be defined as thermodynamically stable, optically isotopic solutions of two immiscible liquids consisting of microdomains of one or both stabilized by an interfacial film of surfactant. The surfactant molecule generally has a polar (hydrophilic) head and a long-chained aliphatic (hydrophobic) tail. Such molecules optimize their interactions by residing at the two-liquid interface, thereby considerably reducing the interfacial tension. Despite promising early studies, there have been only limited reports of controlled titania synthesis from these microemulsions [248,249]. In particular, hydrolysis of titanium alkoxides in microemulsions based on sol–gel methods has yielded uncontrolled aggregation and flocculation [250,251] except at very low concentrations [252,253]. Recently, an improved method using carbon dioxide instead of oil has been applied in preparing nanosized TiO_2 [254].

2.3.1.5 Combustion synthesis. Combustion synthesis (hyperbolic reaction) leads to highly crystalline fine/large area particles [255,256]. The synthetic process involves a rapid heating of a solution/compound containing redox mixtures/redox groups. During combustion, the temperature reaches about 650 °C for a short period of time (1–2 min) making the material crystalline. Since the time is so short, particle growth of TiO_2 and phase transition to rutile is hindered.

2.3.1.6 Electrochemical synthesis. Electrochemical synthesis may be used to prepare advanced thin films such as epitaxial, superlattice, quantum dot and nanoporous ones. Also, varying electrolysis parameters like potential, current density, temperature, and pH can easily control the characteristic states of the films. Although electrodeposition of TiO_2 films by various Ti compounds such as $TiCl_3$ [257–259], $TiO(SO_4)$ [260,261], and $(NH_4)_2TiO(C_2O_4)_2$ [262,263] is reported, use of titanium inorganic salts in aqueous solutions is always accompanied by difficulties, due to the high tendency of the salts to hydrolyze. Therefore, electrolysis requires both an acidic medium and an oxygen-free environment [264]. Non-aqueous solutions represent an option to overcome this problem [265].

2.3.2. Gas phase methods

For thin films, most synthesis routes are performed from the gas phase. These can be chemical or physical of nature. Most of these techniques can also synthesize powder, if a method to collect the produced particles is employed. The main techniques are:

2.3.2.1 Chemical vapour deposition (CVD). CVD is a widely used versatile technique to coat large surface areas in a short span of time. In industry, this technique is often employed in a continuous process to produce ceramic and semiconductor films. The family of CVD is extensive and split out according to differences in activation method, pressure, and precursors. Compounds, ranging from metals to composite oxides, are formed from a chemical reaction or decomposition of a precursor in the gas phase [266,267].

2.3.2.2 Physical vapour deposition (PVD). PVD is another class of thin-film deposition techniques. Films are formed from the gas phase, but here without a chemical transition from precursor to product. This is, therefore, only possible with substances that are stable in the gas phase and can be directed towards the substrate. The most commonly employed PVD technique is thermal evaporation, in which a material is evaporated from a crucible and deposited onto a substrate. PVD is a so-called line-of-sight technique, i.e., the gaseous stream of material follows a straight line from source to substrate. This leads to shadow effects, which are not present in CVD. The substrate can be at room temperature, or heated/cooled, depending on the requirements. In most set-ups, the substrates are placed straight above the source, but other arrangements are also possible. In most cases, evaporation takes place under reduced pressure to minimize collisions of gas molecules and prevent pollution of the deposited films. In electron beam (E-beam) evaporation, a focussed beam of electrons heats the selected material. These

electrons in turn are thermally generated from a tungsten wire that is heated by current. TiO_2 films, deposited with E-beam evaporation, have superior characteristics over CVD grown films where smoothness, conductivity, presence of contaminations, and crystallinity are concerned, but on the other hand, production is slower and more laborious. The use of reduced TiO_2 powder (heated at 900 °C in a hydrogen atmosphere) is necessary to make it conductive enough to focus the electron beam in the crucible [163].

2.3.2.3 Spray pyrolysis deposition (SPD). SPD is an aerosol deposition technique for thin films and powders related to CVD. The main differences are that in spray pyrolysis: (1) an aerosol (a mist of small droplets) is formed from a precursor solution instead of a vapour in CVD. (2) The aerosol is directly focussed onto the sample in most cases, whereas diffusion is a dominant process in CVD. (3) The heated substrates are at ambient pressure, while in CVD, the set-up commonly is under reduced pressure. There are several small derivatives of this technique, mainly differing in the formation step of the aerosol and the character of the reaction at the substrate (gas-to-particle synthesis and droplet-to-particle synthesis). Confusingly, a broad spectrum of names for this class of techniques has evolved. It has been used for preparation of (mixed) oxide powders/films and uses mostly metal-organic compounds or metal salts as precursors [268–277]. In fact, aerosol-based methods are hybrid methods because such routes start from precursors in solutions, which can be further processed in a number of different ways. The size of the particles formed and the morphology of the resulting film are strongly dependent on deposition parameters like substrate temperature, composition and concentration of the precursor, gas flow, and substrate–nozzle distance. Some of these parameters are mutually dependent on each other. Compared to other thin-film deposition methods, spray pyrolysis of TiO_2 has merits such as simplicity, low costs, reproducibility, and the possibility of depositing large areas in a short time, while the films exhibit good electrical and optical properties. Uniformity is in most cases a problem, as is the smoothness of the films.

2.3.2.4 Other methods. There are several other sophisticated thin-film techniques based on vapour-phase deposition. *Sputtering* (either using direct current (DC) [278–280] or radio frequency (RF) [281] currents) is used quite frequently to produce TiO_2 films. The technique uses a plasma consisting of argon and oxygen. Accelerated Ar ions hit an electrode made of TiO_2 or Ti evaporating part of it, which is deposited on a substrate. *Molecular beam epitaxy* [282–284] is a technique that uses a (pulsed) laser to ablate parts of a TiO_2 ceramic target. The material is deposited on the substrate in an argon/oxygen atmosphere or plasma. This leads to high quality films with control over the orientation. *Ion implantation* is seldom used to synthesize TiO_2 and is based on the transformation of precursor plasma to TiO_2, which only becomes crystalline after an annealing step. It is, however, frequently used to implant ions in TiO_2 films (doping) to improve the photocatalytic activity [285]. Another unusual technique is *dynamic ion beam*

mixing [286], which uses high-energy O_2^+ and/or O^+ beams and Ti vapour to deposit TiO_2 films with high speed and control over the composition. Although these methods have the merit to control the film growth and the feasibility to obtain pure materials, they are energy intensive and involve high temperatures. Thus, techniques for film processing should also be developed in view of economical aspects.

TiO_2 is also synthesized in special morphologies. Nanostructures especially have been built in various sizes and shapes [287]. To complete the list, we include: nanorods [288–293] (Fig. 4G), platelets [294] (Fig. 4F), nanowires [295–299], nanowalls [239,290], nanotubes [298,300–302] (Fig. 4A, C), nanoribbons [303] (Fig. 4D), whis-

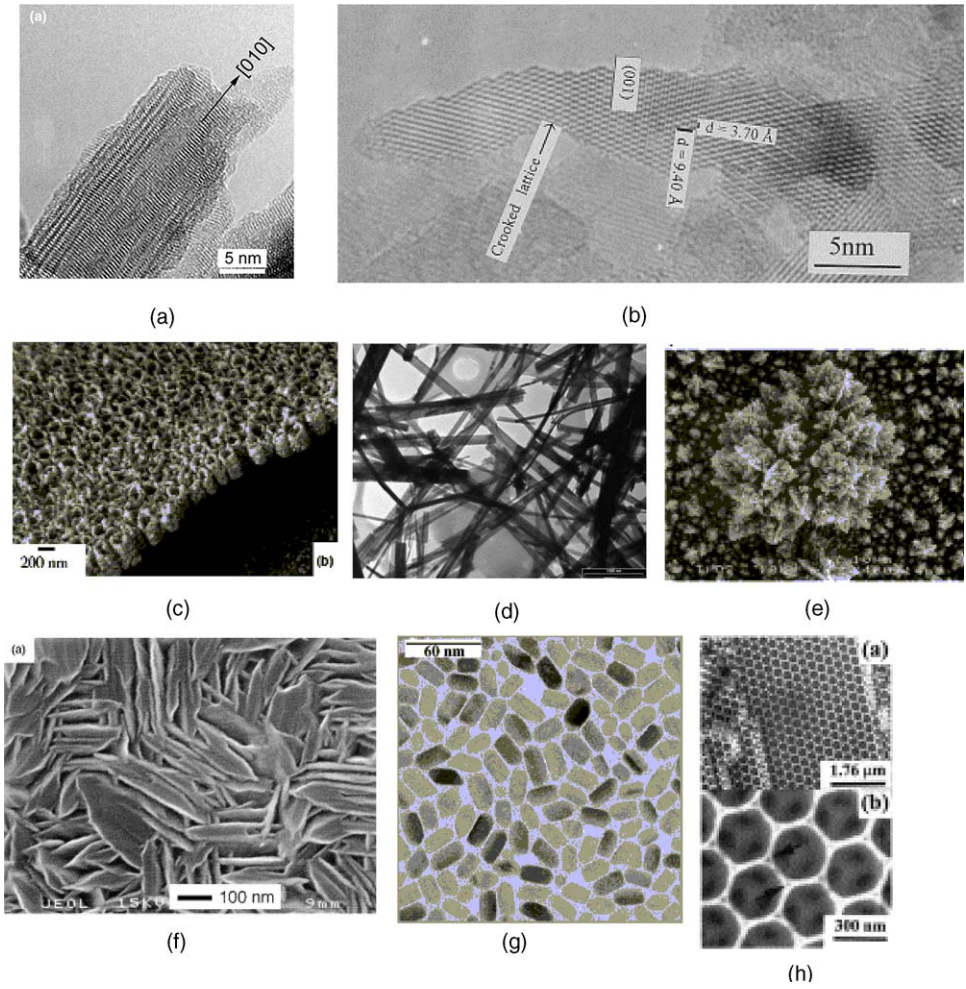

Fig. 4. Morphologies of nanosized TiO_2. For synthesis methods and details, we refer to the respective references: (A) [301]; (B) [304]; (C) [302]; (D) [303]; (E) [308]; (F) [294]; (G) [309]; (H) [310].

kers [304] (Fig. 4B) inverse opals [305–307] (Fig. 4H) (ordered mesoporous materials in which air voids are surrounded by TiO_2 in a 3-D lattice), and fractals [308] (Fig. 4E). In Fig. 4, some interesting morphologies of nanosized TiO_2 are collected.

2.4. Semiconductors and photocatalytic activity

Due to oxygen vacancies, TiO_2 is an n-type semiconductor. These vacancies are formed according to the following reaction:

$$O_o^x \overset{TiO_2}{\rightarrow} V_o^{hh} + 2e^- + 1/2O_2(g) \tag{2.1}$$

where the Kröger–Vink defect notation is used to explain that inside TiO_2 a positive (2+) charged oxide ion vacancy (V_o^{hh}) is formed upon release of two electrons and molecular oxygen. For example, this reaction can be induced by heating (in an oxygen-poor environment).

A photocatalyst is characterized by its capability to adsorb simultaneously two reactants, which can be reduced and oxidized by a photonic activation through an efficient absorption ($h\nu \geq E_g$). Fig. 5 shows the band gap of several semiconductors and some standard potentials of redoxcouples. The ability of a semiconductor to undergo photoinduced electron transfer to an adsorbed particle is governed by the band energy positions of the semiconductor and the redox potential of the adsorbates. The energy level at the bottom of conduction band is actually the reduction potential of photoelectrons. The energy level at the top of valence band determines the oxidizing ability of photoholes, each value reflecting the ability of the system to promote reductions and oxidations. The flatband potential, V_{fb}, locates the energy of both charge carriers at the semiconductor–electrolyte interface, depending on the nature of the material and system equilibrium [311]. From the thermodynamic

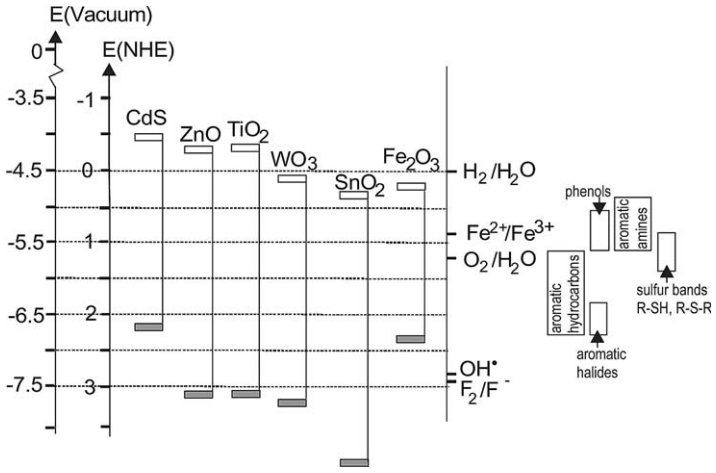

Fig. 5. Band positions (top of valence band and bottom of conduction band) of several semiconductors together with some selected redox potentials. Picture adapted from [314,315].

point of view, adsorbed couples can be reduced photocatalytically by conduction band electrons if they have more positive redox potentials than V_{fb} of the conduction band, and can be oxidized by valence band holes if they have more negative redox potentials than the V_{fb} of the valence band [312]. Because the flatband potential value follows a Nernstian pH dependence, decreasing 59 mV per pH unit [313], the ability of the electrons and holes to induce redox chemistry can be controlled by changes in the pH.

Unlike metals, semiconductors lack a continuum of interband states to assist the recombination of electron–hole pairs, which assure a sufficiently long lifetime of e^-–h^+ pair to diffuse to the catalyst's surface and initiate a redox reaction [316]. The differences in lattice structures of anatase and rutile TiO_2 cause different densities and electronic band structures, leading to different band gaps (for bulk materials: anatase 3.20 eV and rutile 3.02 eV) [317,318]. Therefore, the absorption thresholds correspond to 384 and 410 nm wavelength for the two titania forms, respectively. The mentioned values concern single crystals or well-crystallized samples. Higher values are usually obtained for weakly crystallized thin films [319,320] or nanosized materials [321,322]. The blue shift of the fundamental absorption edge in TiO_2 nanosized materials [321,322] has been observed amounting to 0.2 eV for crystallite sizes in the range 5–10 nm.

3. Photoinduced processes

3.1. General remarks

All photoinduced phenomena are activated by an input of super-band gap energy to the semiconductor TiO_2. Absorption of a photon with enough energy leads to a charge separation due to an electron promotion to the conduction band and a generation of a hole (h^+) in the valence band. The subsequent mode of action of the photogenerated electron–hole pair (e^-–h^+), determines which of the phenomena is the dominant process, because even if they are intrinsically different processes, they can and in fact take place concomitantly on the same TiO_2 surface. If the electrons are used in an outer circuit to perform work, we speak about a photovoltaic solar cell. Photocatalysis is a well-known process and is mostly employed to degrade or transform (into less harmful substances) organic and inorganic compounds and even microorganisms. The recently discovered wettability, termed by Fujishima [323] as 'superhydrophilicity', presents a large range of applications in cleaning and anti-fogging surfaces. The detailed material properties required for enhanced efficiency are different from each other. For enhanced photocatalysis, deep electron traps and high surface acidity are needed to lengthen the lifetime of photoexcited electrons and holes and to ensure better adsorption of organic substances on the surface. Meanwhile, low surface acidity and, most of all, a large quantity of Ti^{3+} is essential for hydrophilic surface conversion. These differences are related to the fact that photocatalysis is more likely to be sensitive to bulk properties, while hydrophilicity can be definite as an interfacial phenomenon.

In the following sections, the above-mentioned photoinduced processes will be treated in more detail.

3.2. Photovoltaic cells

Photovoltaic (PV) cells can produce electricity from (sun)light. They can be composed of various compounds, but all cells are based on semiconductors. Electrons can be promoted from the (occupied) VB to the (empty) CB when photons with energies higher than the band gap are absorbed. These excited electrons can be extracted to an outer circuit where they can perform work. Without a driving force, the lifetime of the excited electron–hole pairs is too short to be used effectively and therefore dopants are introduced in the semiconductor.

Small levels of foreign elements are added to the semiconductor, which increase the conductivity as either the conduction band is partly filled with electrons (n-type doping) or the valence band is partly emptied (which equals partly filled with holes: p-type doping). This p- and n-type character can also develop without the addition of external dopants if defects in the semiconductor are present or are formed in the presence of oxygen. If a p- and an n-type material are connected, electrons and holes recombine at the interface, but the positively charged donors and negatively charged acceptors remain in the lattice and a depletion layer is formed (no free charges present). At a certain thickness of the depletion layer, the growth stops, because electrons from the n-side and holes from the p-side cannot recombine anymore, due to the large charge that is present in the depletion layer. In this so-called p–n junction, an internal electrical field is now present. This is schematically shown in Fig. 6A. In physical terms, the Fermi levels of both sides have to equalize upon contact, thereby creating a flow of electrons from the n-type to the p-type semiconductor. While the edges of the bands are pinned due to the large amount of surface states, band bending occurs between the interface and the bulk of the semiconductors. This is associated with surface charging. Due to the internal electric field, holes will drift to the p-type side and electrons to the n-type side, if they are created by absorption of light in the depletion layer or close enough to reach it by diffusion. The electrons migrate into the external circuit where they can perform work (Fig. 6B).

At present, most commercial solar cells consist of silicon. Although they exhibit quite a high efficiency, they have a number of serious drawbacks. Because of the low doping concentrations (ppm level) needed for efficient p–n junctions, extremely high-purity silicon is required. Furthermore, encapsulation to prevent oxidation in air is necessary. These factors lead to the price of solar electricity being about five times that of electricity based on fossil fuels. Other types of high-purity semiconductor solar cells with even higher efficiencies, like GaAs, are more expensive and sometimes contain hazardous and/or rare elements. These types of cells are mostly used in space applications. The highest theoretical efficiency for single crystalline silicon solar cells is 31%, due to unavoidable spectral mismatch, resistances and recombination losses. Stacks of different solar cell materials (i.e., tandem or multi-junction cells) could increase this efficiency to higher values.

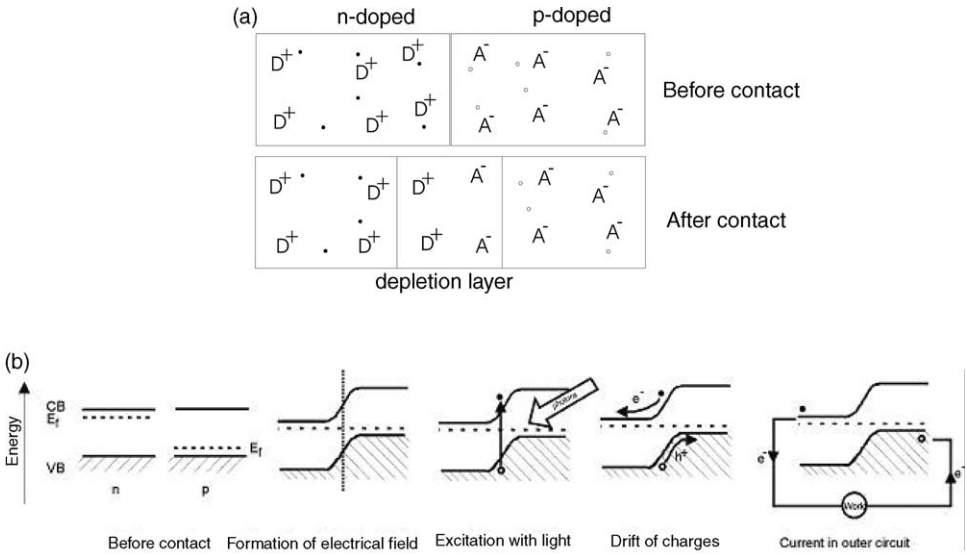

Fig. 6. (A) Formation of a depletion layer upon contact between an n- and a p-type semiconductor, doped with donors (D) and acceptors (A), respectively. (B) Working mechanism of a solar cell.

Research on Si-based solar cells is directed towards higher efficiencies, upscaling of production, and development of amorphous and thin-film devices. A different approach to realize cheap solar cells is the use of organic chromophores. In these so-called organic or hybrid solar cells, a wide band gap semiconductor, mostly an oxide like titanium dioxide or zinc oxide, is combined with a light-absorbing dye, which injects electrons into the conduction band of the metal oxide upon excitation with visible light (Fig. 7). To close the current circuit and to regenerate the oxidized dye molecule, an electron has to be provided to the system. The principle of combining a visible light-absorbing species with a wide band gap semiconductor is called ''sensitization''. Most organic dyes can be treated both as semiconductors with narrow bands and as molecular compounds. If regarded as molecular compounds, excitation takes place between the highest occupied molecular orbital (HOMO) and the lowest unoccupied molecular orbital (LUMO).

Flat film solar cells made of wide band gap (oxide) semiconductors in combination with organic compounds have a low efficiency (mostly less than 1%) [324]. This is caused by the fact that organic materials tend to have a high resistivity, which leads to ohmic losses. The organic films must be thick enough to absorb enough light, but only a very narrow region near the interface between organic dye and inorganic semiconductor is found to be active, as excitons can only move a limited distance before they recombine. If the internal electrical field does not separate them fast enough, they will be lost. The exciton diffusion length is in the order of 5–20 nm for most organic compounds [325–327].

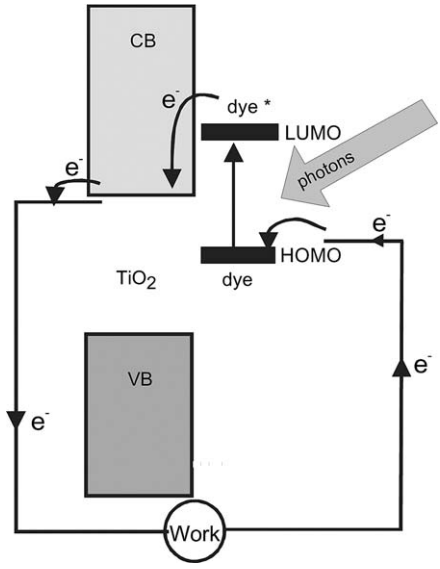

Fig. 7. Working principle of a hybrid solar cell. Photons are absorbed by the dye and an electron is excited to the LUMO level. This electron can be injected into the CB of the TiO_2. The electron can be collected and perform work in the external circuit. It is transported back to regenerate the dye and to close the circuit.

A different approach is to apply a different morphology. In 1991, O'Regan and Grätzel reported the first organic solar cell with high efficiency (8%) [32]. In this so-called Grätzel-type or dye-sensitized cell, anatase TiO_2 is used in nanocrystalline form, to which organic dye molecules (a ruthenium complex) are covalently attached with monolayer coverage (Fig. 8). The use of nanostructured TiO_2 (nc-TiO_2) overcomes the problem of high resistance, since only a monolayer of dye is used. At the same time, the increased surface area ensures enough dye absorption to absorb all the light and provides short-range contact between dye and oxide. A drawback of this device is, however, the need of a liquid electrolyte for regeneration of the oxidized dye molecules after electron injection. This leads to the risk of leakage or even explosion, which is not desirable in commercial devices. The electrolyte also suffers from degradation problems. Nowadays, a laboratory efficiency of 12% is reached [328], but commercial application of these kinds of cells is still in the initial stage.

Much effort is being directed towards the development of similar nanostructured heterojunctions that can function without a liquid electrolyte. An ion-conducting polymer [329–331] or a transparent hole-conducting material can replace the liquid [184,332]. Another possibility is to use dyes that combine both functions and not only absorb light and inject electrons, but can also transport holes [333–338]. Although organic substances exhibit, in general, much lower hole mobilities than

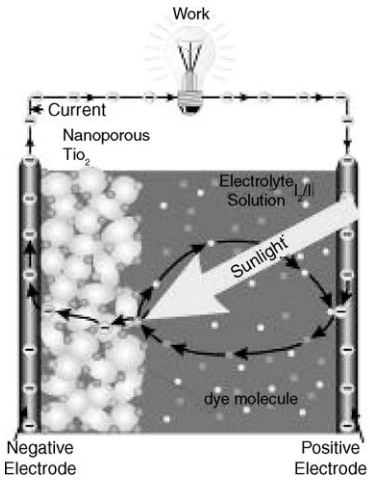

Fig. 8. Schematic principle of a dye-sensitized solar cell. The working principle is similar to Fig. 7. The liquid electrolyte (mostly an I_2/I^- redox couple in an organic solvent) reduces the photo-oxidized dye molecules back to neutral. Injection of electrons from dye to TiO_2 is extremely fast (femtosecond time scale), while recombination rates are low, thus proving that an electrical field due to a p-n junction is not needed in this case, while a depletion layer is not present in nanostructured TiO_2 particles.

inorganic compounds, semiconducting polymers have been shown to approach these high values and are suitable for utilization in these cells [339].

Some excellent review articles about TiO_2-based photovoltaic cells have appeared in recent years [315,324,340–342].

3.3. Photocatalysis

3.3.1. General remarks

Overall, photocatalyzed reactions may be summarized as follows:

$$(\mathrm{Ox}_1)_{\mathrm{ads}} + (\mathrm{Red}_2)_{\mathrm{ads}} \xrightarrow[h\nu > E_g]{\text{semiconductor}} \mathrm{Red}_1 + \mathrm{Ox}_2 \tag{3.1}$$

Depending on whether the sign of the change in Gibbs free energy (ΔG^0) of reaction (3.1) is negative or positive, the semiconductor-sensitized reaction may be an example of *photocatalysis* or *photosynthesis*, respectively [343].

For a semiconductor photocatalyst to be efficient, the different interfacial electron processes involving e^- and h^+ must compete effectively with the major deactivation processes involving e^-–h^+ recombination, which may occur in the bulk or at the surface (Fig. 9).

Ideally, a semiconductor photocatalyst should be chemically and biologically inert, photocatalytically stable, easy to produce and to use, efficiently activated by sunlight, able to efficiently catalyze reactions, cheap, and without risks for the environment or humans. Titanium dioxide (with sizes ranging from clusters to colloids to powders and large single crystals) is close to being an ideal photocatalyst,

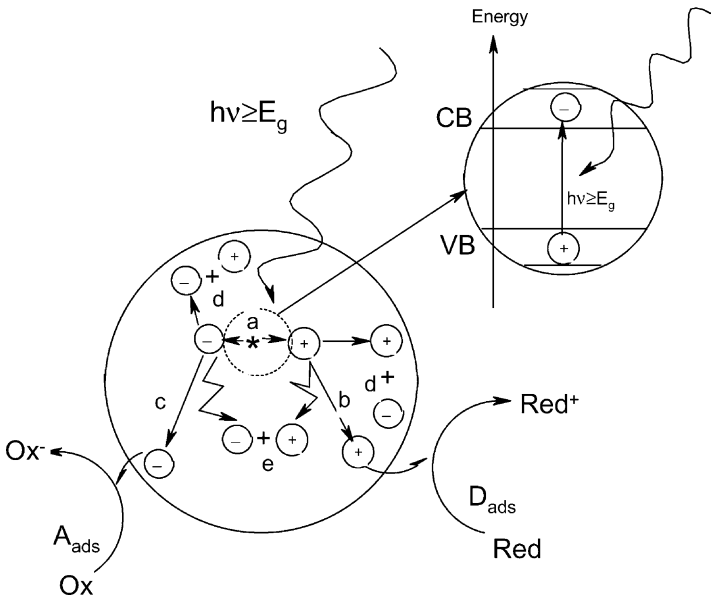

Fig. 9. Main processes occurring on a semiconductor particle: (a) electron–hole generation; (b) oxidation of donor (D); (c) reduction of acceptor (A); (d) and (e) electron–hole recombination at surface and in bulk, respectively. Picture taken from [1].

displaying almost all the above properties. The single exception is that it does not absorb visible light.

Both crystal structures, anatase and rutile, are commonly used as photocatalyst, with anatase showing a greater photocatalytic activity [130,131] for most reactions. It has been suggested that this increased photoreactivity is due to anatase's slightly higher Fermi level, lower capacity to adsorb oxygen and higher degree of hydroxylation (i.e., number of hydroxy groups on the surface) [131,344–346]. Reactions in which both crystalline phases have the same photoreactivity [347] or rutile a higher one [187,348] are also reported. Furthermore, there are also studies which claim that a mixture of anatase (70–75%) and rutile (30–25%) is more active than pure anatase [349–351]. The disagreement of the results may lie in the intervening effect of various coexisting factors, such as specific surface area, pore size distribution, crystal size, and preparation methods, or in the way the activity is expressed. The behaviour of Degussa P25 commercial TiO_2 photocatalyst, consisting of an amorphous state together with a mixture of anatase and rutile in an approximate proportion of 80/20, is for many reactions more active than both the pure crystalline phases [346,351–353]. The enhanced activity arises from the increased efficiency of the electron–hole separation due to the multiphase nature of the particles [345]. Another commercial TiO_2 photocatalyst, Sachtlebem Hombikat UV 100, consisting only of anatase, has a high photoreactivity due to fast interfacial electron-transfer rate [354]. Water splitting is a special case, because band bending is necessary in

order to oxidize water and large rutile particles (with a small surface area) are efficient [355–359].

Efforts have been made to improve the photocatalytic activity of TiO_2 (see Section 5). In this respect, the research can be divided into two categories: (i) to shift the absorption band gap edge to the red in order to enhance activity in the visible portion of the spectra; (ii) to increase the photoactivity of TiO_2 in the near UV and visible portion.

Almost every class of organic/inorganic contaminant present in wastewater and exhaust air has been examined for possible degradation using this technique. Also, the potential of photocatalytical reactions in organic synthesis has been investigated (see Section 6.1).

3.3.2. Photocatalytic synthetic processes versus partial/total photodegradation

In inert solvents or in neat organic substrates, the functional groups of organic compounds may undergo transformations (mainly oxidations), which may be used in organic synthesis if the product is obtained in appreciable quantum yield. In most photosynthesis reactions using TiO_2, ΔG^0 is negative and therefore they are actually photocatalytic reactions rather than photosynthetic reactions.

Practically, every functional group with either a non-bonded lone pair or π-conjugation may exhibit an oxidative reactivity towards TiO_2, undergoing dehydrogenation, oxygenation, or oxidative cleavage. Reductive transformation of organic compounds, which may occur under certain experimental conditions (oxygen absence, proton source [360]), is usually less efficient than the oxidative one due to two reasons. Firstly, the reducing power of a conduction band electron is significantly lower than the oxidizing power of a valence band hole. Secondly, most reducible substrates do not compete kinetically with oxygen in trapping photogenerated conduction band electrons [361]. As a direct consequence, little research has been conducted on the fundamental nature of photocatalytic reductions. However, reductive processes may be convenient for organic synthesis because they are functional group selective [361,362].

If water is used as a solvent, the selectivity of the photocatalytical process favours a partial/complete photodegradation of the organic substrate (instead of photosynthesis), due to the generation of highly oxidizing hydroxyl radicals. Any organic compound can be completely mineralized with irradiated TiO_2, except 1,3,5-triazine-2,4,6 trihydroxy (cyanuric acid), which, fortunately, is non-toxic [363,364]. The term 'photodegradation' usually refers to complete oxidative mineralization, leading the conversion of organics to water, CO_2 and NO_3^-, PO_4^{3-}, halide ions, etc. Often degradation begins with a partial oxidation. Complete oxidative destruction can be realized in inert solvents also, but the efficiency is much lower [9].

Usually, at low reactant levels or when using compounds which do not form important intermediates, complete mineralization and reactant disappearance proceed with similar half-lives, but at higher reactant levels or when important intermediates occur, mineralization is slower than the degradation of the parent compound [365]. Generally, oxygenated compounds are more easily photo-

catalyzed than hydrocarbons, and aromatic compounds more easily than aliphatic ones under the same conditions.

For aromatic compounds, it has been observed that, in general, the time required to achieve dearomatization is clearly lower than that time needed to eliminate the products from the aromatic ring breaking. Their photocatalytical activity can be affected by the nature of substituents and position in the aromatic ring. The photocatalytical activity of some compounds has been correlated to either the Hammett constant (σ) or the 1-octanol–water partition coefficient (K_{OW}). The first, which quantifies the effect of different substituents on the electronic character of a given aromatic system [366], appears to be an adequate descriptor of the photocatalytic degradability for para-substituted phenols. The second is considered to be related to the extent of adsorption of the organic compound on TiO_2. In general, photocatalytical degradation of aromatic pollutants is faster for compounds with electron-donating substituents due to the activation of the aromatic ring with respect to electrophilic attack of the $HO^{\bullet}$ radical. The hydrophobicity, reflecting the extent of adsorption on the catalyst, plays an important role. But, dearomatization is rapid even in the case of deactivating substituents on the aromatic ring [367]. After formation of various phenolic [368–370] and quinonic derivates [370], cleavage of the benzene ring takes place and different aliphatic products such as adipic, acetic, oxalic, formic, and maleic acids are subsequently formed before complete mineralization [371–378]. Hydroxyl radicals preferentially attack the aromatic moiety, but they can also attack the alkyl chain, which is converted subsequently from alkyl to aldehyde and to acid, which is subsequently decarboxlyzed via the photo-Kolbe reaction [379,380]. Such an oxidation pathway is possible even for aliphatic chains linked to nitrogen atoms [374].

The release of halogen anions into solution, from compounds like fluoroalkenes [381], fluoroaromatics [382], and chlor-containing molecules, [383,384] occurs usually faster than mineralization to CO_2. Halide release is expected to be faster for Cl than for F [385,386]. This could be interesting if photocatalysis is combined with a biological treatment (which is generally not efficient for chlorinated compounds).

Nitrogen-containing molecules are mineralized especially into NO_3^- [387], but NH_4^+ is also detected. Ammonium ions are relatively stable and the ammonium/nitrate ratio depends mainly on the initial nitrogen content and irradiation time [388]. At longer irradiation times, conversion of ammonia to nitrate [372,383,386,388,389] is observed. This is usually a sudden conversion, which is attributed to the occurrence of an autocatalytic reaction by the nitrate ions. A possible formation of hydroxylamine has also been postulated [383,389]. For compounds containing ring nitrogen, a higher nitrate concentration (compared to ammonium) is produced than for compounds with the nitrogen atom bonded to the ring or in lateral chains [388].

Sulfur-containing compounds are mineralized to sulfate [368,370,388,390,391] which is deposited on the TiO_2 surface leading to a partial inhibition of the reaction [368,386,392]. The oxidation of thio-alkyl groups is a fast process, faster than

the degradation of nitrogen-containing groups and leads to sulfate via sulfoxide derivates [365,372,393].

Organophosphorous pesticides produce phosphate ions [372,394,395], which may remain absorbed on the TiO_2 surface [396].

The photodegradation of pollutants over TiO_2 is one of the most promising heterogeneous photocatalytic applications, but it cannot be proposed as a general and trouble-free method without a detailed knowledge of the intermediates. This is necessary to assess the applicability of the method (i.e., to check whether more resistant or toxic compounds are formed during the mineralization) as well as to provide a basis for mechanistic approaches [372,397,398].

3.3.3. *Special reactions*

3.3.3.1 Solar production of hydrogen from water. Since the first article by Fujishima and Honda, many research groups have investigated the photocatalytic splitting of water into hydrogen and oxygen under the influence of light [24]. In this first article, rutile TiO_2 is used to catalyze the reaction from water to oxygen and Pt acts as a counter electrode, where hydrogen develops. Some discussion is still continuing the validation of this report regarding the necessity for a (chemical or electrical) bias [1,399]. Various other materials have been tried, but only $SrTiO_3$ showed some results, although the overall solar conversion efficiency is low (1%) [400]. The main problem is that suitable band positions combined with visible light absorption and stability (no photocorrosion) are difficult to be found in one material. A solution is found in the tandem cell [401,402] (Fig. 10) Light passes through two cells in series. A nanocrystalline thin film (of a high band gap material like Fe_2O_3 or WO_3) absorbs the blue part of the spectrum in the front cell oxidizing water to oxygen. Electrons are fed into the second photosystem, where a dye-sensitized film captures the green and red light. The combined photovoltage enables generation of hydrogen in the first cell. The second cell is in fact a dye-sensitized solar cell (Section 3.2), of which the electrons are used to produce hydrogen. This technique is not only commercially interesting for small-scale applications, but also as a non-carbon solution at industrial scales.

Current research on direct photoelectrolysis of water focuses on the introduction of dopants into TiO_2 [403]. This enables the absorption of visible light without a change in the band positions. In Fig. 11, the energy scheme of this reaction is depicted. Other groups investigate the use of sacrificial electron donors or acceptors. These sacrificial materials can, however, also be present as unwanted species and care has to be taken in interpreting data or articles. In this warning, the leakage of oxygen from outside can also cause "false positives".

3.3.3.2 Photofixation of nitrogen. Fixation of nitrogen in biological systems occurs using the enzyme nitrogenase. In industry, the Haber process is used, which requires high temperatures and pressures. An iron-based catalyst is used in this reaction:

$$N_2 + 3H_2 \xrightarrow{\text{catalyst}} 2NH_3 \tag{3.2}$$

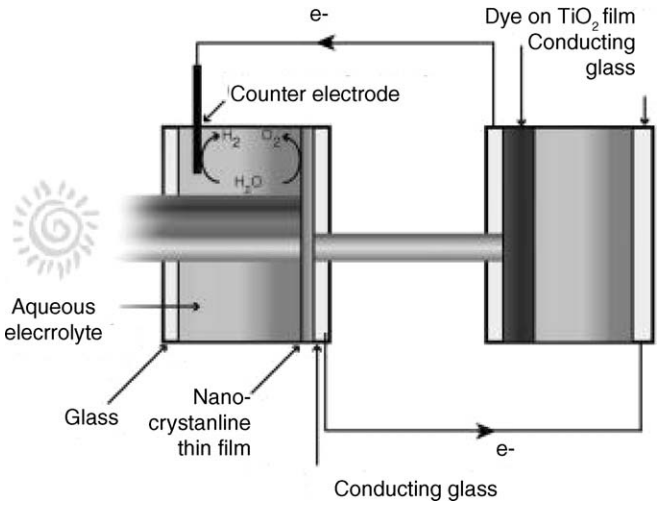

Fig. 10. Scheme of a tandem cell to split water photocatalytically. This is an indirect photoelectrolysis of water to oxygen and hydrogen.

It is important that a cleaner and energy-saving alternative for this process is developed and photocatalysis especially would be a durable option.

Ammonia and other nitrogen compounds (primarily NO_x) are claimed to be formed photocatalytically from atmospheric nitrogen and water according to:

$$2N_2 + 6H_2O \xrightarrow[E \geq E_g]{\text{photocatalyst}} 4NH_3 + 3O_2 \tag{3.3}$$

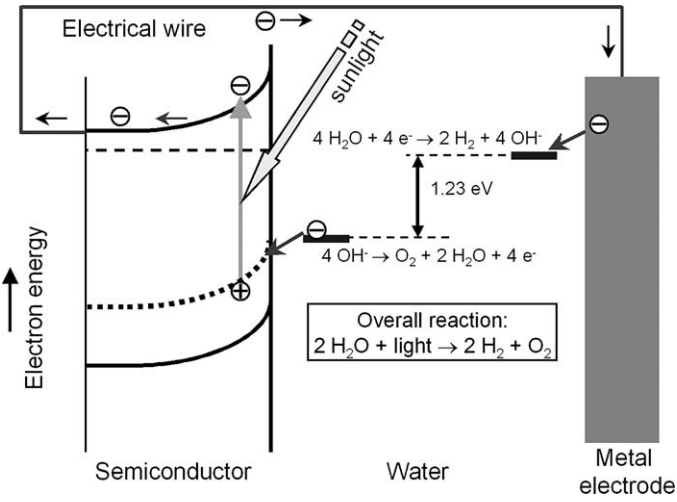

Fig. 11. Band diagram of direct photoelectrolysis of water using doped TiO_2.

The first publication about this subject was in 1941 when Dhar found that soil minerals (consisting for a large part of TiO_2) reduced nitrogen to ammonia [404–406]. This discovery was made some 30 years after predictions that organic material must be able to be formed from inorganic material photocatalytically [407]. Only in 1977, new information appeared from Schrauzer et al., who claimed to have synthesized ammonia using TiO_2 as a photocatalyst [27]. Schrauzer also performed experiments with desert sand and minerals, which also showed to be active for nitrogen reduction [408]. Many research groups have tried to repeat these measurements (successfully and unsuccessfully) and investigated new photocatalysts. However, the yields of ammonia and other nitrogenous compounds were very low and much controversy exists about the correctness of their findings. Davies et al. have tried to collect and check all results and have shown that all findings could be due to contaminations in the experiments [409]. This result is again contested by other authors. In any case, the call for isotope measurements that show an increased ^{15}N amount in the synthesized ammonia and NO_x^- compared to natural abundance references is justified and reliable; repeatable experiments should prove whether or not photofixation of nitrogen is possible.

In recent years, the group of Kisch has published articles, which show that iron titanate films are active in ethanol/water mixtures in the synthesis of ammonia and nitrates [410,411]. The group of Hoshino has found that TiO_2/polymer hybrid systems can fix nitrogen photocatalytically under standard temperatures and pressures [412–414]. For both types of compounds, no isotope measurements have been published so far and contamination by external or internal sources of nitrogen cannot be excluded.

3.3.3.3 Photoreduction of CO_2 (artificial photosynthesis). CO_2 can be catalytically reduced to organic molecules like methane, methanol and formic acid under the influence of light and in the presence of water. The overall reaction is:

$$CO_2 + H_2O \xrightarrow[E \geq E_g]{\text{photocalayst}} \text{carbon products} + O_2 \tag{3.4}$$

This is the same reaction as that taking place in natural photosynthesis, although the main product there is glucose. Reaction 3.3 has not been extensively studied [415] and until now the yield has been low and contamination or the presence of reduction sites (as a result of treatments of the photocatalyst) can lead to "false positives".

3.4. Photoinduced superhydrophilicity

UV illumination of TiO_2 may induce a patchwork of superhydrophilicity (i.e., photoinduced superhydrophilicity or PSH) across the surface that allows both water and oil to spread [33,323,416–418]. This PSH is accompanied by photocatalytic activity, as both phenomena have a common ground; so the surface contaminants will be either photomineralized or washed away by water. A possible application is self-cleaning windows.

PSH involves reduction of Ti(IV) cations to Ti(III) by electrons and simultaneous trapping of holes at lattice sites (usually bridging oxygen) or close to the surface of the semiconductor. Such trapped holes weaken the bond between the associated titanium and lattice oxygen, allowing oxygen atoms to be liberated, thus creating oxygen vacancies. The subsequent dissociative adsorption of water at the site renders it more hydroxylated. An increased amount of chemisorbed –OH leads to an increase of van der Waals forces and hydrogen bonding interactions between H_2O and –OH. Water can easily spread across the surface and hydrophilic properties will be enhanced [419,420] (Fig. 12). Water adsorption does not occur uniformly but produces an amphiphilic surface with alternating hydrophilic and oleophilic regions at the scale of several nanometers (usually <10 nm in size) [33]. The hydrophilic domains align along the bridging oxygen sites. The reduced sites can be reoxidized by air and the weakly bound hydroxyl groups reactively desorb (over some time, typically days in the dark) from the surface that returns to a more hydrophobic form.

The longer the surface is illuminated with UV light, the smaller the contact angle for water becomes (a contact angles close to zero mean that water spreads perfectly across the surface) [416,417]. The hydrophilicizing rate is also increased by repeated UV illumination cycles. This effect is remarkable on (0 0 1) rutile surfaces [421]. The crystal plane dependence can be attributed to differences in oxygen vacancy creation and to the degree of resultant structural distortion between (0 0 1) and (1 1 0) surfaces. This suggests that the hydrophilicizing process of TiO_2 surface is a kind of photocorrosion process [421].

As far as the geometry of the surface is concerned, the hydrophilic properties are known to be enhanced by fine surface roughness [419–423].

To improve the photoinduced superhydrophilic properties of TiO_2 films, doping (Al^{3+}, W^{6+}) [424], nitruration ($TiO_{2-x}N_x$) [425] and combining or mixing the TiO_2 with oxide partners or host oxides such as SiO_2 [426,427] or B_2O_3 [427] is attempted.

Ultrasonic radiation of the amphiphilic surface greatly facilitates the reconversion from amphipilic to hydrophobic surface [417].

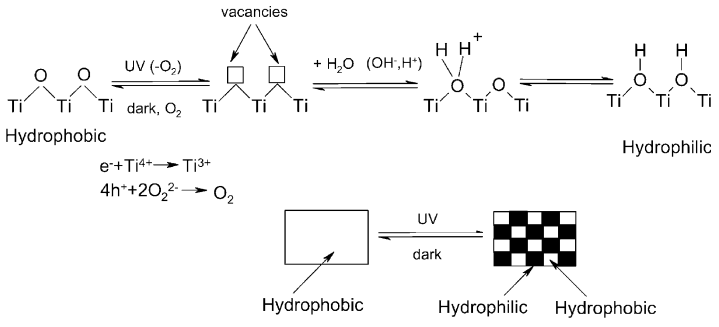

Fig. 12. Mechanism of photoinduced superhydrophilicity of TiO_2.

PSH was found to be of primary commercial importance due to the anti-fogging and self-cleaning properties of the deposits. The technology is now being increasingly used in commercial applications, particularly in Japan.

4. Mechanistical aspects

4.1. Present ideas and models

The main pathway of photomineralization (i.e., the breakdown of organic compounds) carried out in aerated solution may be easily summarized by the following reaction:

$$\text{Organic compound} \xrightarrow[h\nu \geq E_g]{TiO_2} CO_2 + H_2O + \text{mineral acid} \tag{4.1}$$

A schematic representation of this process is displayed in Fig. 13.

The radical ions formed after the interfacial charge transfer reactions can participate in several pathways in the degradation process:

– they may react chemically with themselves or surface-adsorbed compounds;
– they may recombine by back electron-transfer reactions, especially when they are

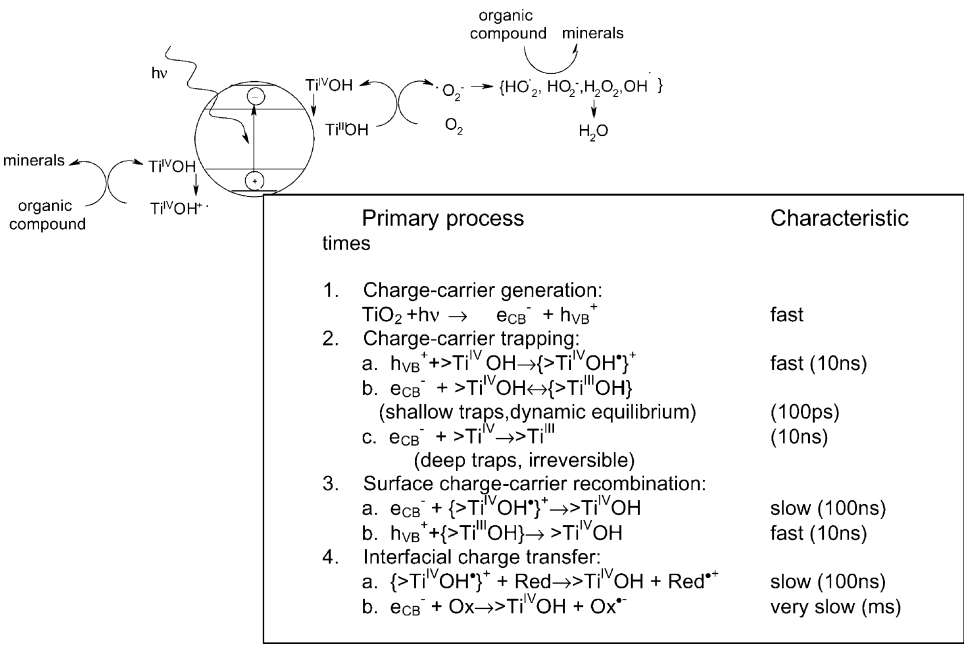

Fig. 13. Major processes and their characteristic times for TiO_2-sensitized photooxidative mineralization of organic compounds by dissolved oxygen in aqueous solutions.

trapped near the surface, due to either the slowed-down outward diffusion or hydrophobicity;
– they may diffuse from the semiconductor surface and participate in chemical reactions in the bulk solution.

The detailed mechanism of the photocatalytic process on the TiO_2 surface is still not completely clear, particularly that concerning the initial steps involved in the reaction of reactive oxygen species and organic molecules. Separate monitoring of oxidation and reduction reactions is employed for a simple macroscopic model that can be used to simulate individual particles [323,428,429] Experiments, carried out at different oxygen partial pressures, [1] yield valuable information in order to determine the photocatalytic mechanism.

A reasonable assumption is that both photocatalytic oxidative and reductive reactions occur simultaneously on the TiO_2 particle, while otherwise charge would built up. In most experiments, the electron transfer to oxygen, which acts as primary electron acceptor, is rate-determining in photocatalysis. Hydroxyl radicals are formed on the surface of TiO_2 by reaction of holes in the valence band (h^+_{vb}) with adsorbed H_2O, hydroxide, or surface titanol groups (>TiOH). The photogenerated electrons are reduce enough to produce superoxide (O_2^-). This superoxide is an effective oxygenation agent that attacks neutral substrates as well as surface-adsorbed radicals and/or radical ions. Theoretically, the redox potential of the electron–hole pair permits H_2O_2 formation, either by water oxidation (by holes) or by two conduction band electron reduction of the adsorbed oxygen. The latter represents the main pathway of H_2O_2 formation [430–432]. H_2O_2 contributes to the degradation pathway by acting as an electron acceptor or as a direct source of hydroxyl radicals due to homolytic scission. Depending upon the reaction conditions, the holes, $^{\bullet}OH$ radicals, O_2^-, H_2O_2, and O_2 can play important roles in the photocatalytical reaction mechanism. These processes are presented in Fig. 14.

If non-oxygenated products, derived from ion radicals, are desired, oxygen has to be replaced with other electron acceptors. Methyl viologen shows a lower

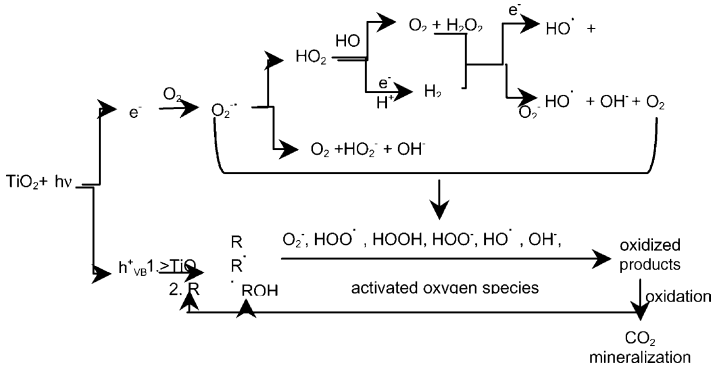

Fig. 14. Secondary reactions with activated oxygen in the mechanism of photooxidative mineralization of organic compounds. Picture taken from [442].

efficiency for electron trapping than oxygen [433], but when hydrogenase is added, the obtained turnover number is about 2–3 orders higher compared to experiments carried out in the presence of oxygen [434].

According to the above-mentioned mechanism and time characteristics, two critical processes determine the overall quantum efficiency of interfacial charge transfer:

- the competition between charge-carrier recombination and trapping (picoseconds to nanoseconds);
- the competition between trapped carrier recombination and interfacial charge transfer (microseconds to milliseconds).

An increase in either charge-carrier lifetime or the interfacial electron-transfer rate is expected to lead to higher quantum efficiency for steady state photolysis.

A first source of debate is whether VB holes can react directly with organic compounds before they are trapped, or whether oxidation occurs indirectly via surface-bound hydroxyl radicals (i.e., a trapped hole at the surface). It was suggested that the first pathway might play an important role at a high coverage of organic compounds [435]. The hydroxyl radical mediated oxidation mechanism was used to explain the degradation of substituted aromatic compounds [436–438] and chlorinated ethanes [439]. For the first class of compounds, hydroxylated structures were detected similar to those found when these aromatics are reacted with a known source of hydroxyl radicals. For the second class of compounds, the rate of oxidation was correlated with C–H bond strengths, which indicates that the abstraction of H atoms by $OH^{\bullet}$ radicals is an important factor in the rate-determining step for oxidation. In conclusion, this hydroxyl radical mediated oxidation mechanism involves two pathways: hydroxyl radical addition and hydrogen abstraction. Both reaction pathways are expected to give oxygenated products in a solution saturated with oxygen. In the absence of water or in competition with water in an aqueous solution, the substrate can undergo a direct electron transfer to the photogenerated holes to yield a radical carbon [440,441]. Then, the radical can react with water or oxygen to form oxygenated compounds. Although hole-catalyzed and hydroxyl radical mediated pathways are vastly different processes, the two give similar product distributions in oxygenated aqueous solutions, thus making the distinction between the two difficult.

Another source of debate is the localization of the degradation process. Adsorption of organic compounds on the semiconductor surface is often reported as a prerequisite for organic photodegradation. Other studies suggest that in the case of radical formation, adsorption of organic contaminants would increase the reaction rate but is not required, since the reactive $HO^{\bullet}$ radicals can diffuse into the solution to react with the organic pollutants [443,444]. Due to their high reactivity, they cannot diffuse far and the reaction has to take place close to the surface [445]. Whether a prerequisite or not, the possibility of adsorption is critical. The summation of chemical and electrostatic forces between substrate molecules and the semiconductor surface includes [442]: inner sphere ligand substitution for metal ions and conventional organic and inorganic ligands; van der Waals force;

(induced) dipole–dipole interactions; hydrogen bonding; outer sphere complexation; ion exchange; surface-matter partitions (i.e., the distribution of the adsorbed molecules on the surface); hydrophobicity of the surface and substrates; and semimicelle formation.

It is agreed upon that the expression for the rate of photomineralization of organic substrates by oxygen sensitized on TiO_2 surfaces follows (with minor variations) the Langmuir–Hinshelwood law (LH), which has been widely used in liquid- and gas-phase photocatalysis [5,446–448]. This law successfully explains the kinetics of reactions that occur between two adsorbed species, a free radical and an adsorbed substrate, or a surface bound radical and a free substrate. The initial rate of substrate removal (R_i) varies proportionally with the surface coverage (θ):

$$R_i = k(S)\theta = -\frac{[S_i]}{dt} = \frac{k(S)K(S)[S_i]}{(1 + k(S)[S_i])} \tag{4.2}$$

where $[S_i]$ is the initial concentration of the organic substrate S; t is the reaction time; $k(S)$ is the Langmuir adsorption constant of S; $K(S)$ is the adsorption equilibrium constant which is a measure of the intrinsic reactivity of the photoactive surface S.

For diluted solutions ($[S_i] < 10^{-3}$ M), $k(S)[S_i] \ll 1$ and the reaction is apparently first order, whereas for concentrations higher than 5×10^{-3} M, $k(S)[S_i] \gg 1$, and the reaction rate is maximum and zero order. In addition, some studies report half order kinetics for dehydrogenation of primary and secondary alcohols [449] and for the degradation of some pesticides, suggesting a reaction with a dissociated adsorbed state of reactants [368,450]. Several variations including light intensity, catalyst dosage, and oxygen concentration have been made in the last few years in order to improve the LH equation [451].

Due to the complex reaction mechanism, it is difficult to develop a model for the dependence of the photocatalytic degradation rate on the experimental parameters for the whole treatment time. Models have so far focussed on the initial disappearance rate of organics [452] or the initial formation rate of CO_2 [451,453]. Some additional complexity may arise from the possibility of different adsorption sites and the presence of pores, which reflect non-ideal (non-Langmuirian) adsorption isotherms and mass-transfer problems [454].

It is also interesting to note that the photocatalytic degradation rate based on the LH-kinetic model depends simultaneously on $k(S)$ and $K(S)$, therefore a higher adsorption constant does not always imply a higher reaction rate.

4.2. Operational parameters

It has been demonstrated that catalyst dosage, character and initial concentration of the target compound, coexisting compound, UV light intensity, oxygen concentration, presence of supplementary oxidizable substance, temperature, circulating flow rate, pH for aqueous treatments, and water concentration for gaseous phases photoreactions are the main parameters affecting the degradation rate. Each of the parameter will be discussed in the following sections.

4.2.1. Catalyst loading

Generally, decomposition increases with catalyst loading due to a higher surface area of the catalyst that is available for adsorption and degradation. An optimum value is present, while above a certain concentration, the solution opacity increases (due to increased light scattering of the catalyst particles) causing a reduction of light penetration in the solution and a consequent rate decrease [452,455–458]. Additionally, at high-TiO_2 concentrations, terminal reactions (such as 4.3 and 4.4) could also contribute to the diminution of photodegradation rate. The formed hydroperoxyl radical is less reactive than the $HO^\bullet$ one:

$$H^\bullet + HO^\bullet \rightarrow H_2O_2 \tag{4.3}$$

$$H_2O_2 + HO^\bullet \rightarrow H_2O + HO_2^\bullet \tag{4.4}$$

In slurry photoreactors, the optimal catalyst dosage reported lies in a wide range (from 0.15 to 8 g/l) for different photocatalyted systems and photoreactors, increasing with increasing light intensity [459–462]. The optimal catalyst dosage or effective optical penetration length, under given conditions, is very important in designing a slurry reactor for effective use of the reactor space and catalyst. If the solution layer thickness exceeds the optical penetration length at any given illumination intensity and catalyst concentration, the photoreactor will be under-utilized.

For TiO_2 immobilized systems, there is also an optimal thickness of the catalyst film. The interfacial area is proportional to the thickness of catalyst, as the film is porous. Thus, thick films favour catalytic oxidation. On the other hand, the internal mass transfer resistance for both organic species and photogenerated electrons/holes will increase with increasing thickness. This increases the recombination possibility of the electron/hole pair and, as a consequence, the degradation performance is reduced.

4.2.2. Concentration of the pollutant

The degradation rate of organic substrates usually exhibits saturation behaviour: the observed rate constant decreases with the increase of initial organic pollutant. Three factors might be responsible for this behaviour:

- the main steps in the photocatalytic process occur on the surface of the solid photocatalyst. Therefore, a high adsorption capacity is associated with reaction favouring. Because most of the reactions follow an LH equation, this means that at a high initial concentration all catalytic sites are occupied. A further increase of the concentration does not affect the actual catalyst surface concentration, and therefore, this may result in a decrease of the observed first-order rate constant.
- the generation and migration of photogenerated electron–hole pairs and their reaction with organic compounds occur in series. Therefore, each step may become rate-determining for the overall process. At low concentrations, the latter dominates the process and, therefore, the degradation rate increases linearly with concentration. However, at high concentrations, the former will become the governing step, and the degradation rate increases slowly with concentration,

and for a given illumination intensity, even a constant degradation rate may be observed as a function of concentration.
– intermediates generated during the photocatalytic process also affect the rate constant of their parent compounds. A higher initial concentration will yield a higher concentration of adsorbed intermediates, which will affect the overall rate.

4.2.3. Temperature

It is well known that the photocatalytical oxidation rate is not much affected by minor changes in temperature [10]. This (weak) dependence of the degradation rate on temperature is reflected by the low activation energy (a few kJ/mol) compared to ordinary thermal reactions. This is caused by the low thermal energy ($kT = 0.026$ eV at room temperature), that has almost no contribution to the activation energy of (the wide band gap) TiO_2. On the other hand, these activation energies are quite close to that of hydroxyl radical formation [463], suggesting that the photodegradation of these organics is governed by hydroxyl radical reactions. The effect of temperature on the rate of oxidation may be dominated by the rate of interfacial electron transfer to oxygen [464]. Alternatively, the more rapid desorption of both substrates and intermediates from the catalyst at higher temperatures is probably an additional factor, leading to a larger effective surface area for the reaction. At lower temperatures, desorption becomes the rate-limiting step of the process [367].

Changes in relative positions of the Fermi level of TiO_2 powders at temperatures between 21 and 75 °C have been reported as relatively small (0.04 eV), but still improved interfacial electron-transfer kinetics are observed when the temperature is increased [465].

4.2.4. Photon flux

There are two regimes of the photocatalytic reaction with respect to the UV-photon flux. They comprise a first-order regime for fluxes up to about 25 mW/cm^2 in laboratory experiments and a half-order regime for higher intensities, respectively. In the former regime, the electron–hole pairs are consumed more rapidly by chemical reactions than by recombination reactions, whereas in the half-order regime, the recombination rate is dominant [466–471]. The variation of reaction rate as a function of the used wavelength follows the adsorption spectrum of the catalyst with a threshold corresponding to its band energy.

4.2.5. Oxygen pressure

Oxygen was found to be essential for semiconductor photocatalytic degradation of organic compounds [472]. Dissolved molecular oxygen is strongly electrophilic and thus an increase of its content probably reduces unfavourable electron–hole recombination routes [466,473]. But higher concentrations lead to a downturn of the reaction rate, which could be attributed to the fact that the TiO_2 surface becomes highly hydroxylated to the extent of inhibiting the adsorption of pollutant at active sites [474].

The influence of the oxygen pressure (P_{O_2}) in the liquid phase is difficult to study because the reaction is polyphasic. Generally, it is assumed that O_2 adsorbs on TiO_2 from the liquid phase, where its concentration is proportional to the gas phase P_{O_2} according to Henry's law. Apart from its conventional electron scavenging function, the dissolved O_2 may play a key role in the degradation of organic compounds [475] (4.5)

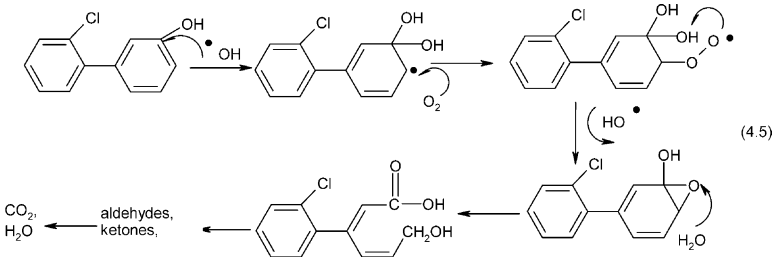

A linear dependence between $HO^{\bullet}$ formation on TiO_2 and P_{O_2} was evidenced [476] and for 2-chlorobiphenyl an increase of mineralization from 16% to 94% is found when P_{O_2} increased from 0.5 to 186 kPa [475]. The role of oxygen in the ring degradation of some hydroxyl intermediates is very important, especially while some of the hydroxyl aromatics products are potentially more toxic than their parent compounds [477].

Dissolved molecular oxygen plays a decisive role in the mechanism of the photocatalytic oxidation of 3,4-dichlorophenol [478]. When it is present, a simple hydroxyl addition to the dichlorophenol occurs. In its absence, the electron transfer from Ti^{3+} sites to the aromatic ring causes partial dechlorination of dichlorophenol. Hence, dissolved molecular oxygen has two important functions in this reaction: as a H-atom acceptor, which is required for direct hydroxyl radical addition to the phenyl ring and as an electron-transfer inhibitor when adsorbed at defective Ti^{3+} sites.

In the case of trichloroethylene, however, the presence of oxygen has less effect than that for other volatile organic carbon (VOCs) compounds, because TCE degradation predominantly occurs through a chain reaction of chlorine radicals [479]. At oxygen concentrations less than 1000 ppmv, the conversion ratio increases with increasing oxygen concentration, while for higher concentrations, the conversion ratio does not increase significantly [480].

4.3. Evaluation of photodegradation efficiency

The results of most studies are presented as percentage of degradation, degradation rate, or half-life. However, because of different experimental factors, these data are difficult to compare in terms of degradation efficiency [481–484]. For this purpose, turnover number, electrical energy per mass or per order, and quantum yields have been used. The turnover number is calculated as the ratio between the

amount of pollutants degraded and the amount of catalyst used. However, the calculation of turnover number does not consider the light energy supplied [485].

Although the photodegradation of most organic compounds does not lead instantaneously to CO_2, but forms sometimes long-living intermediates, only the reaction mechanisms of these photocatalyzed reactions have been investigated to a limited extent. Most research on degradation processes of organic molecules is generally limited either to the initial stage, by measuring the reacted substrate, or to the final stage of the overall reaction by measuring CO_2 formation. Detection and identification of intermediates is required in order to determine which chemical structure is left at the end of process. Simultaneously, toxicity tests are important during the intermediate identification. Furthermore, monitoring the evolution of CO_2 in real wastewater gives only a global estimation of the treatment result without providing information on the real decay of the contaminant. In such cases, the determination of total organic carbon (TOC) [370,374,486,487], the chemical oxygen demand (COD) [398,488], and/or the biological oxygen demand (BOD) [489] of the irradiated solution can be used for monitoring the mineralization reaction.

In an industrial environment, the efficiency of a given process is a significant component to determine its economic viability. Therefore, two figures of merit depending on the initial concentration of the pollutant are suggested [490]. When the initial concentration is high and the kinetics are zero order, the ''electrical energy per unit mass'', i.e. EE/M, is defined as the electrical energy (kW h) needed to degrade 1 kg of pollutant. When the initial concentration is low and the reaction obeys a first order kinetics, the ''electrical energy per order'', i.e. EE/O, is defined as the electrical energy needed to degrade the pollutant by an order of magnitude in 1 m^3 of contaminant water.

Although these figures of merit help to compare the efficiencies of different processes, they do not provide a direct measure of the efficiency of an adsorbed photon to induce a photoinduced process. This is provided by the overall quantum yield ($\Phi_{overall}$) (Eq. (4.6)), calculated as the ratio between the number of molecules (N_{mol}) undergoing an event (degradation of reactants or formation of reaction products) and the number of photons (N_{ph}) absorbed by the reactant(s) or photocatalyst [491]:

$$\Phi_{overall} = \frac{N_{mol}(\text{mol s}^{-1})}{N_{ph}(\text{einstein s}^{-1})} = \frac{\text{rate of reaction}}{\text{rate of absorbtion of photons}} \tag{4.6}$$

Because the rate of absorption is difficult to evaluate as a result of absorption, transmission, and scattering of the semiconductor particles a more useful term is the photonic efficiency (ξ). It is defined as the number of reactant molecules transformed or product molecules formed, divided by the number of photons incident inside the front window of the cell at a given wavelength (Eq. (4.7)):

$$\xi = \frac{N_{mol}(\text{mol s}^{-1})\ \text{transformed/produced}}{N_{ph}(\text{einstein s}^{-1})\ \text{incident inside reactor cell}} \tag{4.7}$$

For comparison of the results obtained by different experiments, standard test reactions such as phenol/Degussa/O_2 or 4-chlorphenol/Degussa/O_2 are suggested [311,451,492]. The comparison between photocatalytical rates in a standard system would provide information about the efficiency of the investigated reactions. The use of standard cells and light intensities would also be advisable. As photodegradation of water or air pollutants is developed for practical applications, the use of solar simulator lamps, as in solar cell research, is highly useful.

4.4. Photodegradation using nanosized TiO_2

As the size of a particle decreases, a gradual transition from semiconductor properties to molecular properties is expected. This quantization effect (macroparticles → colloids → nanoparticles) becomes apparent when the size of semiconductor particles becomes comparable with the Broglie wavelength of the charge carriers, which lies between 5 and 25 nm for individual semiconductors. In quantum-sized particles, the wave functions of the charge carriers spread over the whole semiconductor particle. Thus, charge carriers do not need to diffuse anymore to accomplish reactions with species present at the surface and, as a consequence, it is possible to obtain quantum yields approaching unity.

Another quantitization effect is an increase in the band gap and consequently, a blue shift in the absorption edge [9,493–495]. As a result, the redox potential of photogenerated electrons and holes will be enhanced (i.e., quantum particles will be more photoactive than larger ones), and catalytic reactions different from the photoelectrochemical reactions on bulk TiO_2 powders can occur [464]. On the other hand, the increased potential is detrimental for the near UV-photon absorption. Furthermore, it increases the electron–hole recombination rate due to the increase in electrostatic attraction between them. Also, unfavourable surface species and defects, which are associated with preparative methods [1], are also evidenced. Anchoring methods make the preparation of molecular and/or cluster-sized TiO_2 species incorporated in various supports possible [496].

5. Improving photocatalytic reactions

5.1. General remarks

TiO_2 has a photonic efficiency of less than 10% for most degradation processes. Furthermore, TiO_2 photocatalyzed reactions are non-selective oxidations. Since they are governed by a free radical mechanism, the degradation rate of a large variety of molecules is found to be approximately the same. On one hand, this lack of sensitivity may be advantageous, but a poor selectivity also implies that the catalyst does not differentiate between highly hazardous contaminants and contaminants of low toxicity. This shortcoming is further aggravated by the fact that while many low toxicity contaminants can be degraded by biological means, many of the highly hazardous materials are non-biodegradable. It may even be the case that the degradation products can be more dangerous than the parent compound.

Therefore, it is necessary to develop a photocatalyst system, which can selectively degrade pollutants and that utilizes visible and/or solar light irradiation.

To accomplish these objectives, the following directions are adopted:

- optimization of catalyst synthesis, in order to obtain catalysts with a defined crystal structure, smaller particle sizes, and the ability to use various metal dopants and support materials;
- design and development of second generation of TiO_2 catalyst, with high selectivities, which can operate effectively under visible and/or solar irradiation.

5.2. Structural and morphological aspects

The photocatalytic activity is not necessarily dependent on catalyst surface area, but rather on the availability of active sites [497]. Therefore, properties like crystalline structure, pore size, density of OH groups, surface acidity, number and nature of trap sites (both in lattice and at surface), and adsorption/desorption characteristics play an important role in photocatalytic efficiencies [311].

A *large surface area* can be the determining factor in certain photodegradation reactions, as a large amount of adsorbed organic molecules promotes the reaction rate [187,244,464,498–502]. However, powders with a large surface area are usually associated with large amounts of crystalline defects, which favour the recombination of electrons and holes leading to a poor photoactivity [131,244,503]. Recently, it has been reported that the photocatalytic activity of amorphous TiO_2 is negligible indicating that crystallinity is an important requirement [504]. Then, a balance between surface area and crystallinity must be found in order to obtain the highest photoactivity. It is worth mentioning that the photocatalyst surface can be modified in order to obtain high selectivity. A template synthesis approach, imprinting cavities of target molecules on the photocatalyst's surface, gave very good results in the selective photodegradation of 2,4-dichlorophenoxyacetic acid, when a carboxylic acid derivate of the target molecule was used [502].

Particle size is an important parameter for photocatalytic efficiency, since the predominant way of electron–hole recombination may be different depending on the particle size [503]. It is well known that in the nanometer-size range, physical and chemical properties of semiconductors are modified (compared with bulk). Small variations in particle diameters lead to great modifications in the surface/bulk ratio, thus modifying the significance of volume and surface electron–hole recombinations. Experimental investigations support the existence of an optimum particle size of TiO_2, where photocatalytic oxidation rates of organic substrates are maximized. According to some literature data [503], this value lies around 10 nm, although other authors [152,464] claim improved activity for particles below such value. As for other properties, an optimum value may be discussed only in the context of the used catalyst, organic compound and process parameters [10,504–506]. The use of structured support material, such as structured silica MCM-41 and SBA-15 can induce controlled particle growth [152].

Theoretical investigations, via mathematical models, have also concluded that particle size plays a significant role in the photoactivity of TiO_2. A model based on the mechanism of TiO_2 photocatalysis [507] predicts an increase of the quantum yield when particle sizes decrease from 1000 to 10 nm. It supposes a higher fraction of electron–hole pairs taking part in redox reactions at the surface when fewer electron–hole pairs are generated in the particle [507]. A stochastic model [508] predicts an increase in quantum yield as particle sizes increase from 3 to 21 nm, because the electron–hole recombination rates are lower for the larger particles. This is a result of two assumptions: the average initial distance between electron–hole pairs is proportional to the radius of the TiO_2 particle, and the average number of jumps before a free hole at the surface recombines with trapped electron is proportional to the square radius. Neither model [508] considers the effects of electron–hole recombination within the particle volume.

The *surface hydroxyl groups* have been recognized to play an important role in the photodegradation process due to:

- direct participation in the reaction mechanism by trapping of photogenerated holes that reach the catalyst surface producing very reactive surface $HO^{\bullet}$ [442,509,510];
- a change in the adsorption of reactant molecules both by acting itself as active sites for pollutant adsorption (toluene [495,509,510]) and by covering the sites (exposed titanium cations with unsaturated coordination) where electron trapping by adsorbed oxygen takes place [495]. This process is not only important for producing oxygen radicals but also for hindering electron–hole recombination.

A higher content of OH groups may be attained either by impregnation of the sample with water or by synthesis of nonstoichiometric TiO_x ($0 > x > 2$). A defect structure due to oxygen vacancies affects both adsorption of water on the surface and the dissociation rate of water into hydroxyl groups and protons [130,511–514]. This water dissociation process requires the presence of paired acid/basic sites that are situated at an appropriate distance [515]. Sites with acid character (low coordination titania cations) initially bind the water molecules, while the those with basic characteristics (exposed bridging oxygen) accept the proton. This co-operative effect of acid and basic sites can be obtained if the surface possesses an appropriate structural arrangement at the atomic scale.

The *surface characteristics* may be modified by several pre-treatments of the photocatalyst such as sulfation, reduction with hydrogen, and halogenation in order to enhance the photocatalytic activity.

Recently, TiO_2/SO_4^{2-} solid superacid has been used as a catalyst for a variety of organic reactions [516–518]. It shows an increased photoactivity for several substrates, such as hexane, methanol, benzene, and trichloroethylene (TCE) [347,350,519]. Sulfation of the catalyst leads to an increase of the surface acidity [520–523] and an increase of adsorption strength and therefore to an improvement of the adsorption coverage of the substrates. Also, in sulfated titania, the O═S═O

groups, anchored to the surface, coordinate water, inducing a sulfur electron species which may act as an electron trap. An improvement of the anatase thermal stability [117,175,347,524], against sintering is shown; the anatase phase is preserved up to 700 °C with relatively high surface area values with respect to non-sulfates TiO_2. Undoubtedly, at such temperatures, the SO_4^{2-} content should be negligible, while it is well known that sulfate groups are stable only up to 600 °C during calcination [525,526]. This high calcination temperature is able to eliminate the crystal defects, which could be responsible for the recombination process, and therefore lowers the efficiency. Increase of the photocatalyst life [350] is also evidenced at sulfated samples. It was reported that the active sites in sulfated Degussa were more active than those of TiO_2/SO_4^{2-} [350].

TiO_2, thermally treated with hydrogen, shows a prolonged holes' lifetime caused by a reduced number of recombination centers [527,528]. The presence of oxygen vacancies and Ti^{3+} (in the proper ratio) on the modified TiO_2 surface enhances photocatalytic reactions such as phenol [521] or sulfosalicylic acid degradation [529]. The following mechanism was proposed [529]: both oxygen vacancies and Ti^{3+} species act as hole traps, and when they combine with photogenerated holes, they become charged species. At the same time, oxygen acts as an electron trap. The trapped holes transfer to the organic substrate leading to a degradation reaction and the charged defects recover to their original state of oxygen vacancies and Ti^{3+}.

The introduction of halogen anions on the titania surface by halogenation pre-treatments has two effects. Firstly, an inhibition of the electron–hole recombination takes place, due to the fact that the halogen anions can trap photogenerated holes as they occur. Secondly, they can be converted, via photogenerated holes, into halogen radicals, which can then react with adsorbed hydrocarbon species (e.g., via hydrogen abstraction) Both processes, potentially, yield a rate enhancement [530–532]. Hydrochloric acid (HCl) pre-treated catalysts show an enhancement of the aromatic branched hydrocarbon conversion (toluene, xylene) but are ineffective (significantly lower compared to untreated catalyst) for benzene degradation. TiO_2 catalyst treated with hydrofluoric acid (HF) shows no increased activity, while a pre-treatment with hydrobromic acid (HBr) and hydriodic acid (HI) yields a significantly lower activity than untreated TiO_2. This behaviour was explained by thermodynamic calculations [531] as follows: hydroxyl radicals are capable of initiating the oxidation of branched aromatic contaminants by attacking the side groups. Benzene and other aromatic contaminants may also be attacked by hydroxyl radicals through the aromatic ring, but this reaction is not as energetically favourable. Fluorine radicals, if generated, are predicted to be reactive towards either aromatic reaction sides, but the energy requirements for their formation are not satisfied under near-UV illumination. Chloride radicals are predicted to be effective in oxidizing aromatic side groups, but ineffective in reaction with the aromatic ring. Bromide and iodide radicals are ineffective in oxidizing either aromatic rings or methyl side groups. It is important to mention that a depletion of the chloride leads to a decline of the effectiveness of the treatment over time, so a periodic regeneration is necessary. The photoactivity of TiO_2 and miner-

alization of TCE have been found to correlate with the concentration of HCl employed for perchlorination of TiO_2 [532].

5.3. Doping

Doping the semiconductor with various transition metal ions may lead, to an enhanced efficiency of the photocatalytic systems [533–539]. The photophysical mechanism of doped semiconductors is not always understood. Among others, unsolved problems relate to the surface structure and to the contribution of the charge carriers. Some details of these mechanisms are determined for vanadium-doped TiO_2 in the case of chlorinated hydrocarbon degradations [534]. This method of improving photocatalytic activity is mainly used in aqueous media.

TiO_2 particles can be simply substitutionally or interstially doped with different cations, can form mixed oxides or a mixture of oxides. The dominant parameters include the character and concentration of dopants and the applied thermal treatment [540,541].

The effect of metal ion dopants on the photocatalytic activity is a complex problem. The total induced alteration of the photocatalytic activity is made up from the sum of changes which occur in:

- the light-absorption capability of the TiO_2 photocatalyst;
- adsorption capacity of the substrate molecules at the catalyst's surface;
- interfacial charge transfer rate.

Many controversial results are reported in literature since even the method of doping leads to different morphological and crystalline properties of the photocatalyst. Impregnation, coprecipitation, and sol–gel methods are used to introduce dopants.

For optimal electron/hole separation in semiconductors, the magnitude of the potential drop across the space-charge layer should not fall below 0.2 V [542,543]. The dopant content therefore directly influences the rate of e^-/h^+ recombination, which is reflected in [10]:

$$W = (2\varepsilon\varepsilon_0 V_s/eN_d) \tag{5.1}$$

where W is the thickness of the space-charge layer, ε is the static dielectric constant of the semiconductor, ε_0 is the static dielectric constant in vacuum, V_s is the surface potential, N_d is the number of dopant donor atoms, and e is the electron charge. When W approximates the penetration depth of the light into the solid ($l = 1/a$, where a is the light absorption coefficient at a given wavelength), all the absorbed photons generate e^-/h^+ pairs that are efficiently separated. As the concentration of the dopant increases, the space-charge region becomes narrower; the electron–hole pairs within the region are efficiently separated by the large electric field before recombination. On the other hand, when the concentration of doping is high, the space-charge region becomes very narrow and the penetration depth of light into TiO_2 greatly exceeds the space-charge layer. The recombination of photogenerated electron–hole pairs in the semiconductor therefore increases, because there is no

driving force to separate them. Consequently, there is an optimum concentration of dopant ions [227,544] to make the thickness of space charge layer substantially equal to the light penetration depth. For small colloidal particles, however, there is nearly no band-bending and the electrical field is usually small; so high dopant levels are needed to produce significant potential difference (permanent electric field) between the surface and the center of particles to separate photoinduced electron–hole pair efficiently [545].

Due to the fact that doping ions act as trapping sites, they can influence the *lifetime of charge carriers*. Usually, they enhance the recombination of photogenerated electrons and holes, and therefore do not allow reactions to proceed with any noticeable effect under either under ultraviolet or visible light [226,546–548]. p-Type doping is obtained by dissolving heterocations of valencies lower than that of Ti^{4+} (Al^{3+}, Cr^{3+}, Ga^{3+}, Ln^{3+}) in the TiO_2 lattice, while n-type doping is obtained by heterocations of valencies higher than +4 (Nb^{5+}, Ta^{5+}, Sb^{5+}). The inhibition effect is ascribed to an increase in the electron–hole recombination rate [547,549]. More precisely, p-type dopants act as acceptor centers, which trap photoelectrons and, once negatively charged, attract holes, thus forming recombination centers [229,550]. On the opposite, n-type dopants act as donor centers. By increasing the concentration of conduction electrons, they also favour the electron–hole recombination, which is detrimental for the photoefficiency [229].

Fe^{3+}, Ru^{3+}, Os^{3+}, and Gd^{3+} represent a special position between the metallic dopants. These four metal ions have a half-filled electronic configuration (d^5 and f^7) that is known to be more stable. When these metallic ions trap electrons, the half-filled electronic configuration is destroyed and their stability decreases. The trapped electrons can easily be transferred to oxygen adsorbed on the surface of the catalyst and the metallic ions return to the original stable half-filled electron structure. This might promote charge transfer and efficient separation of the electrons and holes by shallow trapped electrons. The prerequisite for an effective dopant involves the possibility of charge detrapping and migration to the surface.

Codoping may represent a viable way to improve the charge separation. Monocrystalline TiO_2 codoped with Eu^{3+} and Fe^{3+} in an optimal concentration (1 at% Fe^{3+} and 0.5 at% Eu^{3+}) shows a co-operative (synergetic) effect, which significantly increases the photocatalytic degradation of chloroform in solution (five times compared to pure nanocrystalline TiO_2 and about two to six times compared to Fe^{3+} or Er^{3+} doped separately, respectively). Fe^{3+} serves as a hole trap and Eu^{3+} as an electron trap, speeding up the anodic and the cathodic processes, respectively, via improved interfacial charge transfer [213].

The main objective of doping is to induce a *batho-chromic shift* (i.e., a decrease of the band gap or introduction of intra-band gap states, which results in more visible light absorption). Several papers deal with this subject, and titania is doped with different metal ions like: alkaline earth (Ca^{2+}, Sr^{2+} and Ba^{2+}) [137], Fe^{3+} [171,551,552], Cr^{6+} [221,536], Co^{3+} [221], Mo^{5+} [536,553], and rare earth ions (La^{3+}, Ce^{3+}, Er^{3+}, Pr^{3+}, Gd^{3+}, Nd^{3+}, Sm^{3+}) [554] using different preparation techniques. Substitution of Ti^{4+} by d^n metallic ions in the TiO_2 lattice creates allowed energy states in the band gap of TiO_2, which may induce photoactive transitions in

the visible light, due to an excitation of an electron from this energy level into the TiO_2 conduction band [555].

The shift of the absorption edge in metal-ion doped systems may have a complex origin. It may be due to homogeneous substitution of Ti^{4+} or to segregated M_xO_y clusters [552,554,556]. Generally, if the absorbance shifts depend on the concentration of the dopant, it may be attributed to metal ion incorporation (until a critical limit that depends on the solubility of the dopant in TiO_2 is reached). If the shift depends on the annealing temperature, it may be attributed to the formation of metal clusters. While the origin of the shift may not be of crucial importance with respect to the optical applications of these systems (e.g., optical filters), it can be crucial for their photocatalytic activity. In fact, many reports about metal doping of TiO_2 (bulk and thin films) do not take these two different causes for the shift of the absorption edge into account. This may be misleading when trying to interpret photoactivity data of M^{n+}/TiO_2 systems [557,558].

Since surface sites can also be occupied by metal ion dopants, the surface properties as well as the point zero charge (PZC) value may be altered by doping. These changes depend both on the type and amount of the dopant metal. Consequently, a modification of adsorption properties takes place. Lanthanide ions are known for their ability to form complexes with various Lewis bases (e.g., acids, amines, aldehydes, alcohols, thiols, etc.) through interaction of these functional groups with the f-orbitals of the lanthanides [153,559,560] (Fig. 15). La^{3+}, Ce^{3+}, Er^{3+}, Pr^{3+}, Gd^{3+}, Nd^{3+}, and Sm^{3+}, doped TiO_2 photocatalyst present an improved NO_2 adsorption [554]. An enhancement of saturated adsorption capacity and adsorption equilibrium constants (compared to bare TiO_2) for 2-mercaptobenzothiazole [229] (La^{3+} doped) and a mixture salicylic acid, *t*-cinnamic and *p*-chlorophenoxy acids (Eu^{3+}, Pr^{3+}, Yb^{3+} doped) [153,560] is reported. At the same time, doping with lanthanide ions (including La^{3+}, Eu^{3+}, Pr^{3+}, Nd^{3+}, and Sm^{3+}) could improve the photoelectrochemical properties and increase the photocurrent response and the incident monochromatic photon current conversion efficiency in the range 300–400 nm [561,562]. The degradation of rhodamine B is enhanced by doping with Mo^{5+}, due to strong electrostatic interactions with the electron-rich centers of the dye, leading to a higher adsorption and higher photoactivity compared to undoped or Cr^{3+} doped TiO_2 [536].

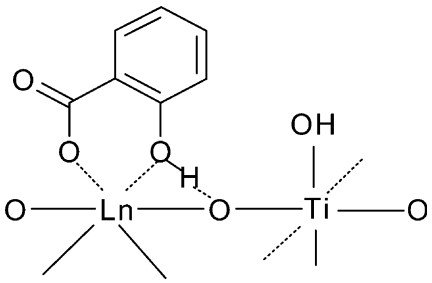

Fig. 15. Surface complex formed between salicylic acid and Ln_2O_3/TiO_2 [153].

In the following sections, special attention will be paid to iron-doped TiO_2 for several reasons:

1. iron cations have a large influence on the charge-carrier recombination time;
2. iron's presence induces a batho-chromic effect;
3. the use of iron-doped photocatalyst is efficient in several important photocatalytical reduction and oxidation reactions.

TiO_2 particles can be substitutionally doped by iron, form mixed oxides or mixtures of simple and mixed oxides. Iron cations occupy substitutional positions [135,563,564] because of the similar radius of Fe^{3+} and Ti^{4+} and form solid solutions with titania at low concentrations (<1 at Fe%). The presence of iron catalyzes the anatase → rutile transformation [565,566], with rutile being detected even at 400 °C [567]. The formation of solid solutions and the existence of solubility limits for Fe ions in TiO_2 lead to formation of α-Fe_2O_3 at higher concentrations. As a function of the applied thermal treatment and iron content, various Fe–Ti mixed oxides can be formed, like Fe_2TiO_5 (pseudobrookite), $Fe_2Ti_3O_9$ (pseudorutile), and $Fe_2Ti_2O_7$.

Substitutional doping of colloidal TiO_2 with Fe^{3+} has a controversial influence on the charge-carrier recombination. Some studies suggest that Fe(III) behaves as an electron/hole recombination center [548,568]. Others indicate that doping with 0.5 at% Fe^{3+} drastically increases the charge-carrier lifetime, which can be extended to minutes and even hours [569–572] (in intrinsic TiO_2, the mean lifetime of an electron–hole pair is about 30 ns).

An enhancement of the intrinsic adsorption edge of TiO_2 from 380 nm to higher wavelengths and a higher absorbance in the range 400–650 nm compared to bare titania (both dependent on the iron content) is evidenced [246,535,573,574]. Additionally, it is shown that iron ions decrease the crystallization rate of TiO_2, leading to small particles [171,230] and also enhance the catalyst's hydrophilic character [171].

Some of the reactions in which Fe-doped TiO_2 photocatalysts are used with good results are the following:

– photoreduction of nitrogen to ammonia. Although anatase and rutile [575] are thermodynamically able to reduce N_2 to NH_3, bare TiO_2 is inactive for kinetic reasons. Catalysts loaded up to 1 at% Fe, forming solid solutions, are active irrespective of the TiO_2 phase (anatase or rutile). Higher iron contents lead to islands of Fe_2O_3, Fe_2TiO_5, or both, and the catalysts are usually less active [535,569,576]. Recently, it was reported that a catalyst containing 50 at% Fe, in the presence of ethanol or humic acids and traces of oxygen, is active in denitrogen fixation to ammonia and nitrate [410]. Such behaviour is attributed to the existence of the $Fe_2Ti_2O_7$ phase. Hidrazine was found as intermediate (see also Section 3.3.3);
– water splitting in the absence of N_2 [27] occurs with higher yields on Fe–TiO_2 catalyst compared to bare TiO_2;

- photooxidation of neat toluene [577] in the presence of O_2, with a selectivity towards benzaldehyde was obtained on a 0.5 wt Fe % impregnated catalyst;
- oxidation of oligocarboxylic acids [534,578]. A mechanism via a [Fe–carboxylic acid]$^{n+}$ complex is proposed. Complexes formed by iron interaction with formic and maleic acids are more photoactive than those formed with acetic or acrylic acids. The slower degradation of these last two acids could be related to a photo-Kolbe reaction or other reduction processes [535]. Impregnation of TiO_2 Degussa with iron nitrate is found to be effective for oxalic and EDTA degradation but less active for malonic acid oxidation [535];
- by oxidation of 4-nitrophenol [541] in water suspension, the reaction rate decreases at higher Fe loadings;
- by oxidation of *o*-cresols [579], the reaction rate decreases with increasing iron content and calcination temperature due to $FeTiO_5$ formation;
- oxidation of 2,4-dichlorophenoxyacetic acid [580] (a herbicide);
- 2.5 at% Fe-doped TiO_2 colloids (5 nm) show high yields for dichloroacetic acid photodegradation in comparison with undoped TiO_2 colloids. The 50 at% Fe catalyst shows photoactivity under visible light irradiation (436 nm) [581].

Magnetic TiO_2 photocatalysts present enhanced separation properties from slurry photoreactors when an external field is applied. These photocatalysts are obtained by coating a Fe_3O_4 or γ-Fe_2O_3 magnetic core with TiO_2 [582–584]. A direct deposition of TiO_2 onto the surface of magnetic oxide particles leads to photocatalysts with high levels of iron oxide phase photodissolution (i.e., dissolution under influence of illumination). The TiO_2 layer probably induces this photodissolution as a result of electronic interactions at the phase junctions [582]. A SiO_2 intermediate passivation layer inhibits the direct electrical contact and hence prevents the photodissolution of the iron oxide phase [583].

More efficient use of solar light (up to 20–30%) is realized with iron-implanted TiO_2 systems, in which the electronic state of the TiO_2 catalysts is modified due to the strong and long distance interactions (but without changes in the chemical properties of the surfaces) [556,585]. Such photocatalysts initiate photocatalytic reactions effectively not only with UV but also with visible light irradiation (>500 nm). The extent of the red shift depends on the amount and type of metal ions implanted, following the sequence: V > Cr > Mn > Fe > Ni [221,586–590]. As a result, under outdoor solar irradiation at ordinary temperatures, a photocatalytic activity several times higher than the original TiO_2 catalyst is registered for V ion implanted TiO_2 for hydrogenation of $CH_3C{\equiv}CH$ (methylacetylene) with H_2O, and for NO decomposition into N_2; O_2 and N_2O using Cr and V-implanted TiO_2 in [556,591].

One new approach to induce visible light activated TiO_2 photocatalysis is by substituting oxygen with anions (N^{3+}, C^{4+}, S^{4+}, X^- (F^-, Cl^-, Br^-)) which leads to a band gap narrowing. Films and powders of $TiO_{2-x}N_x$ have an improvement over bare TiO_2 under visible light (wavelength <500 nm) [425,592–594] in optical absorption and photocatalytical activity either in solution (such as methylene blue)

or gaseous phase (such as acetone). Therefore, many techniques have been used to produce visible light active $TiO_{2-x}N_x$ photocatalyst such as precipitation [595,596], sol gel [597], dip-coating [598], ion implantation [599], NH_3 annealing [600], plasma treatment [601], pulsed laser deposition [594], and mechanochemical reaction [602]. La^{3+} codoping prevents the aggregation of powder in the process of nitrification [603]. Fluorine doping causes red shifts in the absorption edge and the photocatalyst shows higher activity on photocatalytical oxidation of acetone under UV light [604,605]. Bromide and chlorine codoped nano-TiO_2 cause a shift of the adsorption edge from 410 to 425 nm [606]. Codoping of N and F in TiO_2 to $TiO_{x-}N_yF_z$ leads to a band gap absorption edge of 570 nm and is shown to be effective for water oxidation [607]. Chemically modified carbon-substituted TiO_2 ($TiO_{2-2x}C_x$) absorbs light at wavelengths below 600 nm [255,608]. With this photocatalyst higher photocurrent densities and photoconversion efficiencies are obtained [608]. Strong absorption of visible light [609] and high activities for degradation of 2-propanol in aqueous solution and partial oxidation of adamantane in acetonitrile are obtained with a S^{4+}-doped catalyst [610]. Ti-based oxysulfide $Sm_2Ti_2S_2O_5$ is found as a visible light-driven photocatalyst for water splitting [611].

5.4. Metal coating

If the work function of the metal is higher than that of titania, electrons are removed from the TiO_2 particles in the vicinity of each metal particle. This results in formation of a Schottky barrier (Pt produces the highest Schottky barrier [612]) at each metal–semiconductor region, which leads to a decrease in electron–hole recombination, as well as to an efficient charge separation [130,613]. As a consequence of the improved separation of electrons and holes, metal deposition on the TiO_2 surface enhances photocatalytic reactions by accelerating the transfer of electrons to dissolved oxygen molecules. Therefore, deposition of group VIII metals, oxygen reduction catalysts, or noble metals on the photocatalayst surface, should increase the electron-transfer rate to oxygen and thereby the quantum yield [345]. Time-resolved spectroscopic studies clearly indicate the important role played by Pt particles in the dynamic of such photogenerated charge carriers [614].

There is an optimum loading value above which metal deposition has a detrimental effect on the photocatalytic activity. The existence of this optimum loading value may have different reasons. For metal loadings above optimum values, a decrease in electron density occurs, due to electron attraction by numerous metal particles. The resulting complicated field configuration has a detrimental effect on the charge separation, lowering the photocatalytical activity of the catalyst [615]. Also, excessive coverage of TiO_2 catalyst limits the amount of light reaching the surface, reducing the number of photogenerated hole–electron and lowering consequently the photodegradation rate [616]. Lastly, once negatively charged, metal particles, especially for highly loaded samples (%M>5% at), attract holes and subsequently recombine them with electrons [549]. In this case, the metal deposits become recombination centers.

Metals have been immobilized on TiO_2 particles, by sol–gel methods [617,618], mechanical mixing [612,619], chemical deposition [620], precipitation–reduction [612] and photodeposition [7,619,621]. Although the differences in metallizing method may cause differences in photoactivity, this matter is not clear.

Photodeposition is the most commonly used technique in obtaining metals deposits on TiO_2 and involves the reduction of metal ions by conduction band electrons, while the anodic process is represented by the oxidation of water by valence band holes. Oxidizable additives such as acetate, formaldehyde, and methanol are added to improve the rate of photodeposition.

The deposition of metals can be either beneficial or detrimental for photocatalytical degradation in aqueous solutions, depending on the chemical nature of the pollutant [620,622]. For example, the addition of Pd, Pt and Ag reduces the efficiency for degradation of chlorinated hydrocarbons, but leads to an increment of alcohol photodegradation both in aerated and deaerated systems [462,620,623]. In the latter system, the transfer of electrons from TiO_2 to an adsorbed proton is accelerated and the desorption of hydrogen is promoted. In the aerated system, for thermodynamic reasons, oxygen is reduced before protons are reduced, and the deposited metal accelerates the oxygen reduction in the cathodic area. Consequently, on the native TiO_2 surface, the rate-controlling step of photocatalyzed oxidation of alcohols is the cathodic reduction of oxygen or protons, and on Pt/TiO_2 catalyst, the rate-controlling step changes to the anodic oxidation [620]. Pt-loaded TiO_2 is active in the photodecomposition of benzene [624], trichloroethylene [625], phenol [626], methanol [627], ethanol [628–630], *tert*-butyl-alcohol [631], acetone [447], methyl-butyl-ether [631], acetaldehyde [632], EDTA [633], ethyl acetate [634], ozone [635], and azodyes [636]. Different intermediates are obtained in the photocatalytic hydrogenation of alkenes and alkynes in the presence of water when Pt/TiO_2 or TiO_2 is used. The Pt-loaded TiO_2 photocatalyst is found to mainly catalyze hydrogenation without carbon–carbon fission, while unloaded TiO_2 mainly catalyzes hydrogenolysis, leading to smaller hydrocarbons. The next step of the reaction is the formation of oxygen-containing compounds [496]. Ag-loaded TiO_2 improves the photodegradation of phenol [637], 4-chlorophenol [638], and some azodyes [639] and $Au–TiO_2$ promotes 4-chlorophenol decomposition [640]. Pd, Cu, Pt coated photocatalysts (Pd/TiO_2, $Pd–Cu/TiO_2$, Cu/TiO_2, $Pd–Cu–Pt/TiO_2$) show a higher activity in the photodecomposition of 2,4 dinitrophenol, trichloroethylene, and especially formaldehyde (up to five times) [620] in aqueous solutions. The surface morphologies are quite different from bare TiO_2, each metal possessing its own coating pattern [620].

Sometimes the enhanced activity may be detrimental from an environmental point of view. The electron mediation from TiO_2 via Ag deposits (photo) reduces Se^{6+} (derived from SeO_4^{2-}) to Se and toxic H_2Se gas (via Se self-reduction) [641].

It is important to mention here that the oxidation of volatile organic compounds (VOCs) over a Pt/TiO_2 catalyst may not be entirely a photoinduced process, because, depending on the experimental conditions, the noble metal can also catalyze the thermal combustion of the pollutants [447,628]. As a consequence, a moderate increase in the operation temperature enhances the performance of these

systems, and the mineralization of different organic molecules can be fully accomplished [447,624,628].

5.5. Surface sensitization

Surface sensitization of a wide-band gap semiconductor like TiO_2 by electron transfer via chemisorbed or physisorbed dyes/metal complexes can:

- increase the efficiency of the excitation processes;
- expand the used wavelength range through excitation of the sensitizer followed by an electron transfer between the excited dye and the semiconductor conduction band. Depending on its redox environment, the dye is able to donate (in most cases) or receive an electron improving electron–hole separation [642–649].

Dyes and metal complexes that are used as sensitizers include erythrosin B [650], thionine [651], substituted and unsubstituted bipyridine [32,652,653] and phthalocyanine [654–659]. If the oxidative energy level of the excited dye/complex compound is favourable (i.e., more negative) with respect to the conduction band level of semiconductor, the dye molecule can transfer the electron to the conduction band of the semiconductor. A prerequisite for this electron transfer is a low quantum yield of the redox process catalyzed by the dye/complex molecule [660]. The injected electron reacts with surface adsorbed O_2 to yield $O_2^{\bullet-}$(reactions 5.2–5.4), which produces $HO_2^{\bullet}$ on protonation leading to the reduction of the organic molecule (in the presence of a redox couple) or of dye itself (in the absence of a redox couple). In addition to the electron acceptance, oxygen can combine with the organic radical forming an organoperoxy radical [661]. The superoxide radical, a relatively ineffective oxidizing agent by itself, can react with the organoperoxy radicals to form unstable tetroxide that decomposes easily with CO_2 evolving in the early reaction steps [648].

$$\text{Dye} + h\nu \rightarrow \text{Dye}^* \tag{5.2}$$

$$\text{Dye}^* + TiO_2 \rightarrow \text{Dye}^{\bullet+} + TiO_2(e-) \tag{5.3}$$

$$TiO_2(e-) + O_2 \rightarrow TiO_2 + O_2^{\bullet-} \tag{5.4}$$

A novel version of sensitization by electron transfer is obtained by modifying TiO_2 with transition metal salts (Pt^{+4}, Rh^{3+} and Au^{3+} chloride), either in the bulk or at the surface, leading to photocatalysts that are active in 4-chlorophenol degradation with visible light ($\lambda \geq 455$ nm) [662–665]. The excited complex first undergoes a homolytic metal–chloride bond cleavage to yield the metal in a reduced oxidation state and an adsorbed chlorine atom. Subsequent electron transfer from the former to titania and from 4-chlorophenol to the chlorine atom reforms the sensitizer.

5.6. Composite semiconductors

The coupling of two semiconductors, possessing different energy levels for their corresponding conduction and valence bands, provides an approach to achieve a

more efficient *charge separation*, an increased *lifetime* of the charge carriers and an enhanced *interfacial charge transfer* to adsorbed substrates. Two different cases can be distinguished: first only one semiconductor is illuminated and the second is non-activated (Fig. 16a), or both are illuminated (Fig. 16b).

In the first case, a photoelectron generated on the activated semiconductor with a more negative conduction band is injected into the conduction band of the inactivated semiconductor, while the photohole remains on the activated one [130,674,666,667]. This interparticle electron transfer therefore yields vectorial electron transfer, which is irreversible under certain conditions. When both semiconductor are illuminated, a vectorial transfer of electrons and holes from one semiconductor to another occurs: electrons are accumulate at the lower lying conduction band of one semiconductor, while the holes accumulate at the valence band of the other semiconductor [666,668–671]. A proper placement of the individual semiconductors [672] (e.g., convenient energy levels of the coupled photocatalyst) and optimal thickness [672,673] of the covering semiconductor are crucial for efficient charge separation. Undoubtedly, the geometry of particles, surface texture, and particle size also plays a significant role in the interparticle electron transfer [674].

A combination of CdS/TiO_2 leads to an enhancement of the disappearance of 2-chlorophenol and pentachlorophenol by a factor greater than two, consistent with the notion that irradiated CdS electrons are vectorially displaced towards

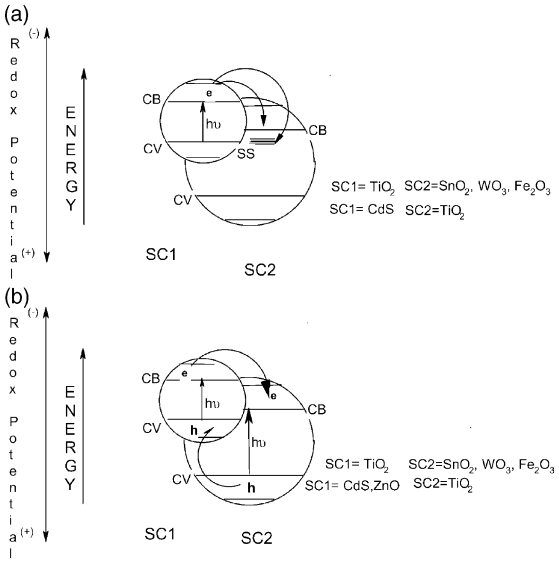

Fig. 16. Energy diagram illustrating the coupling of various semiconductors. SS stands for solid solution [674]. (a) Vectorial electron transfer from the light activated SC to the non-activated SC, (b) both SCs activated and vectorial displacement of electrons and holes.

non-illuminated TiO_2 particles [674]. But from a practical point of view, utilization of CdS alone or in coupled systems is not desirable, as significant quantities of toxic cadmium are released into the aqueous media from the photoanodic corrosion of CdS-based systems.

The photocatalytic properties of coupled systems remain largely unexplored although some TiO_2 composites with CdS [674] CdSe, WO_3 [675–681], Fe_2O_3 [579,682–684], ZnO [684,685] and SnO_2 [478,558,672,686–691] are studied.

5.7. Supports

Different supports and immobilization techniques have been investigated for TiO_2 photocatalysis. A common procedure consists of the fixation of previously prepared titania powder using various techniques such as: silane coupling [692], immobilization in a polymer matrix [693], electrophoretic deposition on conducting glass [694–696], stainless steel [696,697], titanium foil, or tin coated glass [697], and spray coating [697,698]. Another route is the coating of the support by in situ catalyst generation, as a result of a combined physical and chemical transformation like sol–gel synthesis [699–702] and chemical vapourization from $TiCl_4$ [692,703,704]. However, in spite of so many efforts, it is still unclear which methods and supports are most convenient in terms of mechanical stability and photochemical reactivity.

As support materials, glass beads [705], fiber glass [706–708], glass pellets [709,710], glass sheets [711], silica [179,712–717], organo-clays [718–720], stainless steel [721], TiO_2 (rutile) [722], Al_2O_3 fiber textile [723], γ-Al_2O_3 [708], quartz beads [724,725], honeycomb [726], polyethene and polypropylene films [727], fabrics (cotton and polyester) [728,729], paper [730] activated carbon [396,731,732], and zeolites [733–737] are used.

Often, the fixation of TiO_2 on solid supports reduces its photocatalytic efficiency [738,739]. This decline in activity has been correlated with:

- reduction of active surface [715,740];
- mass-transfer limitations [466,741,742];
- presence of foreign cationic impurities (Si^{4+}, Na^+, Cr^{3+}, Fe^{3+}) in a deposit layer (as a consequence of the thermal treatments necessary to improve TiO_2-support adhesion), which increase the e^-/h^+ recombination rate [376,706,726].

The strategies focussed on supported TiO_2 are developed in order to:

(a) immobilize the TiO_2 photocatalyst;
(b) increase the illuminated specific catalyst area;
(c) increase the adsorption capacity and surface area of the photocatalyst;
(d) influence the selectivity of the photocatalytical reaction.

The first demand originates from the requirement to use photocatalysts in continuous processes where the utilization of TiO_2 powder is technologically impracti-

cable. Unfortunately, a small particle size leads to high filtration costs of catalyst removal, hindering its industrial application. For this reason, the synthesis of photocatalysts with high activity and effective separation properties simultaneously is a priority topic.

A photocatalyst surface is active only if it is illuminated. It is difficult to illuminate all the catalyst particles in suspended systems, because the particles further away from the light sources are shielded from radiation by those near the light source. Hence, the penetration depth of light into suspensions is limited. In immobilized systems, it is possible to obtain a configuration in which all catalyst particles are illuminated, e.g., a thin layer coated on a tube surrounding a tube light [742].

Several attempts have been made to obtain hybrid photocatalysts, which are expected to induce synergism because of the *adsorption* properties of organic molecules. Adsorbents such as silica [712,743–745], alumina [744], zeolites [746–748], mesoporous molecular sieves, clays [749–751] (TiO_2 incorporated into the interlayer space of the clays), and active carbon [746,752,753] are used. Adsorption of contaminants in the vicinity of the photocatalytic sites promotes the photodegradation of contaminants that normally do not or in low quantities adsorb on the photocatalyst surface. The basic concept is based on the physisorption of reactants on inert substrates followed by their surface diffusion to the interface between the adsorptive sites and photocatalytic sites. The first step is achieved by using supports with large surface areas for adsorption and high adsorption capacity for the target substances, while the second is achieved only if the adsorption strength is moderate enough to allow diffusion of adsorbed substrates to the loaded TiO_2 [746,754,755]. The net effects may be summarized as follows:

- an enhanced concentration of substrate compounds is progressively built up around the TiO_2 sites, leading to a significant increase of the reaction rate [746,756];
- advanced degradation of the pollutant, succeeding their mineralization even in the case where this was not achieved with bare TiO_2 [746], was due to the fact the reaction intermediates are also adsorbed and then further oxidized. So, toxic intermediates, if formed, are not released in air or in solution, thereby preventing secondary pollution by intermediates if any;
- possibility of photodestruction of low levels of pollutants (either in water decontamination [746] or for indoor applications [757]);
- the continued use of the photocatalyst without deactivation, since the adsorbed substances are oxidized finally to CO_2.

Among the above-mentioned supports, activated carbon is the stronger co-adsorbent, zeolites are supposed to provide an effective separation of photogenerated electrons and holes due to the electric field of their framework [735,737,758], while SiO_2 represents a transparent host (less UV scattering).

Activated carbon has been used either in gas phase (propionaldehyde [746,754], NO_x [757,759], and benzene, toluene, ethyl benzene and xylene (BTEX) [757]

removal from air) or in aqueous phase (dichloromethane [760], propyzamide (3,5 dichloro-*N*(1,1dimethyl-propynyl)benzamide [746,761,762], toluene [763] and 2-naphthol [764]) reactions, but its use as absorbent support for TiO_2 does not always give a photocatalyst with highest activity [746]. A high photoactivity and a long photocatalytical life are registered when TiO_2 is coated with a layer of carbon, in the photodegradation of methylene blue [765]. This TiO_2-mounted, activated carbon does not increase the photoactivity of phenol degradation, but has benefit in suppressing the anatase to rutile transformation [766]. An interesting effect of activated carbon is achieved when it is used as a template during synthesis and is eliminated during the calcination steps [767,768], leading to surface features significantly different from bare TiO_2. The higher performance in phenol photodegradation could be explained as a synergetic effect between surface acidity, carbon content and structural improvement [678].

The presence of SiO_2 is beneficial in the removal of free cyanide [714] and photodegradation of phenol [744], acetophenone [713], and dyes [743] in water. The improved photocatalytical efficiency of mixed silica–titania composites arises through the generation of new active sites, due to the interactions between titania and silica and improved mechanical strength, thermal stability, and surface area of the titania [445,769,770].

Zeolite framework structures have a decisive effect on intra-crystalline diffusion and are likely to limit mass transfer into the catalyst [748,771]. In order to develop enhanced photoactivity of TiO_2, different methods to support TiO_2 on zeolites were investigated, ranging from simple amalgamation of powders through mechanical mixing [772] to impregnation via sol–gel techniques [771], chemical vapour deposition [745], cation exchange [773,774] (pores and channels provide selective exclusion of molecules or ions, enabling entrapment of nanosized TiO_2 particles).

The use of monolithic supports [775] (i.e., solid structures with bored parallel channels, for example $MgSiO_4$), enables a reduction of the pressure drop (caused by passage of the gas through the catalyst) by several orders of magnitude and improves both chemical and photon contact [776]. This permits effective industrial applications where high volumes of gas have to be treated, and gas-phase detoxification must be fast (contact time in the order of seconds).

It is important to mention that the adsorption properties are strongly influenced by the chemical nature of the pollutant and the surface properties of the support (i.e., a high activity of an absorbent is organic compound dependent). Moreover, there is an optimal loading of TiO_2 to achieve the best photoactivity on various supports.

For volatile pollutants such as benzene and chlorobenzenes, molecular sieve supports facilitate the photodegradation reaction by providing a large surface area for adsorption [735,737,779]. The support, in contrast, does not show a positive contribution in degrading hydrophilic pollutants such as phenol. The hydrophobic interlayer surface of the pillared clay [780,781] should be advantageous to adsorb and degrade organic compounds in water such as trichloroethylene [782], di-*n*-butyl [750,783], diethyl- and dimethyl-phthalate [750], and bisphenol A [750]. The hydrophilic nature of vinyl chloride provides a great potential for its adsorption on silica supports [784].

An interesting result in modifying catalyst *selectivity* is obtained on the highly dispersed isolated tetrahedral TiO_2 species within zeolite-Y cavities prepared by an ion exchange method. Used for direct decomposition of NO at 2 °C into N_2 and N_2O a selectivity of 91% and 9%, respectively, is obtained [556]. For impregnated photocatalyst with aggregated octahedrally coordinated TiO_2 species, the obtained selectivities for N_2 are much lower, namely 41% and 25% [736,785]. Such a behaviour is explained by the formation of charge transfer excited complexes of oxides $(Ti^{3+}–O^-)^*$ under UV irradiation, and an electron transfer from the electron-trapped center, Ti^{3+} into the π-antibonding orbital of NO. Simultaneously, electron transfer from the π-bonding orbital of another NO into the trapped hole center, O^-, occurs. These electron transfers lead to the direct decomposition of two molecules of NO on $(Ti^{3+}–O^-)^*$ into N_2 and O_2 even at this temperature. During the illumination of the impregnated catalysts, the photochemical generation of holes and electrons is accompanied by rapid long-distance separation, thus preventing the simultaneous activation of two NO adsorbates on the same active sites. The decomposed N and O species react with NO in different sites to form N_2O and NO_2.

A higher efficiency in NO decomposition [786,787] and also reduction of CO_2 with H_2O into chemically valuable compounds such as CH_3OH or CH_4 [788,789] is obtained with Ti-oxide molecular species obtained by ion implantation or exchange techniques, involving tetrahedral Ti-oxides within the cavities and frameworks of zeolites and mesoporous sieves.

In the photodegradation of 4-nitrophenol using a TiO_2/Al_2O_3 catalyst [722], the support acts as a co-catalyst. Al^{3+} surface sites are well suited for O_2 photo-adsorption [790], and consequently TiO_2 can be assisted also in photoactivation of O_2.

5.8. *Recognition sites*

One of the approaches to obtain highly selective photocatalyst, is the construction of robust, immobile organic molecular recognition sites (MRS) on inert domains, located on or in the vicinity of the photocatalyst that can selectively physisorb the target molecules. Then, the adsorbed molecules will surface-diffuse from site to site towards the interface between the inert domains and photocatalytic domains where they will be destroyed. The use of hiolated β-cyclodextrin chemisorbed on gold as molecular recognition site (hosts) improve the degradation rate of 2-methyl-1,4-naphthoquinone and Chicago Blue (guests), without any significant damage to the organic molecular sites [791].

6. Photocatalytic applications

Photocatalysis provides a number of attractive features:

- a wide variety of compounds may undergo selective redox transformations, decompose, or be deposited;
- it operates at near ambient temperature;

- it utilizes solar energy.

A number of research topics in photocatalysis have emerged that offer potential for commercial development. Of particular promise are the following subjects:

- selective synthesis of organic compounds;
- removal of organic pollutants;
- removal of inorganic pollutants;
- photokilling of pathogenic organisms (viruses, bacteria, algae protozoa and cancer cells);
- self-cleaning and anti-fogging materials.

Heterogeneous photocatalytical reactions can be carried out either in aqueous solution or gas phase, each of them suited for specific applications.

6.1. Selective organic synthesis

6.1.1. General remarks

Heterogeneous photocatalysis in selective organic synthesis is not frequently employed, although nowadays the demands for replacement of traditional oxidation methods with cleaner ones are increasing. TiO_2-sensitized organic photosynthetic reactions include oxidation and oxidative cleavage, reduction, isomerization, substitution, and polymerization. These reactions can be carried out in oxidatively inert solvents [792].

6.1.2. Alkanes and alkenes

The activation of C–H bonds is one of the most challenging chemical problems and is also of great practical importance. Generally, the formation of oxidation products depends on the reaction medium [793]. The different selectivities obtained in gaseous and liquid phase are explained by the ability of the liquid products to act as solvent for primary oxidation products protecting them from further oxidation, as well as by less facile oxygen–surface interactions in the liquid phase.

The oxidation of neat-liquid *n*-heptane and 2,2-dimethylbutane is reported to lead to three ketones and one ketone, respectively, as is expected if the oxidation only takes place on secondary C atoms. No cleavage products are obtained if the same compounds are oxidized in the gas phase [9].

A selective photofluorination substitution of olefins with formation of a single fluorinated product is found in a MeCN medium and in the presence of AgF [794]:

$$(C_6H_5)_3CH \xrightarrow[CH_3CN,\ h\nu]{TiO_2,\ AgF} (C_6H_5)_3CF \tag{6.1}$$

This reaction (6.1) may occur if a single electron transfer leads to the formation of a sufficiently stabile cation radical that can be nucleophilically attacked by fluoride.

Olefins such as 1-decene and 2-hexene are converted to their corresponding carbonyls and epoxides [14,795]. The selectivity of the epoxidation reaction in a mixture of acetonitrile and butyronitrile is improved using rutile (instead of anatase)

and visible light [796]. Recently, the hydrogenation of propine to propene by precious metals (Pt, Ru, Rh, Pd and Ag)-loaded TiO_2 is reported, of which Pd/TiO_2 presents the highest photocatalytical activity [797].

6.1.3. Saturated and unsaturated alicyclic hydrocarbons

The oxidation of cycloalkanes with a 5, 6, 7, and 10 carbon-ring with or without methyl substituents [798,799] leads to ketones as major products. The CO_2 content increases from 12% to 33% when the number of methyl groups on the C_6 ring varies from 0 to 2, showing that the degradation reaction is not limited to partial oxidation products. The highest reactivity is achieved for cyclohexane. *cis*-Decaline is oxidized about 10 times faster than the *trans*-isomer, which may be an interesting synthetic route [9]. Photooxidation of methoxy-substituted 1,1-diarylethenes and 1,1,8,8-tetraaryl-1,7-octadienes catalyzed by TiO_2 proceeds via induced electron transfer to give 3,3,6,6-tetraaryl-1,2-dioxanes in high yields [800]. These reactions are accelerated by the addition of $Mg(ClO_4)_2$ [800] (reaction (6.3)):

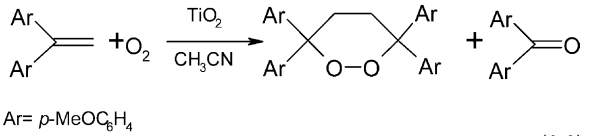

Ar= *p*-$MeOC_6H_4$

Ar= *p*-ClC_6H_4

(6.2)

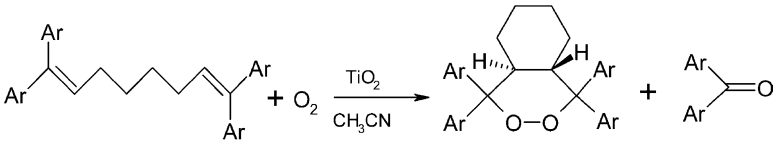

Ar= *p*-$MeOC_6H_4$

Ar= C_6H_5

(6.3)

Cyclohexanol and cyclohexanone, key products in the synthesis of adipic acid and caprolactam, are obtained conventionally by catalytical oxidation of cyclohexane with molecular oxygen at elevated temperatures and pressures in a series of liquid-phase reactors. The single-step conversion of cyclohexane is kept low, usually under 10% to minimize deep oxidation and formation of carbon dioxide [801]. Using photocatalysis with TiO_2, the oxidation of cyclohexane to cyclohexanol and cyclohexanone can be obtained in the liquid phase at room temperature and pressure [497,802,804]. Nanosized particles and the presence of surface Ti^{3+} increase the selectivity of the photocatalytic reaction [805]. Utilizing a proper solvent (that minimizes the adsorption strength of the desired products on TiO_2, does not compete with cyclohexane and oxygen for adsorption sites, and does not form radicals on the illuminated TiO_2 surface) leads to an increase of the reaction rate and the selectivity to cyclohexanol and cyclohexanone over the use of neat cyclohexane [802,804]. The highest product formation rate mentioned in literature is observed for dichloromethane as solvent, which preferentially adsorbs on the TiO_2

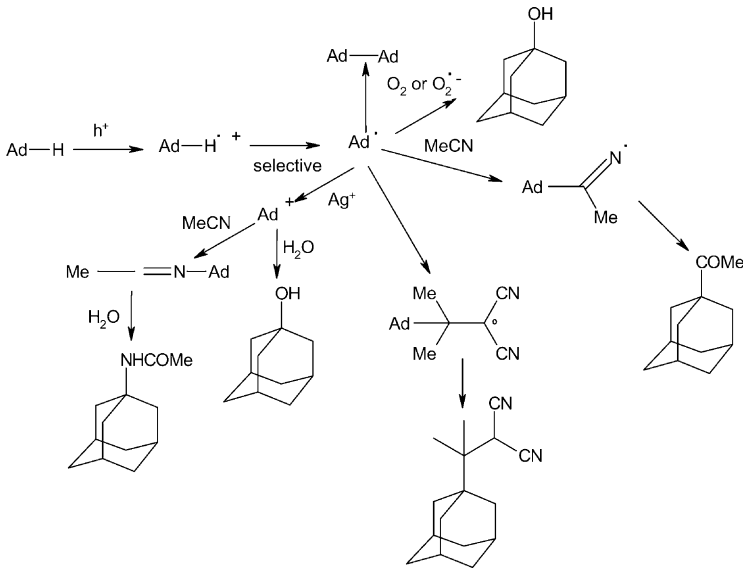

Fig. 17. Adamantane (Ad) oxidation pathways [809].

surface (compared to cyclohexane, cyclohexanol and cyclohexanone), forming a reactive radical which abstracts a hydrogen atom from cyclohexane.

An interesting study of C–H functionalization is performed on adamantane, which may be relatively easily oxidized [806]. This C–H functionalization has been obtained through either oxygen incorporation [807,808] or C–C [806,809] bond forming reactions (Fig. 17). Both oxygen and inorganic/organic oxidants have been used as electron scavengers. While in MeCN, the photocatalysis of adamantane yields 1- and 2-adamantanol and adamantanone, with limited degradation and preference for functionalization at the 1 position (particularly in the presence of Ag^+ salts), the oxidation is less selective in CH_2Cl_2. In N_2-flushed solutions with Ag^+ as sacrificial acceptor, products from trapping of both 1-adamantyl radical (adamantyl methyl ketone) and cation (*N*-adamantylacetamide) are obtained. Furthermore, alkylation of an electrophilic alkene (isopropylydenemalononitrile) is obtained. By addition of H_2O_2 to the MeCN or butyronitrile solution, rutile is more active than anatase in 1-adamantanol, 2-amantanol and 2-adamantanone formation [808].

Unsaturated alicyclic hydrocarbons are more reactive compared to their saturated homologues. Cyclohexene and tetrahydronaphthalene (tetralin) are 1.8 and 15 times faster selectively oxidized at the double bonds than cyclohexane or decahydronaphthalene (decalin) [9] respectively.

The presence of an aromatic nucleus yields a lower CO_2 content, as can be seen, for example, by the oxidation of tetralin (reaction (6.4)), which is oxidized at the allylic position:

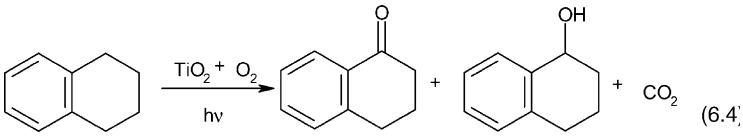

(6.4)

1-Phenylcyclohexene yields 1-phenyl-1,2-epoxycyclohexane selectively [9].

6.1.4. Aromatic compounds

Due to the high stability of the aromatic nucleus, photocatalytic reactions occur only in aqueous solutions and especially show various side chain reactions. The reaction rate is sensitive to ring substitution, with electron-donating groups enhancing and electron-withdrawing groups decreasing the rate [810]. This type of reactions may present a convenient method for the oxidation of benzene ring substituents.

The photooxidation of toluene to benzaldehyde and subsequently to benzoic acid in MeCN (reaction (6.5)) is accelerated by the presence of small amounts of H_2SO_4 [811]. It is assumed that the HSO_4^- anions promote the reaction by mediating the oxidation of the organic substrate by reacting with the photogenerated hole to form highly oxidizing $HSO_4^{\bullet}$ radicals. The formation of benzoic acid is favoured by stronger electron-withdrawing substituents; the oxidation kinetics are also enhanced by the presence of sulfuric acid.

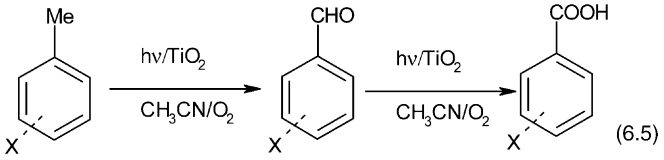

(6.5)

X= H,*p*-CF_3,*p*-NO_2, *p*-Cl, *p*-F, *p*-Me, *p*-tert-butyl, *m*-NO_2, *m*-Cl, *m*-F

In UV-irradiated acetonitrile solutions, the oxidation rate of the alkyl chain of alkylbenzenes decreases with the number of carbon atoms (toluene being an exception) [812]. The carbon atom in the α position with respect to the aromatic ring is the most reactive (reaction (6.6)).

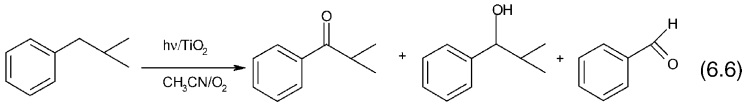

(6.6)

Under these same conditions, xylenes are selectively converted to tolualdehydes and the ethyl and isopropyl substituents are oxidized yielding a mixture of the corresponding ketone and aldehyde (reaction (6.7)). Depending on the structure of the side-chain oxidative cleavage is also possible.

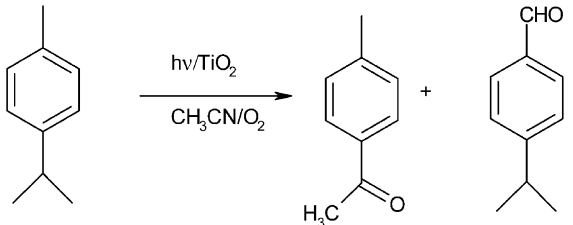

(6.7)

In the case of arylated alkanes, oxirane can be formed, but oxidative cleavage can also occur. The presence of electron-withdrawing groups (such as –CN, $–COCH_3$, and $–COOC_2H_5$) on the olefinic carbon (not bonded to the phenyl group) hinders oxidation [813]. Alkenes substituted with phenyl groups, such as α-methylstyrene [813–815] and 1,1-diphenyl-ethylene [813,816] yield corresponding ketones and aldehydes (reactions (6.8) and (6.9)); however, epoxide formation is not negligible. The reaction rate of reaction (6.8) is ring-substitution sensitive.

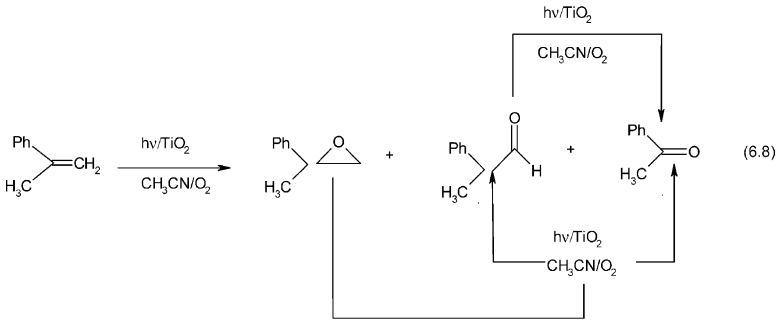

(6.8)

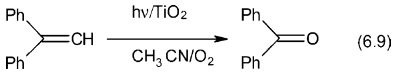

(6.9)

In the absence of water and oxygen, styrene may polymerize [813].

Naphthalene is converted into 2-formylcinnamaldehyde (reaction (6.10)) in a mixed solution of water and MeCN. The best selectivity of 85% and the highest reaction rate are obtained using a photocatalyst containing 90% rutile and 10% anatase [817]. Small particles of anatase are inactive, probably because band bending is necessary for naphthalene oxidation. This synergism between rutile and anatase is explained by an electron transfer from rutile particles to anatase particles, i.e., naphthalene is mainly oxidized in rutile particles and oxygen is mainly reduced on anatase particles.

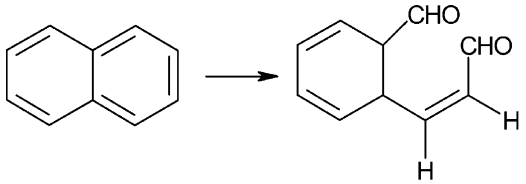

(6.10)

The pyridine nucleus is less stable than the benzene nucleus in photocatalytic conditions, since the oxidation of methylpyridines (picoline) in acetonitrile leads to inorganic products [9]. The absence of selectivity might be due to the relatively strong adsorption through the N atom of picolines, which might prevent desorption of partly oxidized intermediates.

6.1.5. Alcohols

Selective oxidation of alcohols to carbonyls is one of the most important chemical transformations in industrial chemistry. Carbonyl compounds such as ketones and aldehydes are precursors for many drugs, vitamins, and fragrances and are important intermediates in many complex syntheses [818,819]. Most of the employed reactions, however, use toxic, corrosive, or expensive oxidants and require stringent conditions such as high pressure, temperature, or strong mineral acids [820,821]. Additionally, only aldehydes and ketones that withstand high temperatures can be prepared by classical copper-catalyzed dehydrogenation in the gas phase. Photodehydrogenation reactions that take place at room temperature offer an interesting route for aldehyde synthesis.

The C_1–C_4 alcohols are easily converted in the liquid phase and in the presence of oxygen into their corresponding aldehydes or ketones, which may be further transformed by non-catalytic processes into acids. A higher reactivity is registered for primary alcohols [822], which opens up a promising selective synthesis method for hydroxycarboxylic acids.

In the absence of oxygen, the dehydrogenation of neat-liquid aliphatic C_1–C_4 primary and secondary alcohols is very selective, the amount of formed CO_2 being only 1% (methanol) and 4% (ethanol) of the sum of aldehyde and acetal [449]. In MeCN, primary alcohols can be oxidized in preference to secondary ones [823,824]. In benzene or acetonitrile, selective dehydrogenation of various primary and secondary alcohols is also observed [825]. If the alcohol is unsaturated, isomerization may occur, yielding the corresponding saturated aldehyde [826]. Both pathways are illustrated in reactions (6.11) and (6.12).

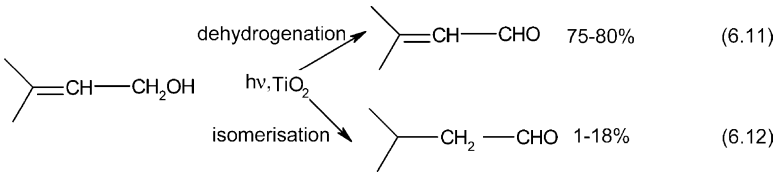

Photodegradation of aryl alcohols [827] leads to the corresponding aldehydes or ketones and small amounts of acids. The low yield of benzoic acid (compounds 1–3 of reaction (6.13)) is understandable in view of the ease of oxidation of aldehydes compared to ketones. For $R_1 = C_6H_5$ and $R_2 = Cl$ (4-chlorobenzhydrol) an oxidative dehalogenation is evidenced (benzophenone and benzoic acid intermediates are formed). 1,2-diaryl alkane-1,2-diol leads to C–C scission of the radical cation after photocatalytic oxidation with aldehydes and acids as major products. The oxidation of polynuclear aromatic alcohols (fluorenols) is selective, leading mainly to the corresponding ketones and a minor amount of the corresponding alkanes (reaction

(6.14)) [828]. The increase of solvent polarity leads to an increase of ketone yield, probably due to the increased stability of the intermediate radical ion [829].

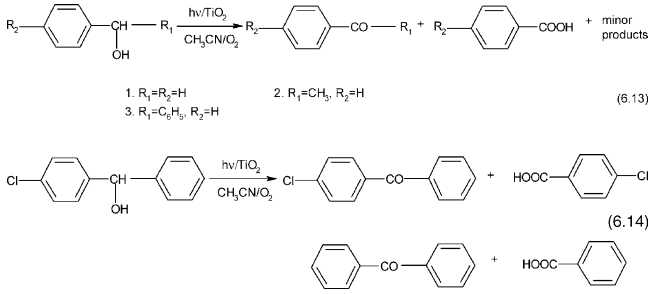

Selective oxidation of alcohols is also obtained in the gas phase, using an annular reactor and temperatures of 150–190 °C [830]. The photooxidation reaction is found to be very dependent on the nature of the used alcohols. Generally, the conversion per pass of primary alcohols is low (with a slightly higher value for secondary alcohols), but the selectivity is high (>95%). The initial step of the proposed mechanism (Fig. 18) is the interaction of a surface hole with the hydroxyl group of the alcohol, forming a metal-oxo species with proton removal. This proton removal step becomes easier with increasing carbon chain length and branching. The higher the number of adjacent hydrogen atoms presents, the easier the removal and the greater the conversion. Cyclopentanol shows a higher conversion than its open-chain counterparts 2- and 3-pentanol. This could be due to the higher strain in the ring structure. However, cyclohexanol shows a lower conversion than *n*-hexanol due to the increased stability of the six-carbon cyclic structure [831]. The presence of a benzene ring generally increases the conversion, but decreases the selectivity. This can be attributed to the electron-deficient nature of the benzene ring, which results in a reduced electron density at the oxygen-hydrogen bond, thereby making the proton abstraction relatively easy. Formation of styrene from 1-phenyl ethanol may be caused by photocatalytic induced dehydration of the alcohols [832]. The presence of oxygen is found to be critical for the

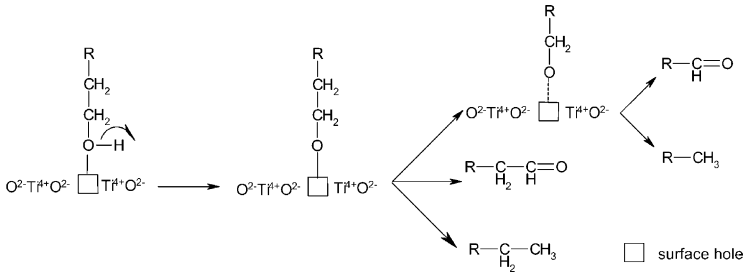

Fig. 18. Photocatalytic oxidation of alcohols to aldehydes/ketones over TiO_2 [830].

photooxidation: if it is absent, the holes formed on the surface abstract oxygen from the alcohols, producing hydrocarbons such as toluene and ethyl benzene.

6.1.6. Aldehydes, ketones, acids

In the absence of oxygen and in aqueous or mixed aqueous/organic solutions, aliphatic carboxylic acids are decarboxylated (reactions (6.15) and (6.16)) to the corresponding reduced hydrocarbons or hydrocarbon dimers [7,833]:

$$RCOOH \rightarrow RH + CO_2 \tag{6.15}$$

$$2RCOOH \rightarrow R\text{–}R + H_2 + 2CO_2 \tag{6.16}$$

The second reaction is attributed to the presence of $R^{\bullet}$ radicals [834], being equivalent to the Kolbe electrosynthesis. Since CH_3COOH represents a common product of biological digestion, the photo-Kolbe reaction could be combined with biological waste treatments to generate combustible fuels.

Parallel to decarboxylation, the presence of a carboxyl group in 4-oxopentanoic acid (levulinic acid) causes oxidative C–C scissions, leading to propionic and acetic acids (which are further converted into ethane and methane), as well as to reductive cleavage in the absence of oxygen, producing acetone and ethanal [835].

In the absence of oxygen, aqueous 1,2-cyclohexandioce acid is singly decarboxylated in aqueous solutions, whereas bis-decarboxylations have been reported using electrochemical oxidation. Such behaviour may be due to the absence of oxygen if the reduction of monodecarboxylated radicals and the subsequent desorption are fast enough to prevent further decarboxylations (at least for short irradiation periods) [836].

In acetonitrile, and in the absence of oxygen, nitrobenzaldehyde undergoes an isomerization to nitrosobenzoic acid [837]. Different light sources and light path distances demonstrate significant impact on the reaction rate constants and half-lives.

6.1.7. Amines

The oxidation of amines can be performed with good selectivity by common oxidation reagents; so no special interest for photocatalytic reactions exists [838].

In acetonitrile suspensions, primary aliphatic amines with secondary carbon atoms are selectively transformed into the corresponding *N*-alkylidene amines [839].

Depending on the initial concentration of 4-phenylbutylamine in water, the oxidation pathway as depicted in reaction 6.17 is proposed. Several other oxidation products occur, displaying a lack of selectivity [840].

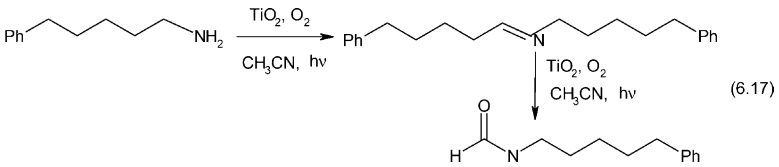

(6.17)

Similarly, α,ω-diamines can undergo an intramolecular process [841]:

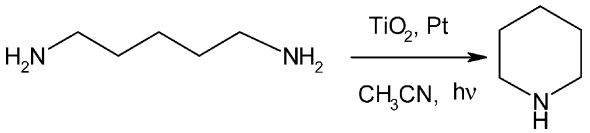

(6.18)

Nevertheless, greater selectivities are obtained in the absence of oxygen, where neat-liquid amines R-NH_2 (R = *n*-propyl, *n*-butyl, *n*-pentyl, benzyl) selectively form symmetrical *N*-alkylidene amines with low amounts of the corresponding dialkylamines [840].

6.1.8. Nitro and nitroso compounds

The yield of the selective reduction of nitro [360,842] and nitroso [843] compounds to amine (reaction (6.19)) is solvent dependent [842].

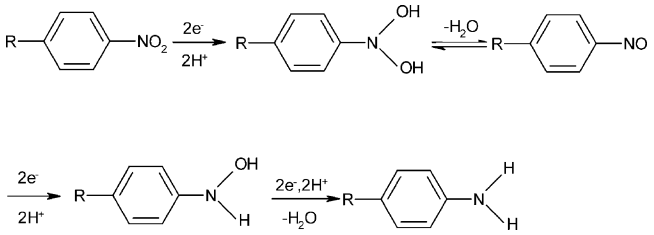

(6.19)

6.1.9. Sulfides

The oxidative degradation of weak C–S bonds (e.g., dibenzyl thioethers) occurs through C–S bond cleavage [799,844]. When stronger C–S bonds [845] are present (e.g., diarylsulfides, diarylthiophes), the carbon skeleton is preserved and oxidation leads to the corresponding sulfoxides and sulfones through sulfide radicals and [$R_2^+SOO^-$] intermediates (reaction (6.20)).

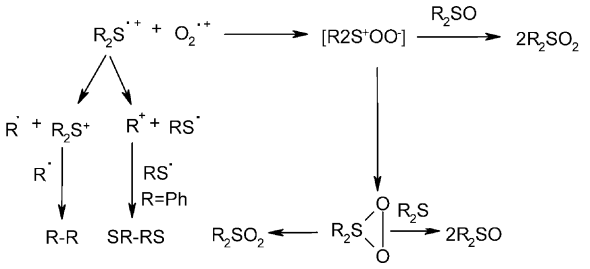

(6.20)

6.2. Water purification

6.2.1. General remarks

The European legislation places emphasis on the cleaning of wastewater effluents from industrial discharges or agrochemical products such as pesticides, fungicides, fertilizers, and land filling domestic wastes [846]. There is a growing demand for effective, economic, and environmentally benign water treatment technologies,

where all materials (used or produced) in the mineralization process are completely harmless to the environment. In developing countries, water resources are limited, which requires recycling of water for reuse in agriculture and industry. In most of these countries, solar energy is abundant, so it can be used as source for photocatalytical detoxification of polluted water.

The activated sludge process (decontamination that involves microorganisms, bacteria (95%), and higher organisms (5%)) is the most commonly applied biological wastewater treatment process. The drawbacks are the slow reaction rates, inefficiency at low pollutant level (sub-ppm), disposal of sludge, control of proper pH and temperature. And, importantly, some toxic substances can endanger the bacteria.

Traditional technologies based on adsorption frequently involve the use of activated carbon. Although activated carbon is usually found to be fairly effective in the extraction of organic materials from water, its regeneration process (e.g., thermal desorption) is rather expensive and induces another pollution problem [847]. A significant fraction of adsorbent is lost cycle by cycle or can be destroyed mechanically. Additionally, activated carbon is a non-selective adsorbent which adsorbs almost all natural organic matter present in water, so there is a rapid decrease of the capacity to accumulate toxic organics [718,719]. In summary, economic reasons explain why the development of re-usable inorganic adsorbents is attracting increasing interest.

Air stripping (decontamination in which volatile organics are extracted from water), is commonly employed for the removal of volatile organic contaminants in wastewater. However, it just transfers pollutants from water phase to air phase rather than destroying them. Thus, most air-stripping processes currently require subsequent treatment of the off-gas.

Chemical oxidation (chlorination, ozonation) is unable to mineralize all organic substances and is only economically viable for the removal of pollutants in high concentrations [849–851]. Secondary pollution may arise using the chlorination process due to the formation of disinfecting by-products (DBPs) such as trihalomethanes known as potential carcinogens [852,853]. Additionally, the efficiency of the chlorination process is affected by the presence of nitrite (nitrification) and suspended solid particles, which also requires high investments for scrubbing safety equipment (i.e., filter systems) and need for dechlorination to meet stringent EPA regulatory limits [854]. Although ozonation, avoids most of the hazardous DBPs associated with the chlorination process, it generates small amounts of bromate ions (3–68 ppb) suspected as cancer agents. Additionally, it has to be generated on site and the off-gases need strict monitoring.

In the last decade, advanced oxidation technologies (AOTs) have been shown to be effective in the destruction of refractory pollutants (e.g., microorganisms, industrial toxins) [367,442,855–857]. They are based on the generation of highly reactive and oxidizing hydroxyl radicals (reaction rate usually in the order of 10^6–10^9 $mol^{-1}s^{-1}$ [858,859]). They offer different possibilities for $HO^{\bullet}$ production [442,446] like O_3/UV, H_2O_2/UV, Fe_2O_3/UV, TiO_2/air/UV, and various combinations of them, allowing a better adaptation to the specific treatment requirements. The

main drawbacks of the method are the use of expensive reactants (like H_2O_2 and O_2) and the fact that this method is only applicable to wastes with relatively small COD contents ($\leq$5.0 g/l) [859].

Photocatalysis based on TiO_2 (anatase) has the following advantages:

- a non-selective destruction of organic and inorganic waste materials may be achieved under normal temperature and pressure in a few hours without production of polycyclic products;
- oxidation of pollutant in ppb range;
- the use of oxygen as the only oxidant;
- capability for simultaneous oxidative and reductive reactions;
- in particular, photocatalysis is known to be effective for inactive substrates such as linear alkanes or their simple derivates [860,861], which opens perspectives in oil spill cleaning [862], elimination of surfactants [863], and dyes [864,865] from industrial water;
- these highly active catalysts are adaptable to specially designed reactor systems.

On the other hand, since hydroxyl radicals [866] react non-selectively with organic compounds, numerous by-products are formed. Cost-effective treatments to complete compound mineralization are usually not practical and the presence of by-products during and at the end of water treatments appears to be unavoidable [365,369].

In summary, heterogeneous photocatalysis for water treatment is still in the research stage as some important problems remain to be solved before efficient applications can be envisaged. In order to make this approach cost alternative to current technologies, more fundamental research is needed in order to:

1. develop a TiO_2 photocatalyst, which works using visible light as well as UV light effectively and without wear;
2. increase the efficiency of the photocatalytic process with a reduced light requirement by a factor of three [867];
3. solve the recovery of the photocatalyst. This can be done using an immobilization technique (see also Section 5.7).

6.2.2. Influence of process parameters

6.2.2.1 Effect of inorganic compounds. Real water systems (wastewater but also natural) are quite complex and contain both inorganic and organic species. The dissolved inorganic species (as cations and anions) may strongly influence the rate and efficiency of the photocatalytical process [373,664,868] or may lead to spontaneous photochemical phenomena [488,867,870]. Additionally, in the last two decades, seawater has become an important source for drinking purposes (e.g., Saudi Arabia currently produces 5.25 M m^3 drinking water from salt water daily). Hence, the influence of inorganic compounds on the photocatalytic properties of TiO_2 becomes an important research field [871].

Effect of inorganic anions. Anions (Cl^-, ClO_4^-, NO_3^-, CO_3^{2-}, HCO_3^-, SO_4^{2-}, PO_4^{3-}) are known to have a retarding effect on oxidation rates of organic compounds by competing for radicals or by blocking the active sites of the TiO_2 catalyst [872–874]. A special case is represented by sulfate and phosphate anions, which may form reactive species such as $SO_4^{\bullet-}$ and $H_2PO_4^{\bullet-}$:

$$h^+ + SO_4^{2-} \rightarrow SO_4^{\bullet-} \tag{6.21}$$

$$h^+ + H_2PO_4^{2-} \rightarrow H_2PO_4^{\bullet-} \tag{6.22}$$

These radicals may initiate oxidation reactions with organic species. The reaction between $SO_4^{\bullet-}$ and organic solutes under CO_2 formation is faster than the corresponding reaction of $H_2PO_4^{\bullet-}$ [872] ($SO_4^{\bullet-}$ is known to be the primary intermediate for destruction of organic molecules in UV/persulfate method of total organic carbon (TOC) analysis). On the other hand, both species are practically immediately adsorbed on the surface of TiO_2, deactivating a portion of the catalyst. Phosphate adsorption at concentrations as low as 1 mM reduces photooxidation of simple organics (ethanol, aniline, and salicylic acid) by ~50% [872]. Their binding with the catalyst is so strong, that removal with water is inefficient and alkali washing is necessary.

Effect of inorganic cations. Both beneficial and detrimental effects have been evidenced. The effect is strongly dependent on the metallic ion nature and their concentration and the rate of photocatalytical degradation can be enhanced up to an optimum value.

Metal ions may increase the photocatalytical rate due to:

- the ability of metallic ions to trap either electrons or holes via oxidizing and reducing reactions,
- alternative homogeneous Fenton-type reactions on the TiO_2 surface [875,876] that lead to an additional $HO^\bullet$ production:

$$M^{(n-1)} + H_2O_2 + H^+ \rightarrow M^{n+} + HO^\bullet + HO^- \tag{6.23}$$

A decrease in reaction rate, as evidenced principally at higher concentrations, can have different reasons:

- short-circuiting reactions that create a cyclic process 'without generation of active $HO^\bullet$ [877–879]:

$$\begin{aligned} &M^{n+} \xrightarrow{e^-} M^{(n-1)+} \xrightarrow{e^-} M^{(n-2)+} \dots \\ &\dots M^{(n-2)+} \xrightarrow{h^+} M^{(n-1)+} \xrightarrow{h^+} M^{n+} \end{aligned} \tag{6.24}$$

- filter effect due to UV absorption of the species;
- precipitation and deposition of the dissolved metallic ions as hydroxides on the TiO_2 surface.

A change in photodegradation rate in both directions may be due to the participation in homogeneous or surface complexes, either with the contaminant or its decomposition products. An example is represented by the aliphatic acid photodecomposition in the presence of Cu^{2+} [880,881]. Copper monocomplexes which are formed at pH <4 are active intermediates (beneficial) because they can act as hole scavengers, whereas diacetate complexes, formed at pH $\geq$5, poison the catalyst.

A considerable controversy on the effect of Cu^{2+} on the photodegradation rate is present in literature. Cu^{2+} enhances the phenol degradation rate until an optimal concentration value [510,882], while others mention a detrimental effect for all concentrations [877,878]. A threefold and eightfold increase of sucrose photodegradation rates is obtained at pH 3.5 and 1.5, respectively, although for the last pH value the overall rate was found to be lower [884]. Copper ions show little adsorption on TiO_2, suggesting that the enhancement of the photocatalytic mineralization rate occurs through a homogeneous pathway mechanism [884]. A detrimental effect is obtained also for 4-nitrophenol degradation [879] at a concentration of 10^{-4} mol/l of pollutant, although other studies mention that the photodegradation of aromatic compounds in aerated solution is increased by Cu^{2+} presence (the higher amounts of hydroxylated products indicate a higher production of $HO^{\bullet}$ radicals either by a heterogeneous pathway or a Fenton-type reaction) [875,885,886].

The presence of Fe^{2+} leads to a small increase of aromatic compound photodegradation in aerated conditions [885,886], while its presence is detrimental in aniline degradation, due to competition of Fe^{2+} with organic substrate for oxidizing species [887]. The presence of Fe^{3+} promotes the occurrence of photocatalytic hydroxylation of benzoic acid and benzoate in deaerated systems [888], also increasing also the phenol [877–889] and toluene [890] degradation until an optimal concentration value is reached. Ferric ions (Fe^{3+}) have a very high adsorption capacity and their presence prevents mercury ions from undergoing photocatalytic reduction, while on the other hand the presence of ferrous (Fe^{2+}) ions improves the rate of Hg^{2+} reduction [8].

The influence of Ag^{+} on phenol and nitrophenol degradation is beneficial even under helium, due to the high efficiency of Ag^{+} as electron scavenger and its reoxidation by a photo-Fenton reaction [876,891,892]. Photocatalytical and electrophotocatalytical degradation of HCOOH is inhibited by Ag^{2+} presence due to the deposition of Ag^{0} on the catalyst surface [893].

Cr^{3+} may be a recombination center, as it is able to create both acceptor and donor surface sites, inhibiting the phenol photodegradation [882].

6.2.2.2 Effect of pH. This reaction pH markedly influences the overall efficiency of the photocatalytical processes [894–896]. The pH dependence can be associated with changes of the surface charge of the photocatalyst, hydrophobicity, net charge of pollutant, changes in its adsorption modes, and amount of produced $HO^{\bullet}$. This can lead to a modification of the overall rate. Additionally, changes in pH may

introduce deactivation problems if the presence of long-living intermediates that poison the photocatalyst is favoured [897].

The interaction of electron donors and acceptors with metal oxide semiconductors is determined, in part, by surface chemistry [898]. In the case of TiO_2, the principal amphoteric surface functionality is the "titanol" moiety, >TiOH. Hydroxyl groups on the TiO_2 surface are known to take part in the following acid–base equilibrium:

$$> TiOH_2^+ \underset{-H^+/+H^+}{\overset{pK_{a1}^s}{\longleftrightarrow}} > TiOH \underset{-H^+/+H^+}{\overset{pK_{a2}^s}{\longleftrightarrow}} > TiO^- \tag{6.25}$$

where pK_{a1}^s and pK_{a2}^s represent the negative log of the microscopic acidity constants of the first and second acid dissociation, respectively. The pH of zero point of charge, pH_{zpc}, is given as follows:

$$pH_{zpc} = 1/2\left(pK_{a1}^s + pK_{a2}^s\right) \tag{6.26}$$

For Degussa P25, the corresponding surface acidity constants are found to be: $pK_{a1}^s = 4.5$ and $pK_{a2}^s = 8$, which yields a pH_{zpc} 6.25 [899]. This implies, that interactions with cationic electron donors and electron acceptors will be favoured at pH $>$ pH_{zpc} conditions, while anionic electron donors and acceptors will be favoured at pH $<$ pH_{zpc} conditions [442,900]. The adsorption of relatively unpolar pollutants such as 1,2-diethyl phthalate is enhanced at a pH close to pH_{zpc}. On the other hand, the difference in pH_{zpc} values of various TiO_2 photocatalysts could affect the reaction mechanism. Furthermore, both the type and the amount of dopant metals influence this value [901].

The state of chemical species present in water is also affected by the pH, being closely related to their dissociation constant. When the pH is lower than the pK_a of the species, they are primarily present in the molecular state. In contrast, they exist in ionic form if pH $>$ pK_a. But relating the dissociation constant of the species to their interaction with the catalyst surface is only a rough approximation because values are in principle valid only for bulk liquids. The formation of a double layer at the liquid–solid interface can influence both the dissociation and the polarizability of reacting molecules.

The pH value may also influence the amount of $HO^\bullet$ formed. Besides the generation of $HO^\bullet$ radicals by the reaction of light-excited holes with H_2O/HO^-, H_2O_2 might be another source, through the following chain reactions (reactions (6.27)–(6.34)) [510]:

$$O_2 + e^- \rightarrow O_2^{\bullet -} \tag{6.27}$$

$$O_2^- + H^+ \leftrightarrow HO_2^\bullet \quad pK_a = 4.88 \tag{6.28}$$

$$HO_2^\bullet + HO_2^\bullet \rightarrow H_2O_2 + O_2 \tag{6.29}$$

$$O_2^{\bullet -} + HO_2^{\bullet} \rightarrow HO_2^- + O_2 \quad (6.30)$$

$$HO_2^- + H^+ \rightarrow H_2O_2 \quad (6.31)$$

$$H_2O_2 + e^- \rightarrow HO^{\bullet} + HO^- \quad (6.32)$$

$$H_2O_2 + O_2^- \rightarrow HO^{\bullet} + HO^- + O_2 \quad (6.33)$$

$$H_2O_2 \xrightarrow{h\nu} 2HO^{\bullet} \quad (6.34)$$

For $HO_2^{\bullet}$ formation, a pH higher than the pK_a leads to an inversion of the reaction. A lack of HO_2• inhibits the formation of H_2O_2, which is the major source of $HO^{\bullet}$. Therefore, at these pHs, $HO^{\bullet}$ is mainly supplied by the reaction of positive holes with water and OH^- on the surface of TiO_2.

pH modification can induce changes in the adsorption mode of pollutant molecules. An interesting example is dichloroacetic acid (DCA). Two different types of adsorbed DCA anions were detected on the TiO_2 surface: mono and bi-dentate complexes. In acidic solutions, at pH < 4, bidentate complexes (where both oxygen atoms of the DCA carboxylic group are coordinated to the surface) are predominant in the system, while monodentate complexes (attached via one oxygen atom) form the majority at pH > 5 [501]. The type of coordination strongly influences the activation and further degradation.

In the case of doped photocatalysts, a change in pH may change the interfacial structure. For example, at pH > 6, the main portion of copper is present in the form of copper hydroxide on the TiO_2 surface of Cu^{2+}-doped catalysts [501].

6.2.3. *Combined processes*

TiO_2 photocatalysis may be used as a complementary method to detoxify drinking water and decontaminate industrial wastewaters. In the following sections, several combinations will be discussed.

6.2.3.1 TiO_2/bacterial or fungal degradation. Classical biological treatments are, at present, the cheapest and the most environmentally compatible methods for wastewater purification. However, in many wastewater streams, organic pollutants are found that cannot be treated by commonly used biological methods because they are not biodegradable or may even be toxic. Examples of these pollutants are organic dyes [902], phenols or phenolic compounds [903], herbicides and insecticides [904], as well as halogenated and non-halogenated hydrocarbons [905,906]. In coupled systems, the photocatalytic pre-oxidation treatment [465,905,907] is meant to modify the structure of pollutants by transforming them into less toxic and easily biodegradable intermediates, making their biological treatment eligible.

Such processes may in the end reduce process costs (compared to the biological process), as they are also able to control bacterial growth within the aqueous medium and reduce the overall value for chemical oxygen demand.

The solution that results after photocatalytical treatment is considered to be biologically compatible after the elimination of [908]:

– the initial biorecalcitrant compounds (i.e., compounds that are not biodegradable);
– inhibitory, toxic and/or non-biodegradable intermediates;
– the residual H_2O_2 or other inhibitory electron acceptors if utilized for the phototreatment.

These requirements combined with knowledge about the evolution of toxicity and biodegradability in phototreated solutions allow the determination of the optimal treatment time. This has to be long enough to permit the formation of intermediates structurally different from the initial biorecalcitrant compounds.

As mentioned earlier, the single compound that cannot be oxidized by TiO_2 mediated photocatalytic reactions, cyanuric acid, can be degraded by bacteria (two distinct *Pseudomonos* species and a strain of *Klebsiella pneumoniae*) [909]. The cyanuric acid is transformed into biuret which is converted into urea and finally yields CO_2 and NH_3 [909,910].

6.2.3.2 TiO_2/inorganic oxidants. Inorganic oxidants such as O_3 [911,912], H_2O_2 [879,913–920], BrO_3^- [913,914], $S_2O_8^{2-}$ [487,914,921,922] and ClO_4^- [921] have been proposed to increase the efficiency of TiO_2/UV treatments due to:

– an increase in the number of trapped electrons, which prevents recombination;
– the avoidance of problems caused by low oxygen concentration;
– the generation of more $HO^\bullet$ radicals or other strongly oxidizing radicals (such as $BrO_2\bullet$ or HOBr) which may, in turn, enhance the photocatalytic degradation of pollutants, according to the following reactions (6.35–6.40):

$$H_2O_2 + e_{CB}^- \rightarrow HO^\bullet + HO^- \tag{6.35}$$

$$S_2O_8^{2-} + e_{CB}^- \rightarrow SO_4^{2-} + SO_4^{\bullet -} \tag{6.36}$$

$$SO_4^{\bullet -} + H_2O \rightarrow SO_4^{2-} + HO^\bullet + H^+ \tag{6.37}$$

$$BrO_3^- + 2H + e_{CB}^- \rightarrow BrO_2^\bullet + H_2O \tag{6.38}$$

$$BrO_3^- + 6H^+ + 6e_{CB}^- \rightarrow [BrO_2^-, HOBr] \rightarrow Br^- + 3H_2O \tag{6.39}$$

$$O_3 + e_{CB}^- \rightarrow O_3^- \tag{6.40}$$

However, at higher concentrations, H_2O_2 is a powerful $HO^\bullet$ scavenger [648,923] (6.41 and 6.42) reacting also with the photogenerated holes (6.43):

$$H_2O_2 + HO^\bullet \rightarrow HO_2^\bullet + H_2O \tag{6.41}$$

$$HO_2^\bullet + HO^\bullet \rightarrow H_2O + O_2 \tag{6.42}$$

$$H_2O_2 + h_{VB}^+ \rightarrow HO_2^\bullet + H^+ \tag{6.43}$$

A recently proposed mechanism for the photocatalytic degradation of 4-chlorophenol in the presence of bromate ions is shown in reaction (6.44) [924]:

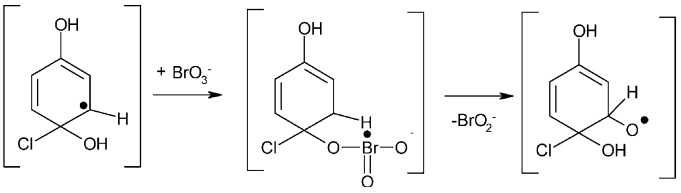

(6.44)

6.2.3.3 TiO_2/adsorptive processes. Combination of adsorption and oxidative destruction appears promising to overcome the detrimental interference between catalyst and support. A suitable adsorbent can selectively adsorb the toxic pollutants without extracting the natural compounds present in water, and the used adsorbent can then be regenerated by removing/oxidizing the organics [720]. Furthermore, the use of such a technique is easy and involves no preparation.

An enhancement of the photodegradation is evidenced when a mixture of TiO_2 and adsorbents like active carbon (AC) [759,925–927] and zeolites [747] is employed for the photooxidation of pollutants. In an AC/TiO_2 mixture [925], a synergetic effect is registered with an increase of the first-order rate constant by a factor of 2.5 for phenol degradation.

6.2.4. Organic compounds

6.2.4.1 Carboxylic acids. The photocatalytic treatment of mono- and polycarboxylic acids is of importance in nuclear industry, which employs these compounds as decontamination and chemical cleaning agents. Oxalate, $[C_2O_4]^{2-}$, is a ubiquitous metabolic product, and its destruction by natural heterogeneous photocatalysis is of importance in aquatic systems.

Formic acid (HCOOH) oxidizes to CO_2 in a single step without forming long-lived intermediates. Less than one-fourth of the formic acid adsorption sites are more than 20 times more active than the other sites. Water, formed during the photocatalytic oxidation, redistributes adsorbed formic acid from less active to more active sites, which enhances the degradation rate [350].

In deaerated solutions, alcohols, acids, aldehydes (or ketones), and alkanes are identified as intermediates during the photocatalytic degradation of C_2–C_4 [833] and 4-oxopentanoic acids. The participation of holes and H_2O [833] or holes and $HO^\bullet$ is proposed. In aerated solutions, heptanol and heptanoic acid are formed during the photodegradation of octanoic acid [661]. Both hole and $HO^\bullet$ participation are proposed to produce $R^\bullet$, which can further react with O_2. In the case of butanoic acid photodegradation, the reaction occurs in two steps [376]. First, an alkyl radical is formed, either by $HO^\bullet$ attack (in the presence of non-dissociated acid), or by a hole (if butanoic acid is dissociated). Next, this alkyl radical reacts with either O_2, RH or $(TiOH_x)^{(x-1)+}$ surface species. The reaction intermediates are pH dependent. At neutral pH, the amounts of formed formic and butanoic

acid are increased, as well as 2-oxobutanoic and oxalic acids, which are not observed at acidic pH (3.6).

Oxalic acid (HOOC–COOH) photodegradation has been widely investigated, because of its role as sacrificial agent [928–930]. The formation of unstable intermediates such as HCO_3^- [928] and $^{\bullet}COOH$ is postulated [931].

A pH-dependent photodegradation is found for maleic acid (*cis*-HOOC–C═C–COOH), fumaric acid (*trans*-HOOC–C═C–COOH), and oxalic acid [932]. At a pH lower than the pH_{pzc} of TiO_2, the photodegradation obeys the LH kinetic model within a certain concentration range. The photodegradation rate constant decreases in the order oxalic acid > maleic acid ≈ fumaric acid. For maleic and fumaric acids, a *cis–trans* isomerization, induced by interaction between adsorbed diacid and semiconductor, occurs. A photo-Kolbe reaction and $HO^{\bullet}$ attack on diacid molecules take place, generating different intermediate products. Three different pathways are proposed for the photocatalytic degradation of fumaric and maleic acids

- maleic/fumaric acid→acrylic acid (H_2C═CH–COOH)→acetic acid (CH_3COOH)→formic acid→CO_2 [376,932]
- maleic/fumaric acid→tartaric acid (HOOC–CH(OH)═CH(OH)–COOH)→tartronic acid (HOOC–CH(OH)–COOH)→glycolic acid (CH_2(OH)–COOH)→oxalic acid →formic acid→CO_2 [376]
- maleic/fumaric acid→malic acid (HOOC–CH_2–CH(OH)–COOH)→oxalic acid-→formic acid→CO_2 [932]

At a pH higher than the pH_{pzc} of TiO_2, adsorption of these three diacids is of low significance, but photocatalytic degradation of fumaric and maleic acids occurs in good yield. *Cis–trans* isomerization is not evidenced anymore and the main intermediate is oxalic acid. For multicomponent systems, at a pH lower than the pH_{pzc} of TiO_2, oxalic acid molecules preferentially occupy the adsorption sites of the TiO_2 surface and are more easily degraded than maleic and fumaric acids. In bicomponent systems containing maleic and fumaric acids, the photocatalytic degradation follows LH kinetics at $pH < pH_{zpc}$.

Four parallel decomposition pathways are reported for malic acid [376]. The main one represents a decarboxylation in the α-position from the OH group according to a ''photo-Kolbe process'' and 3-oxopropanoic acid is formed as intermediate. This indicates that malic acid is preferentially adsorbed through the carboxylic group in the α-position of the HO group (due to the higher affinity of this extremity for chemisorption). The other carboxylic group can also be linked to the surface, since 2-hydroxypropanoic acid (lactic acid) is also formed via the photo-Kolbe process. Competitive oxidation via $HO^{\bullet}$ radicals also occurs, since fumaric/maleic (H abstraction) and tartaric ($HO^{\bullet}$ addition) acids are present as intermediates.

6.2.4.2 Phenol, benzoic acid and their derivates. The degradation of phenol and its derivates has been widely studied [461,933,934] because these compounds are important chemical wastes from industry and research centers.

The photochemical degradation of phenol with TiO_2 has yielded reasonably good results but the process shows a different behaviour depending on the initial phenol concentration. Two different degradation pathways related to the existence of a different surface activation mechanism are mentioned:

- at low phenol concentrations (~0.1 g/l), the insertion of $HO^{\bullet}$ is favoured [10,935]. The presence of low adsorbate concentrations does not affect the yield of this radical.
- at high phenol concentrations (~1g/l), degradation takes place on the catalyst surface by means of peroxocompound formation [935], which is not affected by the $HO^{\bullet}$ insertion process. The formation of such compounds on the catalyst surface is favoured because of the higher amount of chemisorbed phenol molecules, which determine that fewer photons reach the surface and lower amounts of $HO^{\bullet}$ are formed. Consequently, holes can generate phenol-like species ($M–O–C_6H_5$), which subsequently yield phenoxy radicals. The degradation process may be driven by the interaction of these species with $^{\bullet}O_2^-$ and the degradation cycle is then completed on the catalyst surface [936,937]. As intermediates, besides low amounts of hydroquinone and malic acid, chemisorbed formic acid, *ortho*-formates and carbonates, which are responsible for catalyst deactivation, are detected. Adsorbed organic substrates can act as traps for photogenerated holes, either directly or by means of surface hydroxyl radicals [839,938,939].

From these data, it can be concluded that for concentrated phenol solutions chemisorption onto the catalyst can cause the molecule to break, in contrast to the ring break mechanism through successive $HO^{\bullet}$ insertion proposed for low concentrations. These results show that photocatalysis may be also applicable for concentrated pollutants, in combination with a catalyst reactivation method if necessary.

Various studies have shown that the photocatalytic reactivity of aromatic compounds can be affected by the number of substituents, their electronic nature, and their position in the aromatic ring (i.e., ortho, meta, or para), but only few correlate with the photodegradation rate to parameters characterizing the aromatic compound [940–943]. Correlations with the Hammett constant [940,941,943] (σ), the 1-octanol–water partition coefficient [941] $K_{(OW)}$, and quantum chemical properties [943] are recognized. The Hammett constant represents the effect of different substituents on the electronic character of a given aromatic compound. $K_{(OW)}$ reflects the molecular hydrophobicity and is considered to be related to the extent of adsorption of the organic compound on TiO_2. The most critical electronic properties are: the zero-point energy, the total energy divided by the molecular weight, and the quadrupolar moment for the *xy*-plane according to statistical calculations.

Limiting ourselves to the nature and position of the substituted phenols, we can mention the following:

- the photodegradation rates of *para* derivates depend mostly on the effect of the substituents on the aromatic ring, being increased by electron-donating sub-

stituents and decreased by electron-withdrawing substituents [941,943]. For each category of substituents, the activating or deactivating ability of the substituent is directly related with the σ value. An exception to this rule is hydroquinone, which has two electron-donating groups, but is not the most active. This behaviour is related to a keto-enolic short circuiting tautomeric equilibrium [944] (reaction (6.45)).

- a good correlation between the stability of the σ-complexes that may be formed between the aromatic ring and the $HO^{\bullet}$ radical and the photodegradation rate is observed for *ortho*-substituted phenols. The rate decreases in the order guiacol (–OCH_3) > 2-chlorophenol (–Cl) ≈ phenol (–H) > catechol (–OH). The delay in the case of catechol can be also due to the keto-enolic oxido-reductive tautomeric effect [942].

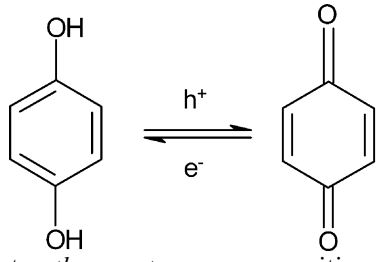

(6.45)

- substituting phenols at *ortho*-, *meta*- or *para*-positions with –NO_2, –Cl, –OH, or –COOH groups does not influence the photocatalytical degradation except in the case of dihydroxybenzenes (catechol (1,2-hydroxybenzene), resorcinol (1,3-hydroxybenzene), and hydroquinone (1,4-hydroxybenzene)) [943]. For these three isomers the degradation efficiency decreases in the order resorcinol > hydroquinone > catechol, due to the *ortho–para* activation of the aromatic ring (OH is an electron-donating substituent). Resorcinol, which has three double activated positions, reacts faster than catechol and hydroquinone, which have the unsubstituted positions, activated only once (Fig. 19). As in the above-mentioned case, delay in the case of catechol can be also due to the keto-enolic oxido-reductive tautomeric effect.

The intermediate product distribution of the photodegradation of *o*-cresol (1-hydroxy-2-methyl benzene) is thought to be different when Fe–TiO_2 catalysts are used [579]. In the TiO_2-mediated decomposition, the detected intermediates are mainly hydroxylated compounds (e.g., methylcatechol, methylhydroquinone, and hydroxybenzaldehyde) [436,945,946], while with Fe–TiO_2, the primary intermediates, *o*-hydroxy benzyl alcohol or hydroxy benzoic acid, are converted into adipic and oxalic acids. An explanation is that the modified catalyst may possess different catalytic sites compared to bare TiO_2.

Ring opening is favoured over hydroxylation and demethoxylation in compounds that contain hydroxyl instead of alkoxyl groups [947]. It is hypothesized that the former are initiated by electron transfer, which requires tight binding

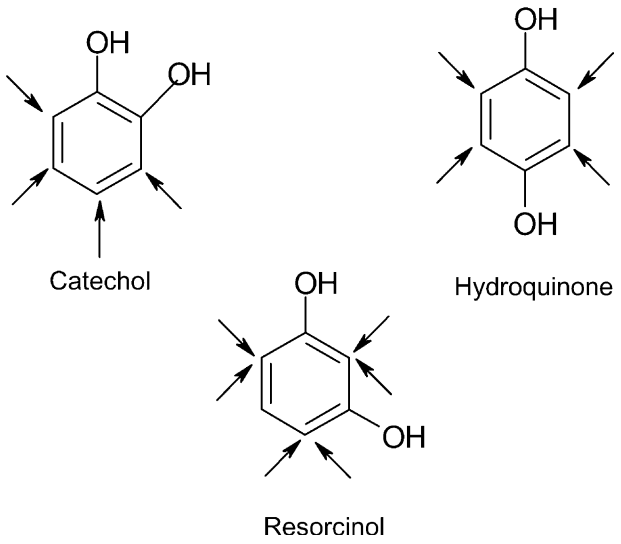

Fig. 19. Schematic representation of the activation of the aromatic ring by the –OH groups at different positions.

achieved by a direct attachment of the deprotonated phenolic groups to the TiO_2 surface, while the other two reactions are based on hydroxyl radical chemistry.

For biphenols (endocrine disruptors), the substitution of the methylene group (which binds the two phenyl groups, Fig. 20) influences the reaction intermediate distribution. The decomposition of bisphenol A (BPA, containing two methyl groups) yields various intermediates (such as 4-isopropylphenol and 4-ethylphenol), ethylidenebisphenol (EBP, containing one methyl group) gives mainly 4-ethylphenol, while 4,4′-methylenebisphenol (MBP, without methyl groups) gives predominantly 4-hydroxybenzaldehyde [948]. The existence of methyl groups leads to differences in the point charges at the C7 position connecting the two phenyl groups. In the three discussed compounds, these point charges are $0.049\ (\mathrm{BPA}) > -0.027(\mathrm{EBP}) > -0.093\ (\mathrm{MBP})$. Since the C3 and C8 positions in each compound bearing two phenyl groups are electron rich, $HO^{\bullet}$ easily attacks at these positions. In the case of MBP (which has the most negatively charged C7 connecting position), the OH adduct intermediate is formed after ring cleavage. On the other hand, BPA has the most positively charged C7 position; hence the hydrogen-adduct intermediate is produced in the decomposition of the aromatic ring structures.

The photodegradation rate of the polycarboxylic benzoic acids: 1,2,3-, 1,2,4-benzene tricarboxylic acid, and 1,2,4,5-tetracarboxylic acid, follows the order 1,2,4,5- >1,2,3 >1,2,4 obeying an LH mechanism and a complete mineralization is accomplished [458]. The two competitive initial steps correspond to a hydroxylation reaction induced by photogenerated $HO^{\bullet}$ radicals and a decarboxylation

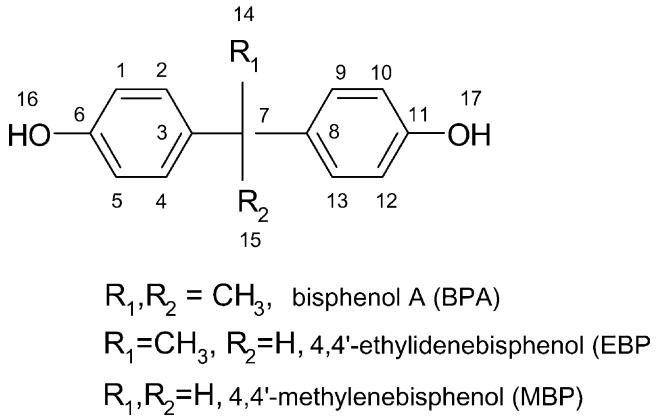

Fig. 20. Structural formula of bisphenol.

(photo-Kolbe) reaction resulting from the direct attack of one carboxylic group by a positive photohole.

6.2.4.3 Chlorine-containing compounds. Volatile chlorine-containing compounds like trichloroethylene (TCE), tetrachloroethylene (PCE), 1,3-dichlorobenzene (DCB), dichloromethane (DCM), and 2-, 4- and 2,4-dichlorophenol (2-CP, 4-CP, 2,4-DCP) are widely used as industrial solvents and have contaminated many soil and water supplies. This contamination has recently become a major issue because these chemicals are toxic, carcinogenic, extremely persistent, and mobile in the environment [949]. The stability of the C–Cl bond in halohydrocarbons is responsible for their toxicity and persistence in biological environments [950–952]. Complete photocatalytic dechlorination (reduction reaction) of many chlorinated compounds tends to be rather slow towards the mineralization of organic carbon atoms (oxidation reaction) to carbon dioxide. Moreover, when organochlorine compounds undergo oxidation, they may produce other organochlorine compounds that may be more toxic than the parent compound itself [953–955]. A rigorous check of the reaction intermediates is therefore necessary.

In the gas phase, degradation may produce unfavourable by-products such as dichloroacetyl chloride and phosgene ($COCl_2$) [956,957]. Additionally, chloroacetic acid is reported to accumulate on the TiO_2 surface [922,958], which inhibits the reaction. Since these by-products are water soluble and are eventually photodegraded to CO_2 in aqueous solutions, the treatment of contaminated water itself is more advantageous to achieve total mineralization [922]. Additionally, photocatalytic treatment can be accompanied by biological depuration (generally not efficient for these type of compounds if used alone).

Mechanistically, the photocatalysis of chlorophenols proceeds through *para*-hydroxylation of the aromatic moiety [959,960]. Further oxidation of the aromatic intermediates leads to ring opening and formation of aliphatic products (e.g., carboxylic acids and hydroxylated carboxylic acids). Phenol, hydroquinone, benzoqui-

none, chloroquinone (CHQ), and hydroxyhydroquinone (HHQ) are found as major intermediates in photodegradation of 2-CP[373]. A decrease of the reaction rate in the following order is evidenced: 2,4,6-CP > 2,4-CP > 2-CP [961].

An interesting example of increased photoreactivity of TiO_2 is shown in the photodegradation of 4-CP with a coke-containing TiO_2 photocatalyst. Highly condensed, coke-like residues are formed during pyrolysis of several alcoholic suspensions in a TiO_2 matrix that act as sensitizing species [962]. The excited photosensitizer injects an electron into the conduction band of TiO_2. Subsequently, the electron is transferred to oxygen adsorbed on the semiconductor surface producing $O_2^{\bullet-}$ (reaction (6.46)).

$$S \xrightarrow{h\nu} {}^1S^* \xrightarrow{TiO_2} TiO_2^{\bullet-} + S^+ \xrightarrow{O_2} TiO_2^{\bullet-} + S^+ + O_2^{\bullet-} \tag{6.46}$$

To become catalytic, the oxidized photosensitizer has to be reduced again, e.g., by oxidation of 4-CP. The catalyst shows an excellent long-time stability, which indicates, that the active site itself is either resistant to photochemical degradation or regenerates itself during the degradation of pollutants. An efficient photodegradation of 4-CP with visible light ($\lambda \geq 455$ nm) is obtained using nitrogen-doped [595] or surface-modified [662–665] (with transition salt) TiO_2.

6.2.4.4 Nitrogen-containing compounds. The final oxidation state of nitrogen after the mineralization of nitrogen-containing organic compounds depends on several factors. The most important are the nature of the initial organic compound and the experimental conditions (pH, O_2 concentration, loading, nature of catalyst, and irradiation time) [388,963].

Photodegradation of aliphatic short-chain alkyl and alkanolamines occurs via an electrophilic attack of $HO^{\bullet}$ radicals, which leads to an abstraction of a hydrogen atom, inducing a cleavage of the C–N bond [964]. The breakdown of the C–N bond is faster than that for C–C bonds. The higher mineralization rate for alkanolamines is attributed to a destabilization of the C–H bond in the hydrocarbon residue as a result of the electron-pulling effect of the hydroxyl group [963].

For *n*-pentylamine (C_5H_{11}–NH_2), piperidine (6 ring structure with one N atom) and pyridine (benzene structure with one N atom), ammonium formation rates are as follows: *n*-pentylamine≫pyridine > piperidine, while the rate for nitrate formation follows the order: pyridine = piperidine > *n*-pentylamine. In general, aliphatic amines produce higher ammonium to nitrate ratios than compounds containing ring nitrogen [388].

The mechanism of ring opening for pyridine is analogous to that of the aromatic ring in the photocatalytic oxidation of benzene. The reaction is initiated by the addition of a hydroxyl radical followed by a rapid addition of oxygen yielding a 2,3-dihydro-2-peroxy-3-hydroxypyridine radical, which finally decomposes in water to produce aldehyde and formaldehyde [388].

In slightly aerated, acidic TiO_2 solutions, the photocatalytic degradation of nitrobenzene [965,966], nitrophenols [965,967], nitrosophenols [965], aniline [965], aminophenols [967], and phenylhydroxylamine [965] yields quantitative formation

of CO_2, whereas nitrogen is converted both through oxidative and reductive pathways into nitrate and ammonium ions. Nitrobenzene (being more strongly adsorbed on the TiO_2 surface compared to phenol [968], *p*-hydroxybenzoic acid [969], and benzoic acid [970]) is degraded with higher rates. For the same reason α-nitrophenol degrades faster than 4-nitrophenol [971].

$HO^{\bullet}$ radicals do not replace the NO_2 group in nitrocompounds as clearly indicated by the fact that phenol is not detected as an intermediate (Fig. 21) [967]. Nitrophenols degrade faster than aminophenols. This can be understood on the basis of facile back reduction of the initial oxidation intermediates (semiquinone and quinonimine species) of aminophenols. Quinoid related structures formed in the initial oxidation steps of aminophenols, which do not directly originate from nitrophenols, are hardly oxidizable, but easily reduced [972,973]. The reaction pathway, together with the formation of negatively charged intermediates such as carboxylate species, accounts for the slow disappearance of total organic carbon (TOC), which is rather remarkable, especially at high pHs.

The three nitrophenol isomers reveal different photoreactivity. Different photoactivity orders are mentioned, like para > ortho > meta [974] or ortho > meta > para [946,967], due to differences in experimental conditions such as catalyst structure, pH, amount of oxygen, and illumination.

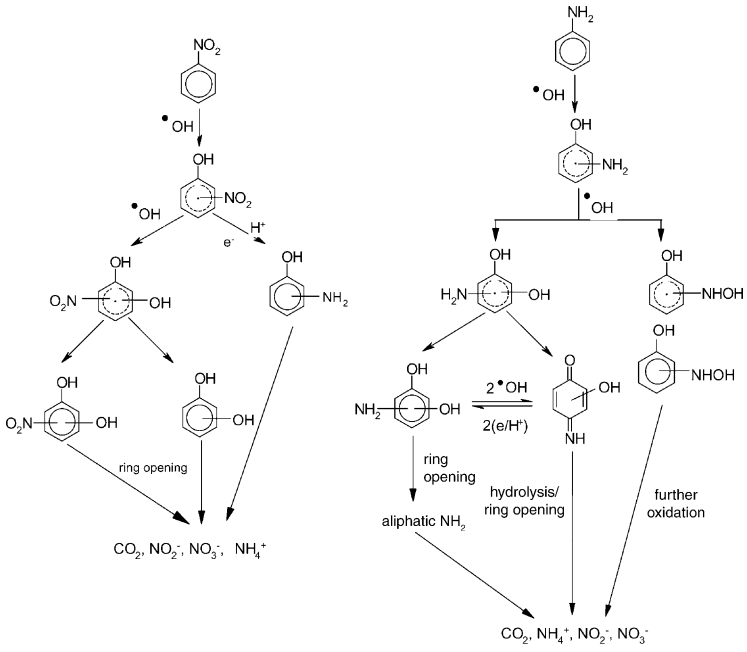

Fig. 21. Decomposition pathways for nitrobenzene and aniline [967].

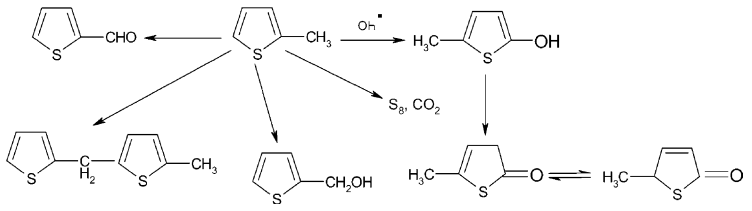

Fig. 22. Photodegradation mechanism of 2-methylthiophene [975].

6.2.4.5 Sulfur-containing compounds. Photodegradation of sulfur-containing heterocyclic compounds is little studied, although alkyl and arylthiophenes are found in petroleum plant wastes. The oxidation of 2-methylthiophene [975] (see Fig. 22) was carried out in a co-solvent system since the compound is not water soluble. The involvement of $HO^{\bullet}$ radicals was proven by the formation of the hydroxylated intermediates 2-hydroxymethylthiophene and 5-methyl-(5H)thiophene-2-one [976]. The formation of dimer structures suggests that the reaction occurs via a radical route. The formation of ring cleavage products S_8 and CO_2 should also be mentioned.

6.2.4.6 Selenium-containing compounds. Selenate compounds (SeO_4^{2-}) poses a great threat due to the fact that they are not easily adsorbed and could end up in drinking water [977]. Photoreduction to Se on TiO_2 is achieved in the presence of formic acid and nitrogen purging [641,978].

6.2.4.7 Humic acids. Humic acids (HAs) are organic macromolecules, formed during degradation of plants and microbial materials [979], with a high molecular weight (100 to several thousands of daltons). Tentatively, the structure exists of a flexible network of aromatic chains bonded by long alkyl structures, containing also oxygen-rich functionalities such as carbonyl, carboxylic, methoxyl, hydroxyl, phenol, and quinoid groups [980]. The structure, molar mass, and functional groups vary depending on origin and age [981]. They account for 90% of dissolved organic carbon in surface water [982] and play an important role as photosensitizer in aquatic processes, complexing agent for heavy metal ions, solubilizing pesticides, hydrocarbons, and organic coating material on mineral surfaces. HAs have received much attention particularly in relation with water treatment since they are precursors of disinfecting by-products (DBPs, e.g., trihalomethanes, haloacetonitriles, haloacetic acids, and 3-chloro-4(dichloromethyl)-5-hydroxy-2(4)furanol [983–985]) due their reaction with chlorine used in water disinfecting. It is therefore imperative that the concentration should be drastically reduced in raw drinking water before chlorination can start.

Some papers reported that humic acids can be effectively degraded (>80%) in TiO_2 suspensions under UV-irradiation [488,986–989]. This photodegradation was studied both in plain and saline waters [990,991]. The kinetics of humic acid degradation are found to be complex due to the heterogeneity and high molecular weight of these compounds. The obtained results are controversial. Some authors

obtain an excellent fit to the LH model [986], others report that this model did not fit [992], due to the high adsorption of humic acid on the TiO_2 surface. The photolysis rate is strongly depending on pH, due to the pH-dependent adsorption of humic acids on TiO_2 (a maximum rate is obtained at pH ≈3–5 [986,988,993,994]) and is also influenced by an increase of the aqueous solutions cation strength ($Ca^{2+} > Mg^{2+}$) [995]. The latter phenomena may originate from a better adsorption of HAs (charge neutralization under neutral pH conditions and bridging via calcium of adsorbed-solution HA [996]).

The photocatalytic degradation occurs via low molecular-weight organic carboxylic acids (4-hydroxybenzoic acid, oxalic acid, succinic acid, malonic acids) as reaction intermediates [982,988,997] to water and CO_2.

Due to the fact that HAs act as natural photosensitizers [866], a viable technology HAs–TiO_2, where HAs serves both as sensitizer and as substrate to be degraded could be developed [488]. But, until now, investigations reveal that visible light irradiation induces little change in DOC, indicating the presence of processes that hinder the photoinduced oxidations. As mentioned earlier, HAs are macromolecules with many redox centers, which could participate both as electron donor centers (oxidation) and as electron accepting centers (reduction). Sequential electron transfer from excited HAs to the TiO_2 conduction band could lead to mineralization with CO_2 evolution, while the electron transfer from the TiO_2 conduction band to HAs tends to inhibit mineralization (Fig. 23). The quinone moieties in the HAs structures have been recognized as the dominant electron acceptors.

6.2.4.8 Cyanobacterial metabolites. The presence of cyanobacterial metabolites such as microcystins (at least 70 hepatotoxic peptides produced primarily by freshwater cyanobacteria) in drinking water causes acute and chronic toxicity [998]. Others, like geosmin (GSM) and 2-methylisoborneol (MIB), are non-toxic, but cause an earthy-muddy taint and imparts nasty taste and odour, which is associated with poor water quality [999]. A complete destruction of GSM and MIB was obtained within 60 minutes of irradiation [1000] and the by-products appear to be non-toxic [1001]. TiO_2 is an efficient photocatalyst for microcystins also, but the rate of photocatalytic destruction is strongly influenced by different amino acid

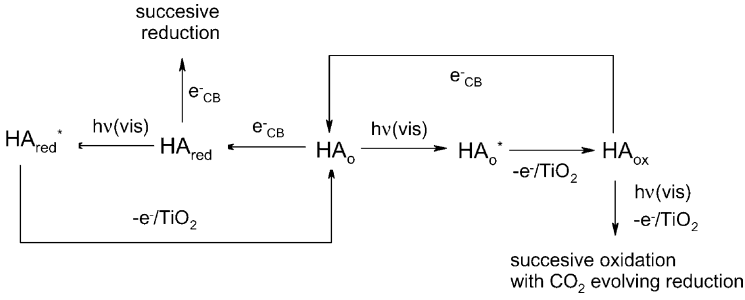

Fig. 23. Sequential photoinduced electron transfers to and from TiO_2 conduction band accompanying transformation of HAs [488].

composition variants of microcystins through charge and hydrophobicity [1002,1003].

6.2.4.9 Oil derivates. Oil derivates belong to the most dangerous compounds for the environment, as they possess large migration abilities both in water and on land. Oil (derivate) spills on water can be cleaned up using TiO_2-coated hollow glass or glass–ceramic microbeads floating at the air–oil interface [1004]. The rate of photooxidation is adequate to maintain the water free of the oily shine often seen around harbours. The photodegradation products are less harmful than those formed from oil destruction by weathering, which produces phenols, polyphenols and eventually tar [1005]. On the other hand, due to the broad spectra of aromatic compounds in oil, polymeric intermediates that strongly absorb may cause photocatalyst deactivation.

TiO_2 deposited on graphite is able to pump up heavy oils into the macropores of the graphite which can subsequently be decomposed by TiO_2 under IR illumination [765].

Despite the fact that mineralization reaches values as high as 90% during photocatalysis of water-soluble crude oil, the generation of transient toxic (for example oxygenated) species has been observed [398].

6.2.4.10 Dyes. Considering the volume and chemical composition of the discharged effluent, the textile dyeing and finishing is one of the major pollutants in industry [1006]. Textile dyes and other commercial dyestuffs have become a focus of environmental remediation in the last few years [1007]. 700,000 t of dyes are annually produced worldwide and about 50% are azodyes [1008]. It is estimated that 15% of the world production of dyes is lost during the dyeing process and is released in the textile effluents [923,1009]. Of dye-containing wastewater more than 4.6×10^7 m^3 in Germany [1010] and more than 1.6×10^9 m^3 in China [648] is discharged annually into the environment. The commonly used method for the treatment of textile wastewater—a combination of biological oxidation and physical chemical treatments [1011]—is quite ineffective in dye decoloration, since dyestuffs are of biorecalcitrant nature, resistant to aerobic degradation [1012] and many may undergo reduction to hazardous compounds (aromatic amines) under anaerobic conditions or in vivo [1013,1014]. Moreover, these chemical treatments only provide a separation of the dyes and produce large quantities of sludge.

In dye photodegradation, most of the visible light in the solar spectrum can be utilized because dyes are able to absorb a large part of the solar spectrum [644,647,1015]. Often, a solar concentrating system is used [1016].

Depending on the nature of the substrate and pH of the solution, three possible mechanisms can contribute to dye degradation: hydroxyl radical attack, direct oxidation by holes, and direct reduction with conduction band electrons (reaction (6.47)) [1017].

$$Dye^* + TiO_2 \rightarrow Dye^{\bullet -} + TiO_2(h^+) \tag{6.47}$$

Photobleaching rates differ significantly among dye families with different functionalities. The first step of the photocatalytic degradation of azo dyes consists of the cleavage of the azo double bond, inducing bleaching in the visible region [643,1008,1018]. Triphenylmethane dyes are found to bleach easier than anthraquinone dyes [1019]. It is also observed that food dyes are, in general, easier to bleach than other dyes [1019]. In terms of the effect of functional groups, the presence of electron withdrawing groups is observed to retard the photosensitized oxidation–bleaching rate [1019].

Additional factors such as sorption characteristic on the TiO_2 surface [648,717,1020–1023], aqueous solubility of the dyes, Fe^{3+} addition [1024,1025], light source [1019], and presence of inorganic salts [1026] may play an important role in the control of photobleaching and mineralization rates [1019].

From a kinetic point of view, most of the processes follow an LH model [1027].

6.2.4.11 Surfactants. Surfactants are increasingly used in domestic and industrial fields [1028] and although most are in principle biodegradable, there are some resistant components or they can be generated during degradation. Alkylbenzenesulfonates, for example, are resistant to bacterial attack.

Photodegradation of dodecylbenzenesulfonate (DBS) and sodium dodecylsulfate (DS) [1029] shows that DS is degraded more slowly than DBS because it has no aromatic ring. The aromatic moiety in DBS is photodegradated more rapidly than its alkyl chain.

6.2.4.12 Pesticides. A wide variety of pesticides is nowadays introduced into water systems from various sources such as industrial effluents, agricultural runoff, and chemical spills [1030,1031]. The production of pesticides has nearly doubled every 5 years since 1975. It is estimated that less than 1% of all pesticides used in agriculture actually reaches air or water. They are toxic (among the possible chronic effects are carcinogenesis, neurotoxicity, and effects on reproduction and cell development particularly in the early stage of life [904]), stable-to-natural decomposition, and persistent in the environment. Therefore, pesticide pollution of water is one of today's greatest environmental problems. The maximum allowed concentrations of pesticides and their degradation products are established by regulations [1032,1033].

Until now, total mineralization was observed for all pesticides at longer irradiation times. An exception is *s*-triazine herbicide, which during degradation formed highly stable triazine nuclei refractory to photocatalytic reactions. In the end, cyanuric acid (2,4,6-trihydroxy-1,3,5-triazine)is formed, which is chemically very stable towards oxidative attack [363, but is fortunately non-toxic.

The large number of compounds detected during degradation of organic pollutants shows the complexity of degradation routes as a result of multi-step and interconnected pathways. The formed reaction intermediates may be more toxic than their parent compounds. As an example, degradation of chlorothalonil and organophosphorous insecticides yields tetrachloro-2,3,4,6-phenol ((2,4,5,6-tetrachloro-1,3-benzenecarbonitirle) [386] and ozone derivates [365].

The degradation and mineralization of some pesticides [925,1034], herbicides [915], and insecticides [925] are found to be higher under solar irradiation compared to artificial irradiation.

The intermediates of pesticide degradation are long-living compounds that are classified into five classes [365]:

- hydroxylated products and derivates (usually after dehalogenation of the parent pesticide if halogen substituents are present);
- oxidation products of the side chains (if present);
- ring-opening products in case of aromatic pesticides;
- decarboxylation products;
- isomerization and cyclization products.

6.2.5. Inorganic compounds

6.2.5.1 Thermodynamic aspects. The most important parameter to determine the thermodynamic potential of a photocatalytic system to reduce or oxidize metallic species is the redox level of the metallic couples related to the levels of conduction and valence bands of the catalyst. Only when the reduction potential E^0 of the M^{n+}/M couple is less negative than the energy level of the bottom of the conduction band, reduction of the metal ion is possible. Metal cations whose potentials do not permit their reduction can be oxidized and deposited on the semiconductor as insoluble oxides [1035].

In the absence of other organic species, the conjugated oxidation reaction of metal-ion reduction is the oxidation of water, which is a kinetically slow for electron-process. The competing recombination of the photogenerated holes and electrons plays an active inhibiting role also [1036]. Therefore, to prevent limitation of the photocatalytical reduction of metals, the addition of hole trapping sacrificial electron donors such as organic acids and alcohols is necessary [1037–1039].

Two kinds of electron-donating processes can occur depending on the nature of the organic additives during the reaction, namely a direct and an indirect one [1038]. In the former case, electrons from organics (e.g., EDTA) are directly injected into the valence band, thereby attenuating the electron–hole recombination, leaving more conduction band electrons available for the reduction of metal ions. As a result, the addition of these organics has a pronounced effect on the reduction of metals. In the latter case (e.g., methanol, 4-nitrophenol, salicylic acid), holes are filled only through the formation of hydroxyl radicals, and these radicals are sequentially consumed by the oxidation of added organics. Thus, organics in this class influence the reduction of metal ions indirectly, resulting in a less prominent effect. Two hole scavengers have to be specially mentioned. Formic acid influences metal reduction in two ways [1040–1042]. Firstly, formate can scavenge the photogenerated holes and, secondly, the initial oxidation of formate by photogenerated holes and/or hydroxyl radicals yields $CO_2^{\bullet-}$ which is strongly reducing ($E^0(CO_2^{\bullet-}/CO_2) = -1.8$ V) and can, hence, also take part in the photoreduction process. The enhancement role of methanol in photoreduction of metals is attrib-

uted to a phenomenon known in electrochemistry as the "current-doubling effect"[1042]. Under UV light and in the presence of TiO_2, methanol is oxidized by photogenerated holes, producing the electron-donating species $^{\bullet}CH_2OH$ ($E^0(^{\bullet}CH_2OH/CH_2O) = -0.95$ V). Due to its large negative potential, this methanol radical can inject an electron into TiO_2 increasing the amount of electrons that can subsequently participate in reduction reactions.

Depending on solution parameters (pH and concentration of metal ions) the photogenerated electrons may reduce protons, water, dissolved oxygen, and metallic ions (Figs. 24 and 25) [8]. pH dependent are only $\varphi(Cr^{6+}/Cr^{3+})$ and the positions of the conduction and valence bands. The photocatalytic reduction of metal ions is favoured by a higher pH. The photocatalytic reduction of Au^{3+}, Cr^{6+}, Hg^{2+} (including $HgCl_2$ and $HgCl_4^{2-}$), Ag^+, Hg_2^{2+}, Fe^{3+}, Cu^+, and Cu^{2+} is thermodynamically feasible. Among the above-mentioned metal ions, Fe^{3+} and Cr^{6+} can only be reduced to Fe^{2+} and Cr^{3+}, respectively. Cd^{2+}, Fe^{2+} and Cr^{3+} cannot be photocatalytically reduced because their reduction potentials are close to or more negative than that of the photogenerated electrons.

Oxygen is a possible electron scavenger, which competes with metal ions for electrons and might retard the photocatalytic reduction activity of metal ions with lower redox potential such as Hg^{2+} [8,1043,1044], Ag^+ [8], and Cu^{2+} [8]. Therefore, if the reaction is performed in a solution purged with nitrogen or air, or

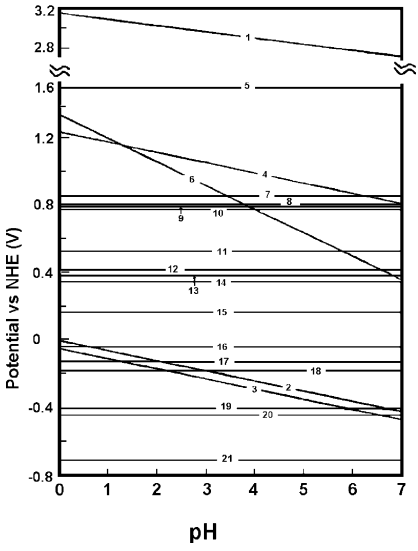

Fig. 24. Positions of the valence and conduction bands of TiO_2 (anatase) and the reduction potentials of metal ions (1 M) at different pHs (calculated from the Nernst equation) [8] 1 E_{VB}; 2 E_{CB}; 3 φ (H^+/H); 4 φ (O_2/H_2O); 5 φ (Au^{3+}/Au); 6 φ (Cr^{6+}/Cr^{3+}); 7 φ (Hg^{2+}/Hg); 8 φ (Ag^+/Ag); 9 φ (Hg^+/Hg); 10 φ (Fe^{3+}/Fe^{2+}); 11 φ (Cu^+/Cu); 12 φ ($HgCl_2/Hg$); 13 φ ($HgCl_4/Hg$); 14 φ (Cu^{2+}/Cu); 15 φ (Cu^+/Cu); 16 φ (Fe^{2+}/Fe); 17 φ (Pb^{2+}/Pb); 18 φ (Ni^{2+}/Ni); 19 (Cd^{2+}/Cd); 20 φ (Fe^{3+}/Fe); 21 φ (Cr^{3+}/Cr).

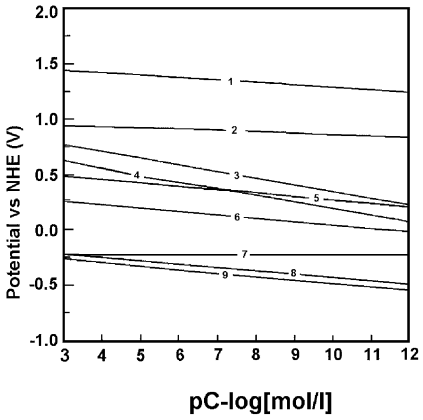

Fig. 25. Position of the conduction band of TiO_2 (anatase) and the reduction potentials of metal ions at pH 3 for different concentrations calculated from the Nernst equation [8] 1 Au^{3+}/Au; 2 Cr^{6+}/Cr^{3+}; 3 Fe^{3+}/Fe^{2+}; 4 Ag^{+}/Ag; 5 $HgCl_2/Hg$; 6 Cu^{2+}/Cu; 7 E_{CB}; 8 Pb^{2+}/Pb; 9 Ni^{2+}/Ni.

sealed to eliminate oxygen reduction, the photocatalytic reduction efficiency of metal ions can be enhanced.

The reduction potential of metal ions is concentration dependent. The driving force for the photocatalytic reduction decreases with the decrease in the concentration of the dissolved ions (Fig. 25). So, in time, the reaction slows down. However, all metal ions with the exception of Pb^{2+} and Ni^{2+} can be photocatalytically reduced, at least thermodynamically, to a concentration as low as 10^{-12} M.

The surface of colloidal TiO_2 can be modified with organic compounds containing two functional groups (e.g., carboxylic and thiol or amino) [1045,1046], which leads to two effects. Firstly, it facilitates a selective adsorption of metal ions on the TiO_2 surface through chelation, because of electrochemical changes in the colloidal and metallic ions, which enhance the reduction properties of conduction band electrons [1047]. Secondly, it introduces also deeper trapping sites outside the photocatalyst particles leading to a greater separation of the photogenerated charges [1048,1049]. As a consequence, reactions not previously possible on the TiO_2 surface are now allowed [1045,1050].

6.2.5.2 Reduction of metal ions. The development of industries increases the demand for metals significantly. Waste metal recovery can potentially resolve two issues: metal pollution prevention and resource conservation. Metal ions are generally non-degradable, they have infinite lifetimes and build up their concentrations in food chains to toxic levels. It is well known that Hg^{2+}, Pb^{2+}, Cd^{2+}, Ag^{+}, Ni^{2+}, and Cr^{6+} ions are very toxic. Their concentration in drinking water has been regulated in many countries and they are included in the list of priority pollutants by the US Environmental Protection Agency (EPA) [1051]. Concentrations lower than 0.005 ppm are allowed for Cr^{6+}, Cu^{2+}, Ni^{2+}, 0.004 ppm for Pb^{2+}, and 0.001 ppm for Hg^{2+}. The recommended level of Cd^{2+} is

<5 ppm, being also included in the priority list of EPA. The toxic effect of Ag^+ is not completely understood, but it is known as an effective bactericide and consequently it can damage biological systems. Therefore, in several US municipal waters concentrations as low as 0.05–5 ppm are permitted and is also included in the EPA list.

Common chemical and physical methods currently adopted for disposal or recovery of metal ions from wastewater include hydroxide precipitation (by far the most commonly used process), activated carbon adsorption, ion exchange, electrolytic processes, and membrane separation [1052]. All these methods have their own advantages and disadvantages. Among the disadvantages, we can mention: pH dependence, unselective metal recovery, inefficiency at extremely low or high concentrations, and generation of wastes (with the exception of electrolytic process) that must be often disposed of as hazardous.

Photocatalytic purification leads to the deposition of environmentally harmful toxic metals on the surface of the semiconductor, which can subsequently be extracted from the slurry by mechanical and/or chemical methods [1053]. Metal cations, whose potential does not permit their reduction, can be oxidized and deposited on the semiconductor as insoluble oxides [1054]. There are reports concerning Cu^{2+} [1055], Hg^{2+} [1056–1058] Ag^+ [1059–1063,1065,1066], Pt^{4+} [1059,1063,1067,1068] Pd^{2+} [1069,1070] Au^{3+} [1069,1071,1072], U^{4+} [1073], Ni^{2+} [1040], and Cr^{6+} [158,739,1038,1039,1074–1076] removal. In the following sections, examples of successful utilization of TiO_2 in metal ion removal are presented.

Chromium (*VI*). Successive one-electron transfer reducing steps are proposed to take place for Cr^{6+} reduction using TiO_2 and Fe–TiO_2 photocatalysts. First, very unstable Cr^{5+} is formed, which is then reduced to Cr^{4+} and Cr^{3+}, the stable final species. The standard redox potential for CrO_4^{2-}/CrO_4^{3-} is 0.1 V [1077], positive enough to allow this first reduction by TiO_2 conduction electrons. The photocatalytical reaction is more feasible at low pH, because the net reaction consumes protons, but neutral and alkaline conditions can be more convenient because Cr^{3+} can be precipitated as hydroxide avoiding expensive separation steps [1078,1079]. The reaction is very slow in the absence of holes or $HO^\bullet$ scavengers, but in the presence of reducing agents, Cr^{6+} reduction is strongly accelerated [548,1079–1081]. The specific nature of the reducing compound is important: low molecular acids, alcohols, and aldehydes do not yield a large effect, while easily oxidizable organics such as EDTA, salicylic acid, and citric acid provide very fast reduction rates.

Nickel(*II*). In the case of Ni^{2+}/Ni^0 ($E^0 = -0.23$ V), conduction band electrons of TiO_2 cannot directly reduce the cation at pH < 7 and an oxidative route is obviously not possible because a higher oxidation state of nickel does not exist in common conditions [1082]. An indirect photoinduced reduction, however, can take place via the strongly reducing intermediate $CO_2^{\bullet -}$, which is produced by oxidation of oxalate, if present in the reaction medium. $Ni^I \rightarrow Ni^0$ reduction further occurs either by an additional $CO_2^{\bullet -}$, a conduction band electron, or by disproportion to Ni^{II} and Ni^0 [1082]. The rate of photocatalytical removal of Ni^{II} salts varies in the order $SO_4^{2-} < Cl^- < CH_3COO_3^-$ and is increased by formate addition [1040].

Copper(*II*). For the removal of Cu^{2+}, the presence of oxygen is generally detrimental, because the reduction of water, H_2O_2, or even superoxide radicals by conduction band electrons is favoured [1083].

Deposition of copper is obtained in the presence of hole scavengers like formate, oxalate, citric acid, EDTA, low molecular weight primary and secondary alcohols, propionic acid, isobutyric acid, chloroacetic acid, and lysine, but not in the presence of *tert*-butanol, acetate, propionate, butyrate, acetone, SA, and ethylacetate [1084,1085,1086]. No correlation between copper deposition and physical–chemical properties of the scavengers is found. An enhanced photoreduction is obtained, when the TiO_2 surface is modified with alanine, which transports photoelectrons from the photocatalyst surface to the metallic cation [1087].

Generally, copper is deposited from aerated solutions as a mixture of Cu^{I} and Cu^0. Cu^{I} is spontaneously reoxidized to Cu^{II}. Cu_2O and Cu^0 deposition is found in the presence of phenol [882], formate [1088], EDTA [1089], and nitriloethanol [1089]. For the last two, neutral or alkaline solutions are requested. At a pH of ~5, only EDTA is able to yield Cu_2O and Cu^0. Cu^0 deposits are reported using formate as a hole scavenger in a deaerated solution [1086].

Ag(*I*). The removal of Ag^+ and deposition as Ag^0 from photographic-processing waste in the presence of $S_2O_3^{2-}$ is reported using UV or solar IR irradiation [1090]. Thiosulfate acts in low concentration as hole scavenger increasing the photoreduction rate, while at high concentrations, it acts as a silver stabilizer, hindering photocatalysis.

Two mechanisms for the formation of colloidal silver particles are proposed:

– aggregation of silver atoms [1059]:

$$m\mathrm{Ag}^0 \rightarrow \mathrm{Ag}_m \tag{6.47}$$

– a sequence of alternating electric and ionic events which build up the Ag^0 particle in a similar way as the latent image cluster in silver halide photography [1059,1091]:

$$\mathrm{Ag}^0 + \mathrm{Ag}^+ \rightarrow (\mathrm{Ag}_2)^+ \xrightarrow{e^-} \mathrm{Ag}_2 \xrightarrow{Ag^+} (\mathrm{Ag}_3)^+ \rightarrow \cdots \mathrm{Ag}_n \tag{6.48}$$

The basis of the latter mechanism is that metal crystallites are rich in photoproduced electrons and constitute sites for cathodic-like reduction of cations, which could progressively increase the size of the metal deposits [1059].

Gold(*III*). The reaction is strongly pH dependent, the optimum pH being around 5–6. At pH 0, photoreduction occurs only by methanol addition as hole scavengers [1092].

Although the recovery of gold from aqueous chloride solution is easy, in the presence of CN^-, the reduction of formed $Au(CN)_4^-$ complexes is achieved only in the presence of hole scavengers like methanol [1093].

Hg(*II*). Generally, the photocatalytic reduction of Hg^{2+} is strongly dependent on the nature of the mercuric salt and pH [373].

In the absence of oxygen, the photocatalytic rate is found to vary in the following order: nitrate > chloride > perchlorate (pH 3.7 and 11 with the faster trans-

formation at pH 11) [1094]. Nitrate yields better removal of Hg(II) from solution compared to chloride, because $Hg(NO_3)_2$ ionizes in solution, whereas $HgCl_2$ is only slightly dissociated and hence more difficult to reduce. Oxygen competes with Hg(II) ions for the photogenerated electrons in air-equilibrated suspensions [1094,1095]. Inhibition by oxygen is observed in acidic and neutral media but not in basic ones [1094,1096]. The deposits consist of Hg^0, HgO and Hg_2Cl_2, depending on the initial conditions.

$Hg(CN)_2$ and $Hg(CN)_4$ pollutants originating from precious metal separation processes, may be removed in an alkaline solution with an yield of more than 99%. Hg^0 and HgO are deposited and CN^- is oxidized to nitrate [1097].

A complete mineralization of phenylmercury chloride (pesticide) [1098] and mercurochrome dye ($C_{20}H_8Br_2HgNa_2O_6$, mebromim) [1043] in oxygenated solutions is obtained with Hg^0 sedimentation. The latter occurs only by the addition of citric acid. Methylmercury (CH_3HgCl) reduction is only possible in the presence of methanol and in the absence of oxygen [1099,1100]. The modification of TiO_2 with thiolactic acid has an inhibitory effect, contrary to Cd^{2+} [1045], probably due to the formation of HgS (Hg has a high affinity for sulfur) [1045].

Platinum(II). The reduction of $[PtCl_6]^{2-}$ to Pt^0 is thermodynamically possible. The presence of hole scavengers such as acetate [1082,1101] and methanol [1102] increases the reaction rate. Low pH [1102–1104], low light intensity [1103], high ionic strength [1103], and low oxygen content [1103] facilitate the photoreduction.

Lead (II). In the case of Pb^{2+}, which has a relatively negative E^0 value ($E^0(Pb^{2+}/Pb^0) = -0.126\ V$), the direct route is forbidden or very difficult using TiO_2 photocatalysts. Pb^{2+} reduction to Pb^0 is possible when TiO_2 particles are complexed with, for example, cysteine [1105], which forms new trapping sites for electrons and holes (thus changing the redox properties of the semiconductor) and increases simultaneously the adsorption of metal ions.

More often the oxidation route through hole attack is used. In air and with TiO_2 and Pt/TiO_2 photocatalysts, PbO and PbO_2 can be deposited, respectively [1106]. In a solution containing nitrobenzene and $Pb(NO_3)_2$ (10^{-5}–10^{-4} M) at pH $\approx$ 6, the degradation of the organic pollutant and PbO_2 deposition simultaneously occurs [387].

Separation of mixtures. The pH and the presence of oxygen and hole scavengers are important parameters for selective separation of metals from a mixture. Some examples:

- the separate extraction of Ag^+ and Cu^{2+} in the presence of $S_2O_3^{2-}$ from photographic fixing baths [1059]. After illumination, Ag^0 is totally and selectively reduced, and $S_2O_3^{2-}$ is simultaneously oxidized to SO_4^{2-};
- the nearly sequential removal of platinum, gold, and rhodium from a mixed solution of their chlorides using a finite level of dissolved oxygen to delay rhodium reduction. In most industrial gold recovery processes, cyanide is present and must be removed before photocatalysts are used to extract gold [1093].
- Mn^{2+}–Fe^{3+}–Co^{2+}–Mn^{2+}–Ni^{2+}-, and Cu^{2+} complexes with EDTA [1107] are degraded (organic compound elimination and deposition of the metallic species), in the following rate order: $Fe^{3+} > Cu^{2+} > Zn^{2+} > Mn^{2+} > Co^{2+}$.

6.2.5.3 Oxidation of inorganic anions. As mentioned earlier, one of the first studies on TiO_2 heterogeneous photocatalysis was the oxidation of cyanide [25,26]. The cyanide ion is converted into isocyanide [25,26,1108], nitrogen [1109], or nitrate [152,713,1110,1111].

In aqueous phase, ammonium undergoes a relatively slow photooxidation, as shown by a low conversion yield (~38%) for ammonium chloride solutions [1112], while nitrite anions are converted to nitrates [1036,1113].

The best investigated inorganic anion is cyanide. The presence of cyanides in effluents related to coal gasification and electroplating processes (in which the utilization of cyanides is almost essential) is an environmental concern, which is not well solved nowadays.

Many mechanistic studies describe the direct charge transfer from TiO_2 to cyanide [25,1108–1110,1114], although oxidation via indirect (adsorbed hydroxyls) or homogeneous pathways (diffused radicals) is also reported [1093,1115].

The elimination of cyanide ions from wastewater is also possible using solar irradiation [1116]. TiO_2/porous silica shows also a reasonable activity for cyanide photodegradation and improved separation properties. The use of mesostructured silica SBA-15 supports leads to the best activity [713].

The photooxidation of $[Fe(CN)_6]^{3-}$ in an aerated solution proceeds simultaneously via two routes [713,870]:

- homogeneous degradation, in which cyanide ions are released from the complex through a substitution reaction of the cyanide ligands by hydroxyl groups and/or water molecules;
- heterogeneous degradation, in which the photocatalyst promotes the subsequent oxidation of released cyanide to cyanate species.

Photooxidation of nitrite to nitrate ions occurs in the presence of H_2O and O_2, as the oxidizing power of the $^{\bullet}OH$ radicals is strong enough. The following mechanism (reactions 6.49–6.56) for the photocatalytic oxidation of nitrite has been proposed [1113,1114]:

$$NO_2^- + {}^{\bullet}OH \rightarrow {}^{\bullet}HNO_3^- \leftrightarrow ({}^{\bullet}NO_3)^{2-} \tag{6.49}$$

$${}^{\bullet}HNO_3^- \rightarrow {}^{\bullet}NO_2^- + OH^- \tag{6.50}$$

$$({}^{\bullet}NO_3)^{2-} + H_2O \rightarrow {}^{\bullet}NO_2^- + 2OH^- \tag{6.51}$$

$$2{}^{\bullet}NO_2^- \rightarrow N_2O_4 \tag{6.52}$$

$$N_2O_4 + H_2O \rightarrow NO_3^- + NO_2^- + 2H^+ \tag{6.53}$$

$${}^{\bullet}NO_2^- + {}^{\bullet}OH \rightarrow HO_2NO \tag{6.54}$$

$$HO_2NO \leftrightarrow NO_3^- + H^+ \tag{6.55}$$

$$({}^{\bullet}NO_3)^{2-} + O_2 \rightarrow NO_3^- + {}^{\bullet}O_2^- \tag{6.56}$$

No significant loss of photocatalytic activity for this oxidation reaction is registered after 150 h of illumination [1117].

Doping TiO_2 with rare earth metals increases the photoactivity of nitrite oxidation in the following order: $Gd^{3+} > Nd^{3+} > La^{3+} > Pr^{3+}(Er^{3+}) > Ce^{3+} > Sm^{3+}$ [554]. The photodegradation rate is higher than that for bare TiO_2 due to the higher absorption (red shift) and increase of interfacial electron rate. The highest enhancement in photoactivity is obtained for ca. 0.5 wt% rare-earth-ion doping (which may favour an efficient separation of the charge carriers). The photocatalytic degradation reaction of nitrite over Gd^{3+}-doped sample follows apparent first-order kinetics, different from the other RE-doped titania, which obey zero-order kinetics, indicating that the photochemical process is dominated by electron–hole recombination (see Table 2).

6.3. Air cleaning

6.3.1. General remarks

Substances emitted into the atmosphere by human activities, in urban and industrial areas, cause many environmental problems including air quality degradation, global warming, climate change, and stratospheric ozone depletion.

Volatile organic compounds (VOCs) are major air pollutants, originating largely from industrial processes. Generally, methods for air cleaning can be divided into two categories, namely combustible and non–combustible processes [1181]. In non-combustible processes, VOCs released from the waste gas are collected. The major techniques in this area include adsorption, condensation, and biological filtration. In combustible processes, VOCs in the gas phase are destroyed by thermal and catalytic incineration. Both of these technologies have disadvantages and limitations in practical applications. For example, the efficiency of activated carbon adsorption significantly decreases at temperatures higher than 38 $^{\circ}C$. Moreover, disposal of the used carbon is a problem. Although thermal incineration is quite effective, it consumes significant amounts of auxiliary fuel. While catalytic incineration may be operated at a lower temperature than that for thermal incineration, catalytic incineration is relatively costly and causes wastage problems as well.

Although, initially TiO_2 photocatalysts were applied for water treatment, in recent years, it has been shown that the photocatalytic detoxification of volatile organic compounds is generally more efficient in the gas phase compared to the liquid phase. Thus, attention for the application of this technology for air treatments increases, including the utilization of pollutant air stripping from the liquid phase (used to separate halogenated and non-halogenated VOCs from water, but ineffective for contaminants with low vapour pressures or high solubilities such as inorganic salts). It has been reported that the use of illuminated TiO_2 can result in the overall degradation of VOCs together with nitrogen oxides and sulfur oxides in air [446,1182–1185].

Photocatalytic oxidation (PCO) is shown to be more cost-effective than incineration, carbon adsorption, or bio-filtration for flow rates up to 20,000 cfm (ft^3/min) for treating a 500 ppm VOC-laden stream [1185].

Photocatalyzed oxidation treatment of air offers the following distinctive advantages when compared to competitive technologies:

Table 2
Organic compounds photodegradated in water

Compounds		Photocatalyst	References
Aromatic hydrocarbons	Benzene	TiO_2/molecular sieves	[735]
		TiO_2/ZSM-5	[897]
	Toluene	TiO_2	[935,1118]
		TiO_2/ZSM-5	[897]
	Naphthalene	TiO_2	[355]
Halogenated compounds	CH_2Cl_2	TiO_2	[1119]
	$CHBr_3$	TiO_2/C	[746]
	Trichlorethane (TCE)	TiO_2	[462,922]
	1,2-Dibromo-3 chloropropane	TiO_2	[1119]
	Monochlorobenzene	TiO_2/molecular sieves	[735]
	1,2 Dichlorobenzene	TiO_2/molecular sieves	[735]
	1,4-Dichlorobenzene	TiO_2	[462]
	2-Chlorobiphenyl	TiO_2	[475]
Hydroxylated compounds	Methanol	Fe–TiO_2	[171]
	2-propanol	TiO_2	[1120]
		Fe–TiO_2	[1121]
	1,2-propylene glycol	TiO_2	[935]
	Phenol	TiO_2	[461,1122,1123]
		TiO_2/molecular sieves	
		TiO_2/silica	[715]
		TiO_2/carbon	[763,767,925]
		TiO_2/zeolite	[747]
		TiO_2 + zeolite	[747]
		TiO_2, $M^{n+}TiO_2$ ($M^{n+} = Li^+, Zn^{2+}$)	[214]
	m-Propyl phenol	TiO_2	[940,943]
	o-Cresol	Fe/TiO_2	[579]
		TiO_2	[942]
	m-Cresol	TiO_2	[940,943]
	o-, *m*-, *p*-Cresol	TiO_2	[436]
	Bisphenol A	TiO_2	[953]
		TiO_2/pillared clays	[750]
	4,4′-Ethylidenebisphenol	TiO_2	[953]
	4,4′-Methylenebisphenol	TiO_2	[953]
Ethers	*o*-Methoxy phenol	TiO_2	[942]
	m-Methoxy phenol	TiO_2	[940–942]
	p-Methoxy phenol	TiO_2	[941]
	Meta- and para-substituted methoxybenzenes, NH_2, NO_2, -F, -Cl	TiO_2	[941]
Sulfur-containing compounds	2-Methylthiophene	TiO_2	[975]
	3-Nitrobenzenesulfonic acid	TiO_2, TiO_2/supports	[1124,1125]
	2,5 Anilinedisulfonic acid	TiO_2, TiO_2/supports	[1124,1125]
	o-Phenol sulfonic acid	TiO_2	[940,943]
	Sulfosalicylic acid	TiO_2	[529]
	2-Mercaptobenzothiazole	La–TiO_2	[229]

Table 2 (*continued*)

Compounds		Photocatalyst	References
Nitrogen-containing compounds	CH_3CN	TiO_2	[1126]
	$C_2H_5NH_2$ $(C_2H_5)2NH_2$	TiO_2	[964]
	Nitrobenzene	TiO_2	[371,965,966]
	Aniline	$TiO_2 + O_3$	[920]
	Phenyltetrazole	TiO_2	[645]
Halogen–nitrogen containing compounds	Cetylpyridinium chloride ($C_{21}H_{38}NCl$)	TiO_2	[238]
S–N containing compounds	Phenylmercaptotetrazole	TiO_2	[645]
	Mercaptotetrazole		[645]
	Phenylmercaptotetrazole	TiO_2	[645]
Aldehydes, ketones	Formaldehyde	TiO_2	[1127]
	Acetophenone	TiO_2/SiO_2	[713]
	Salicylaldehyde	TiO_2	[940,943]
	Methyl salicyl ketone	TiO_2	[940,943]
Acids	Formic acid	TiO_2	[742]
		$TiO_2 + O_3$	[911]
		$Co–TiO_2$	[224]
	Oxalic acid	TiO_2	[928,931,1128]
	Butanoic acid	TiO_2	[376]
	Octanoic acid	TiO_2	[661]
	Malic acid	TiO_2	[194,371,438,725]
	Benzoic acid	W/TiO_2	[224]
	p-Cumaric acid	TiO_2 (70%a + 30%r)	[349]
	Polycarboxylic benzoic acid 1,2,3-, 1,2,4-, 1,2,4,5-	TiO_2	[458]
	Salicylic acid	TiO_2	[158,940,943]
		$ZrO_2–TiO_2$	[158]
		$Ln_2O_3–TiO_2$ (Ln^{3+} = Eu, Pr, Yb)	[153]
		TiO_2/zeolite, molecular sieve	[748]
	Humic acid	TiO_2	[990–993,1130]
		$Fe_2O_3–TiO_2$	[683]
	2-Chlorobenzoic acid	TiO_2	[371]
Amide	Benzamide	TiO_2/glass fiber	[706]
Esters	K hydrogen phthalate	TiO_2	[1131]
	Dimethyl phthalate	TiO_2/pillared clays	[750]
	Diethyl phthalate	TiO_2/pillared clays	[750]
		TiO_2	[913]
	Di-*n*-butyl phthalate	TiO_2/pillared clays	[750]

(*continued on next page*)

Table 2 (*continued*)

Compounds		Photocatalyst	References
Halogenated–hydroxylated compounds	2-Chlorophenol	TiO_2	[489,940,942,943] [933,1132,1133]
		TiO_2/C	[720]
	2-Fluoro, bromo and iodophenol	TiO_2	[940,943]
	4-Chlorophenol	TiO_2	[371,461,514,1134, 1135]
		TiO_2/zeolite	[747]
		TiO_2 + zeolite	[747]
		Au/TiO_2	[640]
		Ag, Pt/TiO_2	[638]
		$TiO_{2-x}N_x$	[595]
		$PtCl_4$, $RhCl_3$, $AuCl_3$/TiO_2	[662–665]
		TiO_2 + coke	[962]
	2,4-Dichlorophenol	TiO_2	[961,1133,1136]
	3,4-Dichlorophenol	TiO_2, TiO_2–SnO_2	[478]
	3,5-Dichlorophenol	TiO_2/TiO_2	[215]
	2,4,6-Trichlorophenol	TiO_2	[961]
	Pentachlorophenol	TiO_2	[442]
Nitro-hydroxylated compounds	2-Nitrophenol	TiO_2	[946,1137]
	3-Nitrophenol	TiO_2	[940,943,1037]
	4-Nitrophenol	TiO_2	[461,879,1137, 1138]
		TiO_2(a)/TiO_2(r) and Al_2O_3	[772]
		W–TiO_2	[224]
		Cu–Pd/TiO_2	[655]
	2,3,4-Trinitrophenol	TiO_2	[436,967,971,974,1133]
	2,3,5-Trinitrophenol	TiO_2	[1133]
	2,4,6-Trinitrophenol	TiO_2	[1139]
	1,2,3,4,5,6-Hexaninitrophenol	TiO_2	[1133]
Amino-hydroxylated compounds	$HOC_2H_4NH_2$, $(HOC_2H_4)_2NH$, $(HOC_2H_4)_3N$,		[964]
	2,3,4-Triaminophenol	TiO_2	[967]
	N methyl-*p* aminophenol	TiO_2 + H_2O_2	[917]
	Pyrimidines Uracil Thymine 6-Methyluracil	TiO_2	[1140]
	EDTA	TiO_2	[1141]
		Pt/TiO_2	[633,1142]
Oil		Ti + KOH	[1143]
		K-, Ca-, Ba^--TiO_2	[1144]
P-containing compounds	Dimethyl phenylphosphone	TiO_2	[1145]
Oestrogen compounds		TiO_2/Ti–6Al–4V	[1146]
Cellulose and paper industry	Lignin fragments, SO_4^{2-}, Cl^-	TiO_2	[916]

Table 2 (*continued*)

Compounds		Photocatalyst	References
Dyes	Azodyes	TiO_2	[639,716,717,749, 907,927,1016,1020, 1022,1023,1147–1155]
		Pt/TiO_2	[636]
	Anthraquinonic dye	TiO_2	[918,1022,1156]
	Heteropolyaromatic dye	TiO_2	[1022]
	Arylmethane	TiO_2	[919,1020,1148]
	Mixtures of dyes	TiO_2	[1021]
Pesticides, herbicides, insecticides	s-Triazines and sulfonylurea herbicides	TiO_2	[368,391,1034,1157–1159]
	Anilide and amide herbicides	TiO_2	[383,1160]
	Pyrimide pesticides	TiO_2	[1161]
	Thiocarbamate herbicides	TiO_2	[370,380,383,1162]
	Phenylurea herbicide	TiO_2	[391,444,1163–1165]
	Organophosphorous insecticides	TiO_2	[391,438,1165–1167]
	Imidazoline herbicide	TiO_2	[915]
	Carbamate insecticides	TiO_2	[487,1165,1168]
	Organochlorine pesticides	TiO_2	[386,1170–1173]
	Phenol based pesticides	TiO_2	[1165,1172,1174,1175]
	Chlorophenol pesticides	TiO_2	[580,1177]
	Miscellaneous	TiO_2	[450,954,1163, 1178–1180]

– it is able to oxidize low-concentration and low flow rate waste streams at, but not limited to, ambient temperatures and pressures [1186];
– gas phase reactions allow the direct application of analytical tools to monitor the composition, structure, and electronic state of the substrate and adsorbates and hence the reaction mechanisms can be directly elucidated [1187,1188];
– photocatalytic reactors may be integrated into new and existing heating, ventilation, and air conditioning systems (HVAC) due to their modular design, room temperature operation, and negligible pressure drop. Additionally, they may be scaled to suit a wide variety of indoor air quality applications [1189];
– it offers potential utilization of solar energy.

Compared to photocatalytic reactions in solution, gas phase processes have the following advantages:

– relatively low levels of UV light are needed;
– the diffusion of both reagents and products is favoured;
– $HO^{\bullet}$ scavengers present in solution (such as Cl^-) do not interfere and electron scavengers such as O_2 are rarely limiting [1190];
– the amount of photons adsorbed by air is negligible

– the values of the formal quantum efficiency of the photodegradation are usually 10-fold higher than those found for photodestruction of some organic substrates in aqueous solutions [468,1186,1191].

As a consequence, the use of TiO_2 photocatalysis for air purification has caught the interest of the industry. The performance of such a treatment system heavily depends on the design of an efficient photocatalytic reactor. Such treatment systems usually employ immobilized photocatalysts on solid substrates, except for reactors using packed powder layers [446] or fluidized powder beds [1192]. The most common immobilized photoreactors are annular plug flow reactors [470,485,530,1193] and honeycomb reactors [1194].

As limitations of the method, we mention [1]:

– incomplete mineralization of some aromatics and halothanes;
– generation of relatively stable intermediate(s) (such as phosgene from trichloroethylene), which are more toxic than the initial substrate;
– not useful in breaking down large volume of soilage, but capable of destroying accumulations;
– deactivation due to by-products. While in aqueous phase, water helps to remove reaction intermediates and reaction products from the catalyst surface, in the gas phase these species tend to accumulate at the surface causing deactivation;
– mass-transport issues associated with high-flow rate systems [1195,1196].

6.3.2. Cofeeding processes

A potential method to increase the PCO efficiency involves the introduction of a second more reactive contaminant such as TCE [471,1188,1197–1198], perchloroethylene (PCE) [1200], or trichloropropene (PCE) [1200] into the gas stream. An enhanced photoefficiency is obtained for methanol [1188], methyl ethyl ketone [1198], butyraldehyde [1198], methyl *tert*-butyl ether [1198], methyl acrylate [1198], 1,4-dioxanehexane [1198], and branched aromatic compounds [1198] (toluene [1200], ethylbenzene, and *m*-xylene). No effect is observed for benzene [1198] and inhibition occurs for acetone and 1,1,1 trichloroethane [1198]. A chain-transfer reaction mechanism is proposed, in which surface chlorine radicals, generated by the degradation of chlorinated compound, react with a second adsorbed reactant via hydrogen abstraction, thereby initiating its oxidation and increasing both removal rate and overall conversion [479].

6.3.3. Organic compounds

6.3.3.1 Hydrocarbons. The conversion of hydrocarbons is strongly dependent on the gas-phase composition and their nature. The carbon atom with the highest electron density and the least steric obstruction is preferentially attacked by oxygen. High concentrations and higher molecular weight hydrocarbons favour partial oxidation over total oxidation to H_2O and CO_2.

In many environmental applications, low hydrocarbon concentrations (ppm) are present together with a large excess of O_2 (10–20%). These conditions are expected to favour total oxidation rather than partial oxidation. A conversion of at least 95% for propane, propane, ethane, and ethane working at 150 °C with 12% O_2 and concentrations up to 2000 ppm is reported without catalyst deactivation after 50 h [1201]. In the absence of oxygen, the hydrocarbon conversion is lower than 5% and a rapid catalyst deactivation occurs [1201]. Using TEM, in situ decomposition of hydrocarbons (CH_4 and C_2H_2) deposited on the catalytic TiO_2 is visualized and the mechanism is elucidated: after polymerization of the hydrocarbon, oxidation occurs through hydroxyl radicals ($HO^{\bullet}$) and oxygen anion radicals ($O^{\bullet -}$) [1202]. A maximum conversion is registered at ~600, 1000, and ~4000 ppm for propene, propane, and ethane, respectively [1201]. Kinetic studies indicate that the rate-determining step for ethylene oxidation is the chemical reaction between C_2H_4OH radicals and oxygen on the catalyst surface. Water competes with ethylene for the same type of catalyst sites, while oxygen molecules adsorb separately on other sites [1203].

The oxidation of higher hydrocarbons, such as *n*-butane [1201], butene [1204], *n*-hexane [1201], *o*-xylene [1205], and toluene [1206] over TiO_2 often yields alcohols, ketones, and aldehydes as a result of partial oxidation [1207–1209]. One of the reasons for the tendency to favour partial oxidation with increasing molecular weight might be a kinetic local ensemble effect. An insufficient oxygen supply favours the production of carbonaceous material that is resistant to oxidation, which leads to a gradual catalyst deactivation.

The low conversion of some aromatic contaminants is enhanced using cofeeding [1198,1200] and catalyst pre-treatment [531] with HCl. Toluene photodegradation is improved over TiO_2, exhibiting a higher surface hydroxylation. The interaction of the aromatic ring with the surface is thereby favoured, thus facilitating direct attack of the aromatic ring, the breakage of which may lead more easily to complete degradation [1210].

6.3.3.2 Chlorinated compounds. The degradation rates of chlorinated compounds are reported to be orders of magnitude higher in the gas phase than in the liquid phase at similar temperatures and levels of irradiation [1211]. The high reaction rate has led to applications involving not only purification of air, but also the purification of contaminated soils and water via processes that combine air stripping of volatile compounds with photocatalytic oxidation in the gas phase [1212]. It is reported that the reactivity of chlorinated compounds is higher than that of non-chlorinated organics [1213–1215], and chlorinated compounds like trichloroethylene or tetrachloroethylene are completely destroyed [468,479,1192,1213–1218]. Experimental studies prove that TCE oxidation occurs via either $OH^{\bullet}$ or holes [1219]. The photodegradation of TCE shows a complex response to temperature changes [1220]. Conversion decreases with increasing temperature, due to decreased adsorption, while mineralization to CO_2 (i.e., selectivity) is significantly improved at increasing temperatures, because adsorption seems to be less relevant for the dechlorination process.

Vinyl chloride is produced in industries in a large scale and is one of the most problematic chlorinated compounds, due to high volatility and low biodegradability. A complete removal and conversion to CO_2 and CO is obtained using a closed cycle batch system [1221], while an 80% removal is achieved with a continuous flow stream system using concentrations up to 160 ppm and gas retention times as low as 0.6 s. The outlet gas contains small amounts of chloroacetaldehyde (C_2H_3ClO) and it is not specified if carbon is evolved as CO_2 or CO [784].

6.3.3.3 Alcohols. Alcohols, commonly used as solvents, are relatively innocuous air pollutants. In the photocatalytic degradation of ethanol, acetaldehyde, which is more toxic, is formed as the main gaseous product [1222–1227]. The following reaction scheme is suggested [1223]:

$$\begin{aligned} CH_3CH_2OH \rightarrow CH_3CHO \rightarrow CH_3COOH \rightarrow HCHO \rightarrow HCOOH \\ \rightarrow CO_2 \end{aligned} \tag{6.57}$$

Several other intermediates such as methyl formate, ethyl formate, methyl acetate [1223], and 1,1-diethoxyethane [1225] are sometimes formed in low concentrations. These products obviously result from condensation reactions between the main intermediate products. CO_2 and H_2O are invariably the final products. Platinum addition to TiO_2 increases the overall rate of oxidation [628].

6.3.3.4 Nitrogen-containing compounds. Not much work has been published on the photocatalytic destruction of gaseous compounds containing nitrogen. Total mineralization is achieved for pyridine, propylamine, and diethylamine but deactivation of the catalyst occurs during the reaction [1229]. The decomposition of amines occurs through an electrophilic attack and cleavage of the C–N bond, which may be due to the higher density of the nitrogen atoms. For pyridine, electrons localized at the nitrogen atom are less available (sp^2 orbital) explaining why pyridine is not efficiently broken down in the absence of oxygen. Some studies mention that during the decomposition of pyridine no nitrogen-containing compounds are identified in the gaseous phase and suggest that the major inorganic products are ammonium and nitrate, without an analysis of these species on the catalyst surface [734]. Another study identifies diethylamine and pyridine (both NH_4^+ and NO_3^-) in the gas phase during photodecomposition of propylamine [1229]. In the absence of oxygen, NH_4^- is the main product observed and the small amount of NO_2^- is probably due to adsorbed O_2 or water from the carrier gas.

6.3.3.5 Sulfur-containing compounds. Reduced sulfur compounds, such as H_2S, CH_3SCH_3, CS_2, OCS, CH_3SH, and CH_3SSCH_3 are significant contaminants when released in the Earth's atmosphere. They are highly toxic and their oxidation leads to the formation of tropospheric SO_2 which eventually becomes H_2SO_4 (one of the main components of acid rain). Additionally, they have a strong unpleasant odour. Two main sources of these compounds are identified. The first is the release of volatile organic sulfur from biological processes. The second is their use as chemical warfare, large quantities being accumulated at least in the USA (25,000 t)

[1230] and Russia (40,000 t) [1231]. In accordance with international obligations, the existing stocks have to be destroyed in a few years.

The problems in photodegradation of these compounds are to obtain a complete oxidation of the organic pollutant and to prevent photocatalyst deactivation. H_2S is degraded with conversions of 99%[1232]. Honeycomb supports increase the concentration of H_2S, which induces deactivation. In the case of diethyl sulfide degradation (a simulant of warfare agent 2,2′-dichlorodiethyl sulfide (mustard gas or **yperite)), the distribution of the gaseous products suggests two main degradation pathways: C–S cleavage and S oxidation.

Products of complete oxidation are detected in small quantities if working in flow reactors with shorter residence times [1233]. If flow reactors with longer residence times [1234] are employed, the final oxidation products are CO_2, H_2O, and surface sulfate. Complete reactivation of the catalyst is achieved by irradiation and subsequent washing [1234]. Compared to diethyl sulfide, 2-chloroethyl ethyl sulfide ($CH_3CH_2SCH_2CH_2Cl$) shows lower reactivity in photocatalytic oxidations [1235]. After the deactivation due to the mineralization of carbonaceous species, oxidation of sulfur continues resulting in surface sulfates. Washing with water removes the monodentate sulfate species as sulfuric acid. Bidentate species are strongly bound to the TiO_2 surface, which prevents their effective removal by water and leads to a permanent deactivation [1235,1236].

6.3.3.6 Siloxane compounds. Silicone products (e.g., grease, oil) may contain some low molecular weight oligomers (siloxanes), which are relatively volatile and tend to outgas into the indoor atmosphere (for example, leading to a deterioration of semiconductor devices [1237]). The photocatalytic degradation of silicon-containing compounds is possible, but the activity decreases in time, due to accumulation of hydroxylated SiO_x on the TiO_2 surface [1238,1239]. The surface may be regenerated by a treatment with dilute alkaline solutions [1239]. The photodegradation of octaphenylcyclotetrasiloxane and poly(methylphenylsiloxane) in water [1240] does not lead to inactivation of the photocatalyst, because the degradation products of soluble silicates do not coat the photocatalytic surface. Thus, aqueous solution degradation of silicone-containing compounds seems to be more adequate.

6.3.4. Inorganic compounds

6.3.4.1 Fixation of nitrogen oxides. NO_x (NO and NO_2) is responsible for tropospheric ozone and particulate build-up (urban smog) through photochemical reactions with hydrocarbon. Furthermore, NO_x is, together with SO_x (SO_2 and SO_3), the major contributor to ''acid rain'', which harms forests and crops, as well as aquatic life [1241–1243]. Thus, NO_x emission has been a focus of environmental regulations, especially in the ozone non-attainment areas.

NO_x control follows two approaches: the reduction of NO_x back to N_2 or the oxidation to NO_2 and HNO_3. The oxidation of nitric acid completes the nitrogen fixation and represents a wonderful example of how a pollutant is converted into a raw material for useful applications such as fertilizers. In the proposed photo-

catalytic oxidation mechanism: $NO \rightarrow HNO_2 \rightarrow NO_2 \rightarrow HNO_3$, $HO^{\bullet}$ radicals play a key role [1244].

In Japan, PCO has been applied to remove NO by coating traffic tunnels, paved roads and buildings with TiO_2 [759]. Applications also include indoor air cleaners and car deodorizers in which indoor VOCs, including NO_x are oxidized over TiO_2 activated by sunlight or fluorescent light [1246]. TiO_2 activity is improved by the addition of an adsorbate such as zeolites (A and Y), which concentrate NO on the surface [772].

A highly selective photoreduction of NO to N_2O and N_2 is reported on metal-implanted TiO_2 [556].

6.3.4.2 Ozone. As a consequence of its high reactivity, ozone is a very toxic material. The recommended threshold level for allowable exposure during an 8 h period is very low (i.e., 0.1 ppm) [1248]. Sources of ozone are commonly found in the (work) environment (cooling air from photocopiers and laser printers, deodorizer in public washrooms and hotels, sterilization processes, wastewater treatments and bleaching of cloth and wood pulp). The following reaction scheme for the degradation of ozone is proposed [348]:

$$e^- + O_3 \rightarrow O_3^- \text{(rate limiting)} \tag{6.58}$$

$$h^+ + OH^- \rightarrow OH^{\bullet} \tag{6.59}$$

$$O_3^- + O_3 \rightarrow O_4^- + O_2 \tag{6.60}$$

$$OH^{\bullet\bullet} + O_3 \rightarrow O_4^- + H^+ \tag{6.61}$$

$$O_4^- + O_3 \rightarrow 2O_2 + O_3^- \tag{6.62}$$

$$H^+ + O_3^- + O_4^- \rightarrow 3O_2 + OH^- \tag{6.63}$$

At ozone concentrations higher than 120 ppm, the photodegradation reaction is zero order with respect to $[O_3]$, and at lower concentrations, the kinetics are described well by an LH-type equation. It is proposed that the rate-determining step is the initial reduction of an adsorbed ozone molecule by a photogenerated electron [348]. The photocatalytic activity is found to be independent of specific surface area, but dependent on the crystal structure, in the order: anatase $\ll$ anatase–rutile mixture $<$ rutile [1249].

6.3.5. Photocatalyst deactivation

Deactivation is an important issue for practical applications of photocatalysts. A comparative study of literature data reveals that photocatalyst deactivation is generally found in single-pass fixed photocatalytic reactors [1250]. Depending on the nature of the organic compound, both reversible or irreversible deactivation are evidenced [1251,1252]. In practice, though, deactivation is not always observed due to low levels of substrate or in experiments carried out using short periods of time.

During the reaction, TiO_2 may be deactivated either by formation of surface species, intermediates, or by-products, that have higher adsorption ability to the

TiO_2 surface than the corresponding reactant or by "heavy products" that are difficult to decompose. Benzoic or butanoic acid formed during photodegradation of benzene [1253], toluene [1253,1262], xylene [1205], toluene/TCE, toluene/PCE, and 1-butanol [466] belong to the first group. Deposits of hydroxylated SiO_x [1239], polymer compounds (formed, for example, by the addition of a radical intermediate to the aromatic ring or double bonds), and carbon belong to the second type.

Since catalyst deactivation has been ascribed to accumulation of intermediates on the TiO_2 surface [1254] or a diminution of surface $HO^\bullet$ radicals, reactivation implies the oxidation (removal) of the products, which block the surface active sites or the regeneration of $HO^\bullet$ radicals. This may be achieved by different regeneration schemes of which we mention the following:

- thermal regeneration by heating at temperatures high enough to decompose the intermediates. Lower temperatures lead to the conversion of reaction intermediates to lesser volatile ones, accelerating the formation of carbonaceous deposits. A temperature of 130–150 °C is not high enough to decompose ethanol by-products [1251], and for toluene intermediates the optimum is above 420 °C [1205]. Pt(0.5%)–TiO_2 is reported to display thermal regeneration at lower temperatures, presumably because platinum serves as an oxidation catalyst at elevated temperatures [1255].
- photocatalytical regeneration using simultaneous UV illumination and exposure to humidified air (xylene [1205], toluene [530,1256], benzene [1189,1255,1256], cyclohexane [1253], cyclohexene [1253]) or pure air (1-butanol [446]). Photocatalytic regeneration may be more practical than thermal regeneration, particularly in indoor air treatment systems because it can be carried out at ambient temperatures. However, since the surface intermediates leading to activity loss are presumably recalcitrant to photocatalytic regeneration, it requires longer regeneration times than thermal regeneration [1205,1255,1256].
- flowing humid air over the catalyst (TCE [1092], nitrogen-containing compounds [1229], sulfur-containing compounds [1234,1235]).
- O_3 purging in the presence of water vapour (benzene [470])
- washing with alkaline solutions (silicon-containing compounds) [1239].

6.3.6. *Influence of water*

The efficiency of air cleaning is greatly affected by the relative humidity (RH) of the test environment [446,448,468,1194,1216,1255,1257,1258]. The ambient water vapour concentration can vary considerably, even if only human comfort conditions are considered (20–70% RH) [468,1257,1258]. The effect of water vapour on the photocatalytic rate in the gas phase depends on its concentration, contaminant species, and process parameters. During photocatalysis, the continuous consumption of hydroxyl radicals requires replenishment to maintain catalyst activity. A suitable equilibrium between consumption and adsorption exists at low water vapour contents. Upon increase of the vapour content, this equilibrium may be

destroyed and more water vapour molecules is adsorbed on the catalyst surface. A competition for the adsorption sites between water and target organic and/or oxygen molecules occurs and a considerable drop in the amount of organic adsorbed on TiO_2 surface is observed in several studies [1182,1211]. Additionally, water adsorption favours electron–hole recombination [1258]. In any case, numerous studies indicate that a certain degree of humidity, usually exceeding the amount produced by the oxidation of organics is necessary to maintain the hydroxylation and to avoid the blockage of the TiO_2 surface by partially oxidized products [1205,1259].

With respect to the nature of the pollutant, both enhancement and inhibition of the degradation rate can be caused by water vapour. It has been demonstrated that water vapour strongly inhibits the oxidation of ethylene [1203,1260], isopropanol [1261], and TCE [466,468,479,1262]. The overall photodegradation for indoor levels of NO (200 ppb) and BTEX (>100 ppb) decreases acutely in the presence of humidity [757]. An enhanced oxidation of cyclohexane [1256] and toluene [448,1219,1253,1263] has been found, but no significant effect on DCM [471], benzene [624], and 1-butanol [446,1207] oxidation is noted. Deposition of Pt leads to a photocatalyst that is active for ozone decomposition under humid conditions in contrast to bare TiO_2 [635]. In the case of acetone, contradictory results are obtained. Several authors report on an inhibitory effect of the presence of water [447,448,1194,1219,1261,1262,1265], while a moderate increase with increasing RH has been detected by others [1266–1268]. This may be due to the differences of the experimental conditions, particularly of the texture of the photocatalyst. Powdered TiO_2 may readily agglomerate at high RH, hindering the adsorption of organic vapours, whereas supported oxides retain their porous structure even after firing.

Water vapour may influence degradation and mineralization rates in different ways. For benzene, the mineralization rate depends on the water content; small amounts of water (<5 ppm) decrease the reaction rate (the reaction itself does not provide enough water to allow complete mineralization to occur) [624]. The presence of water also inhibits the formation of carbon deposits, which would lead to catalyst deactivation [1269]. The rate of methyl-isobutyl ketone (MIBK) degradation decreases at moderate RH (~28%) compared to dry conditions as a consequence of the mutual exclusion of water and slightly hydrophobic MIBK molecules on the TiO_2 surface. On the contrary, mineralization is maximal, due to the rapid photooxidation of acetone formed as intermediate. Furthermore, a considerable increase of the photooxidation is observed at RH > 80%, but the mineralization is decreased [1266].

At low residence times [1233], moderate humidity increases diethylsulfide (DES, $C_4H_{10}S$) conversion compared to dry air. At higher residence times [1234], water has a detrimental effect on the conversion level. A positive effect is a twofold lower value of the SO_2 in effluent at increased humidity.

Another parameter that has to be evaluated in the study of the influence of water on the photoactivity is the hydrophobicity of the organic substrate (which defines the extent of interaction with adsorbed water on the TiO_2 surface) [1255]. A more complex situation can be envisaged when considering not only chemisorbed

water and hydroxyl groups [515], but also physisorbed water [1270], the amount of which depends on the RH and surface characteristics of the TiO_2. Consequently, not only the adsorption of organic molecules on TiO_2 sites, but also their solvation by this physisorbed water could influence the photoactivity [1255].

6.3.7. Indoor applications

Indoor air quality (IAQ) has become a new branch of chemical and medical science, directly linked to the presence of pollutants (VOCs) in confined atmospheres. Odour problems encountered in such environments are connected with the presence of these VOCs.

While concentrations in the parts per million (ppm) range are typical for chemical stream concentration, sub-ppm levels or parts per billion concentrations are commonly associated with indoor (buildings, trains, vehicles, planes, etc.) VOCs. Extrapolation of the oxidation data collected at concentrations much higher than the intended application may not be valid [1182]. It is reported that the photodegradation rate increases with increasing concentration of the pollutants in the range of several hundreds of ppm level [448,466,1271], so it is vital to investigate if photodegradation will be reduced at indoor ppb levels. Although, on average people generally spend 88% of their life in indoor environments [1272], and occupants complain about sickness associated with working in indoor environments (known as the sick building syndrome [1273]), there are limited studies on the photodegradation of pollutants at typical indoor levels [755,757,1182,1274,1275].

TiO_2 photocatalysis depends on the energy of the incident photon, but even the presence of a few photons of required energy may induce photolysis. As a direct application, even ordinary room light may be sufficient to purify indoor air or to keep walls clean.

Photoinduced bactericidal activity of TiO_2 can lead to different applications including disinfection in diverse environments, such as microbiologically sensitive environments like medical facilities and surroundings where biological contamination must be prevented.

For indoor pollutant removal, it is important to use TiO_2 with adsorbents as the concentration is extremely low and the competition for adsorption sites between water vapour and pollutants is most critical [757]. TiO_2 immobilized on an activated carbon (AC) filter significantly increased NO and BTEX removal at short residence times and high humidity levels [757] ($H_2O = 22,000$ ppmv, NO and BTEX obtained degradations TiO_2/TiO_2–AC are 40/66% and 10/60% respectively). NO_2 as an intermediate generated from the photodegradation of NO, is also suppressed.

In a mixture of NO and BTEX at ppb levels, NO promotes the photodegradation of BTEX under low and high humidity levels [757]. The promotion of NO is achieved by $OH^\bullet$ generated from photodegradation of NO [1276] (reactions 6.64 and 6.65):

$$NO + HO_2^\bullet \rightarrow NO_2 + OH^\bullet \tag{6.64}$$

$$NO_2 + NO + H_2O \rightarrow 2HONO \rightarrow 2OH^\bullet + 2NO \tag{6.65}$$

On the other hand, NO conversion is inhibited by the presence of NO_2, BTEX and SO_2 [1277], but no effect is found for CO [1278].

Various TiO_2-based materials for improving indoor environments are commercially available such as TiO_2-coated tiles [1279,1280], TiO_2-films or sheets [1281–1285], TiO_2-glass [1286], TiO_2-papers [730,1287], TiO_2-curtain material [1288], and honeycomb carbon supports [1289] (see Table 3).

6.4. Disinfection and anti-tumoral activity

To remove or kill pathogenic organisms including bacteria, viruses, fungi, protozoa, and algae from water, air, surfaces, and biological hosts represent a top priority. The current disinfection technologies apply either chemical or photochemical damage or physical removal by filtration. Chlorination is a universally practised water-disinfection process, which can prevent waterborne infectious diseases, but it is not efficient in the inactivation of spores, cysts and some viruses [1304–1306]. Chlorination, combined with ozonation, strongly improves the disinfection efficiency for all pathogens of concern like bacteria and viruses, as well as cystforming protozoan parasites [1307,1308]. A contradictory microorganism regrowth potential limits its use [1309].

Increasing appearances of microorganisms in drinking and wastewater has raised concerns for pathogenic related water diseases. Thus, an implementation of more stringent standards on microbial pollution of water and wastewater [1310] is necessary.

Most of the photocatalytic TiO_2 disinfection studies focus on bacteria and cancer cells, but a few study yeasts, viruses, and other types of cells. Most of the work has been done in aqueous phase, but reports of bacteria removal from humid atmosphere are also present [1311–1313]. Municipal wastewater has been treated with TiO_2/UV disinfection technology [1314,1315], leading to the removal of total and faecal coliforms [894].

Escherichia coli, generally considered as an easy target to destroy [1316], is extensively used as a biological indicator of the efficiency for drinking water treatments. If it is not detected, the treated water is regarded as free from faecal contamination [1317]. TiO_2 is proven to be highly efficient in killing very resistant Gram-negative bacteria too, such as *Enterobacter cloacae* which can otherwise not be inactivated [1318].

The nature of the salt content influences the rate of disinfection in a similar manner as the photocatalytic degradation of the organic compounds. The presence of $H_2PO_4^{2-}$ and HCO_3^- decreases the disinfection rate, but while phosphate addition leads to a partially irrreversible deactivation, the bicarbonate one is reversible. $S_2O_3^{2-}$ presence is found to inhibit the photokilling of *E. coli* [1319]. Experiments performed in deionized water may alter the results, due to the loss of calcium and magnesium from the cell membrane surface leading finally to a more permeable or damaged cell membrane [1312].

A negative effect on the bacterial inactivation rate is produced by turbidity, caused by the presence of particulate matter, such as clay, silt, colloidal particles,

Table 3
Compounds photodegraded in gaseous phase

Compounds		Photocatalyst	References
Hydrocarbons	Methane	TiO_2	[1202]
	Ethane	TiO_2	[1201]
	Propane	TiO_2	[1201]
		TiO_2/SiO_2	[744]
	n-Butane	TiO_2	[1201]
	Hexane	TiO_2	[347,1201]
	Heptane	TiO_2	[1290]
	Cyclolhexane	TiO_2	[1253]
	Ethylene	TiO_2	[1201,1203]
		TiO_2/borosilicate glass rings	[1291]
		TiO_2/ZrO_2	[1292]
	Propene	TiO_2	[1201]
	Methylacetylene	V–TiO_2	[591]
	Cyclohexene	TiO_2	[1253]
	Benzene	TiO_2/zeolites	[1253]
		TiO_2	[347,448,624,1189]
	Toluene	TiO_2	[448,1219,1253, 1262,1263,1293]
		TiO_2/silica	[715]
		TiO_2/glass, silicon, alumina	[1294]
		TiO_2/silica, PET + cellulose	[1295]
		TiO_2/fabrics	[729]
Halogenated compounds	DCH (dichloromethane)	TiO_2	[471]
	Trichloromethane	TiO_2/γ-Al_2O_3 or glass fiber	[708]
	TCE	TiO_2	[448,471,532,1220, 1262,1296–1298]
		TiO_2/monolithic	[775]
	PCE	TiO_2	[471]
	Vinyl chloride	TiO_2	[1221]
		TiO_2/silica	[784]
	TCE + PCE	TCE	[775]
	1,3-dichlorobenzene	TiO_2	[471]
Nitrogen-containing compounds	Diethylamine	TiO_2	[1229]
	Propylamine	TiO_2	[1229]
	Pyridine	TiO_2	[1229]
Hydroxylated compounds	Methanol	TiO_2	[347,448,1219,1262]
	Ethanol	TiO_2	[1251]
		Pt/TiO_2	[629,630]
		Fe/TiO_2	[1299]
	2-Propanol	TiO_2/SiO_2	[744]
		TiO_2	[1219]
	Butanol	TiO_2/zeolites	[1300]
	tert-Butyl-alcohol	Pt/TiO_2	[631]

(continued on next page)

Table 3 (*continued*)

Compounds		Photocatalyst	References
Ether	Diethylether	TiO_2	[1219,1233–1235]
	Methyl-butyl-ether		[631]
Sulfur-containing compounds	Diethyl sulfide	TiO_2	[1233–1235]
	2-Chloroethyl ethyl sulfide	TiO_2	[1235,1301]
Silicon-containing compounds	1,3,5,7-Tetramethylcyclotetrasiloxane	TiO_2	[1238]
	Octamethyltrisiloxane	TiO_2	[1239]
Aldehydes, ketones	Formaldehyde	TiO_2	[244,498,1302]
		SiO_2 or WO_3–TiO_2	[668]
	Acetalaldehyde	TiO_2	[1251]
		Pt/TiO_2	[632]
		V, Cr, Mn, Fe, Ni–TiO_2/SiO_2	[221]
		TiO_2/paper	[730]
	Propionaldehyde	TiO_2/mordenite	[746]
	Acetone	TiO_2	[448,776,1219, 1262,1266,]
		Pt/TiO_2	[447]
	Methyl-ethyl ketone	TiO_2/zeolites	[1300]
	Methyl-isobutyl ketone	TiO_2	[1266]
Halogenated derivates of carboxylic acid	Dichloroacetic acid	TiO_2	[471]
Inorganic compounds	NO_x	TiO_2	[1244]
		TiO_2/hydrapatite	[1276]
		TiO_2/zeolite (A and Y)	[772]
		Pt/TiO_2	[1303]
	O_3	TiO_2/glass substrate	[348]
		Pt/TiO_2	[635]
Organic–inorganic compounds	NO + BTEX	TiO_2 (indoor)	[757]
	NO + BTEX + SO_2	TiO_2/AC (indoor)	[757]
		TiO_2/glass fiber	[1278]
		TiO_2/AC (indoor)	[1277]

plankton, and other microscopic organisms in water. The increase in water turbidity reduces the photocatalytic inactivation rate of bacteria in different ways: it can stimulate bacterial growth, diminish the oxygen concentration, cause competition of organic particles with bacteria towards $HO^{\bullet}$ radicals, and lead to reduced light penetration [1320].

One of the most important parameters in inducing an irreversible bacterial inactivation is the minimum illumination time required, either intermittent or continuous, which is characteristic for each microorganism. Some like *E. coli* [1320] or *Bacteriodies fragilis* [1321] require prolonged illumination, while for others such as *Bacillus pumilus* [1322] intermittent illumination is more effective. Combined processes have also shown to be efficient in some photocatalytic reactions. Fifteen minutes of alternating light and dark enhances the killing of *B. pumilus* spores [1322]. The combination of light and ultrasound increases the killing of *E. coli*

[1323], while the elimination of *E. coli* and *C. perfringens* spores is enhanced when a positive voltage bias is applied to the irradiated TiO_2 [1324].

The temperature influences the photocatalytic rate too. For Gram-positive bacteria such as *enterococci*, a temperature increase from 23 to 45 °C improves the photocatalytic rate, whereas for Gram-negative bacteria (except coliforms) the resistance to the photocatalytic treatment is increased with increasing temperature [1320]. The susceptibility of bacteria to heat is also conditioned by other factors, such as concentration of cells, their physiological conditions, and others related to the chemical composition of the solution.

First-order kinetics and modifications thereof have been proposed to describe the TiO_2-photocatalysized degradation of bacteria [1323,1325].

Disinfecting rates or inactivation times are usually not comparable from study to study, due to widely varying operational parameters and reactor configurations. Reactor configurations range from small volume Pyrex beakers and Petri dishes (typically 1–10 cm^3 [422] using illumination from the top by a tubular lamp [1325–1327]) to modifications of commercial UV-disinfecting apparatus [1328], and the design and construction of large volume immobilized flow reactors [1319]. Most investigations use anatase as photocatalyst, but rutile is also reported to be active for killing *S. cricetus* [1329]. Platinum on rutile enhances the photokilling of *E. coli* and *S. aureus* [1330] and silver on rutile is efficient in *E. coli* disinfection [1331].

Photocatalytic inactivation of bacteria is restricted to small volumes of waters with low microbial contamination and is presently used only as an accessory to the chlorination process. The lack of residual disinfection capacity [1332] and the generally slow kinetics of disinfection represent two major disadvantages of photodisinfection sensitized by TiO_2 compared to traditional ones.

The mechanisms leading to cell death have not yet been fully understood and some explanations are contradictory. The first proposed killing mechanism implies an oxidation of the intracellular coenzyme A (CoA), which inhibits cell respiration and subsequently causes cell death as a result of a direct contact between TiO_2 and target cell, leading to cell death [30]. The different sensitivity of microorganisms towards TiO_2 photocatalysis (which follows the order: virus > bacterial cell (Gram-positive > Gram-negative) > bacterial spores [30,1322–1335]) suggests that different microorganisms respond differently to the TiO_2 photocatalyst. This difference is attributed to their structural differences, particularly the complexity and thickness of the cell envelope, which involves the cell wall and cytoplasmic membrane. A second proposed killing mode suggests that bacterial death is caused by a significant disorder in the cell permeability and decomposition of the cell walls [1333]. It is suggested that the cell wall damage might take place prior to cytoplasmic membrane damage [1327,1336]. Photocatalytic treatment progressively increases the cell permeability and subsequently allows free efflux of intracellular constituents, which eventually leads to cell death. Free TiO_2 particles may also access damaged cells and subsequently attack directly intracellular components (alteration of protein structure [30,1322]), which can accelerate cell death [1312]. Kinetic investigation of the photokilling of intact *E. coli* cells was observed to involve two steps, an initial lower rate killing step, followed by a higher one. In

contrast, the photodegradation of *E. coli* spheroplasts, which do not have cell walls, involves only a single step, suggesting that the cell wall of *E. coli* cell acts as barrier in the photocatalytic process [1337].

Pathogenic organisms may respond to the photocatalytic stress by a self-defence mechanism in order to live in an aerobic medium and deal with low levels of UV radiation, Therefore, the disinfection of each target pathogenic organism is a challenge in terms of structure and defence mechanisms to overcome.

All life forms are sensitive to DNA lesions, which consist of formation of dimeric pyrimide photoproducts and are responsible for the inhibition of DNA replication and also bacterial mutation [1338]. Therefore, nature has supplied cells with several defence and repair mechanisms against such damages. Cells that are damaged as a result of UV (300–400 nm) exposure have two mechanisms to repair DNA. The first is known as photoreactivation or photorepair [1339]. The second, which takes place in the dark, consists of excision-resynthesis and post-replication repair [1340] processes. In both cases, different enzymes reverse the detrimental UV photodimerization of pyrimidines by reforming the monomeric pyrimidine.

$$2O_2^{\bullet -} + 2H^+ \xrightarrow{SOD} O_2 + H_2O_2 \qquad H_2O_2 + H_2O_2 \xrightarrow{catalase} O_2 + H_2O \tag{6.66}$$

All aerobic life forms produce superoxide dismutase (SOD) (an enzyme that dismutates the superoxide anions $O_2^{\bullet -}$ to H_2O_2 and O_2) and catalase (an enzyme that reduces the intracellular concentration of H_2O_2 and converts it to H_2O and O_2) [1320] as shown in reaction 6.66.

In some cases, killing of pathogenic organisms is not sufficient. Some Gram-positive bacteria and, less commonly, Gram-negative bacteria release endotoxins and exotoxins if their outer membrane is damaged. Contact with these compounds can give rise to medical problems. Allergic responses can be caused by cell structures that persist even after the cell is not longer viable [1312].

Cancer treatment is one of the most important topics associated with photocatalysis. A cancer cell will die if its membrane is damaged or if the oxidation–reduction compounds needed for adenosine triphosphate (ATP) production in the cell are depleted or exhausted. TiO_2 particles show non-toxicity to cancer cells such as HeLa cells, but a significant ability to sensitize the photokilling [1341] process, which can be enhanced increasing the TiO_2 [1342] amount or by adding superoxide dismutase, which converts superoxide radicals into hydrogen peroxide [1341,1343]. The oxidative damage results obtained using TiO_2 particles are similar to those obtain by the traditional photodynamic therapy (PDT). Ten and 30 min of illumination in the presence of TiO_2 leads to 80% and complete killing of human U 937 monocytic leukemia cells, respectively [1344]. The limitation of this method consists of the weak penetration of the UV light through skin (less than 1 mm), so fiber optics or surgery is needed for this technique [1345].

Some pathogenic organisms photodegraded by TiO_2 are presented in Table 4.

6.5. Photoactive materials

Construction materials that contain TiO_2 possess air-cleaning, antibacterial, and self-cleaning properties, explaining the increasing interest for this kind of materials. If widespread application of such construction materials is achieved, they may become a significant factor in the overall balance of certain contaminants.

6.5.1. Construction materials for air cleaning

Various applications of photocatalyst-modified cement [1364,1365] (Portland [1365]) ranging from self-cleaning facades (e.g., the Jubilee Church and preser-

Table 4
Pathogenic organisms photodegraded by TiO_2

Pathogenic organisms		Photocatalyst	References
Gram-negative bacteria	*Escherichia coli*	TiO_2	[1316,1319,1325,1327, 1337,1346–1349]
		TiO_2–Cu(II) phthalocyanine chloride	[654]
		Cu(II)phthalocyanine-tetrasulfonic acid	[654]
		Fe–TiO_2	[1350]
	Enterobacter cloacae	TiO_2	[1318]
	Streptococcus mutans	TiO_2	[1351]
	Salmonella typhimurium	TiO_2	[1318]
	Salmonella choleraesuis	TiO_2	[1352]
	Serratia marcescens	TiO_2	[1353,1354]
	Streptococcus faecalis	TiO_2	[895]
	Hyphomonas polymorpha	TiO_2	[1347]
	Vibrio parahaemolyticus	TiO_2	[1352]
	Micrococcus luteus	TiO_2	[1347]
	Pseudomonas aeruginosa	TiO_2, Cu or Al-TiO_2	[895,1318]
	Listeria monocytogenes	TiO_2	[1352]
	Klebsiella pneumoniae	TiO_2/cotton fabrics	[728]
Gram-positive bacteria	*Streptococcus sobrinus* AHT	TiO_2	[1333]
	Bacillus subtilis	TiO_2	[1347]
	Lactobacillus helveticus	TiO_2	[1348]
Enzyme	Horseradish peroxidase		[1356]
Protozoan	Giardia lambia		[1357]
Fungus	*Aspergillus niger*	TiO_2	[1323]
Algae	*Chlorella vulgaris*	TiO_2	[30]
Viruses	*Lactobacillus casei* phage PL-1	TiO_2	[1326]
	Bacteriodies fragilis bacteriophage	TiO_2	[30,1358]
	Phage MS 2	TiO_2	[896]
	Poliovirus 1	TiO_2	[894]
Cancer cells	HeLa	TiO_2	[1341,1342,1345,1359,1360]
	T 24	TiO_2	[1343,1361,1362]
	U 937	TiO_2	[1344]

vation of ancient marble Greek statues against environmental damage [1366]) to solar reactors for wastewater treatments have been made in pilot projects [1367,1368]. TiO_2 is used both as an additive in concrete matrices [1364,1365] and as a coating [1125,1369]. The relevant photocatalytic processes may occur both at the air-solid interface and at the liquid–solid interface. Further development of TiO_2-modified materials for self-cleaning building surfaces and even more for the construction of photocatalytic environmental remediation devices requires a better understanding of modified cements. In particular, their sensitivity to ageing processes and the impact of TiO_2 additives on the properties of cement have to be investigated. Cement-bound photocatalysts are especially attractive for large-scale application due to the relatively low cost of cement binders and the versatility of the materials, which can serve simultaneously as a structural component and as a photocatalytically active material.

6.5.2. Self-cleaning and anti-fogging materials

The self-cleaning effect of TiO_2 surface arises from the fact that dirt and grim are washed away on superhydrophilic surfaces. Since water droplets will tend to run off, the surface will also dry very quickly. Complementarily, such materials will not fog, since fogging is characteristic to surfaces with contact angles higher than 20° [323,493]. Additionally, the TiO_2 surface can also destroy organic deposits via photocatalytic degradation, which is an additional self-cleaning action.

For an efficient utilization of near-UV light, either from the sun or artificial sources, the TiO_2 coating should be thick, i.e., typically >1 μm [1370], because thinner films have a low absorbance in this region (i.e., $320 > \lambda > 380$ nm). They should also exhibit clarity, mechanical robustness, and high photoactivity. Some self-cleaning and anti-fogging applications are presented in Table 5.

7. Concluding remarks

Environmental contamination is a growing problem that cannot be neglected as it influences our world and daily life. Eliminating contaminated compounds costs energy, which increases the CO_2 emission that causes global warming. A solution for this dilemma can be found in the field of semiconductor chemistry, which implies the use of an inert "environmentally harmonious" catalyst, non-hazardous oxidants (oxygen) and solar energy input. In this way the contaminated environment can be gently harmonized to restore original conditions. The dominant position of TiO_2 is not limited to basic research, but extends to commercial applications.

TiO_2 is a versatile material. It is used in many applications, in bulk compounds as well as in specialized products. It shows interesting photoinduced properties, which have the same origin but a different appearance. We have treated these processes and their applications, with a special focus on photocatalytic reactions with environmentally unwanted compounds that are present in water or air. Degradation of bio-hazardous materials and cancer therapy are also discussed.

Table 5
Applications of TiO_2 self-cleaning and anti-fogging properties

Function	Material	Application
Cleaning easiness	Materials for road	Tunnel lighting Tunnel wall
	Materials for house	Kitchen parts, bathroom and interior furnishing
	Materials for electric and electronic devices	Computer display, electric wires
	Daily necessities and consumer products	Tableware, kitchenware
Self-cleaning by rainfall	Materials for road	Traffic sign, lighting, soundproof wall, guardrail, decorative laminate panel
	Materials for buildings	Exterior tiles, siding boards, curtain wall, painted steel plate, aluminium panel, building stone, crystallized glass, glass film, window, sash, screen door, gate door, sun parlour, veranda parts
	Materials for electric and electronic devices	Upper glass of a solar cell, insulator
	Materials for vehicles	Painting and coating of vehicles, outside of windows, headlight
Anti-fogging properties	Materials for road	Road mirror
	Materials for buildings	Bathroom mirror
	Materials for stores	Refrigerated showcase
	Materials for vehicles	Inside window, glass film, helmet visor
	Material for optical instrument	Optical lens
	Daily necessities and consumer products	Spray of anti-fogging coat, anti-fogging film
Accelerated drying	Materials for buildings	Toilet, window, bathroom
Preventing dewdrops forming	Materials for electric and electronic devices	Heat exchanger of air conditioner, high voltage cable
	Materials for vehicles	Sideview mirror, rearview mirror, windshield of le, sidemirror film

Summarizing the results of the wealth of literature on this subject we can conclude that much has been investigated and much knowledge has been gained. Detailed investigations require a range of interdisciplinary efforts. Many authors have synthesized TiO_2 photocatalysts and investigated the morphology, structure, and other physical–chemical properties. Others have focussed on photochemistry both fundamentally (including the elucidation of reaction mechanism, the importance of the surface, and theoretical calculations) as well as working towards practical applications (including the manufacture and testing of different photocatalysts, reactants and reactors). Coupled to all these investigations, the ever-important question of how to improve the photocatalytic activity arises. Several attempts are made, with variable success.

However, many questions remain. Disagreement on reaction mechanisms is displayed in several articles, although a general consensus on the first steps and the

importance of OH radicals is clear. Contradicting results are reported on the photocatalytic activity (e.g., activity, selectivity, rate) if dopants, supports, or other supplementaries are introduced or when the reaction parameters are altered. A better understanding of heterogeneous photocatalysis in a multiphase environment represents a continuous challenge in this research topic.

One of the biggest problems at this moment is that most articles are not comparable to each other, due to differences in used TiO_2 and reaction parameters (like light, amount of catalyst, reactor set-up, reaction time and type, concentration of substrates, etc.). This poses a real threat to the progress of the work in this field as no general trends can be detected and the way forward is hard to determine. Now, too much work is conducted, which is interesting in itself, but is not connectable to other results. At this point we do not need more investigations into yet another chemical compound that can be degraded by TiO_2, but need thorough experiments, which really show the potential for practical applications and which also do point out the problems that have to be overcome to get that far. Standardization of reactions is one of the most important steps that should be taken in this field to get beyond the present level. There are some initiatives to come to standardized reactions and we hope that they will be successful soon leading to great progress in the field of photocatalysis. The use of solar simulators in the field of solar cell research has aided the transparency and reliability of the investigations greatly and we hope that the same will be true for standardization of photocatalysis.

A major objective of the future work is the development of a photocatalyst system that can selectively degrade pollutants and that utilizes visible and/or solar light irradiation. If the field of photoinduced processes of TiO_2 is explored successfully, the effective utilization of solar energy, which is clean, safe, and abundant, will in the future be able to provide energy and to solve environmental pollution. Until that time, there is much work to be done, but not without promising prospects.

References

[1] Mills A, Le Hunte S. J Photochem Photobiol A: Chem 1997;108:1.
[2] Lee SK, Mills A. Platinum Metals Rev 2003;47:61.
[3] US Geological Survey Minerals Yearbook, 2002.
[4] Dorfman LM, Adams GE. NSRDS-NB 1973;46:1.
[5] Alberci RM, Jardim WF. Appl Catal B: Environ 1997;14:55.
[6] Hermann JM, Disdier J, Pichat P. In: Gange P, Jacobs PA, Poncdet G, editors. Preparation of catalyst IV. Amsterdam: Elsevier; 1987, p. 285.
[7] Kreutler B, Bard AJ. J Am Chem Soc 1978;100:4317.
[8] Chen D, Ray AK. Chem Eng Sci 2001;56:1561.
[9] Pichat P. Catal Today 1994;19:313.
[10] Fox MA, Dulay MT. Chem Rev 1993;95:54.
[11] Yanagida S, Ishimaru Y, Miyake Y, Shiragami T, Pac C, Hashimoto K, et al. J Phys Chem 1989;93:2576.
[12] Cermanati L, Richter C, Albini A. Chem Commun 1998;7:805.
[13] Karthikeyan A, Almeida RM. J Non-Cryst Solids 2000;274:169.
[14] Ohno T, Nakabeya K, Matsumura M. J Catal 1998;176:76.

[15] Kumar SR, Asha CS, Vasudevan K, Suja R, Mukundan P, Warrier KGK. Mater Lett 1999;38:161.
[16] Braun JH. Prog Org Coat 1987;15:249.
[17] Blakey R. Prog Org Coat 1985;13:279.
[18] Rentschler T, Reller A. ECJ 1999;4:80.
[19] Allen NS, Katami H, Thompson F. Eur Polym J 1992;28:817.
[20] Pugh SL, Guthrie JT. Dyes Pigments 2002;55:109.
[21] Allen NS. Polym Degrad Stab 1990;29:73.
[22] Corralles T, Peinado C, Alle NS, Edge M, Sandoval G, Catalina F. J Photochem Photobiol A: Chem 2003;156:151.
[23] Kubota Y, Niwa C, Ohnuma T, Ohko Y, Tatsuma T, Mori T, et al. J Photochem Photobiol A: Chem 2001;141:225.
[24] Fujishima A, Honda K. Nature 1972;238:37.
[25] Frank SN, Bard AJ. J Am Chem Soc 1977;99:303.
[26] Frank SN, Bard AJ. J Phys Chem 1977;81:1484.
[27] Schrauzer GN, Guth TD. J Am Chem Soc 1977;99:7189.
[28] Pruden AL, Ollis DF. J Catal 1983;82:404.
[29] Hsiav CY, Lee CL, Ollis DF. J Catal 1983;82:418.
[30] Matsunaga T, Tomato R, Nakajima T, Wake H. FEMS Microbiol Lett 1985;29:211.
[31] Fujishima A, Ohtsuki J, Yamashita T, Hayakawa S. Photomed Photobiol 1986;8:45.
[32] O'Regan B, Grätzel M. Nature 1991;353:737.
[33] Wang R, Hashimoto K, Fujishima A, Chikuni M, Kojima E, Kitamura A, et al. Nature 1997;388:431.
[34] Greenwood NN, Earnshaw A. Chemistry of the elements. Oxford: Butterworth-Heinemann; 1997.
[35] Natara NC, Funaga N, No MG. Thin Solid Films 1998;322:6.
[36] Kronos International, 1996.
[37] Adams G. ECJ 1996;6:717.
[38] Philips LG, Barbano DM. J Diary Sci 1997;80:2726.
[39] Hewitt J. Cosmet Toiletries 1999;114:59.
[40] Schulz J, Hohenberg H, Pfück F, Gärtner E, Will T, Pfeiffer S, et al. Adv Drug Deliv Rev 2002;54:157.
[41] Schwaz VA, Klein SD, Hornung R, Knochenmuss R, Wyss P, Fink D, et al. Lasers Surg Med 2001;29:252.
[42] Cord AT, Saunder HF. US Patent No. 273019, 1971.
[43] Hund F. Z Anorg Allg Chem 1985;525:221.
[44] Parker FJ. J Am Ceram Soc 1990;73:929.
[45] Thompson R. Industrial inorganic chemicals; production and uses. The Royal Society of Chemistry; 1995.
[46] Griebler WD, Hocken J, Schulte K. ECJ 1998;1–2:H.
[47] Macleod HA. Thin film optical filters. 2nd ed. New York: MacMillan; 1986, p. 370.
[48] Moseley PT, Tofield BC. Solid state gas sensors. Bristol: Adam Hilger; 1987.
[49] Sberveglieri G, editor. Gas sensors. Dordrecht: Kluwer Academic Publishing House; 1992.
[50] Kumazawa N, Islam MR, Takeuchi M. J Electrochem Chem 1999;472:137.
[51] Logothetis EM. Ceram Proc Eng Sci 1980;1:281.
[52] Savage NO, Akbar SA, Dutta PK. Sensors Actuators B 2001;72:239.
[53] Dutta PK, Ginwalla A, Hogg BD, Patton BR, Chwieroth B, Liang Z, et al. J Phys Chem B 1999;103:4412.
[54] Birkefeld LD, Azad AM, Akbar S. J Am Ceram Soc 1992;75:2964.
[55] Krank PK, Fulkerson MD, Patton BR, Dutta PK. Sensors Actuators B 2002;87:471.
[56] Savage N, Chwieroth B, Ginwalla A, Patton BR, Akbar SA, Dutta PK. Sensors Actuators B 2001;79:17.
[57] Disegi JA, Wyss H. Orthopedics 1989;12:75.

[58] Klinger MM, Rahemtulla FR, Prince CW, Lucas LC, Lemons JE. Crit Rev Oral Biol Med 1998;9:449.
[59] Kasimo B, Laaumaa J. CRC Crit Rev Biocompat 1986;2:335.
[60] Leng YX, Huang N, Yang P, Chen JY, Sun H, Wang J, et al. Surf Coat Technol 2002;156:295.
[61] Mac Donald DE, Deo N, Markovic B, Stranick M, Somasundaran P. Biomaterials 2002;23:1269.
[62] Poluncheck L, Elbel J, Eckert L, Blum J, Wintermantel E, Eppenberger HM. Biomaterials 2000;21:539.
[63] Oh WS, Xu C, Kim DY, Goodman DW. J Vac Sci Technol A 1997;15:1710.
[64] Zhang F, Zheng Z, Chen Y, Liu X, Che A, Jiang Z. J Biomed Mater Res 1998;42:128.
[65] Hadjiivanov KJ, Kissurski DG. Chem Soc Rev 1996;25:61.
[66] Armor JN. Appl Catal B: Environ 1992;1:221.
[67] Went MS, Reimer JA. J Am Chem Soc 1992;114:5768.
[68] Went GT, Leu LJ, Lombardo SJ, Bell AT. J Phys Chem 1992;96:2235.
[69] Topsøe NY, Domestic J. J Catal 1995;151:226.
[70] Schneider H, Tschudin T, Schneider M, Wokauim A, Baiker A. J Catal 1994;147:5.
[71] Forzatti P, Lietti L. Heterogenous Chem Rev 1996;3:33.
[72] Hu S, Apple TM. J Catal 1996;158:199.
[73] Alemany LJ, Berti F, Busca G, Ramis G, Robba D, Toledo GP, et al. Appl Catal B: Environ 1996;10:299.
[74] Vedrine JC, Bond GC, Forzatti P. Catal Today 2000;56:339.
[75] Janssen F, Kerkhoff F, Bosch H, Ross JRH. J Phys Chem 1987;91:5921.
[76] Amridis MD, Duevel RV, Wachs JE. Appl Catal B: Environ 1999;20:111.
[77] Blanco J, Alvarez E, Knapp C. Chem Eng 1999;10:149.
[78] Hums E, Joisten M, Müller R, Sigling R, Spielmann H. Catal Today 1996;27:29.
[79] van der Grift CJG, Woldhuis AF, Maaskant OL. Catal Today 1996;27:23.
[80] Weber R, Sakurai T, Hagenmaier H. Appl Catal B: Environ 1999;20:249.
[81] Angeles Larrubia M, Busca G. Appl Catal B: Environ 2002;39:343.
[82] Krishnamoorthy S, Baker JP, Amiridis MD. Catal Today 1998;40:39.
[83] Boccuzzi F, Chiorino A, Manzoli M, Andreeva D, Tabakowa T, Ilieva L, et al. Catal Today 2002;75:169.
[84] Li J, Jacobs G, Res T, Davis BH. Appl Catal A: Gen 2002;233:255.
[85] Kim CJ. US Patent No. 5227407 to Exxon Res. Eng Co., 1993.
[86] Kim CJ. Eur Appl Patent No. 89304092 to Exxon Res. Eng Co., 1989.
[87] Duvenhage DJ, Coville NJ. Appl Catal A: Gen 2002;233:63.
[88] Duvenhage DJ, Coville NJ. Appl Catal A: Gen 1997;152:43.
[89] Vannice MA, Garten RL. J Catal 1979;56:236.
[90] Bollinger M, Vannice MA. Appl Catal B: Environ 1996;8:417.
[91] Cunnigham D, Tsubota S, Kamijo N, Haruta M. Res Chem Intermed 1993;19:1.
[92] Lin S, Bollinger M, Vannice MA. Catal Lett 1993;17:245.
[93] Tsubota S, Haruta M, Kobayashi T, Ueda A, Nakahara Y. Stud Surf Sci Catal 1991;63:695.
[94] Fan L, Ichikuni N, Shimazu S, Ulmatsu T. Appl Catal A: Gen 2003;246:87.
[95] Chun SW, Jang JY, Park DW, Woo HC, Chung JS. Appl Catal B: Environ 1998;16:235.
[96] Kim H, Park DW, Woo HC, Chung JS. Appl Catal B: Environ 1998;19:233.
[97] Despres J, Koebel M, Kröcher O, Elsener M, Wokaun A. Appl Catal B: Environ 2003;43:389.
[98] Brown WD, Granneman WW. Solid State Electron 1978;21:837.
[99] Li C, Zheng Z, Zhang F, Yang S, Wang H, Chen L, et al. Nucl Instrum Meth Phys Res B 2000;169:21.
[100] Matsumoto Y, Shono T, Hasegawa T, Fukumura T, Kawasaki K, Ahmet P, et al. Science 2001;291:854.
[101] Chambers SA, Thevuthasan S, Farrow RFC, Marks RF, Thiele JU, Folks L, et al. Appl Phys Lett 2001;79:3467.
[102] Kavan L, Fattakhova D, Krtil P. J Electrochem Soc 1999;146:1375.
[103] Simons PY, Dachille F. Acta Cryst 1967;23:334.

[104] Latroche M, Brohan L, Marchand R, Tournoux M. J Solid State Chem 1989;79:78.
[105] Norotsky A, Jamieson JC, Kleppa OJ. Science 1967;158:338.
[106] Jamieson JC, Olinger B. Am Min 1969;54:1447.
[107] Zhang HZ, Banfield JF. J Mater Chem 1998;8:2073.
[108] Zhang H, Banfield JF. J Phys Chem B 2000;104:3481.
[109] Heald EF, Weiss CW. Am Min 1972;57:20.
[110] Nuth JA. Nature 1987;329:589.
[111] Gamarnik MY. Nanostruct Mater 1996;7:651.
[112] Garvie RC. J Phys Chem 1978;82:218.
[113] McHale JM, Auraux A, Perrota AJ, Navrotsky A. Science 1977;277:788.
[114] Bobyrenko YY. Zh Fis Khim 1972;46:1303.
[115] Novrotsky A, Jleppa OJ. J Am Ceram Soc 1968;50:623.
[116] Mitsihashi T. J Am Ceram Soc 1972;62:1305.
[117] Daßler A, Feltz A, Jung J, Ludwig W, Kaiserberger E. J Therm Anal 1988;33:803.
[118] Kumar PN, Keizer K, Burggraff AJ, Okubo T, Nagomoto H, Morooka S. Nature 1992;358:48.
[119] Basca RR, Grätzel M. J Am Ceram Soc 1996;79:2185.
[120] So WW, Park SB, Kim KJ, Shin CH, Moon SJ. J Mater Sci 2001;36:4299.
[121] Shannon RD, Pask JA. Am Min 1964;49:1707.
[122] Ding D, Liu X. J Mater Res 1998;19:2556.
[123] Rao CN, Rao RJ. Phase transitions in solids. New York: McGraw Hill; 1978, p. 82.
[124] Depero LE, Sangaletti L, Allieri B, Bontempi E, Marino A, Zocchi M. J Cryst Growth 1999;198/199:516.
[125] Zhang H, Banfield JF. J Mater Res 2000;15:437.
[126] Gmelin Handbuch der Anorganische Chemie. 8th ed. Titan, Verlag Chemie, GMBH, Veihem/Bugstrasse; 1959, p. 223.
[127] Sureh C, Biju V, Mukundan P, Warrier KGK. Polyhedron 1998;17:3131.
[128] Gennari FC, Pasquevich DM. J Am Ceram Soc 1999;82:1915.
[129] Chan CK, Porter JF, Li YG, Guo W, Chan CM. J Am Ceram Soc 1999;82:566.
[130] Linsbigler AL, Lu GQ, Yates Jr. JT. Chem Rev 1995;95:735.
[131] Tanaka K, Capule MFV, Hisanaga T. Chem Phys Lett 1991;187:73.
[132] Kumar KNP, Keizer K, Burrgraaf AJ. J Mater Chem 1993;3:1141.
[133] Ha PS, Youn HJ, Jung HS, Hong KS, Park YH, Ko KH. J Colloid Interface Sci 2000;223:16.
[134] Chao HE, Yun YU, Xingfang HU, Larbot A. J Eur Ceram Soc 2003;23:1457.
[135] Shannon RD, Pask JA. J Am Ceram Soc 1965;48:391.
[136] Rodriguez R, Vargas S, Arrayo R, Montiel R, Haro E. J Mater Res 1997;12:439.
[137] Al-Salim NY, Abagshaw S, Bittar A, Kemmett T, McQuilla AJ, Mills AM, et al. J Mater Chem 2000;10:2358.
[138] Vargas S, Arrayo R, Haro E, Rodriguez R. J Mater Res 1999;14:3932.
[139] Arrayo R, Códoba G, Padilla J, Lara VH. Mater Lett 2002;54:397.
[140] Karvinen S. Solid State Sci 2003;5:811.
[141] Criado JM, Real C, Soria J. Solid State Ionics 1989;32/33:461.
[142] Rao CNR, Turner A, Honig JM. J Phys Chem 1959;11:173.
[143] Gotic M, Ivanda M, Sekulic A, Music S, Popovic S, Turkovic A. Mater Lett 1966;28:225.
[144] Music S, Gotic M, Ivanda M, Popovic S, Turkovic A, Trojko R, et al. Mater Sci Eng B 1997;47:33.
[145] Hu Y, Tsai HL, Huang CL. J Eur Ceram Soc 2003;23:691.
[146] Kumar KN, Kumar J, Keizer K. J Am Ceram Soc 1994;77:1396.
[147] Banfield JF, Bischoff BL, Anderson MA. Chem Geol 1993;110:211.
[148] Wang CC, Ying JY. Chem Mater 1999;11:3113.
[149] Kumar KNP. Scr Metall Mater 1995;32:873.
[150] Izutsu H, Nair PN, Mizukami F. J Mater Chem 1997;7:855.
[151] Legrand-Buscema C, Malibert C, Bach S. Thin Solid Films 2002;418:79.

[152] van Grieken R, Aguado J, Lopez-Muñoz MJ, Maragan J. J Photochem Photobiol A: Chem 2002;148:315.
[153] Ranjit KT, Wilner I, Bossmann SH, Braun AM. J Catal 2001;204:305.
[154] Leduc CA, Campbell JM, Rossin JA. Ind Eng Chem Res 1996;25:2473.
[155] Fu HZ, Clark LA, Yang Q, Anderson MA. Environ Sci Technol 1996;30:2473.
[156] Yang J, Ferreria JMF. Mater Res Bull 1988;33:389.
[157] Hirano M, Nakahara C, Ota K, Tanaike O, Inagaki M. J Solid State Chem 2003;170:39.
[158] Colón G, Hidalgo MC, Navío JA. Appl Catal A: Gen 2002;231:185.
[159] Zhang YH, Reller A. Mater Sci Eng C 2002;19:323.
[160] Olivery G, Ramis G, Busca G, Escribano VS. J Mater Chem 1993;3:1239.
[161] Gouma PI, Dutta PK, Mills MJ. Nanostruct Mater 1999;11:1231.
[162] Stir M, Traykova T, Nicula R, Burkel E, Baethtz C, Knapp M, et al. Nucl Instrum Meth Phys Res B 2003;199:59.
[163] van de Krol R, Goossens A, Schoonman J. J Electrochem Soc 1997;144:1723.
[164] Errera J, Ketelaar H. J Phys Rad 1932;3:239.
[165] Diebold U. Surf Sci Rep 2003;48:53.
[166] Poznyak SK, Kokorin AI, Kulak AI. J Electroanal Chem 1998;442:99.
[167] Carp O, Reller A. Unpublished results.
[168] Pedraza F, Vasquez A. J Phys Chem Solids 1999;60:445.
[169] Xie Y, Yuan C. Mater Res Bull 2004;39:533.
[170] Yin S, Fujishiro Y, Wu J, Aki M, Sato T. J Mater Proc Tech 2003;137:45.
[171] Kang M. J Mol Catal A: Chem 2003;97:173.
[172] Kim CS, Moon BK, Park JH, Son SM. J Cryst Growth 2003;254:405.
[173] Yanagisava K, Yamamoto Y, Feng Q, Yamasaki N. J Mater Res 1998;13:825.
[174] Ito S, Yoshida S, Wanabe T. Chem Lett 2000;1:70.
[175] Kolen'ko YV, Burukhin AA, Churagulov BR, Oleynikov NN. Mater Lett 2003;57:1124.
[176] Aruna ST, Tirosh S, Zaban A. J Mater Chem 2000;10:2388.
[177] Ovesnstone J, Yanagisawa K. Chem Mater 1990;11:2770.
[178] Inagaki M, Nakazawa Y, Hirano M, Kobayashi Y, Toyoda M. Int J Inorg Mater 2001;3:809.
[179] Hirano M, Ota K. J Mater Sci 2004;39:1841.
[180] Kolen'ko YV, Maximov VD, Garshev AV, Meskin PE, Oleynikov NN, Chragulov BR. Chem Phys Lett 2004;388:411.
[181] Furlong DN, Parfitt CD. J Colloid Interface Sci 1978;65:548.
[182] Qian Y, Chen Q, Chen Z, Fan C, Zhou G. J Mater Chem 1993;3:203.
[183] Iwasaki M, Hara M, Ito S. J Mater Sci Lett 1988;17:1769.
[184] Bach U, Lupo D, Comte P, Moster JE, Weissortel F, Salbeck J. Nature 1998;395:583.
[185] Sivakumar S, Krishna Pillai P, Mukundan P, Warrier K. Mater Lett 2002;52:330.
[186] Matijevic E, Budnik M, Meites L. J Colloid Interface Sci 1997;61:302.
[187] Watson SS, Beydoun D, Scott JA, Amal R. Chem Eng J 2003;95:213.
[188] Haga Y, An H, Yosomiya R. J Mater Sci 1997;32:3183.
[189] Yung KJY, Park SB. J Photochem Photobiol A: Chem 1999;127:177.
[190] Livage J, Henry M, Sanchez C. Prog Solid State Chem 1988;18:259.
[191] Doeuff S, Dromzee Y, Taulelle F. Inorg Chem 1989;28:4439.
[192] Doeuff S, Henry M, Sanchez C. Mater Res Bull 1990;25:1519.
[194] Guillard C, Beaugiraud B, Dutriez C, Herrmann JM, Jaffrezic H, Jaffrezic-Renault N, et al. Appl Catal B: Environ 2002;39:331.
[195] Campostrini R, Ischia M, Palmisano L. J Therm Anal Cal 2003;71:997.
[196] Campostrini R, Ischia M, Palmisano L. J Therm Anal Cal 2003;71:1011.
[197] Campostrini R, Ischia M, Palmisano L. J Therm Anal Cal 2004;75:13.
[198] Harizanov O, Harizanov A. Solar Energy Mater Solar Cells 2000;63:185.
[199] Nakamoto K. Infrared spectra of inorganic compound. New York, London: John Wiley & Sons; 1963.
[200] Dick S, Suhr C, Rehspringer JL, Daire M. Mater Sci Eng A 1989;109:227.

[201] Li S, Condrate RA, Jang SD, Spriggs RM. J Mater Sci 1989;24:3873.
[202] Chandler C, Roger C, Hamden-Smith M. Chem Rev 1993;93:1205.
[203] Barringer EA, Bowen HK. Langmuir 1985;1:420.
[204] Takahashi Y, Matsuoka Y. J Mater Sci 1988;23:2259.
[205] Li Y, White TJ, Lim SH. J Solid State Chem 2004;177:1372.
[206] Hague DC, Mayo MJ. J Am Ceram Soc 1994;77:1957.
[207] Kaliszewski MS, Heur AH. J Am Ceram Soc 1990;73:1504.
[208] Philipse AP, van Bruggen MPB, Pathmamanoharan C. Langmuir 1994;10:92.
[209] Okudera H, Yokogawa Y. Thin Solid Films 2003;423:119.
[210] Tonejc M, Djerdj I, Tonejc A. Mater Sci Eng B 2001;85:55.
[211] Phani R, Santucci S. Mater Lett 2001;50:240.
[212] Chen YF, Lee CY, Yeng MY, Chin HT. J Cryst Growth 2003;247:363.
[213] Yang P, Lu C, Hua N, Du Y. Mater Lett 2002;57:794.
[214] Brezová V, Beažkova A, Karpinsky Ĺ, Grošková J, Jorik V, Cepan M. J Photochem Photobiol A: Chem 1997;109:177.
[215] Arabatzis IM, Antonaraki S, Stergiopoulos T, Hiskia A, Papaconstantinou E, Bernard MC, et al. J Photochem Photobiol A: Chem 2002;149:237.
[216] Teeng HI, Chang WC, Wu JCS. Appl Catal B: Environ 2003;37:37.
[217] Tseng IH, Wu JCS, Chou HY. J Catal 2004;221:432.
[218] Navío JA, Testa JJ, Djedjeian P, Padron JR, Rodriguez D, Litter MI. Appl Catal A: Gen 1999;177:111.
[219] Yuan ZH, Jia HJ, Zhang LD. Mater Chem Phys 2002;73:323.
[220] Sonowane RS, Kale BB, Dongare MK. Mater Chem Phys 2004;85:52.
[221] Wang J, Una S, Klabunde KJ. Appl Catal B: Environ 2004;48:151.
[222] Yamashita H, Harada M, Misaka J, Takeuchi M, Anpo KM. J Photochem Photobiol A: Chem 2002;148:257.
[223] Lopez T, Gomez R, Pecci G, Reyles P, Bokhimi X, Navaro O. Mater Lett 1999;40:59.
[224] Di Paola A, Garcìa-Lòpez E, Ikeda S, Marcì G, Ohtani B, Palmisano L. Catal Today 2002;75:87.
[225] Zhao XF, Cheng XF, Zhang ZH, Liu L, Jia DZ. J Inorg Mater 2004;19:140.
[226] Yuan ZH, Jia JH, Zhang L. Chem Phys 2002;73:323.
[227] Li FB, Li XZ. Appl Catal A: Gen 2002;228:15.
[228] Gaponov Y, Amemiya Y, Ito K, Kamikubo H, Karakchiev I, Lyakov N. Mater Lett 2002;57:330.
[229] Li FB, Li XZ, Hou MF. Appl Catal B: Environ 2004;48:185.
[230] Zhang H, Reller A. J Mater Chem 2001;11:2537.
[231] Stone VF, Davis RJ. Chem Mater 1998;10:1468.
[232] Antonelli DM, Ying JY. Angew Chem Int Ed Engl 1995;34:2014.
[233] Sato S, Oimatsu S, Takahashi R, Sodesawa T, Nozaki F. Chem Commun 1997;2219.
[234] Putnam RL, Nakagawa N, McGrath KMM, Yao N, Aksay IA, Gruner SM. Chem Mater 1997;9:2690.
[236] Thieme M, Schuth F. Micropor Mesopor Mater 1999;27:193.
[237] Cabrera S, El Haskouri J, Beltrán-Porter A, Beltrán-Porter D, Marcos MD, Amóros P. Solid State Sci 2000;2:513.
[238] Singhal B, Porwal A, Sharma A, Ameta R, Ameta SC. J Photochem Photobiol A: Chem 1997;108:85.
[239] Cassiers K, Linssen T, Mathieu M, Bai YQ, Zhu HY, Cool P, et al. J Phys Chem B 2004;108:3713.
[240] Yang P, Zhao D, Margolese DI, Chmelka B, Stucky GD. Nature 1998;396:152.
[241] Li DL, Zhou HS, Hibino M, Honma I. J Mater Res 2003;18:2743.
[242] Kartani I, Meredith P, da Costa JCD, Riches JS, Lu GQM. Curr Appl Phys 2004;4:160.
[243] Thoms H, Epple M, Fröba M, Wong J, Reller A. J Mater Chem 1998;8:1447.
[244] Saadoun L, Ayllón JA, Jimènez-Becerril J, Peral J, Domènech X, Rodríguez-Clemente R. Appl Catal B: Environ 1999;21:269.

[245] Zheng JH, Qiu KY, Wei Y. Mol Cryst Liq Cryst 2000;354:183.
[246] Wang C, Li Q, Wang R. J Mater Chem 2004;39:1899.
[247] Wang C, Xi H, Wang RD. Chem Lett 2004;33:20.
[248] Zhang R, Gao L. Mater Res Bull 2002;37:1659.
[249] Lim KT, Hwang HS, Ryoo W, Johnson KP. Langmuir 2004;20:2466.
[250] Pillai V, Kumar P, Huo MJ, Ayyub P, Shah DO. Adv Colloid Interface Sci 1995;55:241.
[251] Kitahara A, Ohasi O, Kon-no K. J Colloid Interface Sci 1988;78:122.
[252] Chhabra V, Pillai V, Mishra BK, Morrone A, Shah DO. Langmuir 1995;11:3307.
[253] Chhabra V, Ayyub P, Chattopadhay S, Maitra AN. Mater Lett 1996;26:21.
[254] Hong SS, Lee MS, Lee GD, Lim KT, Ha BJ. Mater Lett 2003;57:297.
[255] Nagaveni N, Hegde MS, Ravishankar N, Subbanna GN, Madras G. Langmuir 2004;20:2900.
[256] Nagaveni K, Sivalingam G, Hegde MS, Madras G. Appl Catal B: Environ 2004;48:83.
[257] Kavan L, O'Regan B, Kay A, Grätzel M. J Electroanal Chem 1993;346:291.
[258] Matsumoto Y, Adachi H, Hombo J. J Am Ceram Soc 1993;76:769.
[259] Zhang X, Yao B, Zhao L, Liang C, Mao Y. J Electrochem Soc 2001;148:398.
[260] Natarajan C, Nogami G. J Electrochem Soc 1996;143:1547.
[261] Karuppuchamy S, Amalnekar DP, Yamaguchi K, Yoshida T, Sugiura T, Minoura H. Chem Lett 2001:78.
[262] Matsumoto Y, Ishikawa Y, Nishida M, Ii S. J Phys Chem B 2000;104:4204.
[263] Ishikawa Y, Matsumoto Y. Electrochim Acta 2001;46:2819.
[264] Zhitomirsky I. Mater Lett 1998;33:305.
[265] Kamada K, Mukai M, Matsumoto Y. Electrochim Acta 2002;47:3309.
[266] Jones AC, Chalker PR. J Phys D—Appl Phys 2003;36:R80.
[267] Choy KL. Prog Mater Sci 2003;48:57.
[268] Smith A, Rodriguez-Clemente R. Thin Solid Films 1999;345:192.
[269] Sanchez-Juarez A, Tiburcio-Silver A, Ortiz A. Solar Energy Mater Solar Cells 1998;52:301.
[270] Ahonen PP, Tapper U, Kauppinen EI, Joubert JC, Deschanvres JL. Mater Sci Eng A 2001;315:113.
[271] Ahonen PP, Kauppinen EI, Joubert JC, Deschanvres JL, van Tendeloo G. J Mater Res 1999;14:3938.
[272] Paraguay FD, Estrada WL, Acosta DRN, Andrade EM, Miki-Yoshida M. Thin Solid Films 1999;350:192.
[273] Veluchamy P, Tsuji M, Nishio T, Aramoto T, Higuchi H, Kumazawa S, et al. Solar Energy Mater Solar Cells 2001;67:179.
[274] Zhang SZ, Messing GL. J Am Ceram Soc 1990;73:67.
[275] Lyons SW, Ortega J, Wang LM, Kodas TT. Mater Res Soc Symp Proc 1992;271:907.
[276] Ogihara T, Ookura T, Yanagawa T, Ogata N, Yoshida K. J Mater Chem 1991;1:789.
[277] Dubois B, Ruffier D, Odier P. J Am Ceram Soc 1989;72:713.
[278] Mardare D, Rusu GI. Mater Lett 2002;56:210.
[279] Treichel O, Kirchhoff V. Surf Coat Technol 2000;123:268.
[280] Rodriguez J, Gomez M, Ederth J, Niklasson GA, Ganqvist CG. Thin Solid Films 2000;365:119.
[281] Okimura K, Maeda H, Shibata A. Thin Solid Films 1996;427:281–2.
[282] Ong CK, Wang SJ. Appl Surf Sci 2001;185:47.
[283] Herman GS, Gao Y. Thin Solid Films 2001;397:157.
[284] Marakami M, Matsumoto Y, Nakajima K, Makino T, Segawa Y, Chikyow T, et al. Appl Phys Lett 2001;78:2664.
[285] Fromknecht R, Khubeis I, Massing S, Meyer O. Nucl Instrum Meth Phys Res B 1999;147:191.
[286] Miyake S, Kobayashi T, Satou M, Fujimoto F. J Vac Sci Technol A 1991;9:3036.
[287] Zhu YC, Ding CX. Nanostruct Mater 1999;11:427.
[288] Miao L, Tanemura S, Toh S, Kaneko K, Tanemura M. J Cryst Growth 2004;264:246.
[289] Cozzolli PD, Camarelli R, Fanizza E, Curri ML, Agostina A, Laub D. J Am Chem Soc 2004;126:3868.
[290] Wu JJ, Yu CC. J Phys Chem B 2004;108:3377.

[291] Cozzoli PD, Kornowski A, Welleri H. J Am Chem Soc 2003;125:14539.
[292] Pradhan SK, Reucroft PJ, Yang FQ, Dozier A. J Cryst Growth 2003;256:83.
[293] Lin Y, Wu GS, Xie T, Zhang LD. J Phys Condens Matter 2003;15:2917.
[294] Okuya M, Prokudina NA, Mushika K, Kaneko S. J Eur Ceram Soc 1999;19:903.
[295] Yang HG, Zeng HC. Chem Mater 2003;15:3113.
[296] Zhang YX, Li GH, Jin YX, Zhang Y, Zhang LD. Chem Phys Lett 2002;365:300.
[297] Armstrong AR, Armstrong G, Canales J, Bruce PC. Angew Chemie 2004;43:2286.
[298] Tian ZRR, Voight JA, Liu J, McKenzie B, Xu HF. J Am Chem Soc 2003;125:12384.
[299] Huo ZL, Shi JL, Zhang LX, Ruan ML, Yan JN. Adv Mater 2002;14:830.
[300] Peng TY, Yang HP, Chang G, Dai K, Hirao K. Chem Lett 2004;33:336.
[301] Wang YQ, Hu GQ, Duan XF, Sun HL, Xu QK. Chem Phys Lett 2002;365:427.
[302] Gong D, Grimes GA, Varhghese OK, Hu W, Singh RS, Chen Z, et al. J Mater Res 2001;16:331.
[303] Yuan ZH, Colomer JF, Su BL. Chem Phys Lett 2002;363:362.
[304] Baba K, Hatada R. Surf Coat Technol 2001;136:241.
[305] Holland BT, Blanford CF, Do T, Stein A. Chem Mater 1999;11:795.
[306] Wijnhoven JEGJ, Vos Willem WL. Science 1998;281:802.
[307] Xia Y, Gates B, Yin Y, Lu Y. Adv Mater 2001;12:693.
[308] Goossens A, Maloney EL, Schoonman J. Chem Vapor Deposition 1998;4:109.
[309] Chemseddine A, Moritz T. Eur J Inorg Chem 1999;2:235.
[310] Richel A, Johnson NP, McComb DW. Appl Phys Lett 2000;76:1816.
[311] Serpone N. J Photochem Photobiol A: Chem 1997;104:1.
[312] Rajeshwar K. J Appl Electrochem 1995;25:1067.
[313] Ward MD, White JM, Bard AJ. J Am Chem Soc 1983;105:27.
[314] Serpone N. Solar Energy Mater Solar Cells 1995;38:369.
[315] Grätzel M. Nature 2001;414:338.
[316] Nosaka Y, Fox MA. J Phys Chem 1988;92:1893.
[317] Fujishima A, Hashimoto K, Watanabe T. TiO_2 photocatalysis. Fundaments and applications, 1st ed. Tokyo: BKC; 1999.
[318] Mardare D, Tasca M, Delibas M, Rusu GI. Appl Surf Sci 2000;156:200.
[319] Halley JW, Kozlowski M, Michalewicz M, Smyrl W, Tit N. Surf Sci 1991;226:397.
[320] Radecka M, Zakrewska K, Czternastek H, Stapiński T, Debrus S. Appl Surf Sci 1993;65/66:227.
[321] Madhusudan Reddy K, Gopal Reddy CV, Manorana SV. J Solid State Chem 2001;158:180.
[322] Kumar PM, Badrinarajanan S, Sastry M. Thin Solid Films 2000;358:122.
[323] Fujishima A, Rao TN, Tryk DA. J Photochem Photobiol C: Photochem Rev 2000;1:1.
[324] Wöhrle D, Meissner D. Adv Mater 1991;3:129.
[325] Pettersson LAA, Roman LS, Inganas O. J Appl Phys 1999;86:487.
[326] Theander M, Yartsev A, Zigmantas D, Sundstrom V, Mammo W, Andersson MR, et al. Phys Rev B 2000;61:12957.
[327] van der Zanden B, van de Krol R, Schoonman J, Goossens A. Appl Phys Lett 2004;84:2539.
[328] Nazeerudddin MK, Kay A, Rodicio I, Humphry-Baker R, Müller E, Liska P, et al. J Am Chem Soc 1993;115:6328.
[329] Cao F, Oskam G, Searson PC. J Phys Chem 1995;99:17071.
[330] Nogueira AF, De Paoli MA. Solar Energy Mater Solar Cells 2000;61:135.
[331] Nogueira AF, Durrant JR, De Paoli MA. Adv Mater 2001;13:826.
[332] Krüger J, Plass R, Cevey L, Piccirelli M, Grätzel M. Appl Phys Lett 2001;79:2085.
[333] Kaneko M, Takayama K, Pandey SS, Takashima W, Endo T, Rikukawa M, et al. Synth Met 2001;121:1537.
[334] Tennakone K, Kumara GRRA, Kumarasinghe AR, Wijayantha KGU, Sirimanne PM. Semicond Sci Technol 1995;10:1689.
[335] Salafsky JS. Solid-State Electronics 2001;45:53.
[336] Breeze AJ, Schlesinger Z, Carter SA. Phys Rev B 2001;64:12525.
[337] Arango AC, Carter SA, Brock PJ. Appl Phys Lett 1999;74:1698.

[338] Gebeyehu D, Brabec CJ, Padinger F, Fromherz T, Spiekermann S, Vlachopoulos N, et al. Synth Met 2001;121:1549.
[339] Handbook of oligo- and polythiophenes. Weinheim: Wiley-VCH; 1999.
[340] Grätzel M. Curr Opin Colloid Interface Sci 1999;4:314.
[341] Nelson J. Curr Opin Solid State Mater Sci 2002;6:87.
[342] Grätzel M. Properties and applications of nanocrystalline electronic junctions. In: Nalwa HS, editor. Handbook of nanostructured materials and nanotechnology. Electrical properties, vol. 3. Academic Press; 2000 [Chapter 10].
[343] Bard J. Science 1980;201:139.
[344] Maruska HP, Ghosh AK. Solar Energy 1978;20:443.
[345] Gerischer H, Heller A. J Electrochem Soc 1992;139:113.
[346] Bickley RI, Gonzales-Carreno T, Lees JL, Palmisano L, Tilley RJD. J Solid State Chem 1991;92:178.
[347] Deng X, Yue Y, Gao Z. Appl Catal B: Environ 2002;39:135.
[348] Mills A, Lee SK, Lepre A. J Photochem Photobiol A: Chem 2003;155:199.
[349] Basca RR, Kiwi J. Appl Catal B: Environ 1998;16:19.
[350] Muggli DS, Ding L. Appl Catal B: Environ 2001;32:181.
[351] Ohno T, Sarukawa K, Tokieda K, Matsumura M. J Catal 2001;203:82.
[352] Nargiello M, Herz T. In: Ollis DF, Al-Ekabi H, editors. Photocatalytic purification and treatments of water and air. Amsterdam: Elsevier; 1993, p. 801.
[353] Zhang Q, Gao L, Guo J. Appl Catal B: Environ 2000;26:207.
[354] Martin ST, Hermann H, Choi W, Hoffmann MR. J Chem Soc Faraday Trans 1994;90:3315.
[355] Soana F, Sturini M, Cermenati L, Albini A. J Chem Soc Perkin Trans 2000;4:699.
[356] Bard AJ, Fox MA. Acc Chem Res 1995;28:141.
[357] Ohno T, Haga D, Fujuhara K, Kaizaki K, Matsumura M. J Phys Chem B 1997;101:10605.
[358] Fujihara K, Ohno T, Matsumura M. J Chem Soc Faraday Trans 1998;94:3705.
[359] Ohno T, Fujihara K, Sarakawa K, Tanigawa F, Matsumura M. Z Phys Chem 1999;213:165.
[360] Mahdavi F, Burton TC, Li Y. J Org Chem 1993;58:744.
[361] Li Y. In: Kamat PV, Meisel D, editors. Semiconductor nanocluster. Amsterdam: Elsevier; 1993 [Stud Surf Sci Catal 103].
[362] Ferry JL, Glaze WH. Langmuir 1998;14:3551.
[363] Minero C, Maurino V, Pelizzetti E. Res Chem Intermed 1997;23:291.
[364] Texier I, Ouzzani J, Delaire J, Giannotti C. Tetrahedron 1999;55:3401.
[365] Konstantinou IK, Albanis TA. Appl Catal 2003;42:319.
[366] Smith MB, March J. Effect of structure on reactivity, advanced organic chemistry: reactions, mechanisms and structure, 5th ed. New York: Wiley; 2001.
[367] Hermann JM. Catal Today 1999;53:115.
[368] Vuilliet E, Emmelin C, Chovelon JM, Guillard C, Hermann. Appl Catal B: Environ 2002;38:127.
[369] Hermann JM, Guillard C, Pichat P. Catal Today 1993;17:7.
[370] Maurino V, Minero C, Pelizzetti E, Vincenti M. Colloids Surf A: Physicochem Eng Aspects 1999;151:329.
[371] Hermann JM, Guillard C, Disdier J, Lehaut C, Malato S, Blanco J. Appl Catal B: Environ 2002;35:281.
[372] Bianco Prevot A, Vincenti M, Banciotto A, Pramauro E. Appl Catal B: Environ 1999;22:149.
[373] D'Oliveira JC, Al-Sayyed G, Pichat P. Environ Sci Technol 1990;24:990.
[374] Hermann JM, Tahiri H, Guillard C, Pichat P. Catal Today 1999;54:131.
[375] Galindo C, Jacques P, Kalt A. J Photochem Photobiol A: Chem 1999;130:131.
[376] Guillard C. J Photochem Photobiol A: Chem 2000;125:65.
[377] Sauleda RR, Brillas E. Appl Catal B: Environ 2001;29:135.
[378] Balcioglu A, Getoff N, Bekbölet M. J Photochem Photobiol A: Chem 2000;135:229.
[379] Tanaka K, Robledo SM, Hisanaga T, Ali R, Ramei Z, Bakar WA. J Mol Catal A: Chem 1999;144:425.
[380] Tanaka K, Reddy KSN. Appl Catal B: Environ 2002;39:305.

[381] Hisanaga T, Harada K, Tanaka K. J Photochem Photobiol A: Chem 1990;56:113.
[382] Ohtani B, Ueda Y, Nishimoto S, Kagiya T, Hschisuka H. J Chem Soc Perkin Trans 1990;2:1955.
[383] Konstantinou IK, Sakkas VA, Albanis TA. Appl Catal B: Environ 2001;34:227.
[384] Tahiri H, Ait-Ichou Y, Hermann JM. J Photochem Photobiol A: Chem 1998;114:219.
[385] Calza P, Minero C, Hiskia A, Papaconstantinou E, Pelizzetti E. Appl Catal B: Environ 2001;29:23.
[386] Sakkas VA, Albanis TA. Appl Catal B: Environ 2003;46:175.
[387] Maillard C, Guillard C, Pichat P. New J Chem 1994;18:941.
[388] Low GKC, Mc Evoy SR, Matthews RW. Environ Sci Technol 1991;25:460.
[389] Pramauro E, Vincenti M, Augugliaro V, Palmisano L. Environ Sci Technol 1993;27:1790.
[390] Kerzhentsev M, Giullard C, Pichat JP, Hermann JM. Catal Today 1996;27:215.
[391] Konstantinou IK, Sakellarides TM, Albanis TA. Environ Sci Technol 2001;35:398.
[392] Hous A, Lacheb H, Ksbi M, Elaloui E, Guillard C, Hermann JM. Appl Catal B: Environ 2001;31:145.
[393] Fox MA, Abdel-Wahab AA. Tetrahedron Lett 1990;31:4533.
[394] Harada K, Hisanaga T, Tanaka K. Water Res 1990;24:1415.
[395] Harada K, Hisanaga T, Tanaka K. New J Chem 1987;11:598.
[396] Hermann M, Matos J, Disdier J, Guillard C, Laoine J, Malato S, et al. Catal Today 1999;54:255.
[397] Bianco Prevot A, Pramauro E, de la Guardia M. Chemosphere 1999;39:149.
[398] Ziolli RL, Jardim WF. J Photochem Photobiol A: Chem 2002;147:205.
[399] Halmann M. Nature 1975;275:113.
[400] Wrighton MS, Ellis AB, Wolczanski PT, Morse DL, Abrahamson HB, Ginley DS. J Am Chem Soc 1976;98:2774.
[401] Grätzel M. Cattech 1999;3:4.
[402] Augustynski J, Calzaferri G, Courvoisier JC, Grätzel M, Ulmann M. Proceedings of the 10th International Conference Photochemical Storage of Solar Energy. Switzerland: Interlaken; 1994, p. 229.
[403] Khan SU, Al-Shahry M, Ingler Jr. WB. Science 2002;297:2243.
[404] Dhar NR, Sechacharyubu EV, Mukeji SK. Ann Agron 1941;11:83.
[405] Dhar NR. J Chem Phys 1958;55:983.
[406] Dhar NR, Francis AM. Proc Natl Acad Sci, India, Sect A 1951;20:112.
[407] Moore B, Webster TA. Proc R Soc Lond Ser B 1913;87:163.
[408] Schrauzer GN, Strampach N, Hui LN, Palmer MR, Salehi J. Proc Natl Acad Sci USA 1983;80:3873.
[409] Boucher DL, Davies JA, Edwards JG, Mennad A. J Photochem Photobiol A: Chem 1995;88:53.
[410] Rusina O, Linnik O, Eremenko A, Kisch H. Chem Eur J 2003;9:561.
[411] Rusina O, Eremenko A, Frank G, Strunk HP, Kisch H. Angew Chem Int Ed 2001;40:3993.
[412] Hoshino K, Inui M, Kitamura T, Kokado H. Angew Chem Int Ed 2000;39:2509.
[413] Hoshino K. Chem Eur J 2001;7:2727.
[414] Ogawa T, Kitamura T, Shibuya T, Hoshino K. Electrochem Commun 2004;6:55.
[415] Grätzel E, editor. Energy resources through photochemistry and catalysis. New York: Academic Press; 1983.
[416] Wang R, Hashimoto K, Fujishima A, Chikuni M, Kojima E, Kitamura A, et al. Adv Mater 1998;10:5918.
[417] Sakai N, Wang R, Fujishima A, Watanabe T, Hashimoto H. Langmuir 1998;14:5918.
[418] Wang R, Sakai N, Fujishima A, Watanabe T, Hashimoto H. J Phys Chem B 1999;103:2188.
[419] Yu JG, Zhao XJ, Zhao QN, Wang G. Mater Chem Phys 2001;68:253.
[420] Yu JG, Zhao XJ. J Mater Sci Lett 2001;20:671.
[421] Nakajima A, Koizumi SI, Watanabe T, Hashimoto K. J Photochem Photobiol A: Chem 2001;146:129.
[422] Yu JC, Yu J, Tang HY, Zhang L. J Mater Chem 2002;12:81.
[423] Yu JC, Yu J, Ho W, Zhao J. J Photochem Photobiol A: Chem 2002;148:331.

[424] Lee YC, Hong YP, Lee HY, Kim H, Jung YJ, Ko KH, et al. J Colloid Interface Sci 2000;232:410.
[425] Asachi R, Morikawa T, Ohwaki T, Aoki K, Taga Y. Science 2001;293:269.
[426] Hattori A, Kawahara T, Uemoto T, Suzuki F, Tada H, Ito S. J Colloid Interface Sci 2003;267:127.
[427] Dohshi S, Takeichi M, Anpo M. Catal Today 2003;85:199.
[428] Ikeda K, Sakai R, Baba R, Hoshimoto K, Fujishima A. J Phys Chem B 1997;101:2617.
[429] Maeda H, Ikeda K, Haschimoto K, Ajito K, Morita M, Fujishima A. J Phys Chem 1997; 437:241.
[430] Kormann C, Bahnemann DW, Hoffmann MR. Environ Sci Technol 1988;22:798.
[431] Hoffmann AJ, Carraway ER, Hoffmann MR. Environ Sci Technol 1994;28:776.
[432] Carraway ER, Hoffmann AJ, Hoffmann MR. Environ Sci Technol 1994;28:786.
[433] Muzka J, Fox MA. J Photochem Photobiol A: Chem 1991;57:27.
[434] Mura GM, Ganadu ML, Lombardi P, Lubinu G, Branca M, Maida V. J Photochem Photobiol A: Chem 2002;148:199.
[435] Nosaka Y, Kishimoto N, Nishino J. J Phys Chem 1998;102:10279.
[436] Pelizzetti E, Pramauro E, Minero C, Serpone N, Borgarello E. In: Schiavello M, editor. Photocatalysis and environment: trends and applications. NATO ASI Series C, vol. 238. London: Kluwer Academic Publishers; 1987, p. 469.
[437] Bahnemann DW, Cunningham J, Fox MA, Pelizzetti E, Pichat P, Serpone N. In: Heltz GR, Zepp RG, Crosby DG, editors. Aquatic and surface photochemistry. Boca Raton (FL): Lewis Publishers; 1994, p. 261.
[438] Herrmann JM, Guillard C, Arguello M, Agüera M, Tejedor A, Piedra L, et al. Catal Today 1999;54:353.
[439] Mao Y, Schoneich C, Asmus KD. J Phys Chem 1991;95:80.
[440] Fox MA, Sackett DD, Younathan JN. Tetrahedron 1987;43:1643.
[441] Fox MA, Chen CC. Tetrahedron 1991;95:5261.
[442] Hoffmann MR, Martin ST, Choi W, Bahnemann DW. Chem Rev 1995;95:69.
[443] Turchi CS, Ollis DF. J Catal 1990;122:178.
[444] Para S, Olivero J, Pulgarin C. Appl Catal B: Environ 2002;36:75–85.
[445] Minero C, Catozzo F, Pelizzetti E. Langmuir 1992;8:481.
[446] Peral J, Ollis DF. J Catal 1992;136:554.
[447] Vorontsov AV, Kurkin EN, Savinon EN. J Catal 1999;186:318.
[448] Kim SB, Hong SC. Appl Catal B: Environ 2002;35:305.
[449] Pichat P, Hermann JM, Disdier J, Courbon H, Mozzanega MN. Nouv J Chim 1981;5:627.
[450] Marinas A, Guillard C, Marianas JM, Fernández-Alba A, Agüera A, Hermann JM. Appl Catal B: Environ 2001;34:241.
[451] Mills A, Moris S. J Photochem Photobiol A: Chem 1992;71:75.
[452] Inel Y, Okte A. J Photochem Photobiol A: Chem 1996;96:175.
[453] Matthews RW. J Catal 1988;111:264.
[454] Minero C. Catal Today 1999;54:205.
[455] Turchi CS, Ollis DF. J Catal 1989;119:483.
[456] Bandara J, Kiwi J, Humphry-Baker R, Pulgarin C. J Adv Oxid Technol 1996;1:126.
[457] Le Campion L, Giannotti C, Ouzzani J. Chemosphere 1999;38:1561.
[458] Assabane A, Ichou YA, Tahiri H, Guillard C, Hermann JM. Appl Catal B: Environ 2000;24:71.
[459] Yu Y, Leu RM, Lee KC. Water Res 1996;30:1169.
[460] Okamoto K, Yamamoto Y, Tanaka H, Itaya A. Bull Chem Soc Jpn 1985;58:2023.
[461] Chen D, Ray AK. Appl Catal B: Environ 1999;23:143.
[462] Crittenden JC, Liu J, Hand DW, Perran DL. Water Res 1997;31:429.
[463] Matthews RW. J Phys Chem 1987;91:3328.
[464] Anpo M, Shima T, Kodama S, Kubokawa Y. J Phys Chem 1987;91:4305.
[465] Kiwi J. J Phys Chem 1985;89:2437.
[466] Ollis DF, Pelizzetti E, Serpone N. Environ Sci Technol 1991;25:1522.

[467] Wang KH, Tsai HH, Hseich YH. Appl Catal B: Environ 1998;17:313.
[468] Jacoby WA, Blake DM, Noble RD, Koval CA. J Catal 1995;157:87.
[469] Nimlos MR, Jacoby WR, Blake DM, Milne TA. Environ Sci Technol 1993;24:732.
[470] Wang W, Chiang LW, Ku Y. J Hazard Mater 2003;101:133.
[471] Hager S, Bauer R, Kudielka G. Chemosphere 2000;41:1219.
[472] Al-Ekabi H, Safarzadeh-Amiri A, Sifton W, Story J. Int J Environ Pollut 1991;1:125.
[473] Murov SL, Carmichael I, Huy GL. Handbook of photochemistry. New York: Marcel Dekker; 1993.
[474] Braun AM, Oliveros E. Water Sci Technol 1997;35:17.
[475] Wang Y, Hong CS. Water Res 2000;34:2791.
[476] Schwartz PF, Turro NJ, Bossmann SH, Braun AM, Abdel-Wahab AM, Duerr H. J Phys Chem B 1977;101:7127.
[477] Gierthy JF, Arcado KF, Floyd M. Chemosphere 1997;34:1495.
[478] Axelsson AK, Dunne LJ. J Photochem Photobiol A: Chem 2001;144:205.
[479] Luo Y, Ollis DF. J Catal 1996;163:1.
[480] Hung CH, Marinas BJ. Environ Sci Technol 1997;31(562).
[481] Chu W. Environ Sci Technol 1998;33:421.
[482] Bachman J, Patterson HH. Environ Sci Technol 1998;33:874.
[483] Mio XS, Chu SG, Xu XB. Chemosphere 1999;39:1639.
[484] Stefan MI, Bolton JR. Environ Sci Technol 1999;33:870.
[485] Dullin D, Mill T. Environ Sci Technol 1982;16:811.
[486] Parra S, Sarria V, Malato S, Péringer P, Pulgarin C. Appl Catal B: Environ 2000;27:149.
[487] Malato S, Blanco J, Richter C, Fernández P, Maldonado MI. Solar Energy Mater Solar Cells 2000;64:1.
[488] Cho Y, Choi W. J Photochem Photobiol A: Chem 2002;148:129.
[489] Rao NN, Dubey AK, Monhanty S, Khare P, Jain R, Kaul SN. J Hazard Mater 2003;101:301.
[490] Bolton JR, Bircher KG, Tumas W, Tolman CA. J Adv Oxid Technol 1996;1:13.
[491] Calvert JG, Pitts Jr. JN. Photochemistry. New York: Wiley; 1966, p. 789.
[492] Serpone N, Sauve G, Koch R, Tahiri H, Pichat P, Piccini P, et al. J Photochem Photobiol A: Chem 1996;94:8191.
[493] Paz Y, Luo Z, Rabenberg L, Heller A. J Mater Chem 1995;10:2848.
[494] Fernandez A, Leyrer J, González-Elipe A, Munuera G, Knözinger H. J Catal 1988;112:489.
[495] Maira A, Yeung KL, Yan CY, Yue PL, Chan CK. J Catal 2000;192:185.
[496] Anpo M, Takeuchi M. J Catal 2003;216:505.
[497] Sclafani A, Hermann JM. J Phys Chem 1996;100.
[498] Wang KH, Hsieh YH, Wu CH, Chang CY. Chemosphere 2000;40:389.
[499] Chen Y, Wang K, Lou L. J Photochem Photobiol A: Chem 2004;163:281.
[500] Xiaohong W, Zhaohua J, Huiling L, Shigang X, Xinguo H. Thin Solid Films 2003;441:130.
[501] Bahnemann DW, Kholuiskaya SN, Dillert R, Kulak AI, Kokorin AI. Appl Catal B: Environ 2002;36:161.
[502] Willner I. Unpublished results.
[503] Zhang ZB, Wang CC, Zakaria R, Ying JY. J Phys Chem B 1998;102:10871.
[504] Ohtani B, Ogawa Y, Nishimoto SI. J Phys Chem B 1997;101:3746.
[505] Serpone N, Lawless D, Khairtunov R, Pelizzetti E. J Phys Chem 1995;99:16655.
[506] Wang CC, Zhang Z, Ying JY. Nanostruct Mater 1997;9:583.
[507] Gerischer H. Electrochim Acta 1995;40:1277.
[508] Grela M, Colussi AJ. J Phys Chem 1996;100:18214.
[509] Augugliaro V, Palmisano L, Scalfani A, Minero C, Pelizzetti E. Toxicol Environ Chem 1988;16:89.
[510] Okamota K, Yamanato Y, Tanaka H, Itaya A. Bull Chem Soc Jpn 1985;58:2015.
[511] Kurtz RL, Stockbauer R, Madey TE. Surf Sci 1989;218:178.
[512] Burgeois S, Jomard F, Perdereau M. Surf Sci 1992;278:349.
[513] Smith PB, Bernasek SL. Surf Sci 1987;188:241.

[514] Kim KW, Lee EH, Kim YJ, Lee MH, Kim KH, Shin DW. J Photochem Photobiol A: Chem 2003;159:183.
[515] Henderson MA. Langmuir 1996;12:5093.
[516] Jin TS, Ma YR, Sun X, Liang D, Li TS. J Chem Res (S) 2000;96.
[517] Jin TS, Sun X, Li TS. J Chem Res (S) 2000;128.
[518] Jin S, Ma YR, Sun LX, Li TS. Synth Commun 2001;31:111.
[519] Gómez R, López T, Ortiz-Islas E, Navarrete J, Sánchez E, Tzompantzi F, et al. J Mol Catal A: Chem 2003;193:217.
[520] Corma A, Martinez A, Martinez C. Appl Catal A: Gen 1996;144:249.
[521] Arata K. Appl Catal A: Gen 1996;146:3.
[522] Lopez T, Bosch P, Tzompantzi F, Gomez R, Navarette J, Lopez-Salinas E, et al. Appl Catal 2000;197:107.
[523] Noda LK, de Almeida RM, Gonçalves NS, Probst LFD, Sala O. Catal Today 2003;85:69.
[524] Fu X, Zeltner WA, Yang Q, Anderson MA. J Catal 1997;188:482.
[525] Srinivasan R, Keogh RA, Milburn DR, Davis BH. J Catal 1995;153:123.
[526] Yang X, Jentoft FC, Jentoft RE, Girgsdies F, Ressler T. Catal Lett 2001;81:25.
[527] Harris LA, Schumacher R. J Electrochem Soc: Solid State Sci Technol 1980;127:1186.
[528] Heller A, Degani Y, Johnson Jr. DW, Gallagher PK. J Phys Chem 1987;91:5987.
[529] Liu H, Ma HT, Li XZ, Li WZ, Wu M, Bao XH. Chemosphere 2003;50:39.
[530] d'Hennzel O, Pichat P, Ollis DF. J Photochem Photobiol A: Chem 1990;118:197.
[531] Lewandowski MM, Ollis DF. J Catal 2003;217:38.
[532] Amama PB, Itoh K, Murabayashi M. Appl Catal B: Environ 2002;37:321.
[533] Choi W, Termin A, Hoffmann MR. J Phys Chem 1994;98:13669.
[534] Martin ST, Morrison CI, Hoffman MR. J Phys Chem 1994;98:13695.
[535] Litter MI, Navío JA. J Photochem Photobiol A: Chem 1994;84:183.
[536] Wilke K, Breuer HD. J Photochem Photobiol A: Chem 1999;121:49.
[537] Palmisano L, Augugliaro V, Sclalani A, Schiavello M. J Phys Chem 1992;63:367.
[538] Serpone N, Lawless D, Disdier J, Hermann JM. Langmuir 1994;10:643.
[539] Cao YA, Yang WS, Zhang WF, Liu GZ, Yue PL. New J Chem 2004;28:218.
[540] Soria J, Conesa JC, Augugliaro V, Palmisano L, Sciavello M, Scalfani A. J Phys Chem 1991;95:274.
[541] Palmisano L, Schiavello M, Sclafani A, Martin C, Martin I, Rives V. Catal Lett 1994;24:303.
[542] Gautron JJ, Lemasson P, Marucco JM. Faraday Discuss Chem Soc 1981;70:81.
[543] Pleskov YV. Sov Electrochem 1981;17:47.
[544] Fujihara S, Izumi K, Ohno T. J Photochem Photobiol A: Chem 2000;132:440.
[545] Hagfeldt A, Grätzel M. Chem Rev 1995;95:49.
[546] Anpo M. Catal Surv Jpn 1997;1:169.
[547] Palmisano L, Augugliaro V, Sclafani A, Schiavello M. J Phys Chem 1988;95:6710.
[548] Navío JA, Testa JJ, Djedjeian P, Padrón JR, Rodríguez D, Litter MI. Appl Catal A: Gen 1999;178:191.
[549] Wei M, Hermann JM, Pichat P. Catal Lett 1989;3:73.
[550] Hermann JM, Disdier J, Pichat P. Chem Phys Lett 1984;108:618.
[551] Litter MI, Navío JA. J Photochem Photobiol A: Chem 1996;98:171.
[552] Garcia F, Holgado JP, Yubero F, González-Elipe AR. Surf Coat Technol 2002;158–159:552.
[553] Yang Y, Li XJ, Chen JT, Wang LY. J Photochem Photobiol A: Chem 2004;163:517.
[554] Xu AW, Gao Y, Xu HQ. J Catal 2002;207:151.
[555] Borgarello E, Kiwi J, Grätzel M, Pelizzetti E, Visca M. J Am Chem Soc 1982;104:2996.
[556] Anpo M, Takeuchi M, Ikeue K, Dohshi S. Curr Opin Solid State Mater Sci 2002;6:3812.
[557] Zhao G, Kozuka H, Lin H, Takahashi M, Yoko T. Thin Solid Films 1999;340:125.
[558] Lin J, Yu JC, Lam SK. J Catal 1999;183:368.
[559] Rabenstein DL. Anal Chem 1971;43:1599.
[560] Ranjit KT, Willner I, Bossmann SH, Braun AM. Environ Sci Technol 2001;35:1544.
[561] Wang YQ, Cheng HM, Hao YZ, Ma JM, Li WH, Cai SM. J Mater Sci Lett 1999;18:127.

[562] Wang YQ, Cheng HM, Hao YZ, Ma JM, Li WH, Cai SM. Thin Solid Films 1999;349:120.
[563] Thorp JS, Eggleston HS. J Mater Sci Lett 1985;4:1140.
[564] Amorelli A, Evans JC, Rowlands CC. J Chem Soc Faraday Trans I 1989;85:4031.
[565] Iida Y, Ozaki S. J Am Ceram Soc 1961;44:120.
[566] Nobile Jr. A, Davis Jr. MW. J Catal 1989;116:383.
[567] Carp O, Reller A. Unpublished data.
[568] Serpome N, Lawless D. Langmuir 1994;19:643.
[569] Cordischi D, Burriesci N, D'Alba F, Petrera M, Polizzetti G, Schiavello M. Solid State Chem 1985;56:182.
[570] Bally AR, Korobeinikova EN, Schmid PE, Lévi F, Bussy F. J Phys D Appl Phys 1998;31:1149.
[571] Gennari FC, Pasquevich DM. J Mater Sci 1998;33:1571.
[572] Moser J, Grätzel M. Helv Chim Acta 1982;65:1436.
[573] Bickley RI, González-Carreña T, González-Elipe ART, Munuera G, Palmisano L. J Chem Soc Faraday Trans 1994;90:2257.
[574] Navío JA, Colón G, Litter MI, Bianco GN. J Mol Catal A: Chem 1996;16:267.
[575] Rao MV, Rajeshwar K, Pal VR, Verneker, DuBow J. J Phys Chem 1980;84:1987.
[576] Yue PL, Khan F, Rizzuti L. Chem Eng Sci 1983;38:1893.
[577] Navío JA, Garcìa Gomèz M, Pradera Adrián MA, Fuentes Mota J. In: Guisnet M, editor. Heterogenous catalysis and fine chemicals II. Amsterdam: Elsevier; 1991, p. 445.
[578] Araña J, González-Díaz O, Saracho MM, Doña-Rodríquez JM, Herrera-Melián JA, Pérez-Peña J, et al. Appl Catal B: Environ 2002;36:113.
[579] Pal B, Hata T, Goto K, Nogami G. J Mol Catal A: Chem 2001;169:147.
[580] Kwan CY, Chu W. Water Res 2003;37:4405.
[581] Bahnemann DW. Isr J Chem 1993;33:155.
[582] Beydoun D, Amal R. Mater Sci Eng B 2002;94:71.
[583] Beydoun D, Amal R, Low G, McEvoy S. J Mol Catal A: Chem 2002;180:193.
[584] Chen F, Zhao J. Catal Lett 1999;58:245.
[585] Anpo M. Pure Appl Chem 2000;72:1787.
[586] Anpo M, Kishiguchi S, Ichihashi Y, Takeuchi M, Yamashita H, Ikeue K, et al. Res Chem Intermed 2001;27:459.
[587] Anpo M. Stud Surf Sci Catal 2000;130 (A):157.
[588] Takeuchi M, Yamashita H, Matsuoka M, Anpo M, Hirao T, Itoh N, et al. Catal Lett 2000;66:185.
[589] Takeuchi M, Yamashita H, Matsuoka M, Anpo M, Hirao T, Itoh N, et al. Catal Lett 2000;67:135.
[590] Takeuchi M, Anpo M, Hirao T, Itoh N, Iwamoto N. Surf Sci Jpn 2001;22:561.
[591] Zhang JL, Chen HJ, Xu HS, Anpo M. Chin J Catal 2004;25:10.
[592] Sakatani Y, Koike H. Japan Patent No. P2001-72419A, 2001.
[593] Shara T, Ando M, Sugihara S. Appl Catal A: Gen 2001;5:19.
[594] Suda Y, Kawasaki H, Ueda T, Ohshima T. Thin Solid Films 2004;453–454:162.
[595] Sakthivel S, Kisch H. Chemphyschem 2003;4:487.
[596] Gole JL, Stout JD, Burda C, Lou YB, Chen XB. J Phys Chem B 2004;108:1230.
[597] Rahman MM, Krishna KM, Soga T, Jimbo T, Umena M. J Phys Chem Solids 1999;60:201.
[598] Qiu YM, Guan YC, Yao J. Chemosphere 2001;44:1087.
[599] Zheng SK, Wang TM, Hao WC, Shen R. Vacuum 2002;65:155.
[600] Miyauchi M, Ikezawa A, Tobimatsu H, Irie H, Hashimoto K. Phys Chem Chem Phys 2004;6:865.
[601] Nakamura I, Negishi N, Kutsuna S, Ihara T, Sugihara S, Takeuchi K. J Mol Catal A: Chem 2000;161:205.
[602] Yin S, Yamaki H, Komatsu M, Zhang QW, Wang JR, Tang Q, et al. J Mater Chem 2003;13:2996.
[603] Wei HY, Wu YS, Lun N, Zhao F. J Mater Sci 2004;39:1305.
[604] Yu JC, Yu J, Ho W, Ho W, Ho W, Jiang Z, et al. Chem Mater 2002;14:3808.

[605] Hattori A, Tada H. J Sol–Gel Sci Technol 2001;22:47.
[606] Luo H, Takata T, Lee Y, Zhao J, Domen K, Yan Y. Chem Mater 2004;16:846.
[607] Nukumizu K, Nunoshige J, Takata T, Kondo JN, Hara M, Kobayashi H, et al. Chem Lett 2003;32:196.
[608] Khan SUM, Al-Shahry M, Ingler Jr WB. Science 2002;297:223.
[609] Umebayashi T, Yamaki T, Itoh H, Asai K. Appl Phys Lett 2002;81:454.
[610] Ohno T. Water Sci Technol 2004;49:159.
[611] Ishikawa A, Takata T, Kondo JN, Hara M, Kobayashi H, Domen K. J Am Ceram Soc 2002;124:13547.
[612] Vorontsov AV, Savinov EN, Jin ZS. J Photochem Photobiol A: Chem 1999;125:113.
[613] Einaga H, Futamura S, Ibusuki T. Environ Sci Technol 2001;35:1880.
[614] Furube H, Asachi T, Masuhara H, Yamashita Y, Anpo M. Chem Phys Lett 2001;336:424.
[615] Pichat P. In: Schiavello M, editor. Photocatalysis and environment: trends and applications, NATO advanced study institute on new trends and applications. Dordrecht, Boston: Kluwer Academic Publishers; 1993, p. 339.
[616] Arabatzis IM, Stergiopoulos T, Bernard MC, Labou D, Neophytides SG, Falaras P. Appl Catal B: Environ 2003;42:187.
[617] Moon SC, Mametsuka H, Suzuki E, Nakahara Y. Catal Today 1998;45:79.
[618] Ranjit Viswanathan RT. J Photochem Photobiol A: Chem 1997;107:215.
[619] Ohtani B, Kakimoto M, Nishimoto S, Kagiya T. J Photochem Photobiol A: Chem 1993;70:265.
[620] Chen J, Ollis DF, Rulkens WH, Bruning H. Water Res 1999;33:661.
[621] Jin S, Shiraihi F. Chem Eng J 2003;97:203.
[622] Hu C, Tang Y, Jiang Z, Hao Z, Tang H, Wong PK. Appl Catal A: Gen 2003;253:389.
[623] Sclafani A, Mozzanega MN, Pichat P. J Photochem Photobiol A: Chem 1991;59:181.
[624] Fu X, Zeltner WA, Anderson M. Appl Catal B: Environ 1995;6:209.
[625] Driessen MD, Grassian VH. J Phys Chem B 1998;102:1418.
[626] Blaskovà A, Csolleva I, Brezová V. J Photochem Photobiol A: Chem 1998;113:251.
[627] Bowker M, James D, Stone P, Bennett R, Perkins N, Millard L, et al. J Catal 2003;217:427.
[628] Kenney III JC, Datye AK. J Catal 1998;179:375.
[629] Takeuchi M, Tsujimaru K, Sakamoto K, Matsuoka M, Yamashita H, Anpo M. Res Chem Intermed 2003;29:619.
[630] Vorontsov AV, Dubovitskaya VP. J Catal 2004;221:102.
[631] Preis S, Falconer JL. Water Sci Technol 2004;49:141.
[632] Nakano K, Obuchi E, Nanri M. Chem Eng Res Design 2004;82:297.
[633] Siemon U, Bahnemann D, Testa JJ, Rodriguez D, Litter MI, Bruno N. J Photochem Photobiol A: Chem 2002;148:247.
[634] Papaefthimiou P, Ioannides T, Verykios XE. Catal Today 1999;54:81.
[635] Cho KC, Hwang KC, Sano T, Takeuchi K, Matsuzawa S. J Photochem Photobiol A: Chem 2004;161:155.
[636] Mao LQ, Li QL, Dang HX, Zhang ZH. Surf Rev Lett 2004;11:11.
[637] Liu SX, Qu ZP, Han XW, Sun CL, Bao XH. Chin J Catal 2004;25:133.
[638] Moonsiri M, Rangsunvigit P, Chavadej S, Gulari E. Chem Eng J 2004;97:241.
[639] Ozkan A, Ozkan MH, Gurkan R, Akcay M, Sökmen M. J Photochem Photobiol A: Chem 2004;163:29.
[640] Orlov A, Jefferson DA, Mcleoad N, Lambert RM. Catal Lett 2004;92:41.
[641] Tan TTY, Yip CK, Beydoun D, Amal R. Chem Eng J 2003;95:179.
[642] Gerischer H, Willig F. Top Curr Chem 1976;61:31.
[643] Vinodgopal K, Wynkoop DE, Kamat PV. Environ Sci Technol 1996;30:1660.
[644] Nasr C, Vinodgopal K, Fisher L, Hotchandi S, Chattopadhyay AK, Kamat PV. J Phys Chem 1996;100:8436.
[645] Wang CY, Liu CY, Wang WQ, Shen T. J Photochem Photobiol A: Chem 1997;109:151.
[646] Zheng S, Huang Q, Zhou J, Wang B. J Photochem Photobiol A: Chem 1997;108:235.

[647] Zhang F, Zhao J, Zang L, Shen T, Hidaka H, Pelizzetti E, et al. J Mol Catal A: Chem 1997;120:173.
[648] Zhang F, Zhao J, Zang L, Shen T, Hidaka H, Pelizzetti E, et al. Appl Catal B: Environ 1998;15:147.
[649] Kiriakidou F, Kondarides DI, Verykios KE. Catal Today 1999;54:119.
[650] Kamat PV, Fox MA. Chem Phys Lett 1983;102:379.
[651] Patrick B, Kamat PV. J Phys Chem 1992;96:1423.
[652] Yang M, Thompson DW, Meyer GJ. Inorg Chem 2002;41:1254.
[653] Kamat PV. Chem Rev 1993;93:267.
[654] Yu JC, Xie Y, Tang HY, Zhang L, Chan HC, Zhao J. J Photochem Photobiol A: Chem 2003;156:235.
[655] Mele G, Biccarella G, Vassapollo G, Garćia-López E, Palmisano L, Schiavello M. Appl Catal B: Environ 2002;33:309.
[656] Iliev V. J Photochem Photobiol A: Chem 2002;151:195.
[657] Herrera-Melián JA, Doña-Rodríquez JM, Viera Saurez A, Tello-Rendón E, Valdes do Campo C, Araña J, et al. Chemosphere 2000;41:323.
[658] Ranjit KT, Willner I, Bossmann S, Braun A. J Phys Chem 1998;102:9397.
[659] Hequet V, Le Cloirec P, Gonzalez G, Meunier B. Chemosphere 2000;41:379.
[660] Fan FR, Bard AJ. J Am Chem Soc 1979;101:6139.
[661] Schwitzgebel J, Ekerdt JG, Gerischer H, Heller A. J Phys Chem 1995;99:5633.
[662] Zang L, Lange C, Maier WF, Abraham I, Storck S, Kisch H. J Phys Chem B 1998;102:10765.
[663] Kisch H, Zang L, Lange C, Meissner D. Angew Chem 1998;110:3201.
[664] Zang L, Macyk W, Lange C, Maier WF, Antonius C, Meissner D, et al. Chem Eur J 2000;6:379.
[665] Macyk W, Kisch H. Chem Eur J 2001;7:1862.
[666] Kamat PV, Patrick B. J Phys Chem 1992;96:6834.
[667] Redmond G, O'Keefe A, Burgess C, MacHale C, Fitzmaurice D. J Phys Chem 1993;97:11081.
[668] Spanhel L, Weller H, Henglein A. J Am Chem Soc 1987;109:6632.
[669] Zhang Y, Xiong G, Yao N, Yang W, Fu X. Catal Today 2001;68:89.
[670] Tada H, Hottri A, Tokihisa Y, Imai K, Tohge N, Ito S. J Phys Chem 2000;104:4585.
[671] Levy B, Liu W, Gilbert S. J Phys Chem B 1997;101:1810.
[672] Shang J, Yao W, Zhu Y, Wu N. Appl Catal A: Gen 2004;257:25.
[673] Nasr C, Kamat PV, Hotchandani S. J Phys Chem B 1998;102:10047.
[674] Serpone N, Maruthamuthu P, Pichat P, Pelizzetti E, Hidaka H. J Photochem Photobiol A: Chem 1995;85:247.
[675] Li XZ, Li FB, Yang CL, Ge WK. J Photochem Photobiol A: Chem 2001;141:209.
[676] Alemany LJ, Lietti L, Ferlazzo N, Forzatti P, Busca G, Giamello E, et al. J Catal 1995;155:117.
[677] Engweiler J, Harf J, Baiker A. J Catal 1996;159:259.
[678] Song KY, Park MK, Known YT, Lee HW, Chung WJ, Lee WI. Chem Mater 2001;13:2349.
[679] Ohno T, Tanigawa F, Fujihara K, Izumi S, Matsumura M. J Photochem Photobiol A: Chem 1998;118:41.
[680] Do YR, Lee W, Dwight K, Wold A. J Solid State Chem 1994;108:198.
[681] Kwon YT, Song KY, Lee WI, Choi GJ, Do YR. J Catal 2000;191:192.
[682] Pal B, Sharon M, Nogami G. Mater Chem Phys 1999;59:254.
[683] Sun D, Meng TT, Loong TH, Hwa TJ. Water Sci Technol 2004;49:193.
[684] Yang SG, Quan X, Li XY, Liu YZ, Chen S, Chen GH. Phys Chem Chem Phys 2004;6:659.
[685] Wang C, Zhao JC, Wang XM, Mai BX, Sheng GY, Peng PJ, et al. Appl Catal B: Environ 2002;39:269.
[686] Vinodgopal K, Kamat PV. Environ Sci Technol 1995;29:841.
[687] Pilkenton S, Raftery D. Solid State Nucl Magn Reson 2003;24:236.
[688] Tennakone K, Bandara J. Appl Catal A: Gen 2001;208:335.
[689] Bedja I, Kamat PV. J Phys Chem 1995;99:9182.
[690] Vinodgopal K, Bedja I, Kamat PV. Chem Mater 1996;8:2180.
[691] Shi LY, Ii CZ, Gu HC, Fang DY. Mater Chem Phys 2000;62:62.

[692] Jackson NB, Wang CM, Luo Z, Schwitzgebel J, Ekerdt JG, Brock LR, et al. J Electrochem Soc 1991;138:3660.
[693] Brezová V, Jankoviæová M, Soldan M, Blazcová A, Reháaková M, Surina M, et al. J Photochem Photobiol A: Chem 1993;76:103.
[694] Matthews D, Kay A, Grätzel M. Aust J Chem 1994;47:1869.
[695] Vinodgopal K, Kamat PV. Solar Energy Mater Solar Cells 1995;38:401.
[696] Byrne JA, Eggins ER, Brown NMD, McKinney B, Rouse M. Appl Catal B: Environ 1998;17:25.
[697] Fernández A, Lassaletta G, Jimènez VM, Justo A, González-Elipe AR, Hermann JM, et al. Appl Catal 1995;7:49.
[698] Tenakone K, Tilakaratne CTK, Kottegoda IRM. J Photochem Photobiol A: Chem 1995;87:177.
[699] Sabate J, Anderson MA, Kikkawa H, Edwards M, Hill Jr. CG. J Catal 1991;127:167.
[700] Aguado MA, Anderson MA. Solar Energy Mater Solar Cells 1993;28:345.
[701] Kim DH, Anderson MA. Environ Sci Technol 1994;28:479.
[702] Sobczynsky A, Bard AJ, Campion A, Fox MA, Malloux SE, Webwer SE, et al. J Phys Chem 1987;91:3316.
[703] Anpo M, Aikawa N, Kubotawa Y, Che M, Louis C, Giamello E. J Phys Chem 1985;89:5689.
[704] Sato S, Sobczynski A, White JM, Bard AJ, Campion MA, Malloue T, et al. J Photochem Photobiol A: Chem 1989;50:283.
[705] Xu Y, Chen X. Chem Ind (Lond) 1990;6:497.
[706] Robert D, Piscaro A, Heintz O, Weber JV. Catal Today 1999;54:291.
[707] Matthews RW. Solar Energy 1987;38:405.
[708] Lee SH, Kang M, Cho SM, Han GY, Kim BW, Yoon KJ, et al. J Photochem Photobiol A: Chem 2001;146:121.
[709] Serpone N. Solar Energy 1986;14:121.
[710] Al-Ekabi H, Serpone N. J Phys Chem 1988;119:5726.
[711] Anderson MA, Gieselman MJ, Xu Q. J Membr Sci 1998;39:243.
[712] Sato S. Langmuir 1988;4:1156.
[713] Xu Y, Zheng W, Liu W. J Photochem Photobiol A: Chem 1999;122:57.
[714] Aguado J, Grieken R, Lòpez-Muñoz MJ, Marugán J. Catal Today 2002;75:95.
[715] Alemany LJ, Bañares MA, Paedo E, Galán-Fereres M, Blasco JM. Appl Catal B: Environ 1997;13:289.
[716] Chun H, Yizhong W, Hongxiao T. Appl Catal B: Environ 2001;30:277.
[717] Hu C, Tang Y, Yu JC, Wong PK. Appl Catal B: Environ 2003;40:131.
[718] Najm JN, Snoeyink VL, Suidan MT, Lee CH, Richard Z. J Am Water Works Assoc 1990;82:65.
[719] Milner RJ, Barker DB, Speth TF, Fronk CA. J Am Water Works Assoc 1989;81:43.
[720] Ilisz I, Dombi A, Mogyorósi K, Farkas A, Dékani I. Appl Catal B: Environ 2002;39:247.
[721] Zhu C, Wang L, Fu Y, Cao L. J Mater Chem 2001;11:1864.
[722] Loddo V, Marćı G, Martín C, Palmisano L, Rives V, Sclafani A. Appl Catal B: Environ 1999;20:29.
[723] Ku Y, Ma CM, Shen YS. Appl Catal B: Environ 2001;34:181.
[724] Benoit-Marquiè F, Boisdon MT, Braun AM, Oliveros E, Maurette MT. J Photochem Photobiol A: Chem 2000;132:225.
[725] Hermann JM, Tahiri H, Ait-Ichou Y, Lassetta G, González-Elipe AR, Ternàndez A. Appl Catal B: Environ 1997;13:219.
[726] Fernandez A, Lassalleta G, Jimenez VM, Justo A, González-Elipe AR, Hermann JM, et al. Appl Catal B: Environ 1995;68:173.
[727] Tennakone K, Kottegoda IRM. J Photochem Photobiol A: Chem 1996;93:79.
[728] Doud WA, Xin JH. J Sol–Gel Sci Technol 2004;29:25.
[729] Park OH, Kim CS. J Appl Polym Sci 2004;91:3174.
[730] Iguchi Y, Ichiiura H, Kitaoka T, Tanaka H. Chemosphere 2003;53:1193.
[731] Nozawa M, Tanigawa K, Hosomi M, Chikusa T, Kawada E. Water Sci Technol 2001;44:127.
[732] Takeda N, Iwata N, Torimoto T, Yoneyama H. J Catal 1998;177:240.
[733] Green KYJ, Rudham RJ. Chem Soc Faraday Trans 1993;89:1867.

[734] Sampath S, Uchida H, Yoneyama H. J Catal 1994;149:189.
[735] Xu Y, Langford CH. J Phys Chem 1995;99:11501.
[736] Yamashita H, Ichihashi Y, Anpo M, Hashimoto M, Louis C, Che M. J Phys Chem 1996;100:16041.
[737] Xu Y, Langford CH. J Phys Chem 1997;101:3115.
[738] Mathews RW. Water Res 1990;24:653.
[739] Sabate J, Anderson MA, Aguado MA. J Mol Catal 1992;71:57.
[740] Galán-Fereres M, Alemany LJ, Marisical R, Bañares MA, Anderson J, Fierro JLG. Chem Mater 1995;7:1342.
[741] Ray AK, Beenackers AACM. AIChE J 1997;43:2571.
[742] Dijkstra MFJ, Michorius A, Buwalda H, Panneman HJ, Winkelman JGM, Beenackers AACM. Catal Today 2001;66:487.
[743] Vohra MS, Tanaka K. Water Res 2003;37:3992.
[744] Tanaka T, Teramura K, Yamamoto T, Takenaka S, Yoshida S, Funabiki T. J Photochem Photobiol A: Chem 2002;148:277.
[745] Ding Z, Hu X, Lu GQ, Greenfield PF. Catal Today 2001;68:173.
[746] Yoneyama H, Torimoto T. Catal Today 2000;58:133.
[747] Durgakumari V, Subrahmanyam M, Subba Rao KV, Ratnamala A, Noorjahan M, Tanaka K. Appl Catal A: Gen 2002;234:155.
[748] Reddy EP, Davydov L, Smirniotis P. Appl Catal B: Environ 2003;42:1.
[749] Sun Z, Chen Y, Ke Q, Yang Y, Yuan J. J Photochem Photobiol A: Chem 2002;149:169.
[750] Ooaka C, Yoshida H, Horio M, Suzuki K, Hattori T. Appl Catal B: Environ 2003;41:313.
[751] Ding Z, Zhu HY, Lu Q, Greenfield PF. J Colloid Interface Sci 1999;209:193.
[752] Araña J, Doña-Rodríquez JM, Tello-Rendón E, Garriga i Cabo C, González-Díaz O, Herrera-Melián JA, et al. Appl Catal B: Environ 2003;44:161.
[753] Araña J, Doña-Rodríquez JM, Tello-Rendón E, Garriga i Cabo C, González-Díaz O, Herrera-Melián JA, et al. Appl Catal B: Environ 2003;44:153.
[754] Takeda N, Torimoto T, Sampath S, Kuwabata S, Yoneyama H. J Phys Chem 1995;99:9986.
[755] Legrini O, Oliveros E, Braun A. Chem Rev 1993;93:671.
[756] Chen H, Masumoto A, Nishimija N, Tsutsumi K. Colloids Surf A: Physicochem Eng Aspects 1999;157:295.
[757] Ao CH, Lee SC. Appl Catal B: Environ 2003;44:191.
[758] Takeda N, Ohtani M, Torimoto T, Kuwabata S. J Phys Chem B 1997;101:2644.
[759] Ibusuki I, Takeuchi K. J Mol Catal 1994;88:93.
[760] Tanguay JF, Suib Sl, Coughlin RW. J Catal 1989;117:335.
[761] Uchida H, Ito S, Yoneyama H. Chem Lett 1993;1995.
[762] Torimoto T, Ito S, Kuwabata S, Yoneyama H. Environ Sci Technol 1996;30:1275.
[763] Tryba B, Morawski AW, Inagaki M. Appl Catal B: Environ 2003;41:427.
[764] Qourzal S, Assabane A, Ai-Ichou Y. J Photochem Photobiol A: Chem 2004;163:317.
[765] Tsumura T, Kojitani N, Izumi I, Iwashita N, Toyoda M, Inagaki M. J Mater Chem 2002;12:1391.
[766] Tryba B, Morawski AW, Inagaki M. Appl Catal B: Environ 2003;41:427.
[767] Colón G, Hidalgo MC, Navío JA. Catal Today 2002;76:91.
[768] Colón G, Hidalgo MC, Marcías M, Navío JA, Doña JM. Appl Catal B: Environ 2003;46:203.
[769] Jung KY, Park SB. J Photochem Photobiol A: Chem 1999;127:117.
[770] Gao XT, Bore SR, Fierro JLG, Bañares MA, Wachs IE. J Phys Chem B 1998;102:5653.
[771] Monneyron P, Manero MH, Foussard JN, Benoit-Marquié F, Maurette MT. Chem Eng Sci 2003;53:971.
[772] Hoshimoito K, Wasada K, Osaki M, Shono E, Adachi K, Tonkai N, et al. Appl Catal B: Environ 2001;30:429.
[773] Kim Y, Yoom M. J Mol Catal A: Chem 2001;168:257.
[774] Anandan S, Yoon M. J Photochem Photobiol C: Photochem Rev 2003;4:5.
[775] Ávila P, Sánchez B, Cardona AI, Rebollar M, Candal R. Catal Today 2002;76:271.

[776] Choi W, Yun Ko J, Park H, Shik Chung J. Appl Catal B: Environ 2001;31:209.
[779] Hsieh YH, Chang CF, Chen YH. Appl Catal B: Environ 2001;31:241.
[780] Yamanaka S, Malla PB, Komareni S. J Colloid Interface Sci 1990;134:51.
[781] Malla P, Yamanaka S, Komareni S. Solid State Ionics 1989;32/33:354.
[782] Ooaka C, Akita S, Ohashi Y, Horiuchi T, Suzuki K, Komai S, et al. J Mater Chem 1999;9:2943.
[783] Yoshida H, Kawase T, Miyashida Y, Murata C, Ooaka C, Hattori T. Chem Lett 1999;715.
[784] Mohseni M, David A. Appl Catal B: Environ 2003;46:219.
[785] Zhang SG, Ichihashi Y, Yamashita H, Tatsumi T, Anpo M. Chem Lett 1996;895.
[786] Zhang J, Hu Y, Matsuoka M, Yamashita H, Minagawa M, Hidak H, et al. J Phys Chem B 2001;104:8395.
[787] Zhanpeisov NU, Matsuoka M, Yamashita M, Anpo M. J Phys Chem B 1998;102:6915.
[788] Anpo M, Aikawa N, Kubokawa Y, Che M, Louis C, Giamello E. J Phys Chem 1985;89:5017.
[789] Ikeue K, Yamashita H, Anpo M, Takewaki T. J Phys Chem B 2001;105:8350.
[790] Balard H, Monsour A, Papier E, Pichat P. J Chem Phys 1985;82:1051.
[791] Ghosh-Mukerji S, Haick H, Paz Y. J Photochem Photobiol A: Chem 2003;160:77.
[792] Terzian R, Serpone N, Minero C, Pelizzetti E, Hidaka H. J Photochem Photobiol A: Chem 1990;63:829.
[793] Pichat P. In: Schiavello M, editor. Photoelectrochemistry, photocatalysis and photoreactors. Dordrecht: D. Reidel; 1985, p. 425.
[794] Wang C, Mallouk TE. J Am Chem Soc 1990;112:2916.
[795] Ohno T, Kigoshi T, Nakabeta K, Matsumura M. Chem Lett 1998;877.
[796] Ohno T, Masaki Y, Hirayama S, Matsumura M. J Catal 2001;204:163.
[797] Zhang JL, Anpo M. Chem J Chin Univ—Chin 2004;25:733.
[798] Hermann JM, Mu W, Pichat P. In: Guisnet M, Battault J, Bouchoule C, Duprez D, Pérot G, Maurel R, et al. editors. Heterogenous catalysis and fine chemicals. Studies in surface science and catalysis, vol. 59. Amsterdam: Elsevier; 1991, p. 405.
[799] Fox MA, Abdel-Wahab AA, Dulay M. J Catal 1990;16:693.
[800] Maeda H, Miyamoto H, Mizuno K. Chem Lett 2004;33:462.
[801] Fisher WB, van Pepper JF. In: Grayson M, editor. 3rd ed.. Kirk-Othmer encyclopedia of chemical technology, vol. 7. New York: Wiley; 1979, p. 411.
[802] Boarini P, Carassiti V, Maldotti A, Madelli RA. Langmuir 1998;14:2080.
[804] Almquist CB, Biswas P. Appl Catal A: Gen 2001;214:259.
[805] Li X, Chen G, Po-Lock Y, Kutal C. J Chem Technol Biotechnol 2003;78:1246.
[806] Cermenati L, Dondi D, Fagnoni M, Albini A. Tetrahedron 2003;59:6409.
[807] Giannotti G, LeGreneur G, Watts O. Tetrahedron Lett 1983;24:5071.
[808] Ohno T, Mitsui T, Matsumura M. J Photochem Photobiol A: Chem 2003;160:3.
[809] Cermenati L, Mella M, Albini A. Tetrahedron 1998;54:2575.
[810] Dulay MT, Washington-Dedeaux D. J Photochem Photobiol A: Chem 1991;61:153.
[811] Worsley D, Mills A, Smith K, Hutchings MG. J Chem Soc Chem Commun 1995:1119.
[812] Beaume O, Finiels A, Geneste P, Graffin P, Guida A, Olivé JL, et al. Guisnet M, editor. Heterogenous catalysis and fine chemicals III. Studies in surface science and catalysis, vol. 78. Amsterdam: Elsevier; 1993, p. 401.
[813] Kanno T, Oguchi T, Sakuragai H, Tokumaru K. Tetrahedron Lett 1980;21:467.
[814] Sacket DD, Fox MA. J Phys Org Chem 1988;1:103.
[815] Beaune O, Finiels A, Geneste P, Graffin P, Olivé JL, Saaedan A. J Chem Soc Chem Commun 1992;164:9.
[816] Fox MA, Chen CC. J Am Chem Soc 1981;103:6757.
[817] Ohno T, Tokieda K, Higashida S, Matsumura M. Appl Catal A: Gen 2003;244:383.
[818] Sheldon RA, Kochi JK. Metal-catalyzed oxidation of organic compounds. New York: Academic Press; 1981.
[819] Hudlicky M. Oxidation in organic chemistry. Washington (DC): American Chemical Society; 1990.
[820] Larock RC. Comprehensive organic transformation. New York: VCH; 1989.

[821] Canelli G, Cardillo G. Chromium oxidations in organic chemistry. Berlin: Springer; 1984.
[822] Harwey PR, Rudham R, Ward S. J Chem Soc Faraday Trans I 1983;79:2975.
[823] Fox MA, Ogawa H, Pichat P. J Org Chem 1989;54:3847.
[824] Hussein FH, Pattenden G, Rudham R, Russel JJ. Tetrahedron Lett 1983;24:3363.
[825] Hussein FH, Pattenden G, Russel R. Tetrahedron Lett 1986;1:82.
[826] Pichat P, Disdier J, Mozzanega MN, Herrmann JM. Proceedings of the 8th International Congress in Catal, vol. III. Weinheim: Verlag-Chemie-Dechema; 1984, p. 487.
[827] Mohamed OS, El-Aal A, Gaber M, Abdel-Wahab AA. J Photochem Photobiol A: Chem 2002;148:205.
[828] Mohamed OS. J Photochem Photobiol A: Chem 2002;152:229.
[829] Ling JJ, Liu TJ. J Chin Chem Soc 1986;32:133.
[830] Pillai UR, Sahle-Demessie E. J Catal 2002;211:434.
[831] Smith MB, March J. March's advanced organic chemistry: reactions, mechanism and structure. 5th ed. New York: Wiley-Interscience; 2001, p. 180.
[832] Djeghri N, Teichner SJ. J Catal 1980;62:99.
[833] Sakata T, Kawai T, Hashimoto K. J Phys Chem 1984;88:2344.
[834] Izumi I, Fan FRF, Bard AJ. J Phys Chem 1985;85:218.
[835] Chum HL, Ratcliff M, Posey FL, Nozik AJ, Turner JA. J Phys Chem 1983;87:3089.
[836] Fox MA, Ogawa H, Muzyka J. Photochemistry and electrosynthesis on semiconductor materials. In: Ginley DS, editor. The electrochem society, vol. 14. 1988, p. 9.
[837] Lin YJ, Lee A, Teng LS, Lin HT. Chemosphere 2002;48:1.
[838] Hudlicky M. Oxidation in organic chemistry. Am Chem Soc Monogr 1990;186.
[839] Fox MA, Younathan JN. Tetrahedron 1986;42:6235.
[840] Fox MA, Chen MJ. J Am Chem Soc 1983;105:4497.
[841] Ohtani B, Watanabe T, Honda K. J Am Chem Soc 1986;108:308.
[842] Brezová V, Blazcová A, Šurina I, Halinová B. J Photochem Photobiol A: Chem 1997;107:233.
[843] Brezová V, Tarábek P, Dvoranová D, Staško A, Biskupič S. J Photochem Photobiol A: Chem 2003;155:179.
[844] Eriksen J, Foote CS, Parker TL. J Am Chem Soc 1977;99:6455.
[845] Matsuzawa S, Tanaka J, Sato S, Ibusuki T. J Photochem Photobiol A: Chem 2002;149:183.
[846] Document 391L0271, Official Journal L135, 30/05/1991, p. 0040–52. Council Directive 91/271/EEC of 21 May 1991 concerning wastewater treatment.
[847] Juan KD. Ind Pollut Prev Control 1984;3:88.
[849] Shibaeva IV, Meteletsa DI, Denison ET. Kinet Catal 1969;10:1022.
[850] Eisenhauer HR. J Water Pollut Control Fed 1968;40:1887.
[851] Moza DN, Fytianos K, Samanidou U, Korte F. Bull Environ Contam Toxicol 1988;41:687.
[852] Water chlorination; chemistry, environmental impact ans health effects. Chelsea (MI): Lewis Publishers, Inc.; 1885.
[853] Wei C, Lin W, Zainal Z, Williams NE, Zhu K, Kruzic AP, et al. Environ Sci Technol 1994;28:934.
[854] Heltz GR, Nweke AC. Environ Sci Technol 1995;29:1018.
[855] Sunderstrom DW, Wein BA, Klei HE. Environ Prog 1989;8:6.
[856] Serpone N, Khairutdinov RF. Studies in surface science and catalysis 103. In: Kamat PV, Meisel D, editors. Semiconductor nanoclusters: physical, chemical and catalytic aspects. Netherlands: Elsevier; 1996, p. 417.
[857] Bauer R, Waldner G, Fallmann H, Hager S, Klare M, Krulzler T, et al. Catal Today 1999;53:131.
[858] Hoigné J, Bader H. Water Res 1983;17:185.
[859] Andreozzi R, Caprio V, Insola A, Marotta R. Catal Today 1999;53:51.
[860] Hayashimoto K, Kawari T, Sakato T. J Phys Chem 1984;88:4083.
[861] Pelizzetti E, Minero C, Maurino V, Hidaka H, Serpone N. Ann Chim (Rome) 1990;80:81.
[862] Heller A, Brock JR. In: Helz GR, Zepp RG, Crosby DG, editors. Aquatic and surface photochemistry. Orlando: Lewis Publication; 1994, p. 427.

[863] Chatterjee D, Mahata A. Photochem Photobiol A: Chem 2002;153:199.
[864] Kiwi J, Pulgarin C, Peringer P, Grätzel M. Appl Catal B: Environ 1993;3:85.
[865] Tanaka S, Ichikawa T. Water Sci Technol 1993;28:103.
[866] Zepp RG, Wolfe NI, Baughman GL, Hollis RC. Nature 1977;267:421.
[867] Link H. Solar Energy Research Institute (SERI) report, Golden, CO, 1990.
[868] Litter MI. Appl Catal B: Environ 1999;23:89.
[870] Augugliaro V, Garcìa-Lopez E, Loddo V, Marci G, Palmisano L. Adv Environ Res 1999;3:179.
[871] Takeda K, Fujiwara K. Water Res 1996;30:323.
[872] Abdullah M, Low GKC, Matthews RW. J Phys Chem 1990;94:6820.
[873] Beckbölet M, Boyacioglu Z, Ozkaraova B. Water Sci Technol 1990;24:990.
[874] Jung OJ. Bull Korean Chem Soc 2001;22:1183.
[875] Fujihira M, Satoh Y, Osa T. Chem Lett (Chem Soc Jpn) 1981;1053.
[876] Sclafani A, Palmisano L, Schiavello M. Res Chem Intermed 1992;18:211.
[877] Wei TY, Yang YY, Wan CC. J Photochem Photobiol A: Chem 1990;55:115.
[878] Wei TY, Yang YY, Wan CC. J Photochem Photobiol A: Chem 1992;69:241.
[879] San N, Hatipoğlu A, Koçtürk G, Çinar Z. J Photochem Photobiol A: Chem 2002;146:189.
[880] Bideau M, Claudel B, Faure L, Kazouan H. J Photochem Photobiol A: Chem 1991;61:269.
[881] Bideau M, Claudel B, Faure L, Kazouan H. J Photochem Photobiol A: Chem 1992;67:337.
[882] Brezovà V, Blaskovà A, Borsovà E, Ceppan M, Fiala R. J Mol Catal 1995;98:109.
[884] Beydoun D, Tse H, Amal R, Low G, McEvoy S. J Mol Catal A: Chem 2002;177:265.
[885] Fujihira M, Satoh Y, Osa T. Nature 1981;239:206.
[886] Fujihira M, Satoh Y, Osa T. Chem Soc Jpn 1982;55:666.
[887] Brillas E, Mur E, Sauleda R, Sánchez L, Peral J, Domèch X, et al. Appl Catal B: Environ 1998;16:31.
[888] Matthews RW. J Chem Soc Faraday Trans I 1984;80:457.
[889] Cunningham J, Sedlák P. J Photochem Photobiol A: Chem 1994;77:255.
[890] Butler EC, Davis AP. J Photochem Photobiol A: Chem 1993;90:457.
[891] Sclafani A, Palmisano L, Davi E. New J Chem 1990;14:265.
[892] Sclafani A, Palmisano L, Davi E. J Photochem Photobiol A: Chem 1991;56:113.
[893] Kim DH, Anderson MA. Photochem Photobiol A: Chem 1996;94:221.
[894] Watts RJ, Kong S, Orr MP, Miller GC, Henry BE. Water Res 1995;29:95.
[895] Amèzaga-Madrid P, Nevárez-Moorillón GV, Orrantia-Borunda E, Miki-Yoshida M. FEMS Microbiol Lett 2002;211:183.
[896] Koizumi Y, Taya M. Biochem Eng J 2002;12:107.
[897] Chen J, Eberlein L, Langford CH. J Photochem Photobiol A: Chem 2002;148:183.
[898] Stumm W. Chemistry of solid–water interface. New York: Wiley-Interscience; 1992, p. 428.
[899] Kormann C, Bahnemann DW, Hoffmann MR. Environ Sci Technol 1991;25:494.
[900] Jaffrezic-Renault N, Pichat P, Foissy A, Mercier R. J Phys Chem 1986;90:2733.
[901] Di Paola A, Marci G, Palmisano L, Schiavello M, Uosaki K, Ikeda S, et al. J Phys Chem B 2002;106:637.
[902] Shu HY, Huang CR, Chang MC. Chemosphere 1994;29:2597.
[903] Tong Z, Qingxiang Z, Hui H, Qin L, Yi Z. Chemosphere 1997;34:893.
[904] Burrows HD, Candle ML, Santaballa JA, Steenken S. J Photochem Photobiol B: Biol 2002;67:71.
[905] Yeber MC, Freer J, Martínez M, Mansilla HD. Chemosphere 2000;41:1257.
[906] Sunder M, Hempel DC. Water Res 1997;31:33.
[907] Hu C, Wang Y. Chemosphere 1999;39:2107.
[908] Sarria V, Parra S, Adler N, Péringer P, Benitez N, Pulgarin C. Catal Today 2002;76:301.
[909] Cook AM, Beilstetin P, Grossenbacher H, Hutter R. Biochem J 1985;231:25.
[910] Cook AM. FEMS Microbiol Rev 1987;46:93.
[911] Wang S, Shiraishi F, Nakomo K. Chem Eng J 2002;87:261.
[912] Li L, Zhu W, Zhang P, Chen Z, Han W. Water Res 2003;37:3646.
[913] Muneer M, Theurich J, Bahnemann D. J Photochem Photobiol A: Chem 2001;143:213.

[914] Muneer M, Bahnemann D. Appl Catal B: Environ 2002;36:95.
[915] Garcia JC, Takashima K. J Photochem Photobiol A: Chem 2003;155:215.
[916] Machado AEH, de Miranda JA, de Freitas RF, Duarte ETFM, Ferreira LF, Albuquerque YDT, et al. J Photochem Photobiol A: Chem 2003;155:231.
[917] Accituno M, Stalikas CD, Lumar L, Rubio S, Pérez-Bendito D. Water Res 2002;36:3582.
[918] Saquid M, Muneer M. Dyes Pigments 2002;53:237.
[919] Saquib M, Muneer M. Dyes Pigments 2003;56:37.
[920] Sanchez L, Liu J, Hand DW, Crittenden JC, Perram DL, Mullin ME. Appl Catal B: Environ 1998;19:59.
[921] Pelizzetti E, Carlin V, Minero C. New J Chem 1991;15:351.
[922] Yamazaki-Nishida S, Fu X, Anderson MA, Hori K. J Photochem Photobiol A: Chem 1996;97:175.
[923] Galino C, Jacques P, Kalt A. Chemosphere 2001;45:997.
[924] Linder M. Ph.D. Thesis. Department of Chemistry, University of Hannover, Germanay, 1997.
[925] Hermann JM, Guillard C. C R Acad Sci Paris, Série I, Chimie 2000;3:417.
[926] Matos J, Laine J, Hermann JM. Appl Catal B: Environ 1998;18:281.
[927] Gomez da Silva C, Faria JL. J Photochem Photobiol A: Chem 2003;155:133.
[928] Hermann JM, Mozzanega MN, Pichat P. J Photochem 1983;22:333.
[929] Domènech J, Peral J. J Chem Res 1987;12:360.
[930] Domènech J, Ayllón JA, Peral J. Environ Sci Pollut Res 2001;8:285.
[931] Kosanic MM. J Photochem Photobiol A: Chem 1996;119:119.
[932] Franch MI, Ayllón JA, Peral J, Domènech X. Catal Today 2002;76:221.
[933] Wang K, Hsieh Y, Chou M, Chang C. Appl Catal B: Environ 1999;21:1.
[934] Stafford U, Gray KA, Kamat PV. J Catal 1997;167:25.
[935] Araña J, Tello-Rendón E, Doña-Rodríuez JM, Herrera-Melián JA, Gon Tález Díaz O, Perez Peña J. Appl Catal B: Environ 2001;30:1.
[936] Ilisz I, Lásló Z, Dombi A. Appl Catal A: Gen 1999;180:25.
[937] Ilisz I, Lásló Z, Dombi A. Appl Catal A: Gen 1999;180:35.
[938] Fox MA, Chen CC, Linding BA. J Am Chem Soc 1982;104:5828.
[939] Fox MA, Chen CC. Tetrahedron Lett 1983;24:547.
[940] O'Shea KE, Cardona C. J Org Chem 1994;59:5005.
[941] Almalric L, Guillard C, Blanc-Brude E, Pichat P. Water Res 1996;30:1137.
[942] Peiró AM, Ayllón JA, Peral J, Domènech X. Appl Catal B: Environ 2001;30:359.
[943] Parra S, Olivero J, Pacheco L, Pulgarin C. Appl Catal B: Environ 2003;43:293.
[944] Theurich J, Linder M, Bahnemann DW. Langmuir 1996;12:6368.
[945] Terzian R, Serpone N, Minero C, Pelizzetti E. J Catal 1991;128:352.
[946] Wang RH, Hsieh YH, Chen LJ. J Hazard Mater 1998;59:251.
[947] Li X, Cubbage JW, Jenks WS. J Photochem Photobiol A: Chem 2001;143:69.
[948] Watanabe N, Horikoshi S, Kaeabe H, Sugie Y, Zhao J, Hidaka H. Chemosphere 2003;52:851.
[949] Streit B. Lexikon ökotoxikologie. 1st ed. Weinheim: VCH; 1994, p. 773.
[950] Greenpeace report, the effects of organochlorinrs on aquatic ecosystems. Greenpace International (Publ.); September 1992.
[951] Roques H. Chemical water treatment. Wienheim (Germany): VCH Verlag; 1996.
[952] Krijgsheld KR, van der Gen A. Chemosphere 1986;15:825.
[953] Milne T, Nilmos M. Chem Eng News 1992;22:2.
[954] Jardim WF, Moraes SG, Takiyama MMK. Water Res 1997;31:1728.
[955] Manilal VB, Haridas A, Alexander R, Surender GD. Water Res 1992;26:1035.
[956] Driessen MD, Goodman AL, Miller TM, Zaharis GA, Grassian VH. J Phys Chem B 1998;102:549.
[957] Hwang SJ, Petucci C, Raftery D. J Am Chem Soc 1998;120:4388.
[958] Yamazaki-Nishida S, Cervera-March S, Nagano KJ, Anderson MA, Hori K. J Phys Chem 1995;99:15814.
[959] Dorfman LM, Taub IA, Büchler RE. J Phys Chem 1962;36:3051.

[960] Matthews RW, Sangster DF. J Phys Chem 1967;71:4056.
[961] Hügül M, Erçağ E, Apak R. J Environ Sci Health A: Environ Sci Toxicol Hazard Subst 2002;37:365.
[962] Lettmann C, Hildenbrand K, Kisch H, Macyk W, Maier WF. Appl Catal B: Environ 2001;32:215.
[963] Nohara K, Hidaka H, Pelizzetti E, Serpone N. Catal Lett 1996;36:115.
[964] Klare M, Scheen J, Vogelsang K, Jacobs H, Broekaert JAC. Chemosphere 2000;41:353.
[965] Piccini P, Minero C, Vincenti M, Pelizzetti M. Catal Today 1997;39:187.
[966] Bhatkhande DS, Pangarkar VG, Beenackers AACM. Water Res 2003;37:1223.
[967] Maurino V, Minero C, Pelizzetti E, Piccini P, Serpone N, Hidaka H. J Photochem Photobiol A: Chem 1997;109:171.
[968] Yawalkar AA, Bhatklande DS, Pangarkar VG, Beenackers AACM. J Chemtech Biotech 2001;76:363.
[969] Subramanian V, Pangarkar VG, Beenackers AACM. Clean Prod Process 2000;2:149.
[970] Ajmera AA, Pangarkar VG, Beenackers AACM. J Chem Eng Technol 2002;25:173.
[971] Vione D, Maurino V, Minero C, Vincenti M, Pelizzetti E. Chemosphere 2001;44:237.
[972] Piccini P, Minero C, Vincenti M, Pelizzetti E. J Chem Faraday Trans 1997;93:1993.
[973] Richard C. New J Chem 1994;18:443.
[974] Di Paola A, Augugliaro V, Palmisano L, Pantaleo G, Savinov E. J Photochem Photobiol A: Chem 2003;155:207.
[975] Sökmen M, Allen DW, Hewson AT, Clench MR. J Photochem Photobiol A: Chem 2001;141:63.
[976] Goldstein S, Meyerstein D, Czapski G. Free Radic Biol Med 1993;15:242.
[977] Zhang P, Sparks DL. Environ Sci Technol 1990;24:1848.
[978] Sanuki S, Kojima T, Arai K, Nagaoka S, Majima H. Metall Mater Trans B 1999;30:15.
[979] Stevenson FJ. Humus chemistry: genesis, composition, reactions. New York: Wiley; 1994.
[980] Schulten HR, Plage B, Schnitzer M. Naturwissentshaften 1991;78:311.
[981] Gaffney JS, Marley NA, Clarck SB. ACS Symposium Series, vol. 651, p. 2. Washington (DC): American Chemical Society; 1996.
[982] Corin N, Backlund P, Kulovara M. Chemosphere 1996;33:245.
[983] National Cancer Institute (NCI). Carcinogenesis bioassay of chloropirin. RS No. 65. Washington (DC); 1978.
[984] Li JW, Yu ZB, Gao M. Water Res 1995;30:347.
[985] Singer PC. Water Res 1995;30:25.
[986] Beckbölet M, Ozkosemen G. Water Res 1996;33:189.
[987] Lee SA, Lee KH, Lee HL, Hyeon T, Choi W, Kwon HL. Ind Eng Chem Res 2001;40:1712.
[988] Eggins BR, Palmer FI, Bryne JA. Water Res 1997;31:1223.
[989] Minero C, Pelizzetti E, Sega M, Friberg SE, Sjoblom J. J Dispers Sci Technol 1999;20:643.
[990] Al-Rasheed R, Cardin DJ. Chemosphere 2003;51:925.
[991] Al-Rasheed R, Cardin DJ. Appl Catal A: Gen 2003;246:39.
[992] Palmer FL, Eggins BR, Coleman HM. J Photochem Photobiol A: Chem 2002;148:137.
[993] Zhou J, Banks CJ. Chemosphere 1993;27:607.
[994] Wisniowski J, Robert D, Surmaez-Gorska J, Miksch K, Weber JV. J Photochem Photobiol A: Chem 2002;152:267.
[995] Li XZ, Fan CM, Sun YP. Chemosphere 2002;48:453.
[996] Yoon SH, Lee CH, Kim KJ, Fane AG. Water Res 1998;32:2180.
[997] Beckbölet M, Balcioglu I. Water Res Technol 1996;34:73.
[998] Sivonen K, Jones G. In: Chorus I, Bartram J, editors. Toxic cyanobacteria in water. London: E&FN Spon; 1999, p. 41.
[999] Guire MJ. Water Sci Technol 1995;31:1.
[1000] Lawton L, Robertson PKJ, Rebertson RF, Bruce FG. Appl Catal B: Environ 2003;44:9.
[1001] Liu I, Lawton LA, Cornish B, Robertson PKJ. J Photochem Photobiol A: Chem 2002;148:349.
[1002] Senogles PJ, Scott JA, Shaw G, Stratton H. Water Res 2001;35:1245.
[1003] Lawton LA, Robertson PKJ, Cornish BJPA, Marr IL, Jaspars M. J Catal 2003;213:1009.

[1004] Heller A. Acc Chem Res 1995;28:503.
[1005] Heller A, Schwitzgebel J, Pishko M, Ekerdt JG. In: Rose TL, Murphy O, Rudd E, Conway BE, editors. Waste water treatment. Proceedings in Environmental Catalysis, vol. 94. Pennington (NY): The American Electrochemical Society; 1994, p. 1.
[1006] Correia VM, Stepenson T, Judd SJ. Environ Sci Technol 1994;15:917.
[1007] Ganesh R, Boardman GD, Mochelson D. Water Res 1994;28:1367.
[1008] Bauer C, Jacques P, Kalt A. J Photochem Photobiol A: Chem 2001;140:87.
[1009] Weber EJ, Adams RL. Environ Sci Technol 1995;29:113.
[1010] Renner T, Reichelt A, Wurdack I, Specht O, Wabner D. In: Vogelpohl A, editor. CUTEC Serial Publication No. 46, The Second International Conference on Oxidation Technology for Water and Wastewater Treatment, May 28–31, 2000. p. 39.
[1011] Bahorsky S. Water Environ Res 1997;69:658.
[1012] Pagga U, Brown D. Chemosphere 1986;15:479.
[1013] Shaul GM, Holdswoth TJ, Dempsey CR, Dostal KA. Chemosphere 1991;22:107.
[1014] Raffi F, Franklin W, Cerniglia CE. Appl Environ Microbiol 1990;56:2146.
[1015] Liu G, Wu T, Zhao J, Hidaka H, Serpone N. Environ Sci Technol 1999;33:2081.
[1016] Zhang T, Oyama T, Horikoshi S, Hidaka H, Zhao J, Serpone N. Solar Energy Mater Solar Cells 2002;73:287.
[1017] Tang WZ, Zhang A, Quintana MO, Torres DF. Environ Technol 1997;18:1.
[1018] Bandara J, Mielczarski JA, Kiwi J. Langmuir 2001;140:87.
[1019] Epling GA, Lin C. Chemosphere 2002;46:561.
[1020] Zielińska B, Grzechulska J, Kaleńczuk RJ, Morawski AW. Appl Catal B: Environ 2003;45:293.
[1021] Arslan I, Balcioglu IA, Bahnemann DW. Appl Catal B: Environ 2000;26:193.
[1022] Sivalingam G, Nagaveni K, Hegde MS, Madras G. Appl Catal B: Environ 2003;45:23.
[1023] Grzechulska J, Morawski AW. Appl Catal B: Environ 2002;36:45.
[1024] Baran W, Makowski A, Wardas W. Chemosphere 2003;53:87.
[1025] Mrowetz M, Selli E. J Photochem Photobiol A: Chem 2003;162:89.
[1026] Sökmen M, Özkan A. J Photochem Photobiol A: Chem 2002;147:77.
[1027] Alaton IA, Bacioglu IA. J Photochem Photobiol A: Chem 2001;141:247.
[1028] Esumuri K, Sakai K, Torigoe K, Suhara T, Fukui H. Colloids Surf A 1999;155:413.
[1029] Zhang R, Gao L. Chemosphere 2004;54:405.
[1030] Cohen ZZ, Eiden C, Lober MN. In: Gerner WY, editor. Evolution of pesticides in ground water. ACS Symposium Series, 315. Washington (DC): American Chemical Society; 1986, p. 170.
[1031] Muszkat L, Raucher D, Magaritz M, Ronen D. In: Zoller U, editor. Groundwater contamination and control. New York: Marcel Dekker; 1994, p. 257.
[1032] Prammer B. Directive 98/83/CE relative to the quality of waters for human use. Official Bulletin of the EC, European Union, Brussels; 1998. p. 32.
[1033] World Health Organization. Guidelines for drinking water quality, Geneva: WHO; 1993.
[1034] Miskat L, Bir L, Feigelson L. J Photochem Photobiol A: Chem 1995;87:85.
[1035] Pichat P. In: Schiavello M, editor. Photocatalysis and environment: trends and applications, NATO advanced study institute on new trends and applications. Dordrecht, Boston: Kluwer Academic Publishers; 1993, p. 399.
[1036] Navío JA, Colón G, Trillas M, Peral J, Domènech X, Testa JJ, et al. Appl Catal B: Environ 1998;16:187.
[1037] Foster NS, Noble RD, Koval CA. Bull Chem Jpn 1982;55:2010.
[1038] Prairie MR, Evans LR, Stange BM, Martinez SCL. Environ Sci Technol 1993;27:1776.
[1039] Wang S, Wang Z, Zhung Q. Appl Catal B: Environ 1992;1:257.
[1040] Lin WY, Rajeshwar K. J Electrochem Soc 1997;144:2751.
[1041] Chenthamarakshan CR, Hui Y, Ming Y, Rajeshwar K. J Electroanal Chem 2000;494:79.
[1042] Nguyen VNH, Amal R, Beydoun D. Chem Eng Sci 2003;58:4429.
[1043] Tennakone K, Thaminimulle TK, Senadeera S, Kumarasinghe ARJ. J Photochem Photobiol A: Chem 1993;70:193.
[1044] Tennakone K, Wickramanayake S. J Phys Chem 1986;90:1219.

[1045] Skubal R, Meshkov NK, Rajh T, Thurnauer M. J Photochem Photobiol A: Chem 2002;148:393.
[1046] Skubal LR, Meshkov NK. J Photochem Photobiol A: Chem 2002;148:211.
[1047] Chen LX, Rajh T, Micic O, Wang Z, Thurnauer MC. J Phys Chem 1997;101:10688.
[1048] Marakova OV, Rajh T, Thurnauer MC, Martin A, Klemme P, Cropek D. Environ Sci Technol 2000;34:4797.
[1049] Rajh T, Ostafin AE, Micic OI, Tiede DM, Thurnauer MC. J Phys Chem 1996;100:4538.
[1050] Thurnauer MC, Rajh T, Tiede DM. Acta Chem Scand 1997;51:610.
[1051] Salomons W, Förstner U, Mader P, editors. Heavy metals, problems and solutions. Berlin, Heidelberg: Springer; 1995, p. 386.
[1052] Serpone N, Boragarello E, Pelizzetti E. In: Schiavello M, editor. Photocatalysis and environment, trends and applications. Dordrecht: Kluwer; 1988, p. 527.
[1053] Serpone N, Lawless D, Terzian R, Minero C, Pelizzetti E, Schiavello M, editors. Photochemical conversion and storage of solar energy. Dordrecht: Kluwer Academic Publishers; 1991, p. 451.
[1054] Lawless D, Res A, Harris R, Serpone N. Chem Ind (Milan) 1990;72:139.
[1055] Reiche H, Dunn WW, Bard AJ. J Phys Chem 1979;83:2248.
[1056] Lau L, Rodriguez R, Henery S, Manuel D. Environ Sci Technol 1998;32:670.
[1057] Serpone N, Ah-You YK, Tran TP, Harris R. Solar Energy 1987;391:491.
[1058] Tennakone K, Ketipearachchi US. Appl Catal B: Environ 1995;5:343.
[1059] Hermann JM, Disdier J, Pichat P. J Catal 1988;113:72.
[1060] Sclafani A, Herrmann JM. J Photochem Photobiol A: Chem 1998;113:181.
[1061] Nishimoto SI, Ohtani B, Kajiwara H, Kagiya T. J Chem Soc Faraday Trans I 1983;79:2685.
[1062] Lee W, Shen HS, Dwight K, Wold A. J Solid State Chem 1993;106:288.
[1063] Linder M, Theurich J, Bahnemann DW. Water Sci Technol 1997;35:79.
[1065] Ohtani B, Okugawa Y, Nishimoto SI, Kagiya T. J Phys Chem 1987;91:3550.
[1066] Sundik LM, Norrod KL, Rowlen KL. Appl Spectrosc 1996;50:422.
[1067] Disdier D, Hermann JM, Pichat P. Faraday Trans I 1983;79:651.
[1068] Hermann JM, Disdier J, Pichat P. J Phys Chem 1986;90:6028.
[1069] Borgarello E, Serpone N, Emo G, Harris R, Pelizzetti E, Minero C. Inorg Chem 1986;25:284.
[1070] Papp J, Sen HS, Kershaw R, Dwight K, Wold A. Chem Mater 1993;5:284.
[1071] Albert M, Gao YM, Toft D, Dwight K, Wold A. Mater Res Bull 1992;27:961.
[1072] Gao YM, Lee W, Trehan R, Kershaw R, Dwight K, Wold A. Mater Res Bull 1991;26:1247.
[1073] Eliet V, Bidoglio G. Environ Sci Technol 1998;32:3155.
[1074] Javier D, Javier M. Electrochem Acta 1987;32:1383.
[1075] Muñoz J, Domènech X. J Appl Electrochem 1990;20:518.
[1076] Khalil LB, Mourad W, Rophael MW. Appl Catal B: Environ 1998;17:267.
[1077] Dellien I, Hall FM, Hepler LG. Chem Rev 1976;76:283.
[1078] Domènech X, Muñoz J. J Chem Technol Biotechnol 1990;47:101.
[1079] Ku Y, Jung IL. Water Res 2001;35:135.
[1080] Prairie MR, Evans LR, Martínez SL. Chem Oxid 1992;2:428.
[1081] Prairie MR, Stange BM, Evans LE. In: Ollis DF, Al-Ekabi H, editors. Photocatalytic purification and treatment of water and air. Amsterdam: Elsevier; 1993, p. 1776.
[1082] Forouzan F, Richards TC, Bard AJ. J Phys Chem 1996;100:18123.
[1083] Palik JW, Tantayanon S. J Am Chem Soc 1981;103:6755.
[1084] Foster NS, Lancaster AN, Noble RD, Koval CA. Ind Eng Chem Res 1995;34:3865.
[1085] Kanki T, Yoneda H, Sano N, Toyoda A, Nagai C. Chem Eng J 2003;97:77.
[1086] Yamazaki S, Takemura N, Yoshinaka Y, Yoshida A. J Photochem Photobiol A: Chem 2003;161:57.
[1087] Chen LX, Rajh T, Mićić O, Wang Z, Tiede DM, Thurnauer M. Nucl Instrum Meth Phys Res B 1997;133:8.
[1088] Bideau M, Claudel B, Faure L, Rachimoellah M. J Photochem 1990;39:167.
[1089] Morishita MS. Chem Lett 1992;1979.
[1090] Nishimoto S, Ohtani B, Kajiwara H, Kagiya T. J Chem Soc Faraday Trans I 1983;79:4001.
[1091] Sahyun MR, Serpone N. Langmuir 1997;13:5082.

[1092] Bargarrelo E, Harris R, Serpone N. Nouv J Chim 1985;9:743.
[1093] Serpone N, Borgarello E, Barbeni M, Pelizzetti E, Pichat P, Hermann JM, et al. J Photochem Photobiol A: Chem 1986;36:373.
[1094] Botta SG, Rodriguez DJ, Leyva AG, Litter MI. Catal Today 2002;76:247.
[1095] Wang ZH, Zhuang QX. J Photochem Photobiol A: Chem 1993;75:105.
[1096] Khalil LB, Rophael MW, Mourad WE. Appl Catal B: Environ 2002;36:125.
[1097] Rader WS, Solujic L, Milosavljevic EB, Hendrix JL, Nelson JH. J Solar Energy Eng 1994;116:125.
[1098] Prairie MR, Stange BM, Evans LR. In: Ollis DF, Al-Ekabi H, editors. Photocatalytic purification and treatment of water and air. Amsterdam: Elsevier; 1993, p. 353.
[1099] Sepone N, Ah-You YK, Tran TP, Harris R, Pelizzetti E, Hidaka H. Solar Energy 1987;39:491.
[1100] Serpone N, Borgarrelo E, Pelizzetti E. In: Schiavello M, editor. Photocatalysis and environment. Dordrecht: Kluwer Academic Publishers; 1988, p. 527.
[1101] Koudelka M, Sánchez J, Augustynsky J. J Phys Chem 1982;86:4277.
[1102] Angelidis TN, Koutlemani M, Poulis I. Appl Catal B: Environ 1998;16:347.
[1103] Curran JS, Domènech J, Jaffrezic-Renault N, Phillipe R. J Phys Chem 1985;89:957.
[1104] Xi X, Chen Z, Li Q, Jin Z. J Photochem Photobiol A: Chem 1995;87:249.
[1105] Rajh T, Ostafin AE, Micic OI, Tiede DM, Thurnauer MC. J Phys Chem 1996;100:815.
[1106] Tanaka K, Harada K, Murata S. Solar Energy 1986;36:159.
[1107] Kagaya S, Bitoh Y, Hasegawa K. Chem Lett 1997;155.
[1108] Chiang K, Amal R, Tran T. J Mol Catal A: Chem 2003;193:285.
[1109] Hidaka H, Nakamura T, Ishizaha A, Tsuchiya M, Zhao J. J Photochem Photobiol A: Chem 1992;66:367.
[1110] Augugliaro V, Lodolo V, Marci G, Palmisano L, López-Muñoz MJ. J Catal 1997;166:272.
[1111] Pallema CH, Hendrix J, Milosavljevic EB, Solujic L, Nelson JH. J Photochem Photobiol A: Chem 1992;66:235.
[1112] Wali K, Wang L, Nohara K, Hidaka H. J Mol Catal A: Chem 1995;95:53.
[1113] Botta SG, Navío JA, Hidalgo MC, Litter MI. J Photochem Photobiol A: Chem 1999;129:89.
[1114] Peral J, Muñoz J, Domènech X. J Photochem Photobiol A: Chem 1990;55:251.
[1115] Ahmed MS, Aita YA. J Non-Cryst Solid 1995;186:402.
[1116] Augugliaro V, Blanco Gálvez J, Cáceres Vázquez J, García López E, Loddo V, López Muñoz J, et al. Catal Today 1999;54:245.
[1117] Shifu C, Gengyu C. Solar Energy 2002;73(1):15.
[1118] Almquist C, Biswas P. J Catal 2002;212:145.
[1119] Halmann M, Hunt AJ, Spath D. Solar Energy Solar Cells 1992;26:1.
[1120] Egerton TA, Tooley JR. J Phys Chem B 2004;108:5066.
[1121] Yamashita H, Harada M, Masaka J, Takeuchi M, Neppolian B, Anpo M. Catal Today 2003;84:191.
[1122] Fatou GP, Vermury S, Pratsinis SE. Chem Eng Sci 1994;49:4939.
[1123] Salaices M, Serrano B, Lasa HI. Chem Eng Sci 2004;59:3.
[1124] Rachel A, Sarakha M, Subrahmanyam M, Boule P. Appl Catal B: Environ 2002;37:293.
[1125] Rachel A, Subrahmanyam M, Boule P. Appl Catal B: Environ 2002;37:301.
[1126] Augugliaro V, Prevot AB, Vazquez JC, Garcia-Lopez E, Irico A, Loddo V, et al. Adv Environ Res 2004;8:329.
[1127] Araňa J, Nieto JLM, Melián JAH, Rodriguez JMD, Diaz OG, Pena JP, et al. Chemosphere 2004;55:893.
[1128] Wang H, Adesina AA. Appl Catal B: Environ 1997;14:241.
[1130] Beckbölet M, Suphandag AS, Uygunder CS. J Photochem Photobiol A: Chem 2002;148:121.
[1131] Alhakimi G, Stunicki LH, Al-Ghazali M. J Photochem Photobiol A: Chem 2003;154:219.
[1132] Chan YC, Chen JN, Lu MC. Chemosphere 2001;45:29.
[1133] Dionysiiou DD, Khodadoust AP, Kern AM, Suidan MT, Baudin I, Laîne JM. Appl Catal B: Environ 2000;24:139.

[1134] Guillard C, Disdier J, Hermann JM, Lehaut C, Chopin T, Malato S, et al. Catal Today 1999;54:217.
[1135] Kleine J, Peinemann KV, Schuster C, Warnecke HJ. Chem Eng Sci 2002;57:1661 664.
[1136] Giménez J, Curcó D, Queral MA. Catal Today 1999;54:229.
[1137] Vohra MS, Tanaka K. Water Res 2002;36:59.
[1138] Addoma M, Augugliaro V, Di Paola A, Garcia-Lopez E, Loddo V, Marci G, et al. J Phys Chem B 2004;108:3303.
[1139] Wang ZK, Kutal C. Chemosphere 1995;30:1125.
[1140] Dhananjeyan MR, Annapoorani R, Renganathan R. J Photochem Photobiol A: Chem 1997;109:147.
[1141] Babay PA, Emilio CA, Ferreyra RE, Gettar EA, Litter MI. Water Sci Technol 2001;44:179.
[1142] Emilio CA, Testa JJ, Hufschmidt D, Colón G, Navío JA, Bahnemann DW, Litter MI. J Ind Eng Chem 2004;10:129.
[1143] Grzechulska J, Hamerski M, Morawski AW. Water Res 2000;34:1638.
[1144] Hamerski M, Grechulska J, Morawski AW. Solar Energy 1999;66:395.
[1145] Oh YC, Bao Y, Jenks WS. J Photochem Photobiol A: Chem 2003;161:69.
[1146] Coleman HM, Eggins BR, Byrne JA, Palmer FL, King E. Appl Catal A: Gen 2000;24:L1.
[1147] Saquid M, Muneer M. Desalination 2003;155:255.
[1148] Zielińska B, Grzechulska J, Morawski AW. J Photochem Photobiol A: Chem 2003;157:65.
[1149] Neppolian B, Sakthivel S, Arabindoo B, Palanichamy M, Murugesan V. J Environ Sci Health A: Environ Sci Toxicol Hazard Subst Control 2001;36:203.
[1150] Chen LC, Chou TS. J Mol Catal 1993;85:201.
[1151] Rao KVS, Lavédrine B, Boule P. J Photochem Photobiol A: Chem 2003;154:189.
[1152] Sauer T, Cesconeto Neto G, José HJ, Moreira RFPM. J Photochem Photobiol A: Chem 2002;149:147.
[1153] Sakthivel S, Shankar MV, Palanichamy M, Arabindoo B, Murugesan V. J Photochem Photobiol A: Chem 2002;148:153.
[1154] Muruganandham M, Swaminathan M. Solar Energy Mater Solar Cells 2004;81:439.
[1155] Antharjanam S, Philip R, Das S. Ann Chim 2003;93:719.
[1156] Tang WZ, An H. Chemosphere 1995;31:4171.
[1157] Goutailler G, Valette JC, Guillard C, Païssé O, Faure R. J Photochem Photobiol A: Chem 2001;141:79.
[1158] Macounová K, Urban J, Krýsová H, Krýsa J, Jirkovský J, Ludvik J. J Photochem Photobiol A: Chem 2001;140:93.
[1159] Guillard C, Horikoshi S, Watanabe N, Hidaka H, Pichat P. J Photochem Photobiol A: Chem 2002;149:155.
[1160] Pathirana HMKK, Maithreepala RA. J Photochem Photobiol A: Chem 1997;102:273.
[1161] Agüera A, Almansa E, Tejedor A, Alba ARF, Malato S, Maldonado MI. Environ Sci Technol 2000;34:1563.
[1162] Vidal A, Martin Luengo MA. Appl Catal B: Environ 2001;32:1.
[1163] Malato S, Blanco J, Cáceres J, Ferández-Alba AR, Agüera A, Rodríguez A. Catal Today 2002;76:209.
[1164] Macounová K, Krýová H, Ludvíc J, Jirkovský J. J Photochem Photobiol A: Chem 2003;156:273.
[1165] Herrmann JM, Disdier J, Pichat P, Malato S, Blanco J. Appl Catal B: Environ 1998;17:15.
[1166] Ku Y, Jung IL. Chemosphere 1989;37:2589.
[1167] Sakkas VA, Lambropoulou DA, Sakellarides TM, Albanis TA. Anal Chim Acta 2002;467:233.
[1168] Sanjuán A, Aguirre G, Álvaro M, García H. Water Res 2000;34:320.
[1169] Herrmann JM, Disdier J, Pichat P, Malato S, Blanco J. Appl Catal B: Environ 1998;17:15.
[1170] Pichat P. Water Sci Technol 1997;354:73.
[1171] Vidal A. Chemosphere 1998;36:2593.
[1172] Zaleska A, Hupka J, Wiergowski M, Biziuk M. J Photochem Photobiol A: Chem 2000;135:213.
[1173] Bandala ER, Gelover S, Leal MT, Arancibia-Bulnes C, Jimenez A, Estrada CA. Catal Today 2002;76:189.

[1174] Chen D, Ray AK. Water Res 1998;32:3223.
[1175] Topolov A, Molnár-Gábor D, Kosanic M, Abramovic A. Water Res 2000;34:1473.
[1177] Serpone N, Texier I, Emeline AV, Pichat P, Hidaka H, Zhao J. J Photochem Photobiol A: Chem 2000;136:145.
[1178] Pignatello JJ. Environ Sci Technol 1992;26:994.
[1179] Malato S, Blanco J, Richter C, Curcó D, Gómez J. Water Sci Technol 1997;35:157.
[1180] Roberto D, Malato S. Sci Total Environ 2002;291:85.
[1181] Liu KT. Ind Pollut Prev 1993;48:15.
[1182] Obee TN, Brown RT. Environ Sci Technol 1995;29:1223.
[1183] Lawryk NJ, Wiesel CP. Environ Sci Technol 1996;30:810.
[1184] Li K, Liu SYC, Huang C, Esariyaumpai S, Chen DH. J Adv Oxid Technol 2002;5:227 232.
[1185] http://www.nrel.gov/research/industrial_tech/pollution.html.
[1186] Peral J, Domènech X, Ollis DF. Biotechnology 1997;70:117.
[1187] Hemminger JC, Carr R, Somorjai GA. Chem Phys Lett 1978;57:100.
[1188] Muggli DS, Odland MJ, Schmidt LR. J Catal 2001;203:51.
[1189] Jacoby WA, Blake DM, Fennell JA, Boutler JE, Vargo LM, George MC, et al. Air Waste Manage Assoc 1996;46:891.
[1190] Jardim WF, Alberci RM, Takyama MM, Huang CP. Hazard Ind Waters 1994;26:230.
[1191] Raupp GB, Junio TC. Appl Surf Sci 1993;72:321.
[1192] Dibble LA, Raupp GB. Environ Sci Technol 1992;26:492.
[1193] Canela MC, Alberci RM, Sofia RCR, Eberlin MN, Jardim WF. Environ Sci Technol 1999;33:2788.
[1194] Sauer ML, Ollis DF. J Catal 1994;149:81.
[1195] Nicoella C, Rovatti M. Chem Eng J 1998;69:119.
[1196] Hossain MM, Raupp GB. AIChE J 1999;45:1309.
[1197] Berman E, Dong J. In: Eckenfelder WW, Bowers AR, Roth JA, editors. The Third International Symposium on Chemical Oxidation: Technologies for the Nineties, vol. 3. Chicago: Technomic Publishers; 1993.
[1198] d'Hennzel O, Ollis DF. J Catal 1997;167:118.
[1200] Sauer ML, Helle MA, Ollis DF. J Photochem Photobiol A: Chem 1995;88:169.
[1201] Brigden CT, Poulston S, Twigg MV, Walker AP, Wilkins AJJ. Appl Catal B: Environ 2001;32:63.
[1202] Yoshida K, Yamasaki J, Tanaka N. Appl Phys Lett 2004;84:2542.
[1203] Yamazaki S, Tanaka S, Tsukamoto H. J Photochem Photobiol A: Chem 1999;121:55.
[1204] Cao L, Speiss FJ, Huang A, Suib SL, Obee TN, Hay SO, et al. J Phys Chem B 1999;103:2912.
[1205] Ameen MM, Raupp GB. J Catal 1999;184:112.
[1206] Augugliaro V, Collucia S, Loddo V, Marchese L, Matra G, Palmisano L, et al. Appl Catal B: Environ 1999;20:112.
[1207] Djeghri N, Formenti M, Juillet F, Teichner SJ. Faraday Discuss Chem Soc 1974;58:185.
[1208] Pichat P, Hermann JM, Disdier J, Mozzanega MN. J Phys Chem 1979;83:3122.
[1209] Wada K, Yoshida K, Takatani T, Watanabe Y. Appl Catal A: Gen 1993;99:21.
[1210] Maira AJ, Coronado JM, Augugliaro V, Yeung KL, Conesa JC, Soria J. J Catal 2001;202:413.
[1211] Lichtin NN, Avudaithai M. Environ Sci Technol 1996;30:2014.
[1212] Fu X, Zeltner WA, Anderson MA. In: Kamat PV, Meisel D, editors. Semiconductor nanoclusters: physical, chemical and catalytical aspects. Amsterdam: Elsevier; 1996, p. 445.
[1213] Heldon W, Marcellino A, Valic D, Weedon AC. In: Ollis DF, Al-Ekabi H, editors. Photocatalytic and treatment of water and air. Amsterdam: Elsevier Publication Science; 1993 [Chapter 3].
[1214] Nimlos MR, Jacoby WA, Blake DM, Milne TA. In: Ollis DF, Al-Ekabi H, editors. Photocatalytic and treatment of water and air. Amsterdam: Elsevier Publicaiton Science; 1993 [Chapter 3].
[1215] Nimlos MR, Jacoby WA, Blake DM, Milne TA. Environ Sci Technol 1993;27:732.
[1216] Philips LA, Raupp GB. J Mol Catal 1992;77:297.
[1217] Dibble LA, Raupp GB. Catal Lett 1990;4:345.

[1218] Al-Akabi H, Butters B, Delany D, Holden W, Powel T, Story J. In: Ollis DF, Al-Ekabi H, editors. Photocatalytic and treatment of water and air. Amsterdam: Elsevier Publication Science; 1993 [Chapter 7].
[1219] Hager S, Bauer R. Chemosphere 1999;38:1549.
[1220] Sánchez B, Cardona AI, Romero M, Avila P, Bahamonde A. Catal Today 1999;54:369.
[1221] Sano T, Negishi N, Kutsuna S, Takeuchi K. J Mol Catal A: Chem 2001;168:223.
[1222] Sauer ML, Ollis DF. J Catal 1996;158:570.
[1223] Nimlos MR, Wolfrum EJ, Brewer ML, Fennell JA, Bintner G. Environ Sci Technol 1996;30:3102.
[1224] Vorontsov AV, Savinov EN, Barannik GB, Trotsky VN, Parmon VN. Catal Today 1997;39:207.
[1225] Pinketon S, Hwang SJ, Raftery D. J Phys Chem B 1999;103:11152.
[1226] Hwang SJ, Raftery D. Catal Today 1999;49:353.
[1227] Kozlov DV, Paukshtis EA, Savinov EN. Appl Catal B: Environ 2000;24:77.
[1229] Alberci RM, Canela MC, Eberlin MN, Jardim WF. Appl Catal B: Environ 2001;30:389.
[1230] Yang YC. Chem Ind 1995;1:334.
[1231] Ember LR. Chem News 1990;68:9.
[1232] Canela MC, Alberci RM, Jardim WF. J Photochem Photobiol A: Chem 1998;112:73.
[1233] Vorontsov AV, Savinov ES, Davydov L, Smirniotis PG. Appl Catal B: Environ 2001;32:11.
[1234] Kozlov DV, Vorontsov AV, Smirniotis PG, Savinos EB. Appl Catal B: Environ 2003;42:77.
[1235] Vorontsov AV, Lion C, Savinov EN, Smirniotis PG. J Catal 2003;220:414.
[1236] Vorontsov AV, Savinov EN, Lion C, Smirniotis PG. Appl Catal B: Environ 2003;44:25.
[1237] Saga K, Hattori T. J Electrochem Soc 1996;143:3279.
[1238] Tada H. Langmuir 1996;12:966.
[1239] Sun RD, Nakajima A, Watanabe T, Hashimoto K. J Photochem Photobiol A: Chem 2003;154:203.
[1240] Minero C, Maurino V, Pelizzetti E. Langmuir 1995;11:4440.
[1241] Elsom D. Atmospheric pollution. New York: Basil Blackwell; 1987.
[1242] Seinfeld JH, Pandis SN. Atmospheric chemistry and physics: from air pollution to climate change. New York: Wiley; 1988.
[1243] Cooper CD, Alley FC. Air pollution control: a design approach. Prospect Heights (IL): Waveland Press; 1994.
[1244] Devahasdin S, Fan C, Li K, Chen DH. J Photochem Photobiol A: Chem 2003;156:161.
[1246] Anpo M. Surface science and catalysis. Amsterdam: Elsevier; 2000, p. 93.
[1248] Dhandapani B, Oyama ST. Appl Catal B: Environ 1977;11:129.
[1249] Ohtani B, Zhang SW, Nishimoto S, Kagiya T. J Chem Soc Faraday Trans 1992;88:1049.
[1250] Sauer ML, Ollis DF. J Catal 1996;163:215.
[1251] Piera E, Ayllón JA, Domènech X, Peral J. Catal Today 2002;76:259.
[1252] Peral J, Ollis DF. J Mol Catal A: Chem 1997;115:347.
[1253] Einaga H, Futamura S, Ibusuki T. Appl Catal B: Environ 2002;38:215.
[1254] Larson SA, Falconer JL. Catal Lett 1997;44:57.
[1255] Cao LX, Gao Z, Suib SL, Obee TN, Hay SO, Freihault J. J Catal 2000;196:253.
[1256] Einaga H, Ibusuki T, Futamura S. Environ Sci Technol 2004;38:285.
[1257] Zorn ME, Tompkins DT, Zeltner WA, Anderson MA. Environ Sci Technol 2000;4:5206.
[1258] Park DR, Zhang J, Ikeue K, Yamashita H, Anpo M. J Catal 1999;185:114.
[1259] Maira AJ, Yeung KL, Soria J, Coronado JM, Belver C, Lee CY, et al. Appl Catal B: Environ 2001;29:327.
[1260] Obee N, Hay SO. Environ Sci Technol 1997;31:2034.
[1261] Alberci R, Jardim WF. Appl Catal B: Environ 1997;14:55.
[1262] Kim SB, Hwang HT, Hong SC. Chemosphere 2002;48:437.
[1263] Marta G, Coluccia S, Marchese L, Augugliaro V, Loddo V, Palmisano L, et al. Catal Today 1999;53:695.
[1265] Vorontsov AV, Stoyanova IV, Kozlov DV, Simagina VI, Savinov EN. J Catal 2000;189:360.
[1266] Coronado JM, Zorn ME, Tejedor-Tejedor I, Anderson MA. Appl Catal B: Environ 2003;43:329.

[1267] Zorn ME, Tomkins DT, Zeltner WA, Anderson MA. Appl Catal B 1999;23:1.
[1268] El-Maazawi M, Finken AN, Nair AB, Grassian VH. J Catal 2000;191:138.
[1269] Einaga H, Futamura S, Ibusuki T. Phys Chem Chem Phys 1999;1:4903.
[1270] Vichi FM, Tejedor-Tejedor MI, Anderson MA. Chem Mater 2000;12:1762.
[1271] Lu MC. J Environ Sci Health B 1999;34:207.
[1272] J. Roberts and W. C. Nelson, in *National Human Activity, Pattern Survey Data Base, USEPA*, Research Triangle Park, NC 1995.
[1273] Kreiss K. In: Cone JE, Hodson MJ, editors. Problem buildings: building-associated illness and the sick building syndrome. Philadelphia: Hanley and Belfus; 1985, p. 579.
[1274] Sakamoto K, Tonegawa Y, Ishitani O. J Adv Oxid Technol 1999;4:35.
[1275] Jo WK, Park JH, Chun HD. J Photochem Photobiol A: Chem 2002;148:109.
[1276] Komazaki Y, Shimizu H, Tanaka S. Atmos Environ 1999;33:4363.
[1277] Ao CH, Lee SC. J Photochem Photobiol A: Chem 2004;161:131.
[1278] Ao CH, Lee SC, Yu JC. J Photochem Photobiol A: Chem 2003;156:171.
[1279] Watanabe T, Kitamura A, Kojima E, Nakayama C, Hashimoto K, Fujishima A. In: Ollis D, El-Akabi H, editors. Photocatalytic purification and treatment of water and air. New York: Elsevier; 1995, p. 742.
[1280] TOTO Ltd, Patent No. (PCT) WO95/15816, 1995.
[1281] Negishi N, Iyoda T, Hashimoto K, Fujishima A. Chem Lett 1995;841.
[1282] Noguchi T, Fujishima A. Environ Sci Technol 1998;32:3831.
[1283] Sekine Y, Nishimura A. Atmos Environ 2001;35:2001.
[1284] Ichiura H, Kitaoka T, Tanaka H. J Mater Sci 2002;37:2937.
[1285] Ichiura H, Kitaoka T, Tanaka H. Chemosphere 2003;50:79.
[1286] Sopyan I, Marasawa S, Hashimoto K, Fujishima A. Chem Lett 1994;723.
[1287] Matsubara H, Tanaka M, Koyama S, Hoshimoto K, Fujishima A. Chem Lett 1995;767.
[1288] Sasaki M. R&D Rev Toyota CRDL 2001;36:1.
[1289] Suzuki K. In: Ollis D, El-Akabi H, editors. Photocatalytic purification and treatment of water and air. New York: Elsevier; 1995, p. 421.
[1290] Shang J, Du Y, Xu Z. Chemosphere 2002;46:93.
[1291] Sirisuk A, Hill Jr. CG, Anderson MA. Catal Today 1999;54:159.
[1292] Kataoka S, Tompkins DT, Zeltner WA, Anderson MA. J Photochem Photobiol A: Chem 2002;148:323.
[1293] Blount MC, Falconer JL. Appl Catal B: Environ 2002;39:39.
[1294] Dumitru D, Bally AR, Ballif C, Hones P, Schmid PE, Sanjinès R, et al. Appl Catal B: Environ 2000;25:83.
[1295] Bouzaza A, Laplanche A. J Photochem Photobiol A: Chem 2002;15:207.
[1296] Guo-Min Z, Zhen-Xing C, Min X, Xian-Qing Q. J Photochem Photobiol A: Chem 2003;161:69.
[1297] Wang KH, Hsieh YH, Chao PW, Cgang CY. J Hazard Mater 2002;B 95:161.
[1298] Yeung KL, Yan ST, Maira AJ, Coronado JM, Soria J, Yue PL. J Catal 2003;219:107.
[1299] Piera E, Tejedor-Tejedor MI, Zorn ME, Anderson MA. Appl Catal B: Environ 2003;46:671.
[1300] Monneyron P, Manero MH, Foussard JN, Benoit-Marquie F, Maurette MT. Chem Eng Sci 2003;58:971.
[1301] Han ST, Xi HL, Fu XZ, Wang XX, Ding ZX, Lin ZC, et al. Acta Phys Chim Sinica 2004;20:296.
[1302] Zhang Y, Yang R, Zhao R. Atmos Environ 2003;37:3395.
[1303] Lee BJ, Kuo MC, Chien SH. Res Chem Intermed 2003;29:817.
[1304] King CH, Shotts EB, Wooley RE, Porter KG. Appl Environ Microbiol 1988;54:3023.
[1305] Zszewsyk U, Zszewsyk RU, Manz W, Schleifer KH. Ann Rev Microbiol 2000;54:81.
[1306] Venczel LV, Arrowood M, Hurd M, Sobsey MD. Appl Environ Microbiol 1997;63:1598.
[1307] Abarnou A, Miossec L. Sci Total Environ 1992;126:173.
[1308] Szal GM, Nola PM, Kennedy LE, Barr CP, Bilger MD. Res J WPCF 1991;63:173.
[1309] Cipparone LA, Diehl AC. J AWWA 1997;89:84.
[1310] Yanko WA. Water Environ Res 1993;66:221.
[1311] Goswani DY, Trivedi DM, Block SS. J Solar Energy Eng 1997;119:92.

[1312] Blake DM, Maness PC, Huang Z, Wolfrum EJ, Huang J, Jacoby WA. Sep Purif Methods 1999;28:1.
[1313] Furuzono T, Iwasaki M, Yasuda S, Korematsu A, Yoshioka T, Ito S, et al. J Mater Sci Lett 2003;22:1737.
[1314] Dillert R, Bahnemann D. Chem Eng Technol 1998;21:356.
[1315] Dillert R, Siemon U, Bahnemann D. J Adv Oxid Technol 1999;4:55.
[1316] Sun DD, Tay JH, Tan KM. Water Res 2003;37:3452.
[1317] Baker KH, Herson DS. Water Environ Res 1999;71:530–51.
[1318] Ibáñez JA, Litter MI, Pizzaro RA. J Photochem Photobiol A: Chem 2003;157:81.
[1319] Ireland JC, Klostermann P, Rice EW, Clark RM. Appl Environ Microbiol 1993;59:1668.
[1320] Rincón AG, Pulgarin C. Appl Catal B: Environ 2003;44:263.
[1321] Gourmelon M, Cillard J, Pommepuy M. J Appl Bacteriol 1994;77:105.
[1322] Pham HN, McDowell T, Wilkins E. J Environ Sci Health A: Environ Sci Eng Toxicol Hazard Subst Control A 1995;30:627.
[1323] Stevenson M, Bullock K, Lin WY, Rajeshwar K. Res Chem Intermed 1997;23:311.
[1324] Butterfield IM, Christensen PA, Curtis TP, Gunlazuardi J. Water Res 1997;31:675.
[1325] Bekbölet M, Araz CV. Chemosphere 1996;32:959.
[1326] Kashige N, Kakita Y, Nakashima Y, Miake F, Watanabe K. Curr Microbiol 2001;42:184.
[1327] Huang Z, Maness PC, Blake BM, Wolfrum EJ, Smolinski SL, Jacoby WA. J Photochem Photobiol A: Chem 2000;130:163.
[1328] Kuo WS, Lin YT. J Environ Sci Health A 2000;35:671.
[1329] Ngame S, Oku T, Kambara M, Konishi K. J Dent Res 1989;68:1696.
[1330] Sakurada T. Hyomen Gijutsu 1990;41:1008.
[1331] Thornton HM, Christensen GL, Suri RPS. Hazard Ind Wastes 1997;29:195.
[1332] Wist J, Sanabria J, Dierolf C, Torres W, Pulgarin C. J Photochem Photobiol A: Chem 2002;147:241.
[1333] Saito T, Iwase I, Horis J, Morioka T. J Photochem Photobiol B: Biol 1992;14:369.
[1334] Lee S, Nishida K, Otaki M, Ohgaki S. Water Res Sci Technol 1997;35:101.
[1335] Sjogren JC, Sierka RA. Appl Environ Microbiol 1994;60:344.
[1336] Sunada K, Kikuchi Y, Hoshimoto K, Fujishima A. Environ Sci Technol 1998;32:726.
[1337] Sunada K, Watanabe T, Hashimoto K. J Photochem Photobiol A: Chem 2003;156:227.
[1338] Britt AB. Ann Rev: Plant Physiol Plant Mol Biol 1996;47:75.
[1339] Li S, Paulsson M, Björn LO. J Photochem Photobiol B: Biol 2002;66:62.
[1340] Baron J. Water Environ Res 1997;69:992.
[1341] Cai R, Hashimoto K, Itoh K, Kubota Y, Fujishima A. Bull Chem Soc Jpn 1991;64:1268.
[1342] Cai R, Itoh K, Fujishima A, Kubota Y. Photomed Photobiol 1988;10:253.
[1343] Sakai H, Baba R, Hashimoto K, Kubota Y, Fushima A. Chem Lett 1995;185.
[1344] Huang N, Xu M, Yuan C, Yu R. J Photochem Photobiol A: Chem 1997;108:229.
[1345] Cai R, Kubota Y, Shuin T, Sakai H, Hashimoto K, Fujishima A. Cancer Res 1992;52:2346.
[1346] Dunlop PSM, Byrne JA, Manga N, Eggins BR. J Photochem Photobiol A: Chem 2002;148:355.
[1347] Wolfrum EJ, Huang J, Blake DM, Maness PC, Huang Z, Fiest J, et al. Environ Sci Technol 2002;36:3412.
[1348] Liu HL, Yang TCK. Process Biochem 2003;39:475.
[1349] Tao H, Wei W, Zhang S. J Photochem Photobiol A: Chem 2004;161:193.
[1350] Koizumi Y, Nishi J, Taya M. J Chem Eng Jpn 2002;35:299.
[1351] Morioka T, Saito T, Nara Y, Onoda K. Cariers Res 1998;22:230.
[1352] Kim B, Kim D, Cho D, Cho S. Chemosphere 2003;52:277–81.
[1353] Block SS, Goswami DW. Solar Energy 1995;1:431.
[1354] Armon R, Laot N, Narkis N. J Adv Oxid Technol 1998;3:145.
[1356] Hancock-Chen T, Scaiano JC. J Photochem Photobiol B: Biol 2000;57:193.
[1357] Lee JH, Kang M, Choung SJ, Ogino K, Miyata S, Kim MS, et al. Water Res 2004;38:713.
[1358] Laot N, Narkis N, Neeman I, Vilanovic D, Amon R. J Adv Oxid Technol 1999;4:97.
[1359] Cai R, Hashimoto K, Kubota Y, Fujishima A. Chem Lett 1992;427.

[1360] Kubota Y, Hosaka M, Hashimoto K, Fujishima A. Reg Cancer Treat 1995;8:192.
[1361] Sakai H, Cai R, Kato T, Hashimoto K, Fujishima A, Kubota Y, et al. Photomed Photobiol 1990;12:135.
[1362] Sakai H, Ito E, Cai R, Yoshioka T, Kubota Y, Hashimoto H, et al. Biochim Biophys Acta 1994;1201:259.
[1364] Cassar L, Pepe C. US Patent No. 6,409,821, 1999.
[1365] Lackhoff M, Prieto X, Nestle N, Dehn F, Niessner R. Appl Catal B: Environ 2003;43:205.
[1366] Poulious J, Spathis P, Tsoumparis P. J Environ Sci Health 1999;34:1455.
[1367] Bahnemann D. Nachr Chem Tech Lab 1994;42:378.
[1368] Bockelmann D. Solare reinigung verschmutzter wasser mittels photokatalyse. Göttingen: Cullivier; 1994.
[1369] Linkous CA, Carter GJ, Locuson DV, Ouellete AJ, Slattery DK, Smitha LA. Environ Sci Technol 2000;34:4754.
[1370] Mills A, Hill G, Bhopal S, Parkin IV, O'Neill SA. J Photochem Photobiol A: Chem 2003;160:185.